

University of Szeged  
Albert Szent-Györgyi Medical School  
Doctoral School of Interdisciplinary Sciences

# **Ketone- and cyano-selenoesters as multi-target antibacterial and anticancer derivatives**

PhD Thesis



**Nikoletta Szemerédi**

**Supervisor: Gabriella Spengler, PhD**

**Szeged**

**2024**

## CONTENTS

<b>PUBLICATIONS .....</b>	<b>4</b>
<b>ABBREVIATIONS .....</b>	<b>10</b>
<b>INTRODUCTION.....</b>	<b>13</b>
1. Multidrug resistance in bacteria and cancer .....	13
2. Causes and consequences of antibiotic resistance.....	15
2.1. Efflux pumps in bacteria .....	16
2.2. Formation of biofilm .....	17
2.3. Quorum sensing.....	19
2.4. Efflux pump inhibitors in bacteria.....	20
3. Multidrug resistance in cancer cells .....	21
3.1. Genetic factors.....	22
3.2. Cytokines.....	22
3.3. Increased DNA repair capacity .....	22
3.4. Elevated metabolism of xenobiotics.....	23
3.5. Efflux pumps in cancer cells .....	23
3.6. Efflux pump inhibitors in cancer.....	26
3.7. Apoptosis.....	27
4. Selenium and selenocompounds as chemotherapeutics .....	28
<b>AIMS OF THE STUDY .....</b>	<b>30</b>
<b>MATERIALS AND METHODS.....</b>	<b>32</b>
1. Compounds.....	32
2. Reagents and media.....	33
3. Bacterial strains .....	33
4. Cell lines and their maintenance.....	34
5. Determination of minimum inhibitory concentrations (MIC) by microdilution method .....	35
6. Real-time ethidium bromide (EB) accumulation assay .....	35
7. Assay for quorum sensing (QS) inhibition.....	36
8. Anti-biofilm activity.....	36
8.1. Inhibition of biofilm formation .....	36
8.2. Disruption of mature biofilm.....	37
9. Cytotoxicity assays.....	37
9.1. MTT assay .....	37
9.2. Resazurin assay .....	38
10. Checkerboard combination assay .....	38
11. ABCB1 inhibition by selenoesters .....	39
12. P-gp ATPase activity assay .....	40

13. Apoptosis induction.....	41
<b>RESULTS.....</b>	<b>42</b>
1. Antibacterial activity .....	42
1.1. Determination of minimum inhibitory concentrations (MICs) by microdilution method.....	42
1.2. Inhibition of bacterial efflux pumps .....	43
1.3. Assay for quorum sensing (QS) inhibition.....	47
1.4. Inhibition of biofilms.....	48
2. Antitumor activity .....	49
2.1. Cytotoxicity .....	49
2.2. Interaction of selenoesters with doxorubicin: <i>in vitro</i> model of combination chemotherapy	51
2.3. ABCB1 inhibition by selenoesters .....	53
2.4. Pgp ATPase activity .....	54
2.5. Induction of apoptosis .....	55
<b>DISCUSSION .....</b>	<b>57</b>
1. Antibacterial activity .....	57
2. Efflux pump inhibition in bacteria .....	58
3. Quorum sensing (QS) inhibition and anti-biofilm activity.....	58
4. Antitumor effects.....	60
5. Interaction of selenoesters with doxorubicin.....	60
6. ABCB1 inhibition by selenoesters .....	61
7. P-gp ATPase activity .....	61
8. Induction of apoptosis .....	62
<b>NEW FINDINGS.....</b>	<b>63</b>
<b>SUMMARY.....</b>	<b>64</b>
<b>ÖSSZEFOGLALÁS.....</b>	<b>65</b>
<b>ACKNOWLEDGEMENTS.....</b>	<b>66</b>
<b>REFERENCES.....</b>	<b>67</b>
<b>FINANCIAL SUPPORT.....</b>	<b>79</b>
<b>APPENDIX .....</b>	<b>80</b>
<b>PUBLICATIONS .....</b>	<b>85</b>

## PUBLICATIONS

### 1. Publications related to the thesis:

- I. **Szemerédi N**, Dobiasová S, Salardón-Jiménez N, Kincses A, Nové M, Habibullah G, Sevilla-Hernández C, Benito-Lama M, Alonso-Martínez FJ, Viktorová J, Spengler G, Domínguez-Álvarez E. Cyano- and Ketone-Containing Selenoesters as Multi-Target Compounds against Resistant Cancers. *Cancers (Basel)*. 2021 Sep 11;13(18):4563. doi: 10.3390/cancers13184563. PMID: 34572790; PMCID: PMC8465942.

**IF: 6.575; rank: Q1**

- II. **Szemerédi N**, Kincses A, Rehorova K, Hoang L, Salardón-Jiménez N, Sevilla-Hernández C, Viktorová J, Domínguez-Álvarez E, Spengler G. Ketone- and Cyano-Selenoesters to Overcome Efflux Pump, Quorum-Sensing, and Biofilm-Mediated Resistance. *Antibiotics (Basel)*. 2020 Dec 11;9(12):896. doi: 10.3390/antibiotics9120896. PMID: 33322639; PMCID: PMC7763688

**IF: 4.639; rank: Q1**

**Total IF: 11.214**

### 2. Publications not related to the thesis

- I. Almeida MC, **Szemerédi N**, Durães F, Long S, Resende DISP, Martins da Costa P, Pinto M, Spengler G, Sousa E. Effect of Indole-Containing Pyrazino[2,1-*b*]quinazoline-3,6-diones in the Virulence of Resistant Bacteria. *Antibiotics (Basel)*. 2023 May 17;12(5):922. doi: 10.3390/antibiotics12050922. PMID: 37237825; PMCID: PMC10215404.

**IF: 4.8**

- II. Abu Ghazal TS, Veres K, Vidács L, **Szemerédi N**, Spengler G, Berkecz R, Hohmann J. Furanonaphthoquinones, Diterpenes, and Flavonoids from Sweet Marjoram and Investigation of Antimicrobial, Bacterial Efflux, and Biofilm Formation Inhibitory Activities. *ACS Omega*. 2023 Sep 14;8(38):34816-34825. doi: 10.1021/acsomega.3c03982. PMID: 37780020; PMCID: PMC10536869.

**IF: 4.1**

- III. Sancha SAR, **Szemerédi N**, Spengler G, Ferreira MU. Lycorine Carbamate Derivatives for Reversing P-glycoprotein-Mediated Multidrug Resistance in Human Colon

Adenocarcinoma Cells. *Int J Mol Sci.* 2023 Jan 20;24(3):2061. doi: 10.3390/ijms24032061. PMID: 36768386; PMCID: PMC9916770.

**IF: 5.6**

- IV. Křížková B, Hoang L, Brdová D, Klementová K, **Szemerédi N**, Loučková A, Kronusová O, Spengler G, Kaštánek P, Hajšlová J, Viktorová J, Lipov J. Modulation of the bacterial virulence and resistance by well-known European medicinal herbs. *J Ethnopharmacol.* 2023 Aug 10;312:116484. doi: 10.1016/j.jep.2023.116484. Epub 2023 Apr 10. PMID: 37044231.

**IF: 5.4**

- V. Kovács B, **Szemerédi N**, Kúsz N, Kiss T, Csupor-Löffler B, Tsai YC, Rác B, Spengler G, Csupor D. Antiproliferative and cytotoxic effects of sesquiterpene lactones isolated from *Ambrosia artemisiifolia* on human adenocarcinoma and normal cell lines. *Pharm Biol.* 2022 Dec;60(1):1511-1519. doi: 10.1080/13880209.2022.2103574. PMID: 35952383; PMCID: PMC9377253.

**IF: 3.8**

- VI. Hegedűs D, **Szemerédi N**, Spengler G, Szatmári I. Application of partially aromatic ortho-quinone-methides for the synthesis of novel naphthoxazines with improved antibacterial activity. *Eur J Med Chem.* 2022 Jul 5;237:114391. doi: 10.1016/j.ejmech.2022.114391. Epub 2022 Apr 18. PMID: 35472850.

**IF: 6.7**

- VII. Jesus A, Durães F, **Szemerédi N**, Freitas-Silva J, da Costa PM, Pinto E, Pinto M, Spengler G, Sousa E, Cidade H. BDDE-Inspired Chalcone Derivatives to Fight Bacterial and Fungal Infections. *Mar Drugs.* 2022 May 8;20(5):315. doi: 10.3390/md20050315. PMID: 35621966; PMCID: PMC9147945.

**IF: 5.4**

- VIII. Kerekes D, Horváth A, Kúsz N, Borcsa BL, **Szemerédi N**, Spengler G, Csupor D. Coumarins, furocoumarins and limonoids of *Citrus trifoliata* and their effects on human colon adenocarcinoma cell lines. *Heliyon.* 2022 Aug 29;8(9):e10453. doi: 10.1016/j.heliyon.2022.e10453. PMID: 36097483; PMCID: PMC9463373.

**IF: 4**

- IX. Neves AR, Durães F, Freitas-Silva J, **Szemerédi N**, Martins-da-Costa P, Pinto E, Correia-da-Silva M, Spengler G, Sousa E. Derivatives of Trimethoxybenzoic Acid and Gallic Acid as Potential Efflux Pump Inhibitors: In Silico and In Vitro Studies. *Int J*

Mol Sci. 2022 Nov 21;23(22):14468. doi: 10.3390/ijms232214468. PMID: 36430942; PMCID: PMC9699367.

**IF: 5.6**

- X. Kreutzer D, Gehrman R, Kincses A, **Szemerédi N**, Spengler G, Molnár J, Hilgeroth A. Discovery of a novel class of small-molecule antibacterial agents against *Staphylococcus aureus*. Future Med Chem. 2022 Mar;14(5):299-305. doi: 10.4155/fmc-2021-0272. Epub 2021 Dec 24. PMID: 34951320.

**IF: 4.2**

- XI. Vágvölgyi M, Kocsis E, Nové M, **Szemerédi N**, Spengler G, Kele Z, Berkecz R, Gáti T, Tóth G, Hunyadi A. Diversity-Oriented Synthesis Catalyzed by Diethylaminosulfur-Trifluoride-Preparation of New Antitumor Ecdysteroid Derivatives. Int J Mol Sci. 2022 Mar 22;23(7):3447. doi: 10.3390/ijms23073447. PMID: 35408806; PMCID: PMC8998355.

**IF: 5.6**

- XII. Dobiasová S, **Szemerédi N**, Kučerová D, Koucká K, Václavíková R, Gbelcová H, Ruml T, Domínguez-Álvarez E, Spengler G, Viktorová J. Ketone-selenoesters as potential anticancer and multidrug resistance modulation agents in 2D and 3D ovarian and breast cancer in vitro models. Sci Rep. 2022 Apr 21;12(1):6548. doi: 10.1038/s41598-022-10311-y. PMID: 35449387; PMCID: PMC9023544.

**IF: 4.6**

- XIII. Pereira D, Durães F, **Szemerédi N**, Freitas-da-Silva J, Pinto E, Martins-da-Costa P, Pinto M, Correia-da-Silva M, Spengler G, Sousa E, Cidade H. New Chalcone-Triazole Hybrids with Promising Antimicrobial Activity in Multidrug Resistance Strains. Int J Mol Sci. 2022 Nov 18;23(22):14291. doi: 10.3390/ijms232214291. PMID: 36430768; PMCID: PMC9697807.

**IF: 5.6**

- XIV. Moreira J, Durães F, Freitas-Silva J, **Szemerédi N**, Resende DISP, Pinto E, da Costa PM, Pinto M, Spengler G, Cidade H, Sousa E. New diarylpentanoids and chalcones as potential antimicrobial adjuvants. Bioorg Med Chem Lett. 2022 Jul 1;67:128743. doi: 10.1016/j.bmcl.2022.128743. Epub 2022 Apr 18. PMID: 35447343.

**IF: 2.7**

- XV. Hammadi R, Kúsz N, Dávid CZ, Mwangi PW, Berkecz R, **Szemerédi N**, Spengler G, Hohmann J, Vasas A. Polyoxypregnane Ester Derivatives and Lignans from *Euphorbia*

*gossypina* var. *coccinea* Pax. Plants (Basel). 2022 May 13;11(10):1299. doi: 10.3390/plants11101299. PMID: 35631724; PMCID: PMC9146146.

**IF: 4.5**

- XVI. Domínguez-Álvarez E, Rácz B, Maré MA, Nasim MJ, **Szemerédi N**, Viktorová J, Jacob C, Spengler G. Selenium and tellurium in the development of novel small molecules and nanoparticles as cancer multidrug resistance reversal agents. Drug Resist Updat. 2022 Jul;63:100844. doi: 10.1016/j.drug.2022.100844. Epub 2022 May 2. PMID: 35533630.

**IF: 24.3**

- XVII. Csuvi O, **Szemerédi N**, Spengler G, Szatmári I. Synthesis of 4-Hydroxyquinolines as Potential Cytotoxic Agents. Int J Mol Sci. 2022 Aug 26;23(17):9688. doi: 10.3390/ijms23179688. PMID: 36077085; PMCID: PMC9456289.

**IF: 5.6**

- XVIII. Yazdani M, Béni Z, Dékány M, **Szemerédi N**, Spengler G, Hohmann J, Ványolós A. Triterpenes from *Pholiota populnea* as Cytotoxic Agents and Chemosensitizers to Overcome Multidrug Resistance of Cancer Cells. J Nat Prod. 2022 Apr 22;85(4):910-916. doi: 10.1021/acs.jnatprod.1c01024. Epub 2022 Mar 16. PMID: 35293752; PMCID: PMC9040055.

**IF: 5.1**

- XIX. Stefkó D, Kúsz N, **Szemerédi N**, Barta A, Spengler G, Berkecz R, Hohmann J, Vasas A. Unique Phenanthrenes from *Juncus ensifolius* and Their Antiproliferative and Synergistic Effects with the Conventional Anticancer Agent Doxorubicin against Human Cancer Cell Lines. Pharmaceutics. 2022 Mar 10;14(3):608. doi: 10.3390/pharmaceutics14030608. PMID: 35335985; PMCID: PMC8949129.

**IF: 5.4**

- XX. Durães F, Palmeira A, Cruz B, Freitas-Silva J, **Szemerédi N**, Gales L, da Costa PM, Remião F, Silva R, Pinto M, Spengler G, Sousa E. Antimicrobial Activity of a Library of Thioxanthenes and Their Potential as Efflux Pump Inhibitors. Pharmaceutics (Basel). 2021 Jun 15;14(6):572. doi: 10.3390/ph14060572. PMID: 34203998; PMCID: PMC8232621.

**IF: 6.525**

- XXI. Pivarcsik T, Tóth G, **Szemerédi N**, Bogdanov A, Spengler G, Kljun J, Kladnik J, Turel I, Enyedy ÉA. Comparison of Solution Chemical Properties and Biological Activity of Ruthenium Complexes of Selected  $\beta$ -Diketone, 8-Hydroxyquinoline and Pyrithione Ligands. *Pharmaceuticals (Basel)*. 2021 May 27;14(6):518. doi: 10.3390/ph14060518. PMID: 34072270; PMCID: PMC8226722.  
**IF: 5.215**
- XXII. Kaczor A, **Szemerédi N**, Kucwaj-Brysz K, Dąbrowska M, Starek M, Latacz G, Spengler G, Handzlik J. Computer-Aided Search for 5-Arylideneimidazolone Anticancer Agents Able To Overcome ABCB1-Based Multidrug Resistance. *ChemMedChem*. 2021 Aug 5;16(15):2386-2401. doi: 10.1002/cmdc.202100252. Epub 2021 Jun 7. PMID: 33929088.  
**IF: 3.54**
- XXIII. Durães F, Cravo S, Freitas-Silva J, **Szemerédi N**, Martins-da-Costa P, Pinto E, Tiritan ME, Spengler G, Fernandes C, Sousa E, Pinto M. Enantioselectivity of Chiral Derivatives of Xanthenes in Virulence Effects of Resistant Bacteria. *Pharmaceuticals (Basel)*. 2021 Nov 10;14(11):1141. doi: 10.3390/ph14111141. PMID: 34832923; PMCID: PMC8623869.  
**IF: 5.215**
- XXIV. Cardoso DSP, **Szemerédi N**, Spengler G, Mulhovo S, Dos Santos DJVA, Ferreira MU. Exploring the Monoterpene Indole Alkaloid Scaffold for Reversing P-Glycoprotein-Mediated Multidrug Resistance in Cancer. *Pharmaceuticals (Basel)*. 2021 Aug 28;14(9):862. doi: 10.3390/ph14090862. PMID: 34577562; PMCID: PMC8493801.  
**IF: 5.215**
- XXV. Rimpiläinen T, Nunes A, Calado R, Fernandes AS, Andrade J, Ntungwe E, Spengler G, **Szemerédi N**, Rodrigues J, Gomes JP, Rijo P, Candeias NR. Increased antibacterial properties of indoline-derived phenolic Mannich bases. *Eur J Med Chem*. 2021 Aug 5;220:113459. doi: 10.1016/j.ejmech.2021.113459. Epub 2021 Apr 20. PMID: 33915373.  
**IF: 7.088**
- XXVI. Kúsz N, Stefkó D, Barta A, Kincses A, **Szemerédi N**, Spengler G, Hohmann J, Vasas A. Juncaceae Species as Promising Sources of Phenanthrenes: Antiproliferative Compounds from *Juncus maritimus* Lam. *Molecules*. 2021 Feb 13;26(4):999. doi: 10.3390/molecules26040999. PMID: 33668621; PMCID: PMC7918049.  
**IF: 4.927**



- XXVII. Durães F, **Szemerédi N**, Kumla D, Pinto M, Kijjoo A, Spengler G, Sousa E. Metabolites from Marine-Derived Fungi as Potential Antimicrobial Adjuvants. *Mar Drugs*. 2021 Aug 25;19(9):475. doi: 10.3390/md19090475. PMID: 34564137; PMCID: PMC8470461.  
**IF: 6.085**
- XXVIII. Durães F, Resende DISP, Palmeira A, **Szemerédi N**, Pinto MMM, Spengler G, Sousa E. Xanthonones Active against Multidrug Resistance and Virulence Mechanisms of Bacteria. *Antibiotics (Basel)*. 2021 May 19;10(5):600. doi: 10.3390/antibiotics10050600. PMID: 34069329; PMCID: PMC8158687.  
**IF: 5.222**
- XXIX. Bús C, Kúsz N, Kincses A, **Szemerédi N**, Spengler G, Bakacsy L, Purger D, Berkecz R, Hohmann J, Hunyadi A, Vasas A. Antiproliferative Phenanthrenes from *Juncus tenuis*: Isolation and Diversity-Oriented Semisynthetic Modification. *Molecules*. 2020 Dec 17;25(24):5983. doi: 10.3390/molecules25245983. PMID: 33348712; PMCID: PMC7765930.  
**IF: 4.412**
- XXX. Kincses A, Szabó S, Rácz B, **Szemerédi N**, Watanabe G, Saijo R, Sekiya H, Tamai E, Molnár J, Kawase M, Spengler G. Benzoxazole-Based Metal Complexes to Reverse Multidrug Resistance in Bacteria. *Antibiotics (Basel)*. 2020 Sep 28;9(10):649. doi: 10.3390/antibiotics9100649. PMID: 32998217; PMCID: PMC7600679.  
**IF: 4.639**

## ABBREVIATIONS

<b>AB-A</b>	autoinducer bioassay medium
<b>ABC</b>	ATP-binding cassette
<b>ABCB1</b>	ATP-binding cassette subfamily B member 1
<b>AbgT</b>	p-aminobenzoyl-glutamate transporter family
<b>AI</b>	autoinducer
<b>AMR</b>	antimicrobial resistance
<b>ATCC</b>	American Type Culture Collection
<b>ATP</b>	adenosine triphosphate
<b>BBB</b>	blood-brain barrier
<b>BHI</b>	brain heart infusion
<b>CCCP</b>	carbonyl cyanide m-chlorophenyl hydrazone
<b>CI</b>	combination index
<b>CLSI</b>	Clinical and Laboratory Standard Institute
<b>CPZ</b>	chlorpromazine
<b>CYP</b>	cytochrome P450
<b>DMEM</b>	Dulbecco's Modified Eagle's medium
<b>DMSO</b>	dimethyl sulfoxide
<b>DNA</b>	deoxyribonucleic acid
<b>DPD</b>	dihydropyrimidine dehydrogenase
<b>EB</b>	ethidium bromide
<b>EC<sub>50</sub></b>	effective concentration 50
<b>ED<sub>50</sub></b>	median effective dose
<b>eDNA</b>	extracellular DNA
<b>EDTA</b>	ethylenediaminetetraacetic acid
<b>EMEM</b>	Eagle's Minimal Essential Medium
<b>EP</b>	efflux pump
<b>EPI</b>	efflux pump inhibitor
<b>EPS</b>	extracellular polymeric substance
<b>FAR</b>	fluorescence activity ratio

<b>FBS</b>	foetal bovine serum
<b>FSC</b>	forward scatter count
<b>GST</b>	glutathione-S-transferase
<b>HGT</b>	horizontal gene transfer
<b>IC<sub>50</sub></b>	half-maximal inhibitory concentration
<b>LBA</b>	Luria-Bertani agar
<b>LBB</b>	Luria-Bertani broth
<b>LPS</b>	lipopolysaccharide
<b>MATE</b>	multidrug and toxic compound extrusion family
<b>MDR</b>	multidrug resistant
<b>MFS</b>	major facilitator superfamily
<b>MH</b>	Mueller Hinton
<b>MIC</b>	minimum inhibitory concentration
<b>MMR</b>	mismatch repair
<b>MRSA</b>	methicillin resistant <i>Staphylococcus aureus</i>
<b>MSSA</b>	methicillin-sensitive <i>Staphylococcus aureus</i>
<b>MTT</b>	3-(4,5-dimethylthiazol-2-yl)-2,5-diphenyltetrazolium bromide
<b>MXR</b>	mitoxantrone resistance protein
<b>NC</b>	negative control
<b>NEAA</b>	non-essential amino acid
<b>NER</b>	nucleotide excision repair
<b>PACE</b>	proteobacterial antimicrobial compound efflux family
<b>PBS</b>	phosphate buffered saline
<b>PC</b>	positive control
<b>PMF</b>	proton motive force
<b>PMZ</b>	promethazine
<b>QS</b>	quorum sensing
<b>QSSM</b>	quorum sensing signal molecule
<b>R123</b>	rhodamine 123
<b>RES</b>	reserpine

<b>RF</b>	relative fluorescence
<b>RFI</b>	relative fluorescence index
<b>RLU</b>	relative luminescence unit
<b>RND</b>	resistance-nodulation-division family
<b>ROS</b>	reactive oxygen species
<b>SAR</b>	structure-activity relationships
<b>SD</b>	standard deviation
<b>SDS</b>	sodium dodecyl sulphate
<b>Se</b>	selenium
<b>SI</b>	selectivity index
<b>SMR</b>	small multidrug resistance family
<b>SSC</b>	side scatter count
<b>SSRI</b>	selective serotonin reuptake inhibitor
<b>TMD</b>	transmembrane domain
<b>TPMT</b>	thiopurine methyltransferase
<b>TSA</b>	tryptic soy agar
<b>TSB</b>	tryptic soy broth
<b>TZ</b>	thioridazine
<b>UGT</b>	uridine diphospho-glucuronosyltransferase
<b>WHO</b>	World Health Organization

## INTRODUCTION

### 1. Multidrug resistance in bacteria and cancer

Multidrug resistance (MDR) poses a significant challenge in both bacterial infections and cancer. MDR refers to the ability of microorganisms or tumor cells to withstand the effects of multiple, structurally unrelated drugs, rendering conventional therapies ineffective. Understanding the mechanisms underlying MDR in bacteria and tumor cells is crucial for more efficient therapeutic strategies [1]; [2].

Antibiotic resistance is a growing global problem that has reached alarming levels in all corners of the world. The phenomenon of antibiotic resistance occurs when bacteria lack the sensitivity to a number of antibiotics belonging to different chemical classes by using various mechanisms. There are ongoing efforts to develop new antibiotics, it is unfortunate that none of the upcoming options are projected to effectively combat the most perilous strains of antibiotic resistant bacteria [3]. The World Health Organization (WHO) has provided an estimation that around 4.9 million deaths occur annually as a result of antimicrobial resistance (AMR) mostly caused by 6 pathogens: *Escherichia coli*, *Staphylococcus aureus*, *Klebsiella pneumoniae*, *Streptococcus pneumoniae*, *Acinetobacter baumannii*, and *Pseudomonas aeruginosa* [4]. Furthermore, a study published in The Lancet in 2022 revealed that in 2019 alone, there were 1.27 million deaths associated with AMR, with a significant proportion of 860,000 deaths occurring in Africa.

The rise of multidrug resistance among various pathogens commonly found in hospitals has led to the emergence of superbugs that are exceptionally challenging to treat [5]. Bacteria that have developed resistance to multiple antibiotics called superbugs [6]. According to a report originating from Britain, it is projected that by 2050, the global impact of antimicrobial resistance will result in approximately 10 million fatalities annually [7]. Due to the lack of early identification of causative microorganisms and their antimicrobial susceptibility patterns in patients, there is a prevalent practice of using broad spectrum antibiotics excessively and often unnecessarily in many healthcare settings [8].

Cancer ranks among the top causes of death globally. In women, some of the most frequently occurring types of cancer include breast cancer, cervical cancer, lung cancer, thyroid cancer, and colorectal cancer. On the other hand, the most common types of cancer in men are prostate cancer, lung cancer, colorectal cancer, liver cancer, and stomach cancer [9]. Despite the availability of multiple cancer treatment modalities like radiation therapy, surgery,

immunotherapy, endocrine therapy, and gene therapy, chemotherapy continues to be the predominant approach for treating cancer [10]. Even though there have been notable improvements in cancer therapy, some patients exhibit poor response or fail to respond that can lead to the development of MDR against various anti-cancer drugs [11]. MDR is a term used to describe the phenomenon where cancer cells develop resistance to multiple chemotherapeutic drugs with varying structures and mechanisms of action. It poses a significant challenge in the field of chemotherapy [12]. Chemotherapy is considered a highly effective method for treating cancer and reducing the tumor burden. Unfortunately, in almost 90% of cases, tumor cells develop resistance to chemotherapeutic drugs, leading to increased cancer invasion and metastasis, making it more challenging to treat the disease successfully [13]. MDR is caused by various mechanisms, including increased drug efflux, enhanced DNA damage repair, reduced apoptosis, elevated autophagy, genetics and altered drug metabolism (**Figure 1**) [14]. Several recent studies have shown that combinations of drugs can target and kill drug-resistant cells selectively, while leaving normal cells unharmed [15].

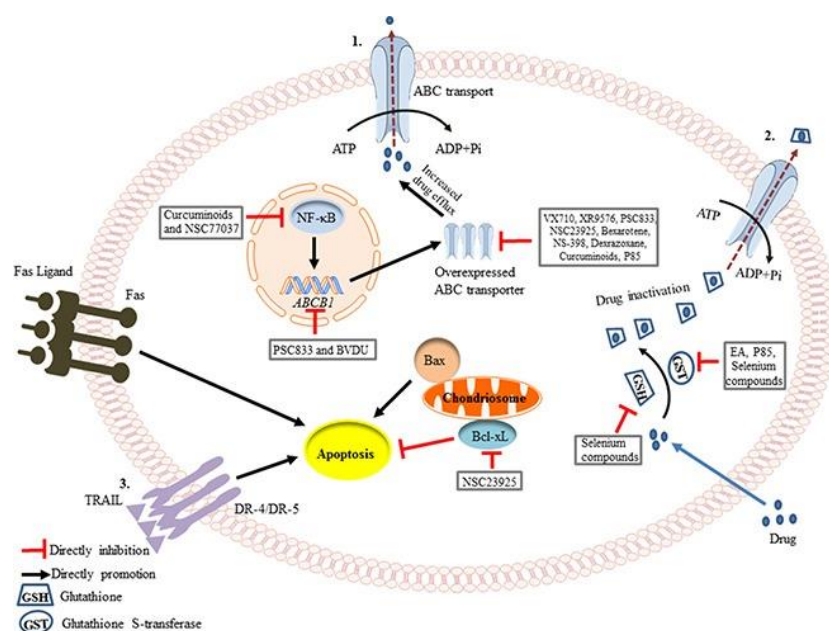


**Figure 1:** Schematic figure of the possible tumor avoidance mechanisms of cancer cells [16].

## **2. Causes and consequences of antibiotic resistance**

Antibiotics are considered to be one of the greatest achievements in the field of the therapy of infectious diseases. Nevertheless, it soon became apparent that bacteria could develop resistance to these drugs. Unfortunately, in recent years, the rate of antibiotic resistance has accelerated, leading to a notable increase in the prevalence of bacterial pathogens that are resistant to antibiotics [17]. Illnesses and the pathogens responsible for them, which were previously assumed to be successfully controlled by antibiotics, are re-emerging in new forms that are resistant to the treatments [18]. The crisis of antibiotic resistance is often linked to the excessive and inappropriate application of these drugs, alongside the pharmaceutical industry's insufficient focus on developing new medications [19]. The advancement of new antibiotics by the pharmaceutical industry, a previously successful strategy to combat resistant bacteria, has faced significant hurdles due to economic and regulatory challenges, resulting in a notable slowdown [20]. The pharmaceutical industry no longer views antibiotic development as a financially lucrative investment. The reason is that antibiotics are typically used for shorter durations and are often curative, making them less profitable compared to medications used to treat chronic conditions like diabetes, psychiatric disorders, asthma, or gastroesophageal reflux [19]. The potential causes of AMR encompass various factors, such as the excessive use of antibiotics in animals (including those used in food production, for pets, and in aquatic settings), the unrestricted availability of antibiotics without prescription, the rise in international travel, inadequate sanitation and hygiene practices, and the release of non-metabolized antibiotics or their remnants into the environment through manure and fecal waste [21]. The extensive misuse of antibiotics undeniably fuels the process of resistance evolution [19,22]. One method to slow down the progression of antibiotic resistance is the reduction of the intensity of natural selection for resistance genes. This can be achieved by minimizing the application of antibiotics: use antibiotics only when prescribed; always follow doctors' advice when using antibiotics; never share or use leftover antibiotics; only prescribe antibiotics when they are needed; regulate and promote the appropriate disposal of antibiotics; not use antibiotics for growth promotion or to prevent diseases in healthy animals in the agriculture sector [22,3]. Bacteria can obtain genetic material that grants resistance through the main mechanisms of genetic acquisition: transformation, transposition, transduction, and conjugation, collectively known as horizontal gene transfer (HGT). Additionally, bacteria can also undergo mutations in their own chromosomal DNA that contribute to the development of resistance [23]. Mutations that give rise to antibiotic resistance commonly arise in three types of genes. These genes encode the

targets of the antibiotics, the transporters responsible for their movement, and the regulators that suppress the expression of transporters or elements involved in antibiotic degradation (primarily chromosomally-encoded enzymes that modify antibiotics and multidrug efflux pumps) [17]. Antimicrobial resistance can be classified into four main categories: (1) limited uptake of a drug; (2) modification a drug target; (3) inactivation a drug; (4) active drug efflux (**Figure 2**) [23]. Out of these resistance mechanisms the present study is focused on the efflux pump related resistance for this reason the role of efflux pumps in bacterial resistance and virulence will be described in the following sections.

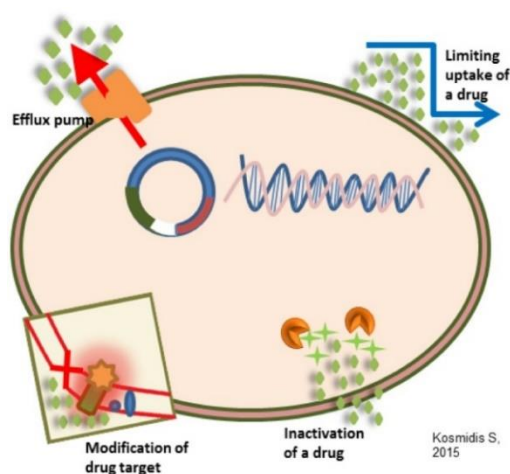


**Figure 2:** Schematic figure of the possible resistance mechanisms of bacterial cells [24].

## 2.1. Efflux pumps in bacteria

Efflux pumps (EPs) are essential membrane proteins present in all bacterial species. They play a crucial role in expelling harmful substances from bacterial cells to the external environment. These pumps are encoded by specific genes, which can be located on bacterial chromosomes or mobile genetic elements like plasmids [25]. Efflux pumps possess the capability to remove a broad spectrum of substances from bacterial cells, including antibiotics, detergents, dyes, toxins, and waste metabolites [26]. In cases where efflux pumps are capable of exporting multiple substrates, including different classes of antibiotics, they may contribute to MDR [27]. These pumps play crucial roles in diverse biological processes such as cell-to-cell communication, known as quorum sensing, as well as biofilm formation [28].

Multidrug efflux pumps present a significant barrier to effectively controlling infections caused by pathogenic bacteria. These pumps can be categorized into seven major



superfamilies (**Figure 3**): the ATP-binding cassette (ABC) superfamily; the small multidrug resistance (SMR) superfamily; the multidrug and toxic compound extrusion (MATE) superfamily; the major facilitator superfamily (MFS); the resistance nodulation and cell division (RND) superfamily; the proteobacterial antimicrobial compound efflux (PACE) superfamily and the p-aminobenzoyl-glutamate transporter family (AbgT) [29]. A notable distinction among efflux pumps lies in the type of energy they utilize: primary transporters of the ABC family operate by hydrolyzing ATP to generate the necessary energy for their function; secondary transporters such as the SMR, MATE, RND, MFS, PACE, and AbgT superfamilies derive energy by utilizing the proton-motive force generated by H<sup>+</sup> or the electrochemical gradient of Na<sup>+</sup> [30]; [31]. ABC, MFS, RND, and MATE are ubiquitous, this means they can be found in archaea to eukaryotes; SMR can be found in archaea and bacteria; PACE and AbgT can be found in bacteria [25,32,33,34,35].

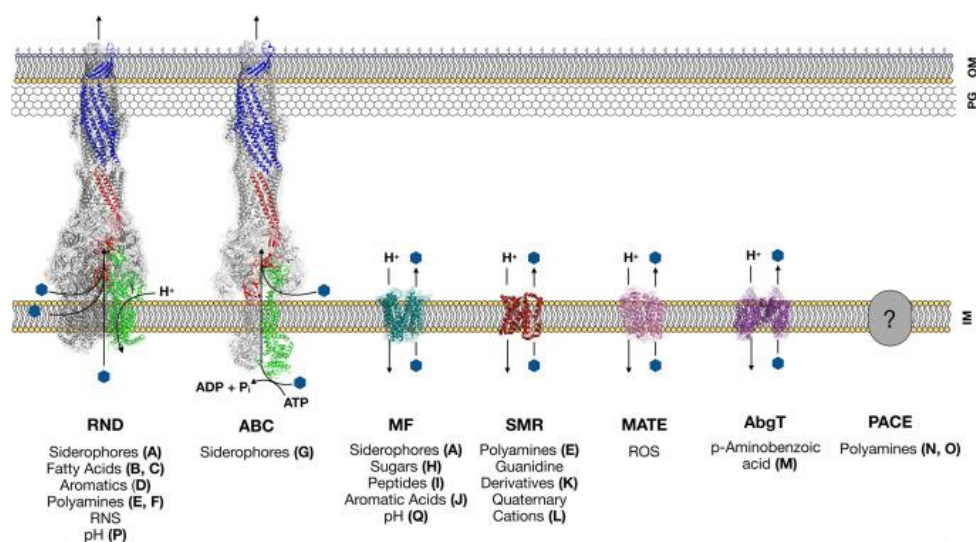


**Figure 3:** The seven major bacterial drug efflux protein families [28].

## 2.2. Formation of biofilm

There is a widely accepted understanding that in natural environments, bacterial cells tend to exist in close proximity to surfaces and interfaces, often forming multicellular aggregates known as biofilms [36]. A biofilm refers to a well-organized collection of bacteria that live within a matrix of extracellular polymers. This matrix is produced by the bacteria themselves and firmly attaches them to either inanimate surfaces or living tissues, requiring prompt rinsing for effective removal [37]. On average, bacteria make up around 5-35% of the

volume within a biofilm, with the remaining volume consisting of the extracellular matrix. The extracellular polymeric substances (EPS) contains proteins, polysaccharides, lipids, and extracellular DNA (eDNA): the composition can vary depending on the bacteria [38, 39]. The production of eDNA within biofilms is thought to involve active mechanisms, including autolysis and vesicular secretion [40]. eDNA plays critical roles within biofilms, serving as essential matrix components. Bacteria utilize eDNA for various vital functions, such as providing structural integrity to biofilms, serving as a nutrient source, and functioning as a reservoir for HGT [41]. Genetic studies have revealed that the formation of biofilms follows a multi-step process. It involves a specific type of cell-to-cell communication called quorum sensing among bacterial cells. Additionally, the transcription of distinct sets of genes is required for biofilm formation, which differs from the genes expressed by the same species in their planktonic (free-floating) forms [42]. The formation of biofilms involves several commonly observed steps, as identified by various researchers. These steps include the initial contact and attachment of bacteria to a surface, subsequent micro-colony formation, the maturation and development of the biofilm's architecture, and finally, the detachment or dispersion of the biofilm (**Figure 4**) [43].

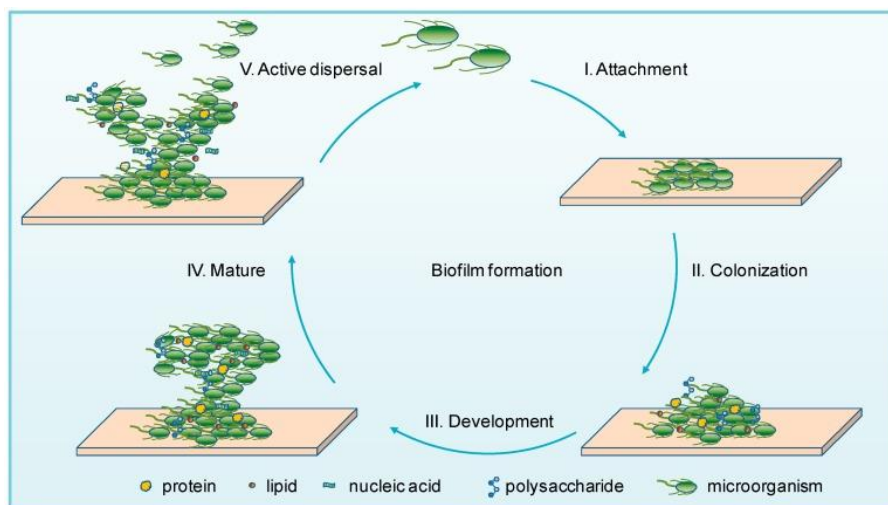


**Figure 4:** The model of microbial biofilm formation.

I. Attachment: microbial cells adhere reversibly to the surface. II. Colonization: microbial cells firmly attach to the surface using structures such as flagella, pili, and exopolysaccharides. III. Development: accumulation of multilayered cells, accompanied by the production of extracellular polymeric substances (EPS). IV. Mature: a stable three-dimensional community is formed. V. Active dispersal: microorganisms disperse from the biofilm aggregate and move to a planktonic state [44].

Research has indicated that biofilms can significantly enhance bacterial resistance to a range of environmental factors, including UV radiation, extreme temperature and pH conditions, high salinity, high pressure, nutrient scarcity, and various antibiotics [44]. When bacteria grow as biofilms, they consistently exhibit a significant increase in resistance to antimicrobial agents compared to cultures grown in suspension (planktonic) in standard liquid media [45]. In order to effectively combat biofilm-forming bacteria, antimicrobial agents must overcome various challenges. These include an elevated presence of resistant mutants, high cell density within the biofilm, molecular exchanges within the biofilm community, efficient substance delivery to the target cells, the presence of efflux pumps that can expel antimicrobial agents, and the presence of persistent cells (persistent refer to a distinct subpopulation of bacterial cells that possess temporary antibiotic resistant phenotypes [46]) that exhibit enhanced resistance to treatment [47].

### **2.3. Quorum sensing**

Quorum sensing (QS) is a vital communication mechanism employed by bacteria to coordinate and control specific processes. It allows bacterial cells to collectively regulate essential activities such as biofilm formation, expression of virulence factors, production of secondary metabolites, and adaptation to stressful conditions [48], and also provide population density-dependent pathogenesis, acquisition of nutrients, transfer of genetic material between cells and motility [49]. Furthermore, QS enables the synchronization of gene expression in response to the density of the population of cells. It is believed that QS plays a pivotal role in coordinating the transition to a biofilm lifestyle once the population density surpasses a certain threshold level [50]. QS signaling is triggered by the release of specific extracellular chemical signals within the surrounding environment, called quorum sensing signal molecules (QSSMs). QS is utilized by both Gram-negative and Gram-positive bacteria [51]. Autoinducers (AIs) are small signaling molecules utilized by quorum-sensing systems in bacteria; the most extensively studied autoinducers can be classified into three main categories: acylated homoserine lactones (AHLs), primarily employed by Gram-negative bacteria (also known as autoinducer-1 [AI-1]); peptide signals, utilized by Gram-positive bacteria; and autoinducer-2 (AI-2), employed by both Gram-negative and Gram-positive bacteria [52]. These signaling molecules play crucial roles in the regulation of bacterial pathogenesis and contribute to the coordination of bacterial activities [53].

Anti-quorum sensing (anti-QS) agents have shown promise as alternatives to antibiotics because of their ability to reduce bacterial virulence and enhance pathogen clearance in various animal models. These agents have been demonstrated to have the potential to prevent bacterial infections. However, the clinical application of anti-QS agents is still in its early stages and requires further development and evaluation [53]. Numerous studies have demonstrated the significant impact of bacterial QS signaling on the formation of biofilms. Blocking specific QS signaling pathways is regarded as an effective approach to prevent biofilm formation by many pathogens. This inhibition of QS can enhance the susceptibility of pathogens to antibacterial agents, leading to improved bactericidal effects of antibiotics [54]. The observation that pathogens need to activate QS signaling to initiate biofilm formation and produce virulence factors implies that disrupting this bacterial "communication" using anti-QS agents can render the pathogens more vulnerable to host immune responses and antibiotics [53].

#### **2.4. Efflux pump inhibitors in bacteria**

Efflux pump inhibitors (EPIs), whether used as a single drug or in combination with antibiotics, have the potential to restore the susceptibility of resistant bacterial strains towards antibiotics [55]. Targeting the efflux pump systems, higher intracellular antibiotic concentration can be achieved using synthetic, natural or repurposed (previously approved) drugs [56]. EPIs should ideally possess minimal or no antibacterial activity when administered alone but should exhibit a synergistic effect when combined with antibiotics [55].

The most studied EPI compound is MC-207,110 (also known as Phe-Arg- $\beta$ -naphthylamide or PABN), was identified in 2001 for its ability to inhibit clinically relevant efflux pumps in *Pseudomonas aeruginosa*. Furthermore, it was demonstrated to be effective against other RND pumps found in Gram-negative bacteria [57]. Additionally, various compounds, such as globomycin (an inhibitor of lipoprotein-precursor-processing enzyme), carbonyl cyanide m-chlorophenyl hydrazone (CCCP, an energy uncoupler that inhibits the proton motive force), quinolines, and arylpiperazine derivatives, have been identified for their potential to reverse multidrug resistance in *E. coli* overexpressing efflux pumps. Among these arylpiperazines, the naphthyl derivative 1-(1-naphthylmethyl)piperazine has shown the capacity to increase the susceptibility of MDR *E. coli* to fluoroquinolones, leading to an elevation in the intracellular concentration of levofloxacin [58].

Regarding repurposed drugs, phenothiazines stand out as a significant class of EPIs. They exert their effects by acting as electron donors on the inner side of the bacterial plasma

membrane, leading to hyperpolarization and the inhibition of membrane-linked processes. Promethazine (PMZ) has demonstrated a synergistic effect when used in conjunction with gentamicin, making it effective in treating recurrent pyelonephritis caused by drug resistant *E. coli*. Thioridazine (TZ) has exhibited the ability to eliminate intracellular *Mycobacterium tuberculosis*, making it a candidate for treating multidrug resistant TB (MDR-TB) or extensively drug-resistant TB (XDR-TB) [59]. Chlorpromazine (CPZ) is a well-known EPI compound that inhibits AcrB-mediated efflux by interfering with substrate binding [60]. Sertraline, a selective serotonin reuptake inhibitor (SSRI) showed synergistic activity with three conventional antibiotics (levofloxacin, piperacillin, and meropenem) against *P. aeruginosa* [61]. Paroxetine, another SSRI, could inhibit the MFS-type NorA pump of *S. aureus* [62]. Proton pump inhibitors (e.g. omeprazole) and calcium channel blockers (e.g. verapamil) can also modulate the function of bacterial efflux pumps [56].

Medicinal plants are also great sources of bacterial EPIs, for this reason some examples will be highlighted based on the literature. A noteworthy discovery made by Lewis et al. involves the traditional Native American medicinal plant, *Berberis fremontii*. This plant produces a potent EPI called 5'-methoxyhydnocarpin (5'-MHC), which effectively inhibits the NorA activity in *S. aureus*, thus restoring its sensitivity to quinolones. However, its clinical application is limited due to toxicity concerns [63]. Another plant-derived compound, trans,trans-1,7-diphenylhepta-4,6-dien-3-one, found in *Alpinia katsumadai*, exhibits weak antimycobacterial properties but demonstrates strong efflux pump inhibitory effects in *Mycobacterium smegmatis* [64]. Sarothrin, derived from the leaf and flower extract of *Alkanna orientalis*, displays efflux pump inhibitory activity against NorA in *S. aureus* [65]. Capsaicin, sourced from *Capsicum annuum*, not only inhibits the NorA efflux pump in *S. aureus* but also possesses the ability to reduce the virulence of the bacterium by inhibiting its invasiveness [66]. Finally, *Momordica balsamina*, an African medicinal plant, contains bioactive EPI compounds, such as karavilagenin C, which inhibits efflux systems in MRSA COL<sub>OXA</sub>, and balsaminagenin B, which targets efflux systems in *E. faecalis* ATCC 29212. These findings highlight the potential of plant-derived compounds in addressing antibiotic resistance [67].

### **3. Multidrug resistance in cancer cells**

Statistical data indicates that drug resistance is a major factor in the mortality of cancer patients, accounting for over 90% of cases. Chemotherapy resistance in cancer cells can be attributed to various mechanisms, such as increased drug efflux, genetic factors, influence of

growth factors, enhanced DNA repair, and elevated metabolism of xenobiotics. Each of these mechanisms reduces the effectiveness of administered drugs, making the treatment of tumors more challenging [10].

### **3.1. Genetic factors**

Gene mutations are commonly observed in tumor cells and are believed to be significant contributors to the resistance of chemotherapy treatment. According to research by Duesberg et al. [68], the development of MDR in cancer cells can be best explained by their aneuploidy nature. Aneuploidy refers to the abnormal number of chromosomes in a cell, and it is suggested that frequent losses of chromosomes or rearrangements during mitosis play a role in the loss of drug-sensitive genes or alterations in biochemical pathways [10]. Recent data underscores the crucial contribution of epigenetic changes within cancer cells to their resistance to anti-cancer drugs. These changes involve processes such as the suppression of tumor suppressor genes through excessive DNA methylation or the amplification of oncogene expression through reduced DNA methylation, both of which may play pivotal roles in the progression of cancer. Throughout the development of tumors, the epigenetic landscape undergoes numerous modifications, including the widespread loss of DNA methylation across the genome, heightened methylation in specific regions, global shifts in histone modification patterns, and fluctuations in the expression of microRNAs [69].

### **3.2. Cytokines**

Both experimental and clinical evidence have established noteworthy links between inflammation and the onset and advancement of cancer. It has been confirmed that acute inflammation supports the elimination of tumors, whereas persistent immune responses contribute to tumor expansion and infiltration. Elevated self-produced cytokines, such as interleukin (IL)-1, IL-4, IL-6, and IL-8, have been detected in MDR cancer cells in contrast to drug-responsive tumors [70,71].

### **3.3. Increased DNA repair capacity**

Other potential mechanism by which tumor cells can acquire resistance to various anticancer drugs is through their capacity to repair DNA damage. In the nucleotide excision repair (NER) pathway, DNA repair endonuclease XPF and DNA excision repair protein ERCC1 play important roles in efficiently mending DNA damage caused by crosslinking and

platinum-based agents [72]. There is a notable association between the overexpression of both XPF and ERCC1 proteins and the development of cisplatin resistance in cancer cells. The limited specificity of many anticancer drugs developed thus far is a key factor contributing to their ineffectiveness in chemotherapy treatment. In contrast to other DNA repair pathways, reduced activity in the DNA mismatch repair (MMR) pathway is linked to increased tolerance to damage, resulting in elevated mutagenicity and resistance to chemotherapy [10].

### **3.4. Elevated metabolism of xenobiotics**

Drug-metabolizing enzymes aid the detoxification of both endogenous and exogenous substances (xenobiotics). Isoforms of cytochrome (CYP) play an essential role in the initial phase of drug metabolism and detoxification. In various types of cancer cells, an increased expression of CYP1B1 has been demonstrated that can alter the way chemotherapeutic drugs like mitoxantrone, flutamide, docetaxel, and paclitaxel are biotransformed [73]. Changes in the expression levels of enzymes involved in drug metabolism including glutathione-S-transferases (GSTs), gamma-glutamyl transferases ( $\gamma$ GTs), uridine diphospho-glucuronosyltransferases (UGTs), thiopurine methyltransferases (TPMTs), and dihydropyrimidine dehydrogenases (DPDs) can potentially contribute to their development of MDR [74].

### **3.5. Efflux pumps in cancer cells**

ATP-binding cassette (ABC) transporters form a widely distributed superfamily of integral membrane proteins, serving as the key drivers for the ATP-driven movement of various substances across cellular membranes. The extensively preserved ABC domains within these transporters act as the energy source, relying on nucleotide-dependent mechanisms to facilitate translocation [75]. ABC transporters play a crucial role in maintaining cellular homeostasis by managing the levels of hormones, lipids, ions, xenobiotics, and various small molecules through their transport across cell membranes.

The initial discovery regarding the active transport of daunomycin out of multidrug resistant mouse Ehrlich ascites cells was credited to Keld Dano. Dano's research led to the proposition that this phenomenon was likely mediated by a membrane transporter. Subsequently, in 1976, Victor Ling identified the ABC transporter known as ABCB1, also referred to as P-glycoprotein (P-gp), in drug resistant Chinese hamster ovary cells [76,77]. The identification of the second member within the ABC transporter family, initially referred to as MRP and later renamed as ABCC1, was reported by Cole and his research team in 1992.

ABCC1 was found to play a role in conferring resistance to several drugs, including doxorubicin, etoposide, and vincristine, among others. However, its widespread expression in various tissues has led to the conclusion that it is unlikely to be a viable target for anticancer therapy [78,79]. The discovery of the third ABC transporter, initially known as breast cancer resistance protein (BCRP or MXR), later renamed as ABCG2, was a remarkable achievement, with three distinct research groups independently reporting their findings within a short span of time [80,81].

The human genome contains 51 genes that encode ABC transporters [91]. These transporters are classified into seven subfamilies labeled from A to G [92, 93]. ABCB1, ABCC1, and ABCG2 are believed to primarily serve excretory and protective functions by facilitating the transport of various substances across biological membranes. In locations such as the blood-brain barrier (BBB), blood-testis barrier, and blood-placental barrier, these transporters are expressed in the capillary endothelial cells to effectively block the entry of external molecules [82]. As a result of their protective functions, these transporters can exert an influence on pharmacokinetic factors related to drug absorption, distribution, metabolism, excretion, and toxicity [76]. Within the ABC superfamily, only ABCB1, ABCG2, and ABCC1 are typically recognized as being associated with MDR [83].

The first MDR transporter discovered, ABCB1, has undergone extensive research as a promising candidate for overcoming chemoresistance. Encoded by the *MDR1* gene located on chromosome 7q21, ABCB1 stands out as the most renowned and thoroughly studied drug transporter within the ABC superfamily. It possesses the capability to expel a wide range of chemotherapeutic agents from cancer cells, contributing to the development of MDR [83].

The P-gp (ABCB1) transporter exhibits a broad spectrum of substrates, encompassing variations not just in size and composition but also in various chemical attributes. The principal determinant for a substance to undergo P-gp efflux lies in its interaction with the lipid bilayer membrane. Consequently, an extensive array of compounds, including those that are cationic, hydrophobic, and planar in nature, become eligible as protein substrates, despite their dissimilar structural characteristics [84].

Studies conducted in the past have established that the occurrence of MDR in cancer is usually linked with the upregulation of ABCB1, which is an adenosine triphosphate-binding cassette (ABC) transporter protein encoded by the *ABCB1* gene [85]. Efflux pump proteins responsible for MDR in human cancers are classified within the ABC superfamily of proteins [86]. ABCB1 (also known as MDR1 or P-glycoprotein) is a type of protein that utilizes energy from ATP molecules to pump a broad range of chemotherapy drugs out of cancer cells, leading



to lower levels of the drugs inside the cells and decreased effectiveness of chemotherapy [87]. ABCB1 is the most extensively researched and well-understood MDR transporter that is linked to cancer chemotherapy resistance [89,90]. ABCB1 is naturally present in various organs and physiological barriers, such as the kidney, intestine, and the blood-brain barrier, where it is expressed continuously [90]. ATP-binding domains, also known as nucleotide-binding folds, are characterized by specific motifs such as the Walker A and Walker B, which are present in all ATP-binding proteins. Functional transporters typically comprise two transmembrane domains and two nucleotide-binding folds. The transmembrane domains consist of 6-12 membrane-spanning  $\alpha$ -helices, which play a crucial role in determining the substrate specificity. The two nucleotide-binding folds bind and hydrolyze ATP, providing the necessary energy for the pump mechanism (**Figure 5**) [91].

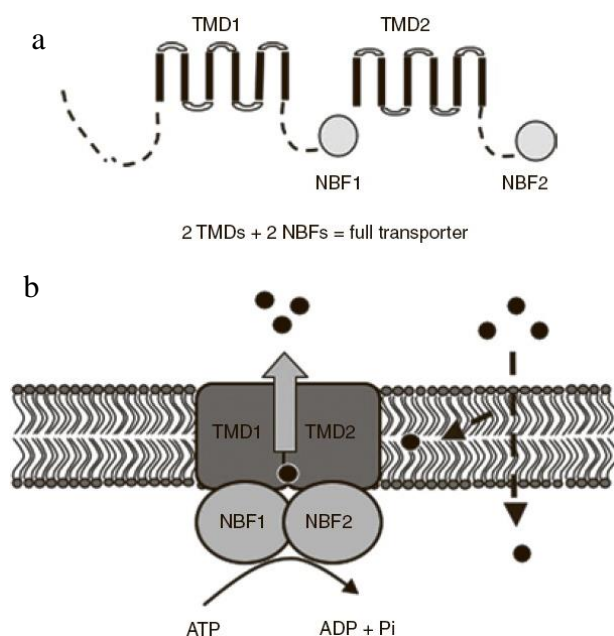


**Figure 5:** The arrangement of ABC transporters.

a) Structural organization of an ABC (full) transporter: A full transporter is composed of two TMDs and two NBF domains; b) ATP-driven transport: ABC transporters utilize the energy derived from ATP hydrolysis to efflux substrates. NBF: nucleotide-binding fold; TMD: transmembrane domain [91].

The emphasis in cancer research regarding ABCB1 has progressively moved towards the creation of a therapeutic strategy aimed at overcoming ABCB1-mediated MDR. One approach involves combining ABCB1 inhibitors with drugs that are substrates of ABCB1. This combination has the potential to restore drug sensitivity in resistant cells, thereby improving the effectiveness of cancer treatment for patients [92].

### 3.6. Efflux pump inhibitors in cancer

*In vitro* studies have demonstrated that inhibitors of ABCB1 can restore the sensitivity of MDR cells to chemotherapy drugs [93]. Most of the clinical trials attempting to inhibit ABCB1 have failed due to various reasons, with a significant one being the requirement of high drug doses to achieve effective inhibition [94]. By inhibiting ABCB1, the intracellular concentration of anticancer drugs can be increased, which in turn could lead to cell cytotoxicity [95]. Verapamil, which is an L-type calcium channel blocker, was the first ABCB1 modulator discovered along with cyclosporin A (first-generation drugs) [96]. However, clinical trials using verapamil as an ABCB1 modulator faced significant challenges due to severe cardiac side effects, resulting in its removal as a viable treatment option [97]. The drugs that belong to this group of inhibitors exhibited low effectiveness in their actions, leading to undesirable levels of systemic toxicity [98]. Chemical alteration of the initial generation agents has been investigated to develop subsequent versions of ABCB1 inhibitors; these are called second-generation drugs, such as dexverapamil and valspoldar, however, these demonstrated high toxicity and valspoldar affected pharmacokinetics of cytotoxic drugs (**Figure 6**) [101,102]; [101]. Despite the attempts made, no feasible inhibitor suitable for clinical use has been identified yet [98]. Third-generation inhibitors, including elacridar, zosuquidar, laniquidar, OC144-093, and tariquidar, are currently undergoing evaluation in clinical trials, they possess safer toxicity profile [104,105]. Developing efficient inhibitors for efflux pumps is a complex task due to the inability of modulators/inhibitors to differentiate between the "physiological" ABCB1 expressed in normal tissues and ABCB1 expressed in cancerous tissues. Inhibiting these proteins can lead to undesired side effects in non-tumor sites of the body [95]. The exploration of a "fourth generation of modulators" remains an active area of research. This field encompasses the investigation of various compounds derived from natural sources and their derivatives, as well as surfactants, lipids, and peptidomimetics [104].

## ABCB1 INHIBITOR DEVELOPMENT

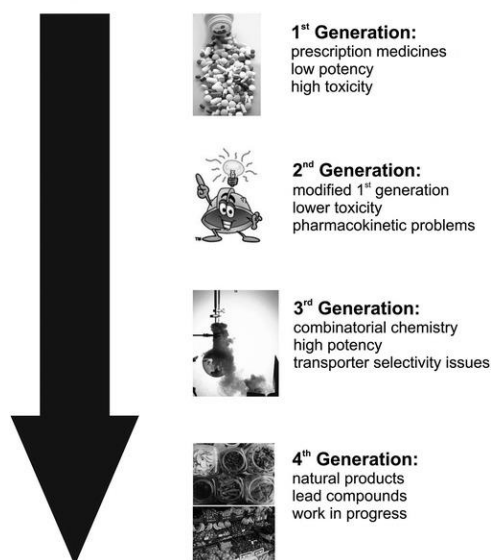


**Figure 6:** Four generations of ABCB1 inhibitors [105].

### 3.7. Apoptosis

Programmed cell death, also called apoptosis, is a crucial and conserved evolutionary process that is essential for the development of organisms and the maintenance of tissue homeostasis [106]. Apoptosis is a controlled and coordinated cellular process that takes place in various physiological and pathological circumstances. In certain conditions, excessive apoptosis can be problematic, as seen in degenerative diseases. Conversely, inadequate apoptosis is a contributing factor in other situations, such as in cancer, where insufficient apoptosis leads to the survival of malignant cells that evade natural cell death mechanisms [107]. Apoptosis is not the only form of tumor related cell death, for instance solid tumors can contain necrotic tissue in the tumor mass. Tumor cells can downregulate or block apoptotic signaling pathways and contribute to oncogenesis. Furthermore, the immune system can exert a selective pressure on cancer cells selecting cells that are resistant to immune-mediated apoptosis [108]. Cancer immunoediting involves three phases known as elimination (also referred to as cancer immunosurveillance), equilibrium, and escape. These phases depict the ongoing interplay between the immune system and cancer cells during the course of cancer development and advancement [109, 110]. Cancer cells possess the capacity to avoid immune surveillance by various mechanisms that includes the transcriptional and translational regulation of anti- or pro-apoptotic genes, as well as influencing the stability of anti- or pro-apoptotic proteins, and post-translational modifications of apoptotic proteins. These mechanisms enable cancer cells to evade apoptosis, and they may utilize one or more strategies to achieve this goal [111].

#### **4. Selenium and selenocompounds as chemotherapeutics**

Selenium (Se) is a vital trace element that plays a crucial role as a micronutrient in various organisms, from bacteria to humans. Its metabolic significance lies in its incorporation as selenocysteine into Se-dependent enzymes. In human cells, there have been 25 selenoproteins identified, each exhibiting diverse biological activities such as redox signaling, antioxidant defense, and immune response modulation. Furthermore, Se is involved in important cellular processes such as cell growth, apoptosis, and the modulation of cell signaling systems and transcription factors [112]. Numerous scientific investigations have consistently revealed a connection between low serum levels of Se and an elevated risk for various diseases, including infections. These epidemiological studies have demonstrated the importance of maintaining adequate Se levels for overall health and disease prevention [113].

The functional characteristics of Se-compounds stem from their specific nature, enabling them to exhibit dual roles as antioxidants and prooxidants. As antioxidants, Se-compounds, particularly selenocysteine, play an important role in maintaining redox homeostasis and protecting phagocytic cells from oxidative stress induced by reactive oxygen species (ROS). Conversely, as prooxidants, Se-compounds can trigger a substantial generation of ROS through the redox cycle, leading to oxidative stress within cancer cells. This dual behavior of Se-compounds highlights their diverse and significant impact on cellular processes [114].

It should be pointed out that not all selenocompounds are uniformly beneficial. The specific chemical form in which they exist is crucial, as certain forms may have toxic effects, while others can exhibit the desired and beneficial biological activities. Hence, the selection of the appropriate form of selenocompounds is vital to ensure their safe and effective application in various contexts [114]. In recent times, there has been a growing interest in selenium, Se-nanoparticles and selenocompounds as promising avenues for discovering potent antibacterials. This attention is especially directed towards combating multidrug resistant bacteria and addressing tumor-related challenges [63,115].

Based on previous studies of our research group, selenoesters containing ketone functional groups in the alkyl moiety bound to the selenium atom exhibited remarkable antibacterial activity. Moreover, symmetrical compounds were also of interest as they allowed for the incorporation of different functional groups, such as nitriles, which also displayed intriguing antibacterial activities [116,117]. It was confirmed that symmetrical selenoesters can

inhibit bacterial efflux pump activity and biofilm formation, furthermore they can also be effective against fungal biofilm [117,118].

Selenocompounds can induce the generation of reactive oxygen species (ROS) and indirectly they can modulate efflux pumps by ROS formation. In addition, selenoanhydrides and selenoesters can modulate the ABCB1 pump in MDR mouse T-lymphoma cells and MDR human colon adenocarcinoma cells by pro-apoptotic effects [116,119]. These derivatives showed synergism with doxorubicin on ABCB1 overexpressing breast cancer cells [120].

## AIMS OF THE STUDY

Bacterial resistance is a well-known phenomenon where bacteria evolve and develop mechanisms to defend themselves against antibiotics. On the other hand, tumor resistance refers to the ability of cancer cells to withstand chemotherapy, radiation therapy, or other cancer treatments. The development of resistance in bacteria and cancer is a complex process that involves multiple factors. Understanding these processes is crucial for developing new and effective treatments. In the present study we aim to address some important resistance mechanisms in both systems and provide an alternative to overcome MDR.

### The main goals of the study:

#### **1. Antibacterial and MDR reversing activity of fifteen selenoesters on Gram-negative and Gram-positive bacterial strains**

- 1.1.** Determination of MICs of compounds using microdilution method on the following bacterial strains: *Staphylococcus aureus* ATCC 25923, methicillin and ofloxacin-resistant *S. aureus* MRSA 272123 clinical isolate, methicillin and oxacillin-resistant *S. aureus* MRSA ATCC 4330, biofilm producing *Pseudomonas aeruginosa* CCM 3955/ATCC 27853, multidrug resistant *P. aeruginosa* NEM 986, wild-type *Salmonella enterica* serovar Typhimurium SL1344 (SE01) expressing the AcrAB-TolC pump system and its *acrB* gene inactivated mutant *S. Typhimurium* SL1344 strain (SE02), *acrA* gene inactivated mutant *S. Typhimurium* SL1344 (SE03), and *tolC* gene inactivated mutant *S. Typhimurium* SL1344 strain (SE39).
- 1.2.** Determination of the efflux pump inhibiting activity of Se-compounds using real-time ethidium bromide accumulation assay in *S. aureus* ATCC 25923, *S. aureus* MRSA ATCC 43300, *S. Typhimurium* SE01, SE02, SE03, and SE39 strains.
- 1.3.** Inhibition of quorum sensing on *Vibrio campbellii* (ATCC BAA-1118<sup>TM</sup> and ATCC BAA-1119<sup>TM</sup>) strains.
- 1.4.** Anti-biofilm activity of Se-compounds on *S. aureus* ATCC 25923 and *P. aeruginosa* CCM 3955 (ATCC 27853) using resazurin assay.

#### **2. Antitumor and MDR reversing activity of fifteen selenoesters in cancer cell lines**

- 2.1.** Determination of the cytotoxic effect of selenoesters using MTT and resazurin assays on different cancer cell lines and normal cells.

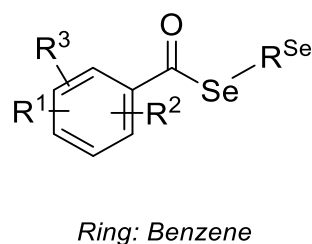
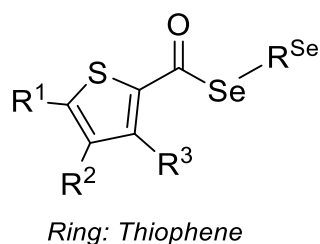
- 2.2.** Combined activity of selenoesters in the presence of doxorubicin using checkerboard assay and Chou-Talalay method on ABCB1 expressing Colo 320 colon adenocarcinoma cell line.
- 2.3.** Inhibition of the ABCB1 efflux pump by rhodamine 123 accumulation assay and flow cytometry.
- 2.4.** Inhibition of Pgp ATPase in the presence of selenoesters using Pgp-Glo™ Assay System (Promega)
- 2.5.** Apoptosis induction in the presence of selenoesters by Annexin V-FITC Apoptosis Detection Kit on Colo 320 cell line by flow cytometry.

## MATERIALS AND METHODS

### 1. Compounds

Fifteen selenocompounds were developed, encompassing eight selenoesters with ketone groups (referred to as **K1–K8** or oxoselenoesters) and seven selenoesters containing cyano groups (designated as **N1–N7** or cyanoselenoesters). These compounds were designed, synthesized, and assessed as innovative agents for combating cancer. They are derived from previously established active selenoesters and were created through a streamlined three-step one-pot synthetic process. The compounds were made within the framework of the EP17382693 (**Table 1**) (The name of the compounds and the synthetic procedure are described in **Appendices 1** and **2**). [121].

Before each biological test, a stock solution of selenoesters (10 mM) was prepared in dimethyl sulfoxide (DMSO).



Cpds.	R <sup>Se</sup>	R <sup>1</sup>	R <sup>2</sup>	R <sup>3</sup>	Ring	Cpds.	R <sup>Se</sup>	R <sup>1</sup>	R <sup>2</sup>	R <sup>3</sup>	Ring
<b>K1</b>	-CH <sub>2</sub> COCH <sub>3</sub>	-H	-H	-H	Thiophene	<b>N1</b>	-CH <sub>2</sub> CN	-H	-H	-H	Thiophene
<b>K2</b>	-CH <sub>2</sub> COCH <sub>3</sub>	2-F	-H	-H	Benzene	<b>N2</b>	-CH <sub>2</sub> CN	3-F	-H	-H	Benzene
<b>K3</b>	-CH <sub>2</sub> COCH <sub>3</sub>	4-Br	-H	-H	Benzene	<b>N3</b>	-CH <sub>2</sub> CN	4-Br	-H	-H	Benzene
<b>K4</b>	-CH <sub>2</sub> COCH <sub>3</sub>	2-CF <sub>3</sub>	-H	-H	Benzene	<b>N4</b>	-CH <sub>2</sub> CN	2-CF <sub>3</sub>	-H	-H	Benzene
<b>K5</b>	-CH <sub>2</sub> COCH <sub>3</sub>	3-CF <sub>3</sub>	-H	-H	Benzene	<b>N5</b>	-CH <sub>2</sub> CN	3-CF <sub>3</sub>	-H	-H	Benzene
<b>K6</b>	-CH <sub>2</sub> COCH <sub>3</sub>	3-Cl	4-F	-H	Benzene	<b>N6</b>	-CH <sub>2</sub> CN	3-Cl	4-F	-H	Benzene
<b>K7</b>	-CH <sub>2</sub> COCH <sub>3</sub>	4-C(CH <sub>3</sub> ) <sub>3</sub>	-H	-H	Benzene	<b>N7</b>	-CH <sub>2</sub> CN	3-CF <sub>3</sub>	5-CF <sub>3</sub>	-H	Benzene
<b>K8</b>	-CH <sub>2</sub> COCH <sub>3</sub>	2-F	4-F	5-F	Benzene						

**Table 1.** Ketone- and cyano-selenoesters investigated in the study (Cpds.: compounds).



## 2. Reagents and media

Phosphate-buffered saline (PBS; pH 7.4), Mueller Hinton (MH) broth (Millipore/Merck KGaA, Darmstadt, Germany), tryptic soy broth (TSB) (Scharlau; Barcelona, Spain). Tryptic soy agar (TSA) (Biolab; Budapest, Hungary). Dimethyl sulfoxide (DMSO), Luria-Bertani broth (LBB), Luria-Bertani agar (LBA), reserpine (RES), CCCP (carbonyl cyanide 3-chlorophenylhydrazone), rhodamine 123 (R123), sodium dodecyl sulfate (SDS), 3-(4,5-dimethylthiazol-2-yl)-2,5-diphenyltetrazolium bromide (MTT), tariquidar, Eagle's Minimal Essential Medium (EMEM) (at concentrations of 100 U/l and 10 mg/l) (containing 4.5 g/l glucose; supplemented with a non-essential amino acid (NEAA) mixture, 2 mM L-glutamine, 1 mM Na-pyruvate, nystatin and a penicillin-streptomycin mixture were purchased from Sigma-Aldrich; St Louis, MO, USA; a selection of vitamins and 10% heat-inactivated foetal bovine serum (FBS) (Biosera; Cholet, France). RPMI 1640 medium at concentrations of 100 U/l and 10 mg/l (supplemented with 10% heat-inactivated-FBS, 2 mM L-glutamine, 1 mM Na-pyruvate, nystatin and a penicillin-streptomycin mixture were purchased from Sigma-Aldrich; St Louis, MO, USA, and 10 mM HEPES (Biosera; Cholet, France). Pgp-Glo™ Assay Systems (Promega; Madison, Wisconsin, USA); Annexin V-FITC Apoptosis Detection Kit (Calbiochem, EMD Biosciences. Inc. La Jolla, CA). Doxorubicin hydrochloride (Teva Pharmaceuticals; Tel-Aviv, Israel).

Autoinducer Bioassay (AB-A) medium, resazurin sodium salt, brain heart infusion (BHI), 100 × antibiotic antimycotic solution, doxorubicin hydrochloride (sold under the trade name Adriamycin, Dulbecco's Modified Eagle's medium—high glucose (DMEM), paclitaxel and trypsin- ethylenediaminetetraacetic acid solution (EDTA) were purchased from Sigma-Aldrich; St Louis, MO, USA.

## 3. Bacterial strains

Gram-positive strains: *Staphylococcus aureus* American Type Culture Collection (ATCC) 25923 strain was used as methicillin-susceptible reference and biofilm producing strain; the methicillin and ofloxacin resistant clinical isolate *S. aureus* MRSA 272123 (kindly provided by Prof. dr. Leonard Amaral, Instituto de Higiene e Medicina Tropical, Universidade Nova de Lisboa, Lisbon, Portugal) and the methicillin and oxacillin-resistant *S. aureus* MRSA ATCC 43300 strains were investigated in the study.

Gram-negative strains: biofilm producing *Pseudomonas aeruginosa* CCM 3955/ATCC 27853, multidrug resistant *P. aeruginosa* NEM 986, wild-type *Salmonella enterica* serovar

Typhimurium SL1344 (SE01) expressing the AcrAB-TolC pump system and its *acrB* gene inactivated mutant *S. Typhimurium* SL1344 strain (SE02), *acrA* gene inactivated mutant *S. Typhimurium* SL1344 (SE03), and *tolC* gene inactivated mutant *S. Typhimurium* SL1344 (SE39) strains were used in the study [117]. *Salmonella* strains were kindly provided by Dr. Jessica M.A. Blair (Institute of Microbiology and Infection, College of Medical and Dental Sciences, University of Birmingham, Birmingham B15 2TT, UK). *P. aeruginosa* CCM 3955 and NEM 986 were obtained from the Czech Collection of Microorganisms (CCM, Masaryk University, Czech Republic) and the Collection of Laboratory of Medical Microbiology (NEM, Czech Laboratory, Inc.). In case of QS tests, the Gram-negative *Vibrio campbellii* ATCC BAA-1118 and ATCC BAA-1119 strains were applied (ATCC).

#### 4. Cell lines and their maintenance

The effect of selenoesters was investigated on several cell lines: the doxorubicin sensitive human colonic adenocarcinoma cell line (Colo 205; ATCC-CCL-222) and the multidrug resistant human colonic adenocarcinoma cell line (Colo 320; ATCC-CCL-220.1) expressing P-gp (MDR1 or ABCB1) and LRP (LGC Promochem, Teddington, UK); human embryonal lung fibroblast cell line (MRC-5; ATCC CCL-171; Sigma-Aldrich, Merck KGaA, Darmstadt, Germany); hepatocellular carcinoma (HepG2; ATCC<sup>®</sup>, CCL-23<sup>™</sup>, Manassas, VA, USA), cervical adenocarcinoma (HeLa; ATCC<sup>®</sup>, CCL-2<sup>™</sup>), skin melanoma (B16; ATCC<sup>®</sup>, CCL-6322<sup>™</sup>), human dermal fibroblast (HDF; Sigma-Aldrich), human keratinocyte (HaCaT, Thermo Fisher Scientific, Waltham, MA, USA) cell lines.

Their culture conditions are the following ones: Colo 205 (ATCC-CCL-222) and Colo 320/MDR-LRP expressing P-gp (MDR1)-LRP (ATCC-CCL-220.1 human colon adenocarcinoma cell lines were cultured in RPMI 1640 as previously described [119]. The cell lines were incubated at 37 °C in a 5% CO<sub>2</sub>, 95% air atmosphere. MRC-5 human embryonal lung fibroblast cells were cultured in Eagle's Minimal Essential Medium (EMEM) as previously described [120]. The cell lines were incubated at 37 °C in a 5% CO<sub>2</sub>, 95% air atmosphere.

HepG2, HeLa, B16 and HaCaT cell lines were cultivated in EMEM medium supplemented with 10% FBS, 2 mM L-glutamine and 1×antibiotic antimycotic solution. All the cells were cultivated in a CO<sub>2</sub> incubator (5% CO<sub>2</sub>, 37 °C, Thermo Fisher Scientific) [122].

## 5. Determination of minimum inhibitory concentrations (MIC) by microdilution method

The study involved determining the minimum inhibitory concentrations (MICs) of ketone- and cyano-selenoesters, following the Clinical and Laboratory Standard Institute (CLSI) guidelines [123]. The results were visually inspected to determine the MIC values of the compounds. DMSO was used as a negative control to rule out any potential antibacterial effects of the solvent.

## 6. Real-time ethidium bromide (EB) accumulation assay

To assess the efflux pump inhibiting activity of Se-compounds on *S. aureus* ATCC 25923, *S. aureus* MRSA ATCC 43300, *S. Typhimurium* SE01, SE02, SE03, and SE39 strains, real-time EB assay was performed that measures the intracellular accumulation of the efflux pump substrate EB. The intracellular accumulation of the fluorochrome EB was recorded by CLARIOstar Plus plate reader (BMG Labtech, UK). Reserpine (RES) was applied at 25  $\mu\text{M}$  and CCCP at 50  $\mu\text{M}$  as a positive control, and DMSO at 1 v/v% as a negative control. The bacterial cultures were incubated at 37°C in a shaking incubator until they reached an optical density (OD) of 0.6 at 600 nm, after they were washed with phosphate buffered saline (PBS; pH 7.4), centrifuged, and resuspended in PBS. The Se-compounds were added at  $\frac{1}{2}$  MIC concentration to PBS containing a non-toxic concentration of EB (2  $\mu\text{g}/\text{mL}$ ). The solutions were then pipetted into a 96-well black microtiter plate (Greiner Bio-One Hungary Kft, Hungary), and 50  $\mu\text{L}$  of bacterial suspension (OD<sub>600</sub> 0.6) were added to each well. The plates were placed into the CLARIOstar plate reader, and the fluorescence was monitored every minute for one hour at excitation and emission wavelengths of 530 nm and 600 nm. Based on the real-time data, the relative fluorescence index (RFI) of the last time point (minute 60) of the EB accumulation assay, was calculated according to the following equation:

$$\mathbf{RFI} = (\mathbf{RF}_{\text{treated}} - \mathbf{RF}_{\text{untreated}})/\mathbf{RF}_{\text{untreated}}$$

where  $\text{RF}_{\text{treated}}$  is the relative fluorescence (RF) at the last time point of EB retention curve in the presence of an inhibitor, and  $\text{RF}_{\text{untreated}}$  is the RF at the last time point of the EB retention curve of the untreated control having the solvent control (DMSO).

## 7. Assay for quorum sensing (QS) inhibition

Anti-quorum sensing (QS) activity of the compounds was investigated in two commercial strains of *V. campbellii* (ATCC BAA-1118<sup>TM</sup> and ATCC BAA-1119<sup>TM</sup>). The wild-type bacteria use both autoinducer-1 (AI-1) and autoinducer-2 (AI-2) types of molecules for its communication, strain 1118 is deficient in communication on the basis of AI-2, while strain 1119 is deficient in AI-1 type communication. The luminescence generation effect of the compounds was evaluated as previously described [124]. An overnight culture of the strains was diluted to  $5 \times 10^5$  CFU/mL in Autoinducer Bioassay medium (NaCl, 17.5 g/L;  $\text{MgSO}_4 \times 7 \text{H}_2\text{O}$ , 12.3 g/L; casamino acids, 2 g/L) [125] split into 96-well plates, and treated with the compounds at 2-fold serial dilutions. The plates were then incubated for 8 h at 30°C with continuous shaking at 100 rpm. Luminescence was recorded for 16 h using a microplate reader set up at 30°C, with an integration time of 10,000 ms and shaking for 60 s prior to measurement. The effective concentration 50 (EC<sub>50</sub>) of the compounds was determined based on the sum of luminescence, and the viability of the culture was checked by resazurin assay to calculate the IC<sub>50</sub> of the compounds. The EC<sub>50</sub> and IC<sub>50</sub> were calculated using GraphPad Prism software version 5.00 for Windows with nonlinear regression curve fit. The compounds were compared based on their EC<sub>50</sub> (the concentration that halves the cell communication) and IC<sub>50</sub> (viability; represents the minimal concentration of a drug that is required for 50% inhibition *in vitro*).

## 8. Anti-biofilm activity

### 8.1. Inhibition of biofilm formation

The study investigated the impact of selenocompounds on biofilm formation in *S. aureus* ATCC 25923 and *P. aeruginosa* CCM 3955 (ATCC 27853) using 96-well microplates. The experiment began by diluting overnight bacterial in Brain Heart Infusion (BHI) broth to obtain an optical density of 0.5 McFarland, followed by distributing the suspension into 96-well plates in 100  $\mu\text{L}$  aliquots per well. Next, Se-compounds were added to the cells in a concentration range of 100  $\mu\text{M}$  to 0.19  $\mu\text{M}$ . The plates were then incubated for 24 hours at 37°C. After incubation, the viability of adherent cells was assessed immediately using resazurin assay. The wells were washed three times with phosphate-buffered saline (PBS), and 100  $\mu\text{L}$  of resazurin in PBS (0.03 mg/L) was added to each well. Fluorescence was measured (560/590 nm, ex./em.) using the SpectraMax i3x Multi-Mode Detection Platform (Molecular Devices, USA), and the assays were carried out in four parallels. The relative viability was evaluated as a percentage according to the formula:

$$\text{RA [\%]}=100\frac{\text{sample fluorescence} - \text{average fluorescence of NC}}{\text{average fluorescence of PC} - \text{average fluorescence of NC}}$$

where RA is relative activity in percentage, PC is positive control (untreated biofilm), and NC is negative control (resazurin incubated without bacterial cells). The IC<sub>50</sub> values were calculated using online tool freely provided by AAT Bioquest – IC<sub>50</sub> Calculator (<https://www.aatbio.com/tools/ic50-calculator>).

## 8.2. Disruption of mature biofilm

The study aimed to examine the efficacy of Se-compounds in damaging mature biofilms formed by two bacterial strains: *S. aureus* ATCC 25923 and *P. aeruginosa* CCM 3955/ATCC 27853. To determine the biofilm disrupting activity resazurin assay was used in 96-well plates. Firstly, overnight cultures of the bacteria were diluted in BHI broth to an optical density of 0.5 McFarland, and then 100 µL aliquots of the bacterial suspension were added to the wells. After 24 hours of incubation at 37 °C, the old medium was discarded, and new BHI broth containing Se-compounds was added to the wells. The plates were then incubated for another 24 hours. Subsequently, the medium was removed, and the wells were washed twice with PBS (pH 7.4). Finally, 100 µL of resazurin in PBS (0.03 mg/L) was added to each well, and fluorescence was measured using the SpectraMax i3x Multi-Mode Detection Platform (Molecular Devices, USA) with excitation and emission wavelengths of 560/590 nm, respectively. The assay was performed in four replicates, and the IC<sub>50</sub> values were calculated using the freely available IC<sub>50</sub> Calculator tool provided by AAT Bioquest (<https://www.aatbio.com/tools/ic50-calculator>).

## 9. Cytotoxicity assays

### 9.1. MTT assay

The experiment involved evaluating how different concentrations of certain compounds affect cell growth. To do this, human colonic adenocarcinoma cells in RPMI medium in 100 µL were added to each well of a 96-well microtiter plate, except for the control wells. The adherent human embryonic lung fibroblast cells in EMEM medium in 100 µL were also seeded overnight in the plate before the assay. Two-fold serial dilutions of the compounds were prepared in a separate plate in 100 µL and then transferred to the corresponding cell line plates. The culture plates were then incubated at 37 °C for 24 hours. Next, 20 µL MTT solution (from a 5 mg/mL stock solution) was added to each well, followed by further incubation at 37 °C for 4 hours. Then, 100 µL SDS solution (10% SDS in 0.01 M HCl) was added to each well, and

the plates were further incubated overnight. The optical density (OD) at 540 nm (ref. 630 nm) was measured using an ELISA reader to determine cell growth inhibition, expressed as IC<sub>50</sub> values. The IC<sub>50</sub> values and standard deviation (SD) of triplicate experiments were calculated using GraphPad Prism software version 5.00 for Windows with a non-linear regression curve fit. The solvent (DMSO) used did not affect cell growth at the tested concentrations. Doxorubicin was used as a positive control [126].

## 9.2. Resazurin assay

In case of HeLa, HepG2, B16, HDF and HaCaT cell line to determine the cell number, the Cellometer AUTO A4 from Nexcelom Bioscience (Lawrence, Massachusetts, USA) was used. For the experiment, cells were seeded into 96-well plates at a concentration of  $1 \times 10^5$  cells/mL to a final volume of 100  $\mu$ L. After 24 hours, the plates were washed with PBS three times, and 199  $\mu$ L of fresh medium was added using a MultiFlo Multi-Mode Dispenser from BioTek (Agilent Technologies, Santa Clara, USA), except for control cells, which contained 100  $\mu$ L. A binary sample dilution was used to prepare the compound concentration range (0.125-4 mM) in new 96-well plates, and a Biomek FXP automatic pipetting station (Beckman Coulter, Prague, Czech Republic) with a 96-channel head was used to add 1  $\mu$ L of sample. The final concentration range of samples was 0.625-20  $\mu$ M. After 72 hours of incubation, the plates were washed once with PBS and a resazurin solution (0.03 mg/mL in 1x PBS) was added for 1 hour. The fluorescence signal was then measured (ex./em. 560/590 nm) using a SpectraMax i3x Multi-Mode Microplate reader with MiniMax Imaging Cytometer from Molecular Devices<sup>®</sup> (San Jose, USA).

The selectivity indices (SI) were calculated by dividing the IC<sub>50</sub> value in non-tumor cells by the IC<sub>50</sub> in cancer cell lines. If the selectivity index (SI) value was SI > 6, the compound's activity towards cancer cells was considered strongly selective. If the SI value was 3 < SI < 6, it was considered moderately selective. For an SI value 1 < SI < 3, the compound's activity was considered slightly selective. A value below 1 indicated that the compound was non-selective towards cancer cells.

## 10. Checkerboard combination assay

Checkerboard microplate method was utilized to investigate the potential synergistic effects of the selenocompounds and doxorubicin on resistant Colo 320 colon adenocarcinoma cells expressing the ABCB1 transporter based on the Chou-Talalay method [127]. The

CalcuSyn software was used to plot 4 or 5 data points for each ratio, and the results were expressed as combination index (CI) values at 50% growth inhibition (ED<sub>50</sub>). The median-effect equation was used to calculate the CI values, where a CI < 1 indicated synergism, CI = 1 indicated an additive effect or no interaction, and CI > 1 indicated antagonism (**Table 2**).

To carry out the experiment, doxorubicin dilutions were prepared in a 100 µL volume horizontally, while the dilutions of Se-compound were prepared vertically in a microtiter plate with a volume of 50 µL. The starting concentration of the doxorubicin was 8.62 µM, the concentration of the Se-compounds was calculated based on their IC<sub>50</sub>. The cells were suspended in culture medium and distributed in 50 µL aliquots into each well containing 6.000 cells. The plates were incubated at 37 °C in a CO<sub>2</sub> incubator for 72 hours, and the cell growth rate was determined using MTT staining. After the incubation period, 20 µL of MTT solution was added to each well, followed by incubation at 37 °C for 4 hours. Next, 100 µL of SDS was added to each well, and the plates were further incubated at 37 °C overnight. Finally, the optical density (OD) was measured at 540/630 nm using a Multiscan EX ELISA reader.

Combination index (CI)	Type of interaction	Combination index (CI)	Type of interaction
0-0.1	very strong synergism	0.9-1.1	additive effect
0.1-0.3	strong synergism	1.1-1.2	slight antagonism
0.3-0.7	synergism	1.2-1.45	moderate antagonism
		1.45-3.3	antagonism
0.7-0.85	moderate synergism	3.3.-10	strong antagonism
0.85-0.9	slight synergism	>10	very strong

**Table 2.** Combination indices and associated interaction types [128].

## 11. ABCB1 inhibition by selenoesters

The study aimed to assess the ability of the tested compounds to inhibit the ABCB1 multidrug efflux pump (also known as P-glycoprotein) in Colo 320 colonic adenocarcinoma cells using flow cytometry. The retention of rhodamine 123 by ABCB1 was measured as an indicator of pump inhibition. To conduct the experiment, colonic adenocarcinoma cells were adjusted to  $2 \times 10^6$  cells/mL and resuspended in serum-free RPMI 1640 medium. The cells were distributed into Eppendorf centrifuge tubes, and the tested compounds were added at different concentrations (0.2 and 2 µM) from stock solutions. After incubation for 10 minutes at room temperature, 10 µL of the fluorochrome rhodamine 123 was added to the samples (with a final

concentration of 5.2  $\mu\text{M}$  from a 260  $\mu\text{M}$  stock solution). The cells were then incubated for 20 minutes at 37  $^{\circ}\text{C}$ , washed twice, and resuspended in PBS for analysis. The fluorescence of the gated cell population was measured using a CyFlow<sup>®</sup> flow cytometer (Partec, Münster, Germany), and the results were obtained from a representative flow cytometry experiment in which at least 20,000 individual cells of the overall population were evaluated for the rhodamine 123 retained inside the cells. The fluorescence activity ratio (FAR) was calculated to determine the percentage of mean fluorescence intensity for treated MDR cells compared to untreated cells. The FAR was calculated using the following equation, which relates the measured fluorescence values:

$$\text{FAR} = \frac{\text{Colo320}_{\text{treated}} / \text{Colo320}_{\text{control}}}{\text{Colo205}_{\text{treated}} / \text{Colo205}_{\text{control}}}$$

Tariquidar was used as a positive control (0.2  $\mu\text{M}$  final concentration), and DMSO was used as the solvent control (at 2 v/v%).

## 12. P-gp ATPase activity assay

The P-glycoprotein ATPase activity was assessed using the Pgp-Glo<sup>™</sup> Assay System from Promega, according to the manufacturer's instructions. In brief, 20  $\mu\text{L}$  of recombinant human P-gp membranes (1.25 mg/mL) were mixed with 20  $\mu\text{L}$  of the Pgp-Glo<sup>™</sup> assay buffer and incubated for 5 minutes at 37 $^{\circ}\text{C}$ . Compounds were tested at a concentration of 25  $\mu\text{M}$ , and sodium orthovanadate ( $\text{Na}_3\text{VO}_4$ ) at 0.25 mM was used as an inhibitor control while verapamil was employed as a substrate control (0.5 mM). A 2% DMSO solution was used as a solvent control. The reaction was started by adding 10  $\mu\text{L}$  of 25 mM MgATP and incubated at 37 $^{\circ}\text{C}$  for 40 minutes. The reaction was stopped by adding 50  $\mu\text{L}$  of ATP Detection Reagent and incubating the samples and controls at room temperature for 20 minutes. The emitted luciferase-generated luminescent signal was measured at 580 nm using a CLARIOstar Plus plate reader from BMG Labtech (Ortenberg, Germany). The relative ATPase activity was determined according to the manufacturer's instruction.

The impact of the compounds under investigation was assessed following the guidelines provided by the manufacturer (**Table 3**).



$\Delta\text{RLU}_{\text{TC}} > \Delta\text{RLU}_{\text{basal}}$	the tested compound is <b>stimulator</b> of Pgp ATPase activity
$\Delta\text{RLU}_{\text{TC}} = \Delta\text{RLU}_{\text{basal}}$	the tested compound has <b>no effect</b> on Pgp ATPase activity
$\Delta\text{RLU}_{\text{TC}} < \Delta\text{RLU}_{\text{basal}}$	the tested compound is an <b>inhibitor</b> of Pgp ATPase activity

**Table 3.** Evaluation of Pgp ATPase activity [129].  $\Delta\text{RLU}_{\text{basal}}$  reflects basal Pgp ATPase activity, and  $\Delta\text{RLU}_{\text{TC}}$  reflects Pgp ATPase activity in the presence of a test compound.

### 13. Apoptosis induction

Annexin V-FITC Apoptosis Detection Kit (Cat. No. PF 032) from Calbiochem (EMD Biosciences, Inc. La Jolla, CA) was used to perform the assay according to the manufacturer's instructions. The Colo 320 cell suspension was adjusted to approximately  $1 \times 10^6$  cells/mL and distributed into 1 mL aliquots ( $1 \times 10^6$  cells) in a 24-well microplate. The cells were incubated overnight at 37 °C with 5% CO<sub>2</sub>. The next day, the medium was removed, and fresh medium was added to the cells. Se-compounds were added to the cells, and the cells were incubated for 3 h at 37 °C. The concentration of 2  $\mu\text{M}$  was selected for apoptosis induction based on previous cytotoxicity results (IC<sub>50</sub> values). Additionally, 12*H*-benzo( $\alpha$ )phenothiazine (M627) was used as a positive control at a final concentration of 20  $\mu\text{M}$  [120]. After the 3 h induction period, the culture medium was removed, and fresh medium was added to the cells. The 24-well plates were incubated overnight at 37 °C with 5% CO<sub>2</sub>. The supernatant was collected in a microfuge tube after the incubation, and 200  $\mu\text{L}$  of 0.25% trypsin (Trypsin-Versene) was added to the wells until the cells detached from the surfaces of the wells. The cells were centrifuged at 2000 $\times$  g for 2 min at room temperature, and the supernatant was removed. The cells were resuspended in fresh serum-free medium, and the apoptosis assay was carried out according to the rapid protocol of the kit using Annexin V-FITC and propidium iodide staining. The fluorescence was immediately analysed using a CyFlow<sup>®</sup> flow cytometer (Partec, Münster, Germany), and the results were obtained from a representative flow cytometry experiment evaluating at least 20,000 individual cells of the overall population in a sample. FlowJo<sup>™</sup> software (BD Biosciences, San Jose, NJ, USA) was used to analyse the data.

## RESULTS

It has been confirmed by previous studies that selenoesters possess diverse biological activities including antiviral, antibacterial, antifungal, and anticancer effects. Furthermore, selenoesters could decrease the virulence of bacteria by inhibition of QS and biofilm formation. Regarding cancer cells, chemosensitizing effect was observed in the presence of selenoesters. Based on these antecedents, the ketone- and cyano-selenoesters investigated in this study were tested in both bacterial and tumor models *in vitro* [114].

### 1. Antibacterial activity

#### 1.1. Determination of minimum inhibitory concentrations (MICs) by microdilution method

The results suggest that the ketone-selenoesters have a robust antibacterial effect against the Gram-positive bacteria studied. Notably, the derivatives **K1**, **K7**, and **K8** exhibited the highest potency, being active against all three *S. aureus* strains examined, with MIC values ranging from 0.39 to 1.56  $\mu\text{M}$  (see **Table 4**).

Cpds.	MIC Determination [ $\mu\text{M}$ ]									
	<i>S. aureus</i> ATCC 25923	<i>S. aureus</i> MRSA ATCC 43300	<i>S. aureus</i> MRSA 272123	<i>S. Typhimurium</i> SE01 wild-type	<i>S. Typhimurium</i> SE02 <i>ΔacrB</i>	<i>S. Typhimurium</i> SE03 <i>ΔacrA</i>	<i>S. Typhimurium</i> SE39 <i>ΔtolC</i>	<i>P. aeruginosa</i> CCM 3955	<i>P. aeruginosa</i> NEM 986	
<b>K1</b>	1.56	1.56	0.78	50	100	100	100	100	50	
<b>K2</b>	1.56	3.125	0.78	> 100	> 100	> 100	> 100	100	50	
<b>K3</b>	1.56	3.125	0.78	50	50	50	50	>100	>100	
<b>K4</b>	3.125	3.125	1.56	> 100	> 100	> 100	> 100	100	50	
<b>K5</b>	1.56	3.125	0.78	100	50	50	> 100	100	50	
<b>K6</b>	1.56	3.125	0.39	100	100	100	100	100	50	
<b>K7</b>	1.56	1.56	0.39	50	> 100	100	> 100	100	100	
<b>K8</b>	1.56	1.56	0.78	50	> 100	100	100	100	50	
<b>N1</b>	12.5	100	25	50	50	100	100	>100	>100	
<b>N2</b>	12.5	100	50	50	100	100	100	>100	>100	
<b>N3</b>	12.5	50	25	50	50	50	50	>100	>100	
<b>N4</b>	12.5	100	50	100	100	100	100	>100	>100	
<b>N5</b>	12.5	50	50	100	100	100	100	>100	>100	
<b>N6</b>	12.5	50	25	100	50	100	100	>100	>100	
<b>N7</b>	12.5	50	25	50	50	50	100	>100	>100	

**Table 4.** Antibacterial activity of selenocompounds on Gram-positive and Gram-negative bacteria.

Cpds: compounds; *S. aureus*: *Staphylococcus aureus*; *S. Typhimurium*: *Salmonella Typhimurium*; *P. aeruginosa*: *Pseudomonas aeruginosa*.

In contrast to the cyano-selenoesters, the ketone-selenoesters showed greater activity against Gram-positive strains, such as *S. aureus* ATCC 25923, *S. aureus* MRSA 272123, and MRSA 43300. This is presumably because Gram-negative bacteria possess a more intricate cell wall structure compared to Gram-positive bacteria. This includes an outer membrane that serves as an additional barrier to the penetration of drugs. The outer membrane of Gram-negative bacteria contains lipopolysaccharides (LPS), which can contribute to the bacteria's resistance to antibiotics. In contrast, Gram-positive bacteria have a simpler cell wall structure, making them generally more susceptible to certain types of antibiotics [130].

Cyano-selenoesters were found to be less effective against MRSA strains, with MIC values ranging from 25 to 100  $\mu\text{M}$ , compared to the reference *S. aureus* ATCC 25923 strain, which had an MIC of 12.5  $\mu\text{M}$ . It is probably due to the variations in membrane lipids between clinical strains of *S. aureus* that are susceptible to antibiotics and those that have developed resistance. These differences in membrane composition may influence the resistance mechanisms associated with cell membrane structure and flexibility [131]. The primary distinguishing factor between MRSA and methicillin-sensitive *S. aureus* (MSSA) cells remains their susceptibility to antibiotics. MRSA cells are resistant to all  $\beta$ -lactam antibiotics and have a propensity to acquire resistance to other antibiotics easily, resulting in the emergence of multidrug resistant strain [132]. Moreover, the overexpression of efflux pumps, which are involved in antibiotic resistance, is frequently observed in MRSA isolates and is more prevalent than in MSSA strains, as reported in various regions worldwide [133]. Among the seven cyano-selenoesters tested, **N3**, **N6**, and **N7** exhibited the highest antibacterial potency.

However, both the ketone-selenoesters and the cyano-selenoesters had marginal antibacterial activity against the tested *P. aeruginosa* strain and only mild activity against the *S. Typhimurium* strains studied (with MIC values ranging from 50 to 100  $\mu\text{M}$ , as shown in **Table 4**). This is probably due to the above-mentioned difference in Gram-negative and Gram-positive bacteria.

## 1.2. Inhibition of bacterial efflux pumps

With the aid of the real-time ethidium bromide accumulation assay it was examined whether the ketone- and cyano-selenoesters could inhibit efflux pumps in Gram-negative and Gram-positive bacterial strains (**Table 5**). The efflux pump inhibiting (EPI) activity was studied

on five strains, including *S. aureus* ATCC MRSA 43300, *S. aureus* ATCC 25923 and *S. Typhimurium* SE01, SE02, SE03, and SE39. Among the Salmonella strains tested, the ketone-selenoester **K7** demonstrated the most potent EPI activity, as it could inhibit the AcrAB-TolC system. In case of the  $\DeltaacrB$  strain lower EB concentration and lower EPI activity was observed than in the wild type. However, regarding the  $\DeltaacrA$  and  $\Delta tolC$  strains higher EB concentration was recorded compared to the wild-type strain with RFI of 1.15 and 1.67, respectively. This compound may have caused membrane destabilization, leading to the observed increase in EB accumulation. It can be supposed that the inhibition of the outer membrane channel component TolC or inhibition of the periplasmic membrane fusion protein AcrA can disturb the function of the AcrAB-TolC system. Additionally, ketone-selenoesters **K4** and **K5** inhibited EB accumulation in the *tolC* inactivated mutant strain (see **Figure 7**). The cyano-selenoesters **N4** and **N7** exhibited the most notable activity on the *tolC* inactivated mutant strain (see **Figure 7**).

Cpds.	Relative fluorescence index (RFI)					
	<i>S. aureus</i> MRSA ATCC 43300	<i>S. aureus</i> ATCC 25923	<i>S.</i> Typhimurium SE01 wild-type	<i>S.</i> Typhimurium SE02 $\DeltaacrB$	<i>S.</i> Typhimurium SE03 $\DeltaacrA$	<i>S. Typhimurium</i> SE39 $\Delta tolC$
<b>K1</b>	-0.02	1.19	0.17	0.20	0.29	0.31
<b>K2</b>	-0.04	1.12	0.18	0.21	0.30	0.42
<b>K3</b>	-0.10	1.17	0.60	0.27	0.24	0.44
<b>K4</b>	-0.09	1.02	0.19	0.35	0.68	0.95
<b>K5</b>	-0.08	1.17	0.41	0.11	0.35	0.91
<b>K6</b>	-0.09	1.19	0.17	0.43	0.52	0.80
<b>K7</b>	-0.02	1.13	1.02	0.30	1.15	1.67
<b>K8</b>	-0.04	1.10	0.08	0.31	0.28	0.70
<b>N1</b>	0.05	1.40	0.04	0.10	0.37	0.84
<b>N2</b>	-0.02	1.31	-0.06	-0.05	0.16	0.19
<b>N3</b>	-0.05	1.49	0.003	0.03	0.38	0.24
<b>N4</b>	0.35	1.78	0.22	0.39	0.36	1.00
<b>N5</b>	-0.03	1.43	0.02	0.02	0.32	0.43
<b>N6</b>	-0.01	1.32	0.03	-0.03	0.45	0.38
<b>N7</b>	-0.06	0.28	0.003	0.14	0.32	1.11
<b>CCCP</b>	-	-	3.37	1.83	3.30	1.61
<b>RES</b>	0.30	5.5	-	-	-	-

**Table 5.** Efflux pump inhibition in the presence of selenoesters on Gram-positive and Gram-negative bacteria.

The inhibitory effects of selenoesters at MIC/2 on efflux pumps in *S. aureus* and *S. Typhimurium* strains have been investigated by assessing their impact on relative fluorescence index (RFI) values. Higher RFI values indicate more effective inhibition of efflux pumps (Cpds: compounds; RES: reserpine (25  $\mu$ M); CCCP: carbonyl cyanide m-chlorophenyl hydrazone 50  $\mu$ M).

Regarding the *S. aureus* ATCC MRSA 43300 and *S. aureus* ATCC 25923 strains, only one derivative, the cyano-selenoester **N4** exhibited potent efflux pump inhibition as shown in Figure 7. Furthermore, the effect of **N4** was more pronounced (with a relative fluorescence intensity, RFI of 0.351) than that observed in the presence of the reference EPI reserpine (RFI: 0.300). Since there were no mutant strains of *S. aureus* in our study, the observed EPI activity is the result of a bulk signal due to the inhibition of several efflux pumps.

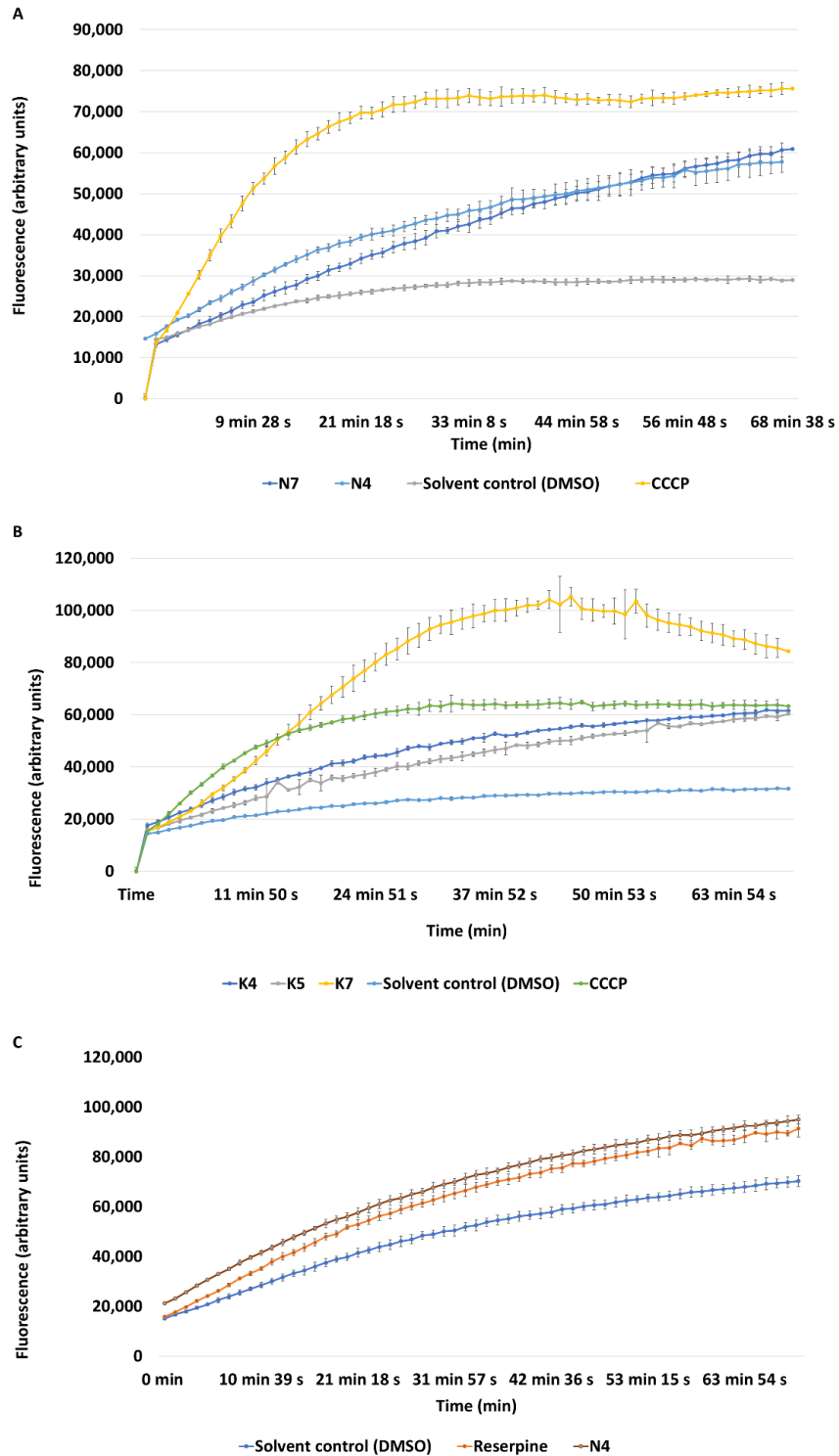


**Figure 7:** Efflux pump inhibition in the presence of the most potent selenoesters.

**A:** Accumulation of ethidium bromide (EB) in the presence of selenoesters **K4**, **K5**, and **K7** at half of the MIC on *S. Typhimurium* SE39  $\Delta tolC$  strain. **B:** Accumulation of EB in the presence of **N4** and **N7** at MIC/2 on *S. Typhimurium* SE39  $\Delta tolC$  strain. **C:** Accumulation of EB in the presence of selenoester **N4** at MIC/2 on *S. aureus* MRSA 43300. DMSO: dimethyl sulfoxide (solvent) (2%); CCCP: carbonyl cyanide 3-chlorophenylhydrazone (50  $\mu$ M) (positive control).

### 1.3. Assay for quorum sensing (QS) inhibition

To differentiate between the concentration that induces toxicity and the concentration that inhibits cell-to-cell communication (quorum sensing), the IC<sub>50</sub> was compared (the concentration that reduces viability by 50%) with the EC<sub>50</sub> (the concentration that halves cell-to-cell communication). This comparison was essential to determine the efficacy of the tested compounds. If the concentration required for toxicity was higher than the concentration needed for quorum sensing inhibition, the compound was deemed as effective.

The ability of selenocompounds to inhibit quorum sensing was tested using two strains of *Vibrio campbellii*. The wild-type of *V. campbellii* uses both autoinducer-1 (AI-1) and autoinducer-2 (AI-2) types of molecules for its communication, strain 1118 is deficient in communication on the basis of AI-2, while strain 1119 is deficient in AI-1 type communication. The impact of different concentrations of a compound on cell-to-cell communication (EC<sub>50</sub>) and cell viability (IC<sub>50</sub>) was examined, and compared to determine the selectivity index (SI) of each compound. The SI was calculated as the ratio of IC<sub>50</sub> and EC<sub>50</sub>, allowing to differentiate between toxic and quorum sensing inhibiting concentrations. Compounds with higher SI values were considered more effective in QS inhibition. **Table 6** shows that all compounds (except **N5**) demonstrated an ability to inhibit bacterial communication.

Cpd.	<i>V. campbellii</i> BAA 1118			<i>V. campbellii</i> BAA 1119		
	IC <sub>50</sub> [μM]	EC <sub>50</sub> [μM]	SI	IC <sub>50</sub> [μM]	EC <sub>50</sub> [μM]	SI
<b>K1</b>	5.76 ± 0.07	0.22 ± 0.01	26.2	2.02 ± 0.15	0.71 ± 0.05	2.8
<b>K2</b>	4.38 ± 0.47	0.25 ± 0.03	17.5	3.23 ± 0.14	0.22 ± 0.02	14.7
<b>K3</b>	1.12 ± 0.02	0.17 ± 0.01	6.6	0.77 ± 0.07	0.23 ± 0.02	3.3
<b>K4</b>	33.18 ± 3.45	4.68 ± 0.32	7.1	6.66 ± 0.13	0.29 ± 0.05	23.0
<b>K5</b>	2.42 ± 0.29	1.35 ± 0.03	1.8	1.32 ± 0.10	0.45 ± 0.01	2.9
<b>K6</b>	3.28 ± 0.19	2.29 ± 0.02	1.4	0.97 ± 0.09	1.20 ± 0.00	0.8
<b>K7</b>	10.54 ± 0.19	1.77 ± 0.19	6.0	4.27 ± 0.23	0.15 ± 0.01	28.5
<b>K8</b>	1.23 ± 0.07	0.11 ± 0.01	11.2	1.39 ± 0.03	0.46 ± 0.03	3.0
<b>N1</b>	2.21 ± 0.19	1.45 ± 0.02	1.5	2.28 ± 0.12	0.26 ± 0.03	8.8
<b>N2</b>	7.36 ± 0.70	0.34 ± 0.04	21.6	2.40 ± 0.12	0.73 ± 0.02	5.1
<b>N3</b>	2.199 ± 0.16	0.34 ± 0.04	6.5	2.35 ± 0.03	< 0.06	37.6
<b>N4</b>	2.52 ± 0.03	1.29 ± 0.04	2.0	6.41 ± 0.42	0.73 ± 0.02	8.8
<b>N5</b>	12.51 ± 0.05	> 5	-	3.57 ± 0.08	> 5	-
<b>N6</b>	1.37 ± 0.02	0.37 ± 0.05	3.7	2.28 ± 0.12	0.22 ± 0.00	10.4
<b>N7</b>	3.84 ± 0.15	1.44 ± 0.06	2.7	7.71 ± 0.10	0.25 ± 0.02	30.8

**Table 6.** Quorum sensing inhibition in the presence of selenocompounds on *Vibrio campbellii* strains.

Cpd: compound, IC<sub>50</sub>: half-maximal inhibitory concentration, EC<sub>50</sub>: half-maximal effective concentration, SI: selectivity index (IC<sub>50</sub>/EC<sub>50</sub>)

According to previous studies, a selectivity index (SI) higher than 10 is desirable for practical application [134]. Based on this criterion, the most promising ketone-selenoesters for QS inhibition are **K1**, **K2**, and **K8**, while the most effective cyano-selenoester is **N2**. Among the tested compounds, **K2** was the only one that inhibited communication based on either AI-1 or AI-2 molecules with an SI higher than 10 (17.5 and 14.7, respectively). **K1** was the most promising compound regarding the inhibition of AI-1 based communication, with an SI of 26.2, while **N2** was the second most potent AI-1 inhibitor, with an SI of 21.6. Among the cyano-selenocompounds, **N3** and **N7** were the most effective inhibitors of AI-2 based communication, with SIs of 37.6 and 30.8, respectively (**Table 6**).

#### 1.4. Inhibition of biofilms

The ability of the compounds to inhibit biofilm formation and disrupt mature biofilms was evaluated against pathogenic bacteria that are known for their biofilm formation, including *S. aureus* and *P. aeruginosa*. Biofilm inhibition can be achieved through several strategies, e.g. (a) preventing bacterial surface adhesion during the initial stages (anti-adhesion effect), (b) chemically inhibiting biofilm maturation (anti-biofilm effect), and (c) disrupting mature biofilms (anti-biofilm effect) [135].

The results, as presented in **Table 7**, indicate that all tested selenocompounds showed efficacy against both stages of biofilm formation. It should be noted that biofilms act as a protective layer for cells, making the concentrations required to disrupt mature biofilms several times higher than those required for inhibiting bacterial adhesion [136]. This was most evident with compound **N3**, which required up to 26- and 11-times higher concentrations to disrupt the biofilm produced by *S. aureus* and *P. aeruginosa*, respectively, compared to the concentrations needed for inhibition of bacterial adhesion. In contrast, compound **K5** exhibited the least difference in efficacy between inhibition of bacterial adhesion and disruption of mature biofilms, requiring only 5- and 4-times higher concentrations for *S. aureus* and *P. aeruginosa*, respectively. Interestingly, the selenocompounds were generally more effective against *P. aeruginosa* than against *S. aureus*.



Compounds	<i>Staphylococcus aureus</i> ATCC 25923		<i>Pseudomonas aeruginosa</i> CCM 3955	
	Anti-adhesion [ $\mu\text{M}$ ]	Anti-biofilm [ $\mu\text{M}$ ]	Anti-adhesion [ $\mu\text{M}$ ]	Anti-biofilm [ $\mu\text{M}$ ]
<b>K1</b>	1.84 $\pm$ 0.26	32.80 $\pm$ 3.25	1.15 $\pm$ 0.01	10.21 $\pm$ 0.48
<b>K2</b>	1.72 $\pm$ 0.17	28.08 $\pm$ 1.17	1.10 $\pm$ 0.11	8.78 $\pm$ 0.66
<b>K3</b>	1.39 $\pm$ 0.13	11.64 $\pm$ 0.99	1.14 $\pm$ 0.05	6.00 $\pm$ 0.74
<b>K4</b>	3.59 $\pm$ 0.48	28.70 $\pm$ 4.18	3.04 $\pm$ 0.33	21.85 $\pm$ 2.04
<b>K5</b>	2.84 $\pm$ 0.13	15.44 $\pm$ 0.42	1.51 $\pm$ 0.22	6.45 $\pm$ 0.30
<b>K6</b>	2.96 $\pm$ 0.16	12.87 $\pm$ 0.37	2.33 $\pm$ 0.25	14.29 $\pm$ 1.62
<b>K7</b>	3.08 $\pm$ 0.24	40.80 $\pm$ 3.12	2.16 $\pm$ 0.29	11.06 $\pm$ 1.92
<b>K8</b>	1.35 $\pm$ 0.16	9.22 $\pm$ 0.61	0.86 $\pm$ 0.09	6.98 $\pm$ 0.22
<b>N1</b>	2.46 $\pm$ 0.15	24.79 $\pm$ 2.65	1.78 $\pm$ 0.07	15.51 $\pm$ 1.65
<b>N2</b>	3.14 $\pm$ 0.12	48.08 $\pm$ 3.82	2.86 $\pm$ 0.17	18.06 $\pm$ 0.72
<b>N3</b>	1.19 $\pm$ 0.15	30.46 $\pm$ 2.72	0.92 $\pm$ 0.01	10.56 $\pm$ 0.95
<b>N4</b>	1.49 $\pm$ 0.08	28.91 $\pm$ 2.00	2.49 $\pm$ 0.43	13.48 $\pm$ 0.82
<b>N5</b>	3.01 $\pm$ 0.35	34.55 $\pm$ 3.00	3.40 $\pm$ 0.10	24.81 $\pm$ 2.12
<b>N6</b>	1.83 $\pm$ 0.15	21.75 $\pm$ 2.61	1.34 $\pm$ 0.08	13.46 $\pm$ 1.77
<b>N7</b>	1.99 $\pm$ 0.26	16.53 $\pm$ 0.76	1.81 $\pm$ 0.04	11.09 $\pm$ 0.82

**Table 7.** Anti-biofilm activity: concentration of selenoesters ( $\text{IC}_{50}$ ) halving the adhesion of biofilms and disrupting the biofilm of *S. aureus* ATCC 25923 and *P. aeruginosa* CCM 3955 strains.

## 2. Antitumor activity

### 2.1. Cytotoxicity

The ketone-selenoesters displayed strong cytotoxic activity against the sensitive Colo 205 and resistant Colo 320 cancer cell lines, with  $\text{IC}_{50}$  values ranging from 1 to 4  $\mu\text{M}$  for both cell lines. However, they also exhibited similar toxicity on normal lung fibroblast cells (MRC-5), suggesting that they lack selectivity towards cancer cells. On the other hand, cyano-selenoesters did not affect MRC-5 cells ( $\text{IC}_{50} > 100 \mu\text{M}$ ), but were highly toxic on both colon cancer cell lines. The cyano-selenoesters were less potent on the resistant Colo 320 cells ( $\text{IC}_{50}$ : 3.78-7.64  $\mu\text{M}$ ) compared to the sensitive Colo 205 cells ( $\text{IC}_{50}$ : 1.98-2.96  $\mu\text{M}$ ). Both ketone- and cyano-selenoesters were more active against cancer cells than the positive control doxorubicin. The SI were calculated, it was demonstrated that cyano-selenoesters exhibited high selectivity ( $>6$ ) in all cases, while ketone-selenoesters showed moderate ( $3 < \text{SI} < 6$ ) and slight ( $1 < \text{SI} < 3$ ) selectivity, except for K2 ( $\text{SI} < 1$ ) (**Table 8**).

Cpd.	Colo 205 (IC <sub>50</sub> )		Colo 320 (IC <sub>50</sub> μM)		MRC-5 (IC <sub>50</sub> μM)		SI	
	Me	SD	Mean	SD	Mean	SD	MRC-5/Colo 205	MRC-5/Colo 320
<b>K1</b>	1.53	± 0.46	1.47	± 0.02	2.24	± 0.29	1.46	1.52
<b>K2</b>	3.35	± 0.58	2.38	± 0.23	2.53	± 0.4	0.76	1.06
<b>K3</b>	2.28	± 0.05	2.15	± 0.03	2.86	± 0.36	1.25	1.33
<b>K4</b>	1.05	± 0.04	1.48	± 0.06	3.63	± 0.37	3.46	2.45
<b>K5</b>	2.14	± 0.08	2.17	± 0.27	3.11	± 3.93	1.45	1.43
<b>K6</b>	2.09	± 0.02	2.1	± 0.05	3.62	± 0.41	1.73	1.72
<b>K7</b>	2.69	± 0.07	2.57	± 0.15	3.72	± 0.17	1.38	1.45
<b>K8</b>	2.24	± 0.16	2.37	± 0.11	2.5	± 0.056	1.12	1.05
<b>N1</b>	2.37	± 0.27	7.64	± 0.15	>100	-	>6	>6
<b>N2</b>	2.96	± 0.09	7.01	± 0.69	>100	-	>6	>6
<b>N3</b>	2.1	± 0.06	4.37	± 0.097	>100	-	>6	>6
<b>N4</b>	1.97	± 0.14	5.57	± 0.226	>100	-	>6	>6
<b>N5</b>	2.1	± 0.1	5.22	± 0.08	>100	-	>6	>6
<b>N6</b>	2.24	± 0.07	5.19	± 0.37	>100	-	>6	>6
<b>N7</b>	1.98	± 0.16	3.78	± 0.23	>100	-	>6	>6
<b>Doxorubicin</b>	3.46	± 0.34	7.61	± 0.29	2.73	± 0.34		

**Table 8.** Cytotoxic effect of selenocompounds on Colo 205 and Colo 320 colon adenocarcinoma cell lines and on MRC-5 normal embryonal fibroblast cells.

Selectivity indices (SI) were calculated to evaluate the potential selectivity of these compounds towards cancer cells compared to normal cells. Doxorubicin was used as a positive control. (Cpd=compound; SD=standard deviation).

The anticancer potential of ketone-selenoesters and cyano-selenoesters was also evaluated on cancer cells derived from various organs such as liver, cervix, and skin. The ketone-selenoesters showed a range of IC<sub>50</sub> values between 2.2 to 4.3 μM for HepG2 cells, 1.9 to 2.7 μM for HeLa cells, and 1.1 to 2.0 μM for B16 cells (**Table 9**). The cyano-selenoesters, on the other hand, exhibited IC<sub>50</sub> values ranging from 5.2 to 11.8 μM for HepG2 cells, 1.3 to 5.2 μM for HeLa cells, and 1.4 to 2.6 μM for B16 cells.

Cpd.	HepG2	HeLa	B16	Cpd.	HepG2	HeLa	B16
IC <sub>50</sub> [ $\mu$ M]; SD +/-				IC <sub>50</sub> [ $\mu$ M]; SD +/-			
<b>K1</b>	2.3 $\pm$ 0.2	2.5 $\pm$ 0.2	1.4 $\pm$ 0.1	<b>N1</b>	11.3 $\pm$ 0.9	2.0 $\pm$ 0.05	1.9 $\pm$ 0.4
<b>K2</b>	2.2 $\pm$ 0.15	2.5 $\pm$ 0.45	1.2 $\pm$ 0.12	<b>N2</b>	5.6 $\pm$ 0.32	5.2 $\pm$ 0.48	2.6 $\pm$ 0.4
<b>K3</b>	3.1 $\pm$ 0.18	2.1 $\pm$ 0.15	1.7 $\pm$ 0.16	<b>N3</b>	9.6 $\pm$ 0.9	2.4 $\pm$ 0.1	2.8 $\pm$ 0.5
<b>K4</b>	4.3 $\pm$ 0.1	1.9 $\pm$ 0.03	2.0 $\pm$ 0.2	<b>N4</b>	5.2 $\pm$ 0.25	2.5 $\pm$ 0.04	1.4 $\pm$ 0.3
<b>K5</b>	2.4 $\pm$ 0.17	2.5 $\pm$ 0.1	1.1 $\pm$ 0.1	<b>N5</b>	9.8 $\pm$ 0.62	2.5 $\pm$ 0.15	1.4 $\pm$ 0.3
<b>K6</b>	2.9 $\pm$ 0.28	2.3 $\pm$ 0.1	1.3 $\pm$ 0.1	<b>N6</b>	9.6 $\pm$ 0.41	1.3 $\pm$ 0.1	1.7 $\pm$ 0.3
<b>K7</b>	3.7 $\pm$ 0.28	2.7 $\pm$ 0.27	1.4 $\pm$ 0.13	<b>N7</b>	11.8 $\pm$	2.1 $\pm$ 0.05	1.6 $\pm$ 0.4
<b>K8</b>	4.0 $\pm$ 0.2	2.0 $\pm$ 0.01	1.4 $\pm$ 0.1				

**Table 9.** Cytotoxic effect of selenocompounds on hepatocellular carcinoma (HepG2), cervical adenocarcinoma (HeLa), and skin melanoma (B16) cell lines. (Cpd=compounds; SD=standard deviation).

## 2.2. Interaction of selenoesters with doxorubicin: *in vitro* model of combination chemotherapy

The checkerboard combination assay is a common method used to assess drug interactions *in vitro*. It calculates combination indices and determines the most effective ratios of drugs. In this study, ketone- and cyano-selenoesters were combined with doxorubicin on Colo 320 cells and their interactions were evaluated using MTT staining. The results were analyzed with the aid of Calcsyn software [137]. The IC<sub>50</sub> values were previously determined and the starting concentration of the compounds for the checkerboard assay was calculated based on this value, a concentration 3x or 4x higher than the IC<sub>50</sub> was applied.

The combination of six ketone-selenoesters (**K1**, **K3**, **K4**, **K5**, **K6**, **K8**) with doxorubicin resulted in a synergistic interaction, with **K5** and **K6** showing consistent synergistic effects at all ratios. Similar findings were observed for five cyano-selenoesters (**N1**, **N2**, **N3**, **N4**, **N7**), which exhibited a synergistic effect when combined with doxorubicin (see **Appendix 3** for complete results) (**Tables 10** and **11**).

Compounds	Starting conc. ( $\mu\text{M}$ )	Ratio*	CI at ED <sub>50</sub>	SD (+/-)	Type of interaction
<b>K1</b>	5	4.8:1	0.88	0.13	<b>Slight synergism</b>
<b>K3</b>	6	1.4:1	0.37	0.15	<b>Synergism</b>
		2.8:1	0.73	0.1	Moderate synergism
<b>K4</b>	5	0.6:1	0.54	0.07	<b>Synergism</b>
		4.8:1	0.74	0.1	Moderate synergism
		9.6:1	0.85	0.06	<b>Slight synergism</b>
<b>K5</b>	6	0.7:1	0.51	0.06	<b>Synergism</b>
		1.4:1	0.81	0.05	<b>Moderate synergism</b>
		2.8:1	0.55	0.04	<b>Synergism</b>
		5.6:1	0.58	0.02	<b>Synergism</b>
		11.2:1	0.64	0.02	<b>Synergism</b>
		22.4:1	0.68	0.06	<b>Synergism</b>
<b>K6</b>	6	0.7:1	0.51	0.06	<b>Synergism</b>
		1.4:1	0.81	0.05	<b>Moderate synergism</b>
		2.8:1	0.55	0.04	<b>Synergism</b>
		5.6:1	0.58	0.02	<b>Synergism</b>
		11.2:1	0.64	0.02	<b>Synergism</b>
<b>K8</b>	6	22.4:1	0.68	0.06	<b>Synergism</b>
		0.7:1	0.12	0.09	<b>Strong synergism</b>

**Table 10.** Interaction of selected ketone-selenoesters with doxorubicin on MDR Colo 320 colon adenocarcinoma cells.

The combination index (CI) values at 50% growth inhibition (ED<sub>50</sub>) were determined using CalcuSyn software. The CI values were calculated by plotting 4 or 5 data points for each ratio and using the median-effect equation. (CI=combination index; ED<sub>50</sub> = 50% growth inhibition).

Compounds	Starting conc. ( $\mu\text{M}$ )	Ratio*	CI at ED <sub>50</sub>	SD (+/-)	Type of interaction
<b>N1</b>	15	3.4:1	0.34	0.04	<b>Synergism</b>
		6.8:1	0.51	0.04	<b>Synergism</b>
		27.2:1	0.56	0.09	<b>Synergism</b>
		54.4:1	0.21	0.21	<b>Strong synergism</b>
<b>N2</b>	15	54.4:1	0.21	0.21	<b>Strong synergism</b>
		1.7:1	0.62	0.19	<b>Synergism</b>
		6.8:1	0.58	0.03	<b>Synergism</b>
<b>N3</b>	10	4.8:1	0.85	0.1	<b>Moderate synergism</b>
<b>N4</b>	10	4.8:1	0.85	0.1	<b>Moderate synergism</b>
<b>N7</b>	8	3.6:1	0.9	0.23	<b>Slight synergism</b>

**Table 11.** Interaction of cyano-selenoesters with doxorubicin on MDR Colo 320 colon adenocarcinoma cells.

The combination index (CI) values at 50% growth inhibition (ED<sub>50</sub>) were determined using CalcuSyn software. The CI values were calculated by plotting 4 or 5 data points for each ratio and using the median-effect equation. (CI=combination index; ED<sub>50</sub> = 50% growth inhibition).

### 2.3. ABCB1 inhibition by selenoesters

The effect of selenoesters on ABCB1 inhibition in MDR Colo 320 cells was evaluated by measuring the intracellular accumulation of the ABCB1 substrate, rhodamine 123, using flow cytometry. To assess the effectiveness of the selenoesters, fluorescence activity ratio (FAR) values were calculated. The effectiveness of the ABCB1 transporter inhibition by ketone-selenoesters was evaluated by analyzing the intracellular accumulation of rhodamine 123, a fluorescent substrate, at two different concentrations (0.2  $\mu\text{M}$  and 2  $\mu\text{M}$ ). According to the results obtained by flow cytometry, some of the ketone-selenoesters exhibited potent inhibition on the ABCB1 transporter, with **K1**, **K2**, **K3**, **K7**, and **K8** being the most effective ones. These compounds showed a FAR value of 45.73, 37.35, 39.17, 40.38, and 36.09 at 2  $\mu\text{M}$ , respectively. **K3** and **K8** were effective at both concentrations (0.2  $\mu\text{M}$  and 2  $\mu\text{M}$ ), with a FAR value of 3.99 and 3.38, respectively, at 0.2  $\mu\text{M}$  (**Figure 8**). The other ketone-selenoesters showed inhibitory activity only at 2  $\mu\text{M}$ . In contrast, the cyano-selenoesters did not show any modulating activity towards the ABCB1 transporter.

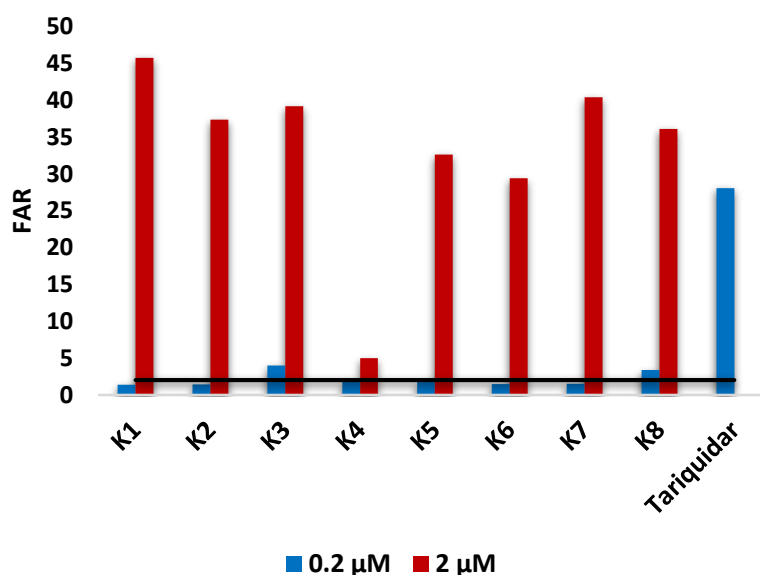


**Figure 8:** Inhibition of the MDR efflux pump ABCB1 by selenoesters on Colo 320 colon adenocarcinoma cells.

Tariquidar was used as a positive control at 0.2  $\mu\text{M}$ , while DMSO served as solvent control at 2%. FAR values above 2 (highlighted in bold by a black line) were considered to be indicative of an effective inhibition. (The table containing the FAR values can be found in **Appendix 4**.)

The flow cytometric experiments involved the evaluation of various parameters, including the forward scatter count (FSC), which provides information about the size of the cells, the side scatter count (SSC), which is proportional to the granularity or internal complexity of the cells, and FL-1, which refers to the mean fluorescence of the cells. FAR values were also calculated using the equation provided above.

#### **2.4. Pgp ATPase activity**

The Pgp-Glo™ Assay is designed to identify and quantify the influence of different compounds on the activity of ABCB1. The assay can determine the effectiveness of compounds to alter the ABCB1 activity: the compounds can be stimulator or inhibitor of the ABCB1 ATPase activity. The study examined the relative ATPase inhibition of selected ketone-selenoesters on ABCB1. The effects were measured as the relative ATPase activity, with the luminescence decrease in untreated samples compared to samples treated with sodium-vanadate representing the basal ABCB1 ATPase activity (**Figure 9**). Similarly, the luminescence decreases in verapamil-treated samples indicated the verapamil-stimulated ABCB1 ATPase activity (**Figure 9**). A lower relative ATPase activity indicated a more effective inhibitor.

Only compounds that exhibited ABCB1 inhibitory activity were evaluated in this assay. Figure X demonstrates that **K1**, **K4**, **K7**, and **K8** had  $\Delta\text{RLU}$  values lower than  $\Delta\text{RLU}_{\text{basal}}$ , indicating that they are inhibitors of ABCB1 ATPase activity. On the other hand, the remaining compounds stimulated ATPase activity. Verapamil, which is a substrate of ABCB1 and stimulates ATPase activity, was used as a control in this assay. The ABCB1 ATPase activity could not be determined for **K2** and **K6** because of the inconsistency of the experimental data (**Figure 9**).

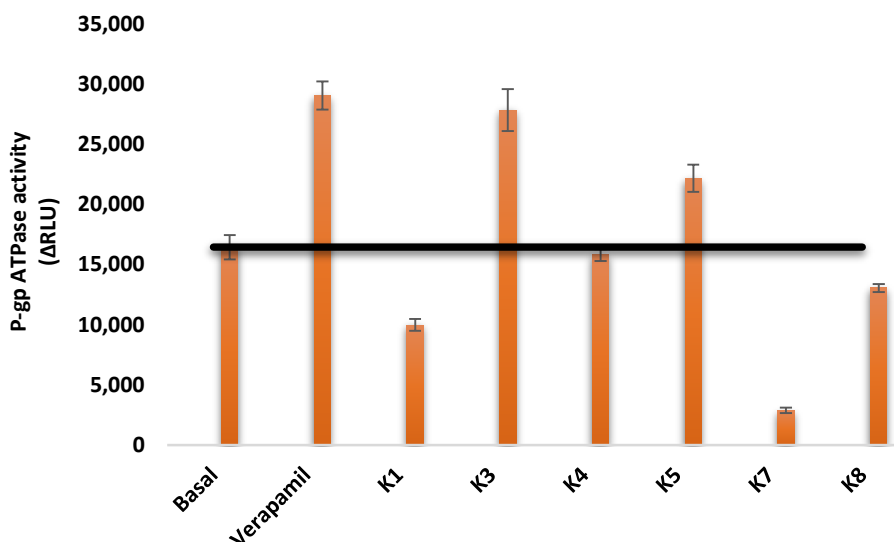


**Figure 9:** Inhibition of P-gp (ABCB1) ATPase by selected ketone-selenoesters.

A lower relative ATPase activity indicates a more effective inhibitor. The results presented are the means  $\pm$  standard deviation (SD) from experiments conducted in triplicate, and the black line represents the level of basal activity.

## 2.5. Induction of apoptosis

In cancer, the normal apoptotic pathway that leads to programmed cell death is often disrupted. One common mechanism is the overexpression of antiapoptotic proteins, which prevent cells from undergoing apoptosis. These changes can lead to resistance to chemotherapy. To overcome this phenomenon, apoptosis induction is a common target in anticancer therapy [138].

The MDR Colo 320 colon adenocarcinoma cells were subjected to apoptosis-inducing activity tests with the highly effective ABCB1 inhibiting ketone-selenoesters. The positive control used for comparison was 12*H*-benzo[ $\alpha$ ]phenothiazine (M627). The results showed that **K3** was the most potent compound, inducing early apoptosis in 18.6% of the cell population. Furthermore, **K3** was the most effective in late apoptosis induction, with a rate of 25.6% in the cell population. It was interesting to note that all the derivatives contributed to late apoptosis in the studied cell population, with activities ranging from 16.1% to 33.9% in the treated cells (**Figure 10**).

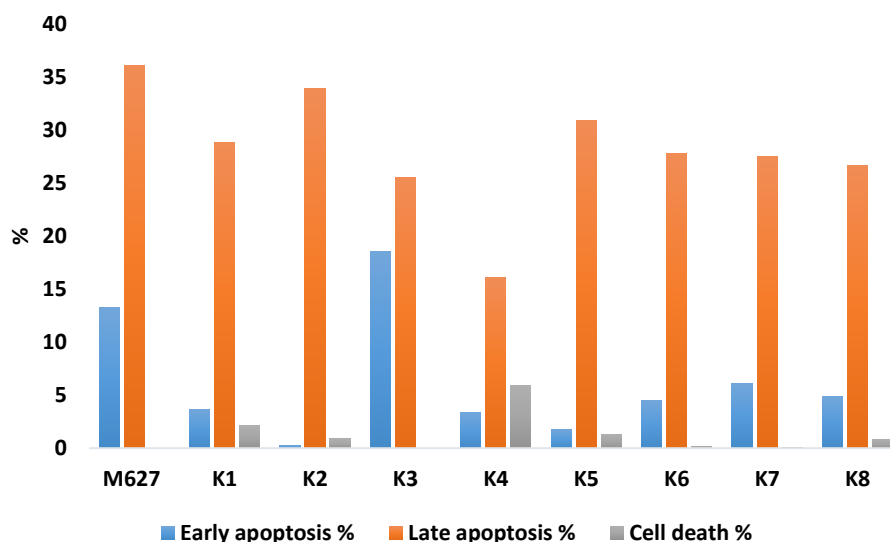


**Figure 10:** Apoptosis induction by ketone-selenoesters on MDR Colo 320 adenocarcinoma cells.

The positive control, 12*H*-benzo( $\alpha$ )phenothiazine (M627), was used for comparison. Flow cytometry analysis was conducted after staining the cells with Annexin V-FITC and propidium iodide. The figure illustrates the percentage of cells in early apoptosis (annexin positive, propidium iodide negative) (A+, P-), late apoptosis (annexin positive, propidium iodide positive) (A+, PI+), and dead cells (annexin negative, propidium iodide positive) (A-, PI+). The induction with the compounds lasted for 3 hours (see **Appendix 5** for complete data regarding apoptosis in the cell population).



## DISCUSSION

### 1. Antibacterial activity

Previously, it was demonstrated that a methylketone selenoester possess potent activity against Gram-positive bacteria. In addition, two other selenocompounds, namely a selenoanhydride and a diselenodiester, exhibited inhibitory properties against the AcrAB-TolC system of *E. coli*. A series of symmetrical selenoesters was also investigated to evaluate their potential as anti-biofilm agents and inhibitors of efflux pumps. It was confirmed that selenoesters containing a methyloxycarbonyl group displayed significant inhibition of biofilm formation and efflux pumps. Furthermore, a specific methyloxycarbonyl selenoester demonstrated a notable ability to inhibit quorum sensing, a process involved in bacterial communication [139,119]. The ketone-selenoesters demonstrated potent activity against both sensitive and methicillin-resistant *S. aureus* strains. Furthermore, cyano-selenoesters showed slightly greater activity than the ketone-selenoesters against the evaluated strains of *Salmonella enterica* serovar Typhimurium.

Among the synthesized compounds, **K6** stood out as the most active compound. It contained a *tert*-butyl group in the *para*-position and displayed impressive MIC values of 1.56  $\mu\text{M}$  against the sensitive strains and 0.39-3.13  $\mu\text{M}$  against the methicillin-resistant *S. aureus* (MRSA) strains. Interestingly, **K6** was the only compound in our study that had an electron-donating substituent. This is noteworthy since previous studies on selenoesters have indicated that electron-withdrawing substituents generally exhibit higher biological activity.

The nitrile derivatives (**N1-N7**) demonstrated comparable activity against the sensitive *S. aureus* ATCC 25923 strain, with a MIC of 12.5  $\mu\text{M}$ . Considering the results obtained from the MRSA and *S. Typhimurium* strains, the most potent compounds were identified as **N1** (unsubstituted), **N3** (4-Br-substituted), **N6** (3-Cl-substituted), and **N7** (3,5-bis(trifluoromethyl)-substituted). These findings indicate that among the monosubstituted compounds, those containing a bromine or chlorine atom attached to the ring exhibit superior activity compared to those with a fluoro or trifluoromethyl group. Furthermore, the inclusion of a second trifluoromethyl group contributes to antibacterial activity comparable to that observed for the bromine or chlorine derivatives.

It is important to note that the compound **K4**, which demonstrated lower activity, contained a bulky substituent (trifluoromethyl group) at the *ortho* position of the selenoester. This bulky substituent may cause steric hindrance, potentially hindering the hydrolysis of the selenoester within the cells. It is suggested that the hydrolysis of the selenoester is a crucial

mechanism underlying its biological activity. Interestingly, when this bulky substituent was replaced with the smallest possible substituent (-H in compound **K1**), the MIC value decreased by twofold across the three tested strains of *S. aureus*. Furthermore, substitution with a fluorine atom (an intermediate between -H and -CF<sub>3</sub>) resulted in a twofold reduction in MIC values against *S. aureus* ATCC 25923 and *S. aureus* MRSA 272123.

## 2. Efflux pump inhibition in bacteria

Bacteria can develop multidrug resistance by employing drug efflux mechanisms, which actively expel antibiotics from within their cells. EPIs have the potential to restore the sensitivity of bacteria to antibiotics, thereby enhancing the efficacy of antibiotic treatments [55]. In the case of the ketone- and cyano-selenoesters investigated in this study, only one cyano-selenoester, **N4** exhibited potent EPI activity against methicillin-resistant *S. aureus*, surpassing the effect of the reference EPI reserpine. Moreover, ketone-selenoester **K7** demonstrated effective EPI activity on *S. Typhimurium* strains, likely due to its ability to destabilize the bacterial membrane. Interestingly, all compounds containing at least one trifluoromethyl group (**K4**, **K5**, **N4**, and **N7**), except for **N5**, demonstrated moderate inhibitory effects on efflux pumps in the *S. Typhimurium* SE39  $\Delta tolC$  strain, as observed in the real-time ethidium bromide accumulation assay. Hence, the presence of the -CF<sub>3</sub> moiety and the -C(CH<sub>3</sub>)<sub>3</sub> moiety in **K7** appeared to be significant for the efflux pump inhibitory activity in the *S. Typhimurium* SE39  $\Delta tolC$  strain.

## 3. Quorum sensing (QS) inhibition and anti-biofilm activity

The control of bacterial infections can be achieved through the inhibition of bacterial cell-to-cell communication. This communication mechanism enables bacteria to monitor their population density and regulate their behavior accordingly, for example they can initiate the production of biofilms and some of them can inhibit mammalian ABC transporter as well [140]. Currently, quorum-sensing modulators offer promising tools to decrease bacterial virulence, they might be potent against biofilm formation.

Based on our findings, we have identified several promising compounds that can be utilized as inhibitors of bacterial communication. Compound **K2**, in particular, displayed significant selectivity in inhibiting communication rather than bacterial growth. This selectivity is advantageous for non-pathogenic bacteria, such as those found in the human microflora. Among the compounds evaluated, ketone-selenoester **K1** emerged as the most promising inhibitor of AI-1-based communication, followed by **N2**, the only cyano-selenocompound

capable of inhibiting this type of communication. Both **K1** and **N2** demonstrated inhibitory activity at remarkably low concentrations of 0.25  $\mu\text{M}$  and 0.34  $\mu\text{M}$ , respectively. Interestingly, both **K2** (ketone-selenoester) and **N2** (cyano-selenoester) share a common 2-fluorophenyl moiety attached to the selenoester, suggesting its importance in inhibition of AI-1 communication. Notably, the presence of fluorine atoms without other substituents proved to be beneficial for activity, as evidenced on of the most active compound **K8** with a 2,4,5-trifluoro substitution. However, the activity of the most potent inhibitor, **K1**, may not be solely attributed to the absence of substitution, as its nitrile equivalent (**N1**) displayed no activity. Since *P. aeruginosa* primarily relies on AI-1-based communication, compounds inhibiting AI-1 communication in *V. campbellii* (strain BAA 1118) are expected to impede the adhesion of *P. aeruginosa* as well. Compounds **K1**, **K2**, and **K8** exhibited QS selectivity indices above 10 and demonstrated significant inhibition of *P. aeruginosa* adhesion in the anti-biofilm assay.

In contrast, the cyano-selenocompounds demonstrated superior efficacy in inhibiting AI-2-based communication. Among them, **N3** and **N7** proved to be the most potent compounds, with **N3** exhibiting remarkable inhibition even at a concentration as low as 60 nM. Interestingly, these compounds featured distinct substitutions on the phenyl ring compared to the AI-1 inhibitors.

The quorum sensing process in Gram-positive bacteria is typically mediated by peptide molecules, which differ from the communication signals utilized by *Vibrio* bacteria. Therefore, the results obtained in this study cannot be directly correlated. However, many of the tested compounds exhibited significant inhibition of *S. aureus* adhesion, indicating the potential of Se-compounds for modulating the activity of efflux pumps. Autoinducers-2 (AI-2) are commonly utilized by both Gram-positive and Gram-negative bacteria. For instance, *S. aureus*, *Bacillus* genus, and members of the *Enterobacteriaceae* family employ ABC transporters as part of their communication system [141]. However, in the AI-2 system, these transporters are involved in the uptake of communication molecules [142]. Interestingly, compounds **K2**, **K4**, **K7**, **N3**, **N6**, and **N7** displayed notable inhibitory effects on this universal communication system, which is shared by both Gram-positive and Gram-negative bacteria.

In the anti-biofilm assay, all tested compounds exhibited biofilm adhesion inhibition against the evaluated bacterial strains (*S. aureus* ATCC 25923 and *P. aeruginosa* CCM 3955) at concentrations below 4  $\mu\text{M}$ . Notably, two compounds (**K8** and **N3**) demonstrated remarkable inhibition of *P. aeruginosa* biofilm adhesion at nanomolar concentrations (0.86  $\mu\text{M}$  and 0.92  $\mu\text{M}$ , respectively). No specific structure-activity relationships (SARs) could be established, it was observed that the ketone-selenoesters were more potent disruptors compared to the cyano-

selenoesters. Additionally, the compounds showed higher effectiveness against *P. aeruginosa* biofilms compared to *S. aureus* biofilms.

#### 4. Antitumor effects

Oxoselenoesters, with a few exceptions, have shown greater cytotoxicity compared to cyano-selenoesters in MDR Colo 320, HepG2, and B16 cancer cell lines. The difference in activity is particularly pronounced in Colo 320 and HepG2 cells. While cyano-selenoesters had no effect on MRC-5 cells, they exhibited significant toxicity in both colon cancer cell lines, albeit less potent in resistant cells. The most active compound in each cell line, with the second and third most active compounds in brackets, were as follows: **K4** in Colo 205 (**K1**, **N4**); **K1** in Colo 320 (**K4**, **K6**); **K2** in HepG2 (**K1**, **K5**); **N6** in HeLa (**K4**, **K3**); and **K5** in B16 cells (**K2**, **K6**). Interestingly, most of the most active compounds are oxoselenoesters, with the presence of substituents without halogens, such as **K7**, leads to a decrease in activity. Compounds with a trifluoromethyl group or one or two halogens bound to the phenyl ring exhibited better activity. However, the inclusion of a third fluorine atom on the phenyl ring (**K8**) was found to be less favorable for cytotoxicity. Furthermore, the recurrent appearance of **K1** and **K4** among the most active compounds against each cell line (three times each) suggests that the thionyl ring and the presence of a trifluoromethyl group in the ortho position of the phenyl ring enhance cytotoxicity. Notably, **K5**, which has a 3-CF<sub>3</sub> substituent on the ring, also displayed significant activity, while the cyano-selenoester **N4**, with a 2-CF<sub>3</sub> substituent on the ring, was perhaps the most active derivative among the cyano-selenoesters. These findings support the observation that the trifluoromethyl group, preferably in the ortho position, plays a crucial role in the cytotoxic activity, although the compound with this substituent in the meta position showed comparable activity in all cell lines, except for HepG2, where it was significantly less active.

The selenoesters containing ketone groups demonstrated toxicity against normal MRC-5 cells, whereas none of the derivatives containing cyano groups exhibited toxicity at concentrations below 100  $\mu$ M. This suggests that all the cyano-selenoesters displayed strong selectivity (selectivity index, SI > 6) towards cancer cells.

#### 5. Interaction of selenoesters with doxorubicin

When studying the interaction between ketone-selenoesters, cyano-selenoesters, and the cytotoxic drug doxorubicin, it was found that eleven out of the fifteen evaluated selenoesters exhibited synergistic interactions with doxorubicin in at least one of the tested ratios on resistant colon adenocarcinoma cells. The selenoesters that demonstrated synergism were **K1**, **K3**, **K4**,

**K5, K6, K8, N1, N2, N3, N4, and N7.** Interestingly, no clear structure-activity relationships (SARs) could be established, as compounds **K5** and **K6** showed varying degrees of synergism with doxorubicin across all tested ratios, while their cyano-selenoester counterparts (**N5** and **N6**) displayed antagonistic interactions in five out of the six ratios tested. Similarly, the thiophene cyano-selenoester **N1** exhibited synergistic interactions with doxorubicin in four out of the six ratios, whereas its ketone analog, **K1**, only displayed synergism in one out of the five ratios. Notably, the **N1** derivative showed a particularly strong synergistic interaction at a ratio of 54.4:1 with doxorubicin.

## 6. ABCB1 inhibition by selenoesters

To overcome efflux-related multidrug resistance (MDR), the inhibition of the ABCB1 pump was investigated in the presence of selenocompounds. It was found that the presence of a 2-oxopropyl group in ketone-selenoesters was crucial for their activity as ABCB1 inhibitors. All ketone-selenoesters, except for **K4**, exhibited greater potency as ABCB1 inhibitors, whereas none of the cyano-selenoesters demonstrated ABCB1 inhibitory activity. These findings align with previous studies [143,139], which also highlighted the importance of the 2-oxopropyl group and a 3,3-dimethyl-2-oxobutyl group as highly effective components.

Among the compounds evaluated, **K1** emerged as the most active compound, featuring a thiophene ring instead of a phenyl ring. Notably, the introduction of a bulky trifluoromethyl group at the two-position of the phenyl ring (**K4**) significantly diminished its activity. Interestingly, relocating this group to the three-position, thereby eliminating steric hindrance, resulted in a sixfold increase in activity (**K5**). Surprisingly, two oxoselenoesters, namely **K7** with a 4-*tert*-butylphenyl ring, and **K8** with a 2,4,5-trifluorophenyl ring, exhibited lower cytotoxicity, but demonstrated strong inhibition of ABCB1, comparable to the activity of **K2** (with a 2-fluorophenyl moiety) and **K3** (with a 4-bromophenyl moiety).

## 7. P-gp ATPase activity

The P-glycoprotein (P-gp) ATPase activity was assessed exclusively for the oxoselenoesters, as they were the only compounds that exhibited ABCB1 inhibitory activity. Among the tested oxoselenoesters, the ATPase activity of **K2** and **K6** could not be determined. However, all the other compounds, except for **K4**, which exhibited activity similar to the basal control, demonstrated modulation of the ATPase activity. Remarkably, the most potent ABCB1 inhibitors, namely **K1** and **K7**, significantly inhibited the ATPase activity, with **K7** showing particularly strong inhibition. Additionally, **K8** displayed a milder inhibition of the ATPase

activity. Given that ABCB1 activity can protect cells from apoptosis, the inhibition of ATP supply to this pump can promote apoptosis, as supported by our findings [119]. In fact, the aforementioned derivatives (**K1**, **K7**, and **K8**) induced late apoptosis in MDR Colo 320 cells, further confirming the link between ABCB1 inhibition and the induction of apoptosis.

## 8. Induction of apoptosis

The connection between ABCB1 inhibition and the induction of apoptosis was explored in the case of ketone-selenoesters. Overall, the ketone-selenoesters exhibited notable capacity to trigger apoptotic events, except for **K4**. Notably, compound **K3** outperformed the reference phenothiazine in inducing early apoptosis and demonstrated comparable potency to the reference (89.5%) when considering both early and late apoptosis induction. Among the other tested derivatives, no clear structure-activity relationships (SARs) could be identified based on the available data. However, it was evident that the inclusion of a bromine atom at the four-position of the phenyl ring (**K3**) enhanced apoptosis induction, while the introduction of a bulky substituent at the two-position (such as the trifluoromethyl moiety) of the phenyl ring reduced the ability to trigger apoptotic events. Furthermore, the presence of selenium in the compounds can promote the generation of free radicals, leading to apoptosis and cell death in cancer cells [144,145,146]. The MDR transporter proteins, particularly ABCB1, play a role in evading apoptosis by suppressing the extrinsic apoptotic pathway (including TRAIL protein and caspases three and eight) and stabilizing cell membrane phospholipids through outward flippase activity. The interconnection between overexpressed efflux pumps and programmed cell death may explain the activity of the compounds [120,147].

## NEW FINDINGS

### 1. Selenoesters as antibacterial agents

- ❖ Ketone-selenoesters showed an outstanding antibacterial effect against methicillin susceptible and methicillin resistant *Staphylococcus aureus* strains. In addition, cyano-selenoesters showed also potent antibacterial activity on these Gram-positive strains.  
Ketone- and cyano-selenoesters had a slight antibacterial activity on the Gram-negative *Salmonella* Typhimurium SE01, SE02, SE03, SE 39, *Pseudomonas aeruginosa* ATCC 27853 and NEM 986 strains.

### 2. Modification of bacterial virulence: inhibition of efflux pumps, quorum sensing and biofilm formation

- ❖ The ketone-selenoester **K7** could inhibit the AcrAB-TolC system of wild-type *Salmonella* Typhimurium.
- ❖ Cyano-selenoester **N4** inhibited the function of the AcrAB-TolC system on *S. Typhimurium*, and the highest inhibition was achieved on the *tolC* deficient mutant SE39 strain of *S. Typhimurium*. Cyano-selenoester **N4** inhibited the efflux pump activity of *S. aureus* MRSA 43300 strain.
- ❖ All ketone- and cyano-selenoesters, except one compound, were able to reduce bacterial communication of *Vibrio campbellii* strains lacking either the autoinducer-1 or autoinducer-2 types quorum sensing molecules. The most potent ketone selenoesters are **K1, K2, K4, K7**, and **K8**, among the cyano selenoesters compounds **N2, N3**, and **N7** should be highlighted.
- ❖ All ketone- and cyano-selenoesters had an inhibitory effect on biofilm formation and could disrupt mature biofilms of *S. aureus* ATCC 25923 and *Pseudomonas aeruginosa* CCM 3955 strains.

### 3. Antitumor and cytotoxic effects of selenoesters

- ❖ All ketone- and cyano-selenoesters had a cytotoxic effect on the tested colon adenocarcinoma (Colo 205 and 320), hepatocellular carcinoma (HepG2), cervical adenocarcinoma (HeLa), and skin melanoma (B16) cell lines. An outstanding result is that the cyano-selenoesters were selective, this means that they had no cytotoxic effect on the normal MRC-5 lung fibroblast cell line.
- ❖ The ketone-selenoesters **K1, K3, K4, K5, K6, K8** and the cyano-selenoesters **N1, N2, N3, N4, N7** presented synergistic interaction with doxorubicin on resistant Colo 320 colon adenocarcinoma cells, as they were able to reduce the IC<sub>50</sub> value of doxorubicin.

### 4. Reversal of cancer MDR by selenoesters

- ❖ Among the selenoesters, only the ketone-selenoesters proved to be effective in ABCB1 inhibition, and the most potent derivatives were **K1, K2, K3, K7**, and **K8**.
- ❖ Ketone-selenoesters **K1, K4, K7**, and **K8** proved to be the inhibitors of ABCB1 ATPase activity.
- ❖ Ketone-selenoesters were able to induce late apoptosis in resistant Colo 320 colon adenocarcinoma cells, only compound **K3** induced early apoptosis.

## SUMMARY

Multidrug resistance (MDR) is an important challenge in antibacterial and anticancer therapies. It refers to the ability of microorganisms or tumor cells to withstand the effects of multiple drugs of different structural classes, making conventional therapies ineffective. Antimicrobial resistance can occur by different mechanisms, such as limited uptake of a drug, modification of the drug target, inactivation of a drug, and active drug efflux. Out of these factors the present study is focused on the efflux pump related resistance. As a result of anticancer chemotherapy many patients develop MDR against anticancer drugs, making the treatment less effective. MDR in cancer cells is caused by various mechanisms, such as increased drug efflux, enhanced DNA damage repair, reduced apoptosis, elevated autophagy, and altered drug metabolism. Understanding the mechanisms behind MDR in both bacteria and cancer is crucial for developing more efficient therapeutic strategies.

Based on previous studies selenium-containing compounds proved to be effective against MDR in bacteria and cancer. For this reason, new ketone- and cyano-selenoesters were synthesized and their antibacterial and anticancer activities were investigated. The antibacterial, efflux pump inhibitory, anti-biofilm, and the anti-QS effects were determined on Gram-negative and Gram-positive bacterial strains. Methyloxycarbonyl-selenoesters could inhibit bacterial biofilm formation, efflux pump activity, and the bacterial communication or quorum sensing. Oxoselenoesters displayed more pronounced cytotoxicity than cyano-selenoesters in MDR colon adenocarcinoma, hepatocellular carcinoma, and skin melanoma cell lines. Cyano-selenoesters showed no toxicity in normal cells, however they had cytotoxic activity in both colon cancer cell lines. Regarding the interaction with doxorubicin, eleven out of fifteen selenoesters demonstrated synergism on MDR colon adenocarcinoma cells. Ketone-selenoesters with a 2-oxopropyl group were active ABCB1 (P-glycoprotein) inhibitors, furthermore several oxoselenoesters modulated the ATPase activity of ABCB1. In addition, ketone-selenoesters were able to trigger apoptosis in MDR colon adenocarcinoma cells.

It can be concluded that ketone- and cyano-selenoesters could provide promising scaffolds for antibacterial and anticancer drugs, however additional *in vitro* and *in vivo* experiments have to be completed in the future.



## ÖSSZEFOGLALÁS

A multidrog rezisztencia (MDR) fontos kihívás az antibakteriális és rákellenes terápiákban. A mikroorganizmusok vagy a daganatsejtek képesek ellenállni több, különböző szerkezeti osztályba tartozó gyógyszer hatásának, ami hatástalanná teszi a hagyományos terápiákat. Az antimikrobiális rezisztencia különböző mechanizmusok révén léphet fel, mint például a gyógyszer korlátozott felvétele, a gyógyszer célpontjának módosítása, a gyógyszer inaktíválása és a gyógyszer aktív kipumpálása efflux pumpák révén. Ezen tényezők közül jelen tanulmány az efflux pumpákkal kapcsolatos rezisztenciára összpontosít. A rákellenes kemoterápia eredményeként sok betegnél rezisztencia alakul ki a rákellenes gyógyszerekkel szemben, így a kezelés kevésbé hatékony. A rákos sejtekben az MDR-t különböző mechanizmusok okozzák, mint például a fokozott gyógyszerkiáramlás, a DNS-károsodás helyreállítása, az apoptózis csökkenése, az emelkedett autofágia és a megváltozott gyógyszermetabolizmus. Az MDR mögött meghúzódó mechanizmusok megértése mind a baktériumok, mind a rák esetében kulcsfontosságú a hatékonyabb terápiás stratégiák kidolgozásához.

Korábbi vizsgálatok alapján a szeléntartalmú vegyületek hatékonynak bizonyultak az MDR ellen baktériumokban és tumorsejtekben. Ezen oknál fogva új keton- és ciano-szelenoészterek szintézise történt, melyeknek antibakteriális és rákellenes hatását vizsgáltuk. Gram-negatív és Gram-pozitív baktériumtörzseken határoztuk meg az antibakteriális, efflux pumpát gátló, antibiofilm és anti-QS hatásokat. A metiloxikarbonil-szelenoészterek gátolták a bakteriális biofilm képződést, az efflux pumpák aktivitását, és a bakteriális kommunikációt, vagyis a quorum sensing-et. Az oxoszelenoészterek erősebb citotoxicitást mutattak, mint a ciano-szelenoészterek rezisztens vastagbél adenokarcinóma, hepatocelluláris karcinóma és bőr melanoma sejtvonalakon. A ciano-szelenoészterek nem mutattak toxicitást normál sejtekben, azonban citotoxikus hatásúnak bizonyultak mindkét vastagbélrák sejtvonalon. A doxorubicinnel való kölcsönhatást illetően, tizenöt szelenoészterből 11 mutatott szinergizmust a rezisztens vastagbél adenokarcinóma sejteken. A 2-oxopropil-csoportot tartalmazó keton-szelenoészterek aktív ABCB1 (P-glikoprotein) inhibitorok voltak, továbbá számos oxoszelenoészter modulálta az ABCB1 ATPáz aktivitását. Ezen kívül a keton-szelenoészterek képesek voltak apoptózist kiváltani rezisztens vastagbél adenokarcinóma sejtekben.

Megállapítható, hogy a keton- és ciano-szelenoészterek ígéretes kiindulópontjai lehetnek az antibakteriális és rákellenes gyógyszereknek, azonban a jövőben további *in vitro* és *in vivo* kísérletek szükségesek.

## ACKNOWLEDGEMENTS

I want to convey my deep appreciation to **Dr. Gabriella Spengler**, my supervisor, for granting me the chance to be a part of her research team and for her invaluable guidance throughout the course of my research. The completion of this thesis owes much to her insightful recommendations, unwavering support, and boundless patience.

I would like to thank **Prof. Dr. Katalin Burián**, chair of the Department of Medical Microbiology, for the possibility to work at the department, also for her outstanding help for the PhD students working in our institute.

I am extremely grateful to our collaborators **Dr. Enrique Domínguez-Álvarez**, **Prof. Dr. József Molnár**, and **Dr. Jitka Viktorova**. I would also like to thank Dr. Jitka Viktorová for allowing me to spend time in their laboratory, studying and gaining new knowledge.

I would like to thank **Dr. Annamária Kincses**, **Dr. Márta Bozóki-Nové**, **Gábor Tóth**, **Dr. Imre Ocsovszki**, **Simona Dobiasová**, and **Katerina Rehorova** for their help during my work. I would also like to thank Annamária and Márta for sharing their laboratory knowledge.

I would like to give my special thanks to **Györgyi Müllerné Deák**, **Anikó Vigyikánné Váradi**, **Szilvia Urbán**, and **Lidia Mucea** for their technical assistance.

I am deeply grateful to **Dr. Anita Varga-Bogdanov** and **Edina Miklósné Bódi** for their selfless help and encouragement during my PhD.

I am grateful to **all the members of the department** for their support and for creating a pleasant working environment during my studies.

Lastly, I feel a deep sense of gratitude to my **family** for their love, a lot of patience and support.

## REFERENCES

1. Abushaheen, M.A.; Muzaaheed; Fatani, A.J.; Alosaimi, M.; Mansy, W.; George, M.; Acharya, S.; Rathod, S.; Divakar, D.D.; Jhugroo, C.; et al. Antimicrobial Resistance, Mechanisms and Its Clinical Significance. *Disease-a-Month* **2020**, *66*, 100971, doi:10.1016/j.disamonth.2020.100971.
2. Simon, S.M.; Schindler, M. Cell Biological Mechanisms of Multidrug Resistance in Tumors. *Proc. Natl. Acad. Sci. U.S.A.* **1994**, *91*, 3497–3504, doi:10.1073/pnas.91.9.3497.
3. <https://www.who.int/news-room/fact-sheets/detail/antibiotic-resistance>.
4. Pei, S.; Blumberg, S.; Vega, J.C.; Robin, T.; Zhang, Y.; Medford, R.J.; Adhikari, B.; Shaman, J.; for the CDC MIND-Healthcare Program Challenges in Forecasting Antimicrobial Resistance. *Emerg. Infect. Dis.* **2023**, *29*, 679–685, doi:10.3201/eid2904.221552.
5. Hassan, K.A.; Elbourne, L.D.H.; Li, L.; Gamage, H.K.A.H.; Liu, Q.; Jackson, S.M.; Sharples, D.; Kolstø, A.-B.; Henderson, P.J.F.; Paulsen, I.T. An Ace up Their Sleeve: A Transcriptomic Approach Exposes the AceI Efflux Protein of *Acinetobacter Baumannii* and Reveals the Drug Efflux Potential Hidden in Many Microbial Pathogens. *Front. Microbiol.* **2015**, *6*, doi:10.3389/fmicb.2015.00333.
6. Mitra, S.; Sultana, S.A.; Prova, S.R.; Uddin, T.M.; Islam, F.; Das, R.; Nainu, F.; Sartini, S.; Chidambaram, K.; Alhumaydhi, F.A.; et al. Investigating Forthcoming Strategies to Tackle Deadly Superbugs: Current Status and Future Vision. *Expert Review of Anti-infective Therapy* **2022**, *20*, 1309–1332, doi:10.1080/14787210.2022.2122442.
7. Gradisteanu Pircalabioru, G.; Popa, L.I.; Marutescu, L.; Gheorghe, I.; Popa, M.; Czobor Barbu, I.; Cristescu, R.; Chifiriuc, M.-C. Bacteriocins in the Era of Antibiotic Resistance: Rising to the Challenge. *Pharmaceutics* **2021**, *13*, 196, doi:10.3390/pharmaceutics13020196.
8. Akova, M. Epidemiology of Antimicrobial Resistance in Bloodstream Infections. *Virulence* **2016**, *7*, 252–266, doi:10.1080/21505594.2016.1159366.
9. <https://www.who.int/news-room/fact-sheets/detail/cancer>.
10. Bukowski, K.; Kciuk, M.; Kontek, R. Mechanisms of Multidrug Resistance in Cancer Chemotherapy. *IJMS* **2020**, *21*, 3233, doi:10.3390/ijms21093233.
11. Neophytou, C.M.; Trougakos, I.P.; Erin, N.; Papageorgis, P. Apoptosis Deregulation and the Development of Cancer Multi-Drug Resistance. *Cancers* **2021**, *13*, 4363, doi:10.3390/cancers13174363.
12. Li, Y.-J.; Lei, Y.-H.; Yao, N.; Wang, C.-R.; Hu, N.; Ye, W.-C.; Zhang, D.-M.; Chen, Z.-S. Autophagy and Multidrug Resistance in Cancer. *Chin J Cancer* **2017**, *36*, 52, doi:10.1186/s40880-017-0219-2.
13. Goodman, L.S. NITROGEN MUSTARD THERAPY: Use of Methyl-Bis(Beta-Chloroethyl)Amine Hydrochloride and Tris(Beta-Chloroethyl)Amine Hydrochloride for Hodgkin's Disease, Lymphosarcoma, Leukemia and Certain Allied and Miscellaneous Disorders. *JAMA* **1946**, *132*, 126, doi:10.1001/jama.1946.02870380008004.

14. Szakács, G.; Paterson, J.K.; Ludwig, J.A.; Booth-Genthe, C.; Gottesman, M.M. Targeting Multidrug Resistance in Cancer. *Nat Rev Drug Discov* **2006**, *5*, 219–234, doi:10.1038/nrd1984.
15. Blagosklonny, M.V. Targeting Cancer Cells by Exploiting Their Resistance. *Trends in Molecular Medicine* **2003**, *9*, 307–312, doi:10.1016/S1471-4914(03)00111-4.
16. Wang, J.; Seebacher, N.; Shi, H.; Kan, Q.; Duan, Z. Novel Strategies to Prevent the Development of Multidrug Resistance (MDR) in Cancer. *Oncotarget* **2017**, *8*, 84559–84571, doi:10.18632/oncotarget.19187.
17. Martinez, J.L. General Principles of Antibiotic Resistance in Bacteria. *Drug Discovery Today: Technologies* **2014**, *11*, 33–39, doi:10.1016/j.ddtec.2014.02.001.
18. Levy, S.B.; Marshall, B. Antibacterial Resistance Worldwide: Causes, Challenges and Responses. *Nat Med* **2004**, *10*, S122–S129, doi:10.1038/nm1145.
19. Ventola, C.L. The Antibiotic Resistance Crisis: Part 1: Causes and Threats. *P T* **2015**, *40*, 277–283.
20. Bartlett, J.G.; Gilbert, D.N.; Spellberg, B. Seven Ways to Preserve the Miracle of Antibiotics. *Clinical Infectious Diseases* **2013**, *56*, 1445–1450, doi:10.1093/cid/cit070.
21. Aslam, B.; Wang, W.; Arshad, M.I.; Khurshid, M.; Muzammil, S.; Rasool, M.H.; Nisar, M.A.; Alvi, R.F.; Aslam, M.A.; Qamar, M.U.; et al. Antibiotic Resistance: A Rundown of a Global Crisis. *IDR* **2018**, *Volume 11*, 1645–1658, doi:10.2147/IDR.S173867.
22. Read, A.F.; Woods, R.J. Antibiotic Resistance Management. *Evolution, Medicine, and Public Health* **2014**, *2014*, 147–147, doi:10.1093/emph/eou024.
23. C Reygaert, W.; Department of Biomedical Sciences, Oakland University William Beaumont School of Medicine, Rochester, MI, USA An Overview of the Antimicrobial Resistance Mechanisms of Bacteria. *AIMS Microbiology* **2018**, *4*, 482–501, doi:10.3934/microbiol.2018.3.482.
24. C Reygaert, W.; Department of Biomedical Sciences, Oakland University William Beaumont School of Medicine, Rochester, MI, USA An Overview of the Antimicrobial Resistance Mechanisms of Bacteria. *AIMS Microbiology* **2018**, *4*, 482–501, doi:10.3934/microbiol.2018.3.482.
25. Alav, I.; Sutton, J.M.; Rahman, K.M. Role of Bacterial Efflux Pumps in Biofilm Formation. *J Antimicrob Chemother* **2018**, *73*, 2003–2020, doi:10.1093/jac/dky042.
26. Marquez, B. Bacterial Efflux Systems and Efflux Pumps Inhibitors. *Biochimie* **2005**, *87*, 1137–1147, doi:10.1016/j.biochi.2005.04.012.
27. Alav, I.; Sutton, J.M.; Rahman, K.M. Role of Bacterial Efflux Pumps in Biofilm Formation. *Journal of Antimicrobial Chemotherapy* **2018**, *73*, 2003–2020, doi:10.1093/jac/dky042.
28. Teelucksingh, T.; Thompson, L.K.; Cox, G. The Evolutionary Conservation of Escherichia Coli Drug Efflux Pumps Supports Physiological Functions. *J Bacteriol* **2020**, *202*, e00367-20, doi:10.1128/JB.00367-20.

29. Hassan, K.A.; Liu, Q.; Elbourne, L.D.H.; Ahmad, I.; Sharples, D.; Naidu, V.; Chan, C.L.; Li, L.; Harborne, S.P.D.; Pokhrel, A.; et al. Pacing across the Membrane: The Novel PACE Family of Efflux Pumps Is Widespread in Gram-Negative Pathogens. *Research in Microbiology* **2018**, *169*, 450–454, doi:10.1016/j.resmic.2018.01.001.
30. Huang, L.; Wu, C.; Gao, H.; Xu, C.; Dai, M.; Huang, L.; Hao, H.; Wang, X.; Cheng, G. Bacterial Multidrug Efflux Pumps at the Frontline of Antimicrobial Resistance: An Overview. *Antibiotics* **2022**, *11*, 520, doi:10.3390/antibiotics11040520.
31. Delmar, J.A.; Yu, E.W. The AbgT Family: A Novel Class of Antimetabolite Transporters: AbgT Family of Antimetabolite Transporters. *Protein Science* **2016**, *25*, 322–337, doi:10.1002/pro.2820.
32. Pasqua; Grossi; Zennaro; Fanelli; Micheli; Barras; Colonna; Prosseda The Varied Role of Efflux Pumps of the MFS Family in the Interplay of Bacteria with Animal and Plant Cells. *Microorganisms* **2019**, *7*, 285, doi:10.3390/microorganisms7090285.
33. Henderson, P.J.F.; Maher, C.; Elbourne, L.D.H.; Eijkelkamp, B.A.; Paulsen, I.T.; Hassan, K.A. Physiological Functions of Bacterial “Multidrug” Efflux Pumps. *Chem. Rev.* **2021**, *121*, 5417–5478, doi:10.1021/acs.chemrev.0c01226.
34. Nikaido, H. RND Transporters in the Living World. *Research in Microbiology* **2018**, *169*, 363–371, doi:10.1016/j.resmic.2018.03.001.
35. Hassan, K.A.; Liu, Q.; Elbourne, L.D.H.; Ahmad, I.; Sharples, D.; Naidu, V.; Chan, C.L.; Li, L.; Harborne, S.P.D.; Pokhrel, A.; et al. Pacing across the Membrane: The Novel PACE Family of Efflux Pumps Is Widespread in Gram-Negative Pathogens. *Research in Microbiology* **2018**, *169*, 450–454, doi:10.1016/j.resmic.2018.01.001.
36. Branda, S.S.; Vik, Å.; Friedman, L.; Kolter, R. Biofilms: The Matrix Revisited. *Trends in Microbiology* **2005**, *13*, 20–26, doi:10.1016/j.tim.2004.11.006.
37. Jamal, M.; Ahmad, W.; Andleeb, S.; Jalil, F.; Imran, M.; Nawaz, M.A.; Hussain, T.; Ali, M.; Rafiq, M.; Kamil, M.A. Bacterial Biofilm and Associated Infections. *Journal of the Chinese Medical Association* **2018**, *81*, 7–11, doi:10.1016/j.jcma.2017.07.012.
38. Sun, D.; Accavitti, M.A.; Bryers, J.D. Inhibition of Biofilm Formation by Monoclonal Antibodies against *Staphylococcus Epidermidis* RP62A Accumulation-Associated Protein. *Clin Vaccine Immunol* **2005**, *12*, 93–100, doi:10.1128/CDLI.12.1.93-100.2005.
39. Secchi, E.; Savorana, G.; Vitale, A.; Eberl, L.; Stocker, R.; Rusconi, R. The Structural Role of Bacterial eDNA in the Formation of Biofilm Streamers. *Proc. Natl. Acad. Sci. U.S.A.* **2022**, *119*, e2113723119, doi:10.1073/pnas.2113723119.
40. Barnes, A.M.T.; Ballering, K.S.; Leibman, R.S.; Wells, C.L.; Dunny, G.M. *Enterococcus Faecalis* Produces Abundant Extracellular Structures Containing DNA in the Absence of Cell Lysis during Early Biofilm Formation. *mBio* **2012**, *3*, e00193-12, doi:10.1128/mBio.00193-12.
41. Peng, N.; Cai, P.; Mortimer, M.; Wu, Y.; Gao, C.; Huang, Q. The Exopolysaccharide–eDNA Interaction Modulates 3D Architecture of *Bacillus Subtilis* Biofilm. *BMC Microbiol* **2020**, *20*, 115, doi:10.1186/s12866-020-01789-5.

42. Donlan, R.M. Biofilms: Microbial Life on Surfaces. *Emerg. Infect. Dis.* **2002**, *8*, 881–890, doi:10.3201/eid0809.020063.
43. Sutherland, I. The Biofilm Matrix – an Immobilized but Dynamic Microbial Environment. *Trends in Microbiology* **2001**, *9*, 222–227, doi:10.1016/S0966-842X(01)02012-1.
44. Yin, W.; Wang, Y.; Liu, L.; He, J. Biofilms: The Microbial “Protective Clothing” in Extreme Environments. *IJMS* **2019**, *20*, 3423, doi:10.3390/ijms20143423.
45. Gilbert, P.; Collier, P.J.; Brown, M.R. Influence of Growth Rate on Susceptibility to Antimicrobial Agents: Biofilms, Cell Cycle, Dormancy, and Stringent Response. *Antimicrob Agents Chemother* **1990**, *34*, 1865–1868, doi:10.1128/AAC.34.10.1865.
46. Miyaue, S.; Suzuki, E.; Komiyama, Y.; Kondo, Y.; Morikawa, M.; Maeda, S. Bacterial Memory of Persisters: Bacterial Persister Cells Can Retain Their Phenotype for Days or Weeks After Withdrawal From Colony–Biofilm Culture. *Front. Microbiol.* **2018**, *9*, 1396, doi:10.3389/fmicb.2018.01396.
47. Dincer, S.; Masume Uslu, F.; Delik, A. Antibiotic Resistance in Biofilm. In *Bacterial Biofilms*; Dincer, S., Sümengen Özdenefe, M., Arkut, A., Eds.; IntechOpen, 2020 ISBN 978-1-78985-899-0.
48. Pena, R.T.; Blasco, L.; Ambroa, A.; González-Pedrajo, B.; Fernández-García, L.; López, M.; Bleriot, I.; Bou, G.; García-Contreras, R.; Wood, T.K.; et al. Relationship Between Quorum Sensing and Secretion Systems. *Front. Microbiol.* **2019**, *10*, 1100, doi:10.3389/fmicb.2019.01100.
49. <sup>1</sup>Department of Biochemistry and Molecular Biology, University of Bucharest, Faculty of Biology, Bucharest, Romania; Preda, V.G.; Săndulescu, O.; Department of Infectious Diseases I, Carol Davila University of Medicine and Pharmacy, National Institute for Infectious Diseases “Prof. Dr. Matei Balș”, Bucharest, Romania Communication Is the Key: Biofilms, Quorum Sensing, Formation and Prevention. *Discoveries (Craiova)* **2019**, *7*, e10, doi:10.15190/d.2019.13.
50. Solano, C.; Echeverz, M.; Lasa, I. Biofilm Dispersion and Quorum Sensing. *Current Opinion in Microbiology* **2014**, *18*, 96–104, doi:10.1016/j.mib.2014.02.008.
51. Verbeke, F.; De Craemer, S.; Debunne, N.; Janssens, Y.; Wynendaele, E.; Van De Wiele, C.; De Spiegeleer, B. Peptides as Quorum Sensing Molecules: Measurement Techniques and Obtained Levels In Vitro and In Vivo. *Front. Neurosci.* **2017**, *11*, doi:10.3389/fnins.2017.00183.
52. LaSarre, B.; Federle, M.J. Exploiting Quorum Sensing To Confuse Bacterial Pathogens. *Microbiol Mol Biol Rev* **2013**, *77*, 73–111, doi:10.1128/MMBR.00046-12.
53. Jiang, Q.; Chen, J.; Yang, C.; Yin, Y.; Yao, K. Quorum Sensing: A Prospective Therapeutic Target for Bacterial Diseases. *BioMed Research International* **2019**, *2019*, 1–15, doi:10.1155/2019/2015978.
54. Sankar Ganesh, P.; Ravishankar Rai, V. Attenuation of Quorum-Sensing-Dependent Virulence Factors and Biofilm Formation by Medicinal Plants against Antibiotic Resistant

*Pseudomonas Aeruginosa*. *Journal of Traditional and Complementary Medicine* **2018**, *8*, 170–177, doi:10.1016/j.jtcme.2017.05.008.

55. Spengler, G.; Kincses, A.; Gajdács, M.; Amaral, L. New Roads Leading to Old Destinations: Efflux Pumps as Targets to Reverse Multidrug Resistance in Bacteria. *Molecules* **2017**, *22*, 468, doi:10.3390/molecules22030468.

56. Laws, M.; Shaaban, A.; Rahman, K.M. Antibiotic Resistance Breakers: Current Approaches and Future Directions. *FEMS Microbiology Reviews* **2019**, *43*, 490–516, doi:10.1093/femsre/fuz014.

57. Lomovskaya, O.; Warren, M.S.; Lee, A.; Galazzo, J.; Fronko, R.; Lee, M.; Blais, J.; Cho, D.; Chamberland, S.; Renau, T.; et al. Identification and Characterization of Inhibitors of Multidrug Resistance Efflux Pumps in *Pseudomonas Aeruginosa*: Novel Agents for Combination Therapy. *Antimicrob Agents Chemother* **2001**, *45*, 105–116, doi:10.1128/AAC.45.1.105-116.2001.

58. Sjuts, H.; Vargiu, A.V.; Kwasny, S.M.; Nguyen, S.T.; Kim, H.-S.; Ding, X.; Ornik, A.R.; Ruggerone, P.; Bowlin, T.L.; Nikaido, H.; et al. Molecular Basis for Inhibition of AcrB Multidrug Efflux Pump by Novel and Powerful Pyranopyridine Derivatives. *Proc. Natl. Acad. Sci. U.S.A.* **2016**, *113*, 3509–3514, doi:10.1073/pnas.1602472113.

59. Amaral, L.; Martins, M.; Viveiros, M.; Molnar, J.; Kristiansen, J. Promising Therapy of XDR-TB/MDR-TB with Thioridazine an Inhibitor of Bacterial Efflux Pumps. *CDT* **2008**, *9*, 816–819, doi:10.2174/138945008785747798.

60. Grimsey, E.M.; Fais, C.; Marshall, R.L.; Ricci, V.; Ciusa, M.L.; Stone, J.W.; Ivens, A.; Malloci, G.; Ruggerone, P.; Vargiu, A.V.; et al. Chlorpromazine and Amitriptyline Are Substrates and Inhibitors of the AcrB Multidrug Efflux Pump. *mBio* **2020**, *11*, e00465-20, doi:10.1128/mBio.00465-20.

61. Adamson, D.H.; Krikstopaityte, V.; Coote, P.J. Enhanced Efficacy of Putative Efflux Pump Inhibitor/Antibiotic Combination Treatments versus MDR Strains of *Pseudomonas Aeruginosa* in a *Galleria Mellonella in Vivo* Infection Model. *Journal of Antimicrobial Chemotherapy* **2015**, *70*, 2271–2278, doi:10.1093/jac/dkv111.

62. Kaatz, G. Phenylpiperidine Selective Serotonin Reuptake Inhibitors Interfere with Multidrug Efflux Pump Activity in *Staphylococcus Aureus*. *International Journal of Antimicrobial Agents* **2003**, *22*, 254–261, doi:10.1016/S0924-8579(03)00220-6.

63. Witek, K.; Nasim, M.; Bischoff, M.; Gaupp, R.; Arsenyan, P.; Vasiljeva, J.; Marć, M.; Olejarz, A.; Latacz, G.; Kieć-Kononowicz, K.; et al. Selenazolinium Salts as “Small Molecule Catalysts” with High Potency against ESKAPE Bacterial Pathogens. *Molecules* **2017**, *22*, 2174, doi:10.3390/molecules22122174.

64. Gröblacher, B.; Kunert, O.; Bucar, F. Compounds of *Alpinia Katsumadai* as Potential Efflux Inhibitors in *Mycobacterium Smegmatis*. *Bioorganic & Medicinal Chemistry* **2012**, *20*, 2701–2706, doi:10.1016/j.bmc.2012.02.039.

65. Bame, J.; Graf, T.; Junio, H.; Bussey, R.; Jarmusch, S.; El-Elimat, T.; Falkinham, J.; Oberlies, N.; Cech, R.; Cech, N. Sarothrin from *Alkanna Orientalis* Is an Antimicrobial Agent and Efflux Pump Inhibitor. *Planta Med* **2013**, *79*, 327–329, doi:10.1055/s-0032-1328259.

66. Kalia, N.P.; Mahajan, P.; Mehra, R.; Nargotra, A.; Sharma, J.P.; Koul, S.; Khan, I.A. Capsaicin, a Novel Inhibitor of the NorA Efflux Pump, Reduces the Intracellular Invasion of *Staphylococcus Aureus*. *Journal of Antimicrobial Chemotherapy* **2012**, *67*, 2401–2408, doi:10.1093/jac/dks232.
67. Amaral, L.; Spengler, G.; Martins, A.; Armada, A.; Handzlik, J.; Kiec-Kononowicz, K.; Molnar, J. Inhibitors of Bacterial Efflux Pumps That Also Inhibit Efflux Pumps of Cancer Cells. *Anticancer Res* **2012**, *32*, 2947–2957.
68. Duesberg, P.; Stindl, R.; Hehlmann, R. Explaining the High Mutation Rates of Cancer Cells to Drug and Multidrug Resistance by Chromosome Reassortments That Are Catalyzed by Aneuploidy. *Proc. Natl. Acad. Sci. U.S.A.* **2000**, *97*, 14295–14300, doi:10.1073/pnas.97.26.14295.
69. Kanwal, R.; Gupta, S. Epigenetic Modifications in Cancer. *Clinical Genetics* **2012**, *81*, 303–311, doi:10.1111/j.1399-0004.2011.01809.x.
70. Ham, I.-H.; Oh, H.J.; Jin, H.; Bae, C.A.; Jeon, S.-M.; Choi, K.S.; Son, S.-Y.; Han, S.-U.; Brekken, R.A.; Lee, D.; et al. Targeting Interleukin-6 as a Strategy to Overcome Stroma-Induced Resistance to Chemotherapy in Gastric Cancer. *Mol Cancer* **2019**, *18*, 68, doi:10.1186/s12943-019-0972-8.
71. Setrerrahmane, S.; Xu, H. Tumor-Related Interleukins: Old Validated Targets for New Anti-Cancer Drug Development. *Mol Cancer* **2017**, *16*, 153, doi:10.1186/s12943-017-0721-9.
72. Gentile, F.; Elmenoufy, A.H.; Ciniero, G.; Jay, D.; Karimi-Busheri, F.; Barakat, K.H.; Weinfeld, M.; West, F.G.; Tuszynski, J.A. Computer-aided Drug Design of Small Molecule Inhibitors of the ERCC1-XPF Protein–Protein Interaction. *Chem Biol Drug Des* **2020**, *95*, 460–471, doi:10.1111/cbdd.13660.
73. Pathania, S.; Bhatia, R.; Baldi, A.; Singh, R.; Rawal, R.K. Drug Metabolizing Enzymes and Their Inhibitors' Role in Cancer Resistance. *Biomedicine & Pharmacotherapy* **2018**, *105*, 53–65, doi:10.1016/j.biopha.2018.05.117.
74. Ramsay, E.E.; Dilda, P.J. Glutathione S-Conjugates as Prodrugs to Target Drug-Resistant Tumors. *Front. Pharmacol.* **2014**, *5*, doi:10.3389/fphar.2014.00181.
75. Rees, D.C.; Johnson, E.; Lewinson, O. ABC Transporters: The Power to Change. *Nat Rev Mol Cell Biol* **2009**, *10*, 218–227, doi:10.1038/nrm2646.
76. Robey, R.W.; Pluchino, K.M.; Hall, M.D.; Fojo, A.T.; Bates, S.E.; Gottesman, M.M. Revisiting the Role of ABC Transporters in Multidrug-Resistant Cancer. *Nat Rev Cancer* **2018**, *18*, 452–464, doi:10.1038/s41568-018-0005-8.
77. Juliano, R.L.; Ling, V. A Surface Glycoprotein Modulating Drug Permeability in Chinese Hamster Ovary Cell Mutants. *Biochimica et Biophysica Acta (BBA) - Biomembranes* **1976**, *455*, 152–162, doi:10.1016/0005-2736(76)90160-7.
78. Cole, S.; Bhardwaj, G.; Gerlach, J.; Mackie, J.; Grant, C.; Almquist, K.; Stewart, A.; Kurz, E.; Duncan, A.; Deeley, R. Overexpression of a Transporter Gene in a Multidrug-Resistant Human Lung Cancer Cell Line. *Science* **1992**, *258*, 1650–1654, doi:10.1126/science.1360704.



79. Mirski, S.E.; Gerlach, J.H.; Cole, S.P. Multidrug Resistance in a Human Small Cell Lung Cancer Cell Line Selected in Adriamycin. *Cancer Res* **1987**, *47*, 2594–2598.
80. Allikmets, R.; Schriml, L.M.; Hutchinson, A.; Romano-Spica, V.; Dean, M. A Human Placenta-Specific ATP-Binding Cassette Gene (ABCP) on Chromosome 4q22 That Is Involved in Multidrug Resistance. *Cancer Res* **1998**, *58*, 5337–5339.
81. Doyle, L.A.; Yang, W.; Abruzzo, L.V.; Krogmann, T.; Gao, Y.; Rishi, A.K.; Ross, D.D. A Multidrug Resistance Transporter from Human MCF-7 Breast Cancer Cells. *Proc. Natl. Acad. Sci. U.S.A.* **1998**, *95*, 15665–15670, doi:10.1073/pnas.95.26.15665.
82. Kannan, P.; John, C.; Zoghbi, S.S.; Halldin, C.; Gottesman, M.M.; Innis, R.B.; Hall, M.D. Imaging the Function of P-Glycoprotein With Radiotracers: Pharmacokinetics and In Vivo Applications. *Clin Pharmacol Ther* **2009**, *86*, 368–377, doi:10.1038/clpt.2009.138.
83. Dong, J.; Yuan, L.; Hu, C.; Cheng, X.; Qin, J.-J. Strategies to Overcome Cancer Multidrug Resistance (MDR) through Targeting P-Glycoprotein (ABCB1): An Updated Review. *Pharmacology & Therapeutics* **2023**, *249*, 108488, doi:10.1016/j.pharmthera.2023.108488.
84. Srivalli, K.M.R.; Lakshmi, P.K. Overview of P-Glycoprotein Inhibitors: A Rational Outlook. *Braz. J. Pharm. Sci.* **2012**, *48*, 353–367, doi:10.1590/S1984-82502012000300002.
85. Glavinas, H.; Krajcsi, P.; Cserepes, J.; Sarkadi, B. The Role of ABC Transporters in Drug Resistance, Metabolism and Toxicity. *CDD* **2004**, *1*, 27–42, doi:10.2174/1567201043480036.
86. Eckford, P.D.W.; Sharom, F.J. ABC Efflux Pump-Based Resistance to Chemotherapy Drugs. *Chem. Rev.* **2009**, *109*, 2989–3011, doi:10.1021/cr9000226.
87. Gottesman, M.M.; Fojo, T.; Bates, S.E. Multidrug Resistance in Cancer: Role of ATP-Dependent Transporters. *Nat Rev Cancer* **2002**, *2*, 48–58, doi:10.1038/nrc706.
88. Robinson, K.; Tiriveedhi, V. Perplexing Role of P-Glycoprotein in Tumor Microenvironment. *Front. Oncol.* **2020**, *10*, 265, doi:10.3389/fonc.2020.00265.
89. Choi, Y.; Yu, A.-M. ABC Transporters in Multidrug Resistance and Pharmacokinetics, and Strategies for Drug Development. *CPD* **2014**, *20*, 793–807, doi:10.2174/138161282005140214165212.
90. Wu, Z.-X.; Yang, Y.; Wang, J.-Q.; Zhou, W.-M.; Chen, J.; Fu, Y.-G.; Patel, K.; Chen, Z.-S.; Zhang, J.-Y. Elevated ABCB1 Expression Confers Acquired Resistance to Aurora Kinase Inhibitor GSK-1070916 in Cancer Cells. *Front. Pharmacol.* **2021**, *11*, 615824, doi:10.3389/fphar.2020.615824.
91. Moitra, K.; Lou, H.; Dean, M. Multidrug Efflux Pumps and Cancer Stem Cells: Insights Into Multidrug Resistance and Therapeutic Development. *Clin Pharmacol Ther* **2011**, *89*, 491–502, doi:10.1038/clpt.2011.14.
92. Hegedűs, C.; Özvegy-Laczka, C.; Apáti, Á.; Magócsi, M.; Németh, K.; Órfi, L.; Kéri, G.; Katona, M.; Takáts, Z.; Váradi, A.; et al. Interaction of Nilotinib, Dasatinib and Bosutinib with ABCB1 and ABCG2: Implications for Altered Anti-Cancer Effects and Pharmacological

Properties: Interaction of Bcr-Abl Inhibitors and MDR-ABC Proteins. *British Journal of Pharmacology* **2009**, *158*, 1153–1164, doi:10.1111/j.1476-5381.2009.00383.x.

93. Seiden, M.V.; Swenerton, K.D.; Matulonis, U.; Campos, S.; Rose, P.; Batist, G.; Ette, E.; Garg, V.; Fuller, A.; Harding, M.W.; et al. A Phase II Study of the MDR Inhibitor Biricodar (INCEL, VX-710) and Paclitaxel in Women with Advanced Ovarian Cancer Refractory to Paclitaxel Therapy. *Gynecologic Oncology* **2002**, *86*, 302–310, doi:10.1006/gyno.2002.6762.

94. Kumar, A.; Jaitak, V. Natural Products as Multidrug Resistance Modulators in Cancer. *European Journal of Medicinal Chemistry* **2019**, *176*, 268–291, doi:10.1016/j.ejmech.2019.05.027.

95. Callaghan, R.; Luk, F.; Bebawy, M. Inhibition of the Multidrug Resistance P-Glycoprotein: Time for a Change of Strategy? *Drug Metab Dispos* **2014**, *42*, 623–631, doi:10.1124/dmd.113.056176.

96. Tsuruo, T.; Iida, H.; Tsukagoshi, S.; Sakurai, Y. Increased Accumulation of Vincristine and Adriamycin in Drug-Resistant P388 Tumor Cells Following Incubation with Calcium Antagonists and Calmodulin Inhibitors. *Cancer Res* **1982**, *42*, 4730–4733.

97. Ozols, R.F.; Cunnion, R.E.; Klecker, R.W.; Hamilton, T.C.; Ostchega, Y.; Parrillo, J.E.; Young, R.C. Verapamil and Adriamycin in the Treatment of Drug-Resistant Ovarian Cancer Patients. *JCO* **1987**, *5*, 641–647, doi:10.1200/JCO.1987.5.4.641.

98. Crowley, E.; McDevitt, C.A.; Callaghan, R. Generating Inhibitors of P-Glycoprotein: Where to, Now? In *Multi-Drug Resistance in Cancer*; Zhou, J., Ed.; Methods in Molecular Biology; Humana Press: Totowa, NJ, 2010; Vol. 596, pp. 405–432 ISBN 978-1-60761-415-9.

99. Boote, D.J.; Dennis, I.F.; Twentyman, P.R.; Osborne, R.J.; Laburte, C.; Hensel, S.; Smyth, J.F.; Brampton, M.H.; Bleehen, N.M. Phase I Study of Etoposide with SDZ PSC 833 as a Modulator of Multidrug Resistance in Patients with Cancer. *JCO* **1996**, *14*, 610–618, doi:10.1200/JCO.1996.14.2.610.

100. Warner, E.; Hedley, D.; Andrulis, I.; Myers, R.; Trudeau, M.; Warr, D.; Pritchard, K.I.; Blackstein, M.; Goss, P.E.; Franssen, E.; et al. Phase II Study of Dexverapamil plus Anthracycline in Patients with Metastatic Breast Cancer Who Have Progressed on the Same Anthracycline Regimen. *Clin Cancer Res* **1998**, *4*, 1451–1457.

101. Ichiro, N.; Kimitoshi, K.; Junko, K.; Michihiko, K.; Shin-Ichi, A.; Akira, K.; Ken-Ichi, S.; Yohji, Y.; Cornwell, M.M.; Pastan, I.; et al. Analysis of Structural Features of Dihydropyridine Analogs Needed to Reverse Multidrug Resistance and to Inhibit Photoaffinity Labeling of P-Glycoprotein. *Biochemical Pharmacology* **1989**, *38*, 519–527, doi:10.1016/0006-2952(89)90393-6.

102. Lai, J.-I.; Tseng, Y.-J.; Chen, M.-H.; Huang, C.-Y.F.; Chang, P.M.-H. Clinical Perspective of FDA Approved Drugs With P-Glycoprotein Inhibition Activities for Potential Cancer Therapeutics. *Front. Oncol.* **2020**, *10*, 561936, doi:10.3389/fonc.2020.561936.

103. Werle, M.; Takeuchi, H.; Bernkop-Schnürch, A. New-Generation Efflux Pump Inhibitors. *Expert Review of Clinical Pharmacology* **2008**, *1*, 429–440, doi:10.1586/17512433.1.3.429.

104. Wu, C.-P.; Ohnuma, S.; V. Ambudkar, S. Discovering Natural Product Modulators to Overcome Multidrug Resistance in Cancer Chemotherapy. *CPB* **2011**, *12*, 609–620, doi:10.2174/138920111795163887.
105. Crowley, E.; McDevitt, C.A.; Callaghan, R. Generating Inhibitors of P-Glycoprotein: Where to, Now? In *Multi-Drug Resistance in Cancer*; Zhou, J., Ed.; Methods in Molecular Biology; Humana Press: Totowa, NJ, 2010; Vol. 596, pp. 405–432 ISBN 978-1-60761-415-9.
106. Mohammad, R.M.; Muqbil, I.; Lowe, L.; Yedjou, C.; Hsu, H.-Y.; Lin, L.-T.; Siegelin, M.D.; Fimognari, C.; Kumar, N.B.; Dou, Q.P.; et al. Broad Targeting of Resistance to Apoptosis in Cancer. *Seminars in Cancer Biology* **2015**, *35*, S78–S103, doi:10.1016/j.semcancer.2015.03.001.
107. Wong, R.S. Apoptosis in Cancer: From Pathogenesis to Treatment. *J Exp Clin Cancer Res* **2011**, *30*, 87, doi:10.1186/1756-9966-30-87.
108. Messmer, M.N.; Snyder, A.G.; Oberst, A. Comparing the Effects of Different Cell Death Programs in Tumor Progression and Immunotherapy. *Cell Death Differ* **2019**, *26*, 115–129, doi:10.1038/s41418-018-0214-4.
109. Dunn, G.P.; Old, L.J.; Schreiber, R.D. The Immunobiology of Cancer Immunosurveillance and Immunoediting. *Immunity* **2004**, *21*, 137–148, doi:10.1016/j.immuni.2004.07.017.
110. O'Donnell, J.S.; Teng, M.W.L.; Smyth, M.J. Cancer Immunoediting and Resistance to T Cell-Based Immunotherapy. *Nat Rev Clin Oncol* **2019**, *16*, 151–167, doi:10.1038/s41571-018-0142-8.
111. Fernald, K.; Kurokawa, M. Evading Apoptosis in Cancer. *Trends in Cell Biology* **2013**, *23*, 620–633, doi:10.1016/j.tcb.2013.07.006.
112. Alcolea, V.; Pérez-Silanes, S. Selenium as an Interesting Option for the Treatment of Chagas Disease: A Review. *European Journal of Medicinal Chemistry* **2020**, *206*, 112673, doi:10.1016/j.ejmech.2020.112673.
113. Di Bella, S.; Grilli, E.; Cataldo, M.A.; Petrosillo, N. Selenium Deficiency and HIV Infection. *Infectious Disease Reports* **2010**, *2*, e18, doi:10.4081/idr.2010.e18.
114. Domínguez-Álvarez, E.; Rácz, B.; Marć, M.A.; Nasim, M.J.; Szemerédi, N.; Viktorová, J.; Jacob, C.; Spengler, G. Selenium and Tellurium in the Development of Novel Small Molecules and Nanoparticles as Cancer Multidrug Resistance Reversal Agents. *Drug Resistance Updates* **2022**, *63*, 100844, doi:10.1016/j.drug.2022.100844.
115. Satarzadeh, N.; Sadeghi Dousari, A.; Amirheidari, B.; Shakibaie, M.; Ramezani Sarbandi, A.; Forootanfar, H. An Insight into Biofabrication of Selenium Nanostructures and Their Biomedical Application. *3 Biotech* **2023**, *13*, 79, doi:10.1007/s13205-023-03476-4.
116. Domínguez-Álvarez, E.; Gajdács, M.; Spengler, G.; Palop, J.A.; Marć, M.A.; Kieć-Kononowicz, K.; Amaral, L.; Molnár, J.; Jacob, C.; Handzlik, J.; et al. Identification of Selenocompounds with Promising Properties to Reverse Cancer Multidrug Resistance. *Bioorganic & Medicinal Chemistry Letters* **2016**, *26*, 2821–2824, doi:csonka.

117. Nové, M.; Kincses, A.; Szalontai, B.; Rácz, B.; Blair, J.M.A.; González-Prádena, A.; Benito-Lama, M.; Domínguez-Álvarez, E.; Spengler, G. Biofilm Eradication by Symmetrical Selenoesters for Food-Borne Pathogens. *Microorganisms* **2020**, *8*, 566, doi:10.3390/microorganisms8040566.
118. De La Cruz-Claure, M.L.; Céspedes-Llave, A.A.; Ulloa, M.T.; Benito-Lama, M.; Domínguez-Álvarez, E.; Bastida, A. Inhibition–Disruption of *Candida Glabrata* Biofilms: Symmetrical Selenoesters as Potential Anti-Biofilm Agents. *Microorganisms* **2019**, *7*, 664, doi:10.3390/microorganisms7120664.
119. Gajdács, M.; Spengler, G.; Sanmartín, C.; Maré, M.A.; Handzlik, J.; Domínguez-Álvarez, E. Selenoesters and Selenoanhydrides as Novel Multidrug Resistance Reversing Agents: A Confirmation Study in a Colon Cancer MDR Cell Line. *Bioorganic & Medicinal Chemistry Letters* **2017**, *27*, 797–802, doi:10.1016/j.bmcl.2017.01.033.
120. Csonka, A.; Kincses, A.; Nové, M.; Vadas, Z.; Sanmartín, C.; Domínguez-Álvarez, E.; Spengler, G. Selenoesters and Selenoanhydrides as Novel Agents Against Resistant Breast Cancer. *Anticancer Res* **2019**, *39*, 3777–3783, doi:10.21873/anticancer.13526.
121. Domínguez Álvarez E., Spengler G., Jacob C., Sanmartín Grijalba M.C. Selenoester-Containing Compounds for Use in the Treatment of Microbial Infections or Colorectal Cancer. EP18382693. European Patent. 2018 Sep 28;
122. Szemerédi, N.; Dobiasová, S.; Salardón-Jiménez, N.; Kincses, A.; Nové, M.; Habibullah, G.; Sevilla-Hernández, C.; Benito-Lama, M.; Alonso-Martínez, F.-J.; Viktorová, J.; et al. Cyano- and Ketone-Containing Selenoesters as Multi-Target Compounds against Resistant Cancers. *Cancers* **2021**, *13*, 4563, doi:10.3390/cancers13184563.
123. <https://www.nih.org.pk/wp-content/uploads/2021/02/CLSI-2020.pdf>.
124. Viktorová, J.; Stupák, M.; Řehořová, K.; Dobiasová, S.; Hoang, L.; Hajšlová, J.; Van Thanh, T.; Van Tri, L.; Van Tuan, N.; Ruml, T. Lemon Grass Essential Oil Does Not Modulate Cancer Cells Multidrug Resistance by Citral—Its Dominant and Strongly Antimicrobial Compound. *Foods* **2020**, *9*, 585, doi:10.3390/foods9050585.
125. Holasová, K.; Křížkovská, B.; Hoang, L.; Dobiasová, S.; Lipov, J.; Macek, T.; Křen, V.; Valentová, K.; Ruml, T.; Viktorová, J. Flavonolignans from Silymarin Modulate Antibiotic Resistance and Virulence in *Staphylococcus Aureus*. *Biomedicine & Pharmacotherapy* **2022**, *149*, 112806, doi:10.1016/j.biopha.2022.112806.
126. Spengler, G.; Kincses, A.; Rácz, B.; Varga, B.; Watanabe, G.; Saijo, R.; Sekiya, H.; Tamai, E.; Maki, J.; Molnár, J.; et al. Benzoxazole-Based Zn(II) and Cu(II) Complexes Overcome Multidrug-Resistance in Cancer. *Anticancer Res* **2018**, *38*, 6181–6187, doi:10.21873/anticancer.12971.
127. Chou, T.-C. Drug Combination Studies and Their Synergy Quantification Using the Chou-Talalay Method. *Cancer Research* **2010**, *70*, 440–446, doi:10.1158/0008-5472.CAN-09-1947.
128. Chou, T.-C. Theoretical Basis, Experimental Design, and Computerized Simulation of Synergism and Antagonism in Drug Combination Studies. *Pharmacol Rev* **2006**, *58*, 621–681, doi:10.1124/pr.58.3.10.

129. Dongping, M.,; Cali, J.J.: Identify P-Glycoprotein Substrates and Inhibitors with the Rapid, HTS Pgp-Glo™ Assay System. *Promega Notes* 96: 11-14., 2007.
130. Richter, M.F.; Hergenrother, P.J. The Challenge of Converting Gram-Positive-Only Compounds into Broad-Spectrum Antibiotics: Challenges in Developing Broad-Spectrum Antibiotics. *Ann. N.Y. Acad. Sci.* **2019**, *1435*, 18–38, doi:10.1111/nyas.13598.
131. Nikolic, P.; Mudgil, P.; Harman, D.G.; Whitehall, J. Untargeted Lipidomic Differences between Clinical Strains of Methicillin-Sensitive and Methicillin-Resistant *Staphylococcus Aureus*. *Infectious Diseases* **2022**, *54*, 497–507, doi:10.1080/23744235.2022.2049863.
132. Rozgonyi, F.; Kocsis, E.; Kristóf, K.; Nagy, K. Is MRSA More Virulent than MSSA? *Clinical Microbiology and Infection* **2007**, *13*, 843–845, doi:10.1111/j.1469-0691.2007.01780.x.
133. Hassanzadeh, S.; Ganjloo, S.; Pourmand, M.R.; Mashhadi, R.; Ghazvini, K. Epidemiology of Efflux Pumps Genes Mediating Resistance among *Staphylococcus Aureus*; A Systematic Review. *Microbial Pathogenesis* **2020**, *139*, 103850, doi:10.1016/j.micpath.2019.103850.
134. Peña-Morán, O.; Villarreal, M.; Álvarez-Berber, L.; Meneses-Acosta, A.; Rodríguez-López, V. Cytotoxicity, Post-Treatment Recovery, and Selectivity Analysis of Naturally Occurring Podophyllotoxins from *Bursera Fagaroides* Var. *Fagaroides* on Breast Cancer Cell Lines. *Molecules* **2016**, *21*, 1013, doi:10.3390/molecules21081013.
135. Ghosh, A.; Jayaraman, N.; Chatterji, D. Small-Molecule Inhibition of Bacterial Biofilm. *ACS Omega* **2020**, *5*, 3108–3115, doi:10.1021/acsomega.9b03695.
136. Macia, M.D.; Rojo-Molinero, E.; Oliver, A. Antimicrobial Susceptibility Testing in Biofilm-Growing Bacteria. *Clinical Microbiology and Infection* **2014**, *20*, 981–990, doi:10.1111/1469-0691.12651.
137. BIOSOFT. CalcuSyn, Version 2.00; BIOSOFT: Cambridge, UK, 2005; Available Online: [Http://Www.Biosoft.Com](http://www.biosoft.com) (Accessed on 23 Februar).
138. Pfeffer, C.; Singh, A. Apoptosis: A Target for Anticancer Therapy. *IJMS* **2018**, *19*, 448, doi:10.3390/ijms19020448.
139. Mosolygó, T.; Kincses, A.; Csonka, A.; Tönki, Á.S.; Witek, K.; Sanmartín, C.; Maré, M.A.; Handzlik, J.; Kieć-Kononowicz, K.; Domínguez-Álvarez, E.; et al. Selenocompounds as Novel Antibacterial Agents and Bacterial Efflux Pump Inhibitors. *Molecules* **2019**, *24*, 1487, doi:10.3390/molecules24081487.
140. Yong, Y.-C.; Zhong, J.-J. Impacts of Quorum Sensing on Microbial Metabolism and Human Health. In *Future Trends in Biotechnology*; Zhong, J.-J., Ed.; Advances in Biochemical Engineering/Biotechnology; Springer Berlin Heidelberg: Berlin, Heidelberg, 2012; Vol. 131, pp. 25–61 ISBN 978-3-642-36507-2.
141. Rezzonico, F.; Smits, T.H.M.; Duffy, B. Detection of AI-2 Receptors in Genomes of Enterobacteriaceae Suggests a Role of Type-2 Quorum Sensing in Closed Ecosystems. *Sensors* **2012**, *12*, 6645–6665, doi:10.3390/s120506645.

142. Taga, M.E.; Semmelhack, J.L.; Bassler, B.L. The LuxS-Dependent Autoinducer AI-2 Controls the Expression of an ABC Transporter That Functions in AI-2 Uptake in *Salmonella Typhimurium*: Autoinducer-Dependent Gene Regulation. *Molecular Microbiology* **2008**, *42*, 777–793, doi:10.1046/j.1365-2958.2001.02669.x.
143. Zhu, Z.; Kimura, M.; Itokawa, Y.; Aoki, T.; Takahashi, J.A.; Nakatsu, S.; Oda, Y.; Kikuchi, H. Apoptosis Induced by Selenium in Human Glioma Cell Lines. *Biol Trace Elem Res* **1996**, *54*, 123–134, doi:10.1007/BF02786259.
144. Ghosh, J. Rapid Induction of Apoptosis in Prostate Cancer Cells by Selenium: Reversal by Metabolites of Arachidonate 5-Lipoxygenase. *Biochemical and Biophysical Research Communications* **2004**, *315*, 624–635, doi:10.1016/j.bbrc.2004.01.100.
145. Zu, Y.; Yang, Z.; Tang, S.; Han, Y.; Ma, J. Effects of P-Glycoprotein and Its Inhibitors on Apoptosis in K562 Cells. *Molecules* **2014**, *19*, 13061–13075, doi:10.3390/molecules190913061.
146. Stavrovskaya, A.A.; Moiseeva, N.I. Non-Canonical Functions of the Cellular Transporter P-Glycoprotein. *Biochem. Moscow Suppl. Ser. A* **2016**, *10*, 241–250, doi:10.1134/S1990747816040085.

## FINANCIAL SUPPORT

The work on which this thesis was based on was supported by the following organizations and grants:

- Szeged Foundation for Cancer Research (Szegedi Rákkutatásért Alapítvány)
- COST Action CA17104 (STRATAGEM) - STSM
- New National Excellence Programme (ÚNKP) (2021 - UNKP-21-3-SZTE-103; 2022 - ÚNKP-22-3 - SZTE-285; 2023 - ÚNKP-23-4 -SZTE-347)
- GINOP-2.3.2-15-2016-00038
- EFOP-3.6.3-VEKOP-16-2017-00009
- SZTE ÁOK-KKA 2018/270-62-2 (Selenium derivatives as novel promising antibacterial agents) of the University of Szeged, Faculty of Medicine
- 2018-2.1.15-TÉT-PT-2018-00017 Bilateral Portuguese-Hungarian Science & Technology Cooperation (FCT/NKFIH, 2019/2020).
- OTKA K132446
- International Visegrad Fund (No. 22010090)

## APPENDIX

### Appendix 1. Names of the selenocompounds.

*Se*-(2-Oxopropyl) Thiophene-2-carboselenoate (**K1**)

*Se*-(2-Oxopropyl) 2-Fluorobenzoselenoate (**K2**)

*Se*-(2-Oxopropyl) 4-Bromobenzoselenoate (**K3**)

*Se*-(2-Oxopropyl) 2-(Trifluoromethyl)benzoselenoate (**K4**)

*Se*-(2-Oxopropyl) 3-(Trifluoromethyl)benzoselenoate (**K5**)

*Se*-(2-Oxopropyl) 3-Chloro-4-fluorobenzoselenoate (**K6**)

*Se*-(2-Oxopropyl) 4-(Tert-butyl)benzoselenoate (**K7**)

*Se*-(2-Oxopropyl) 2,4,5-Trifluorobenzoselenoate (**K8**)

*Se*-(Cyanomethyl) Thiophene-2-carboselenoate (**N1**)

*Se*-(Cyanomethyl) 3-Fluorobenzoselenoate (**N2**)

*Se*-(Cyanomethyl) 4-Bromobenzoselenoate (**N3**)

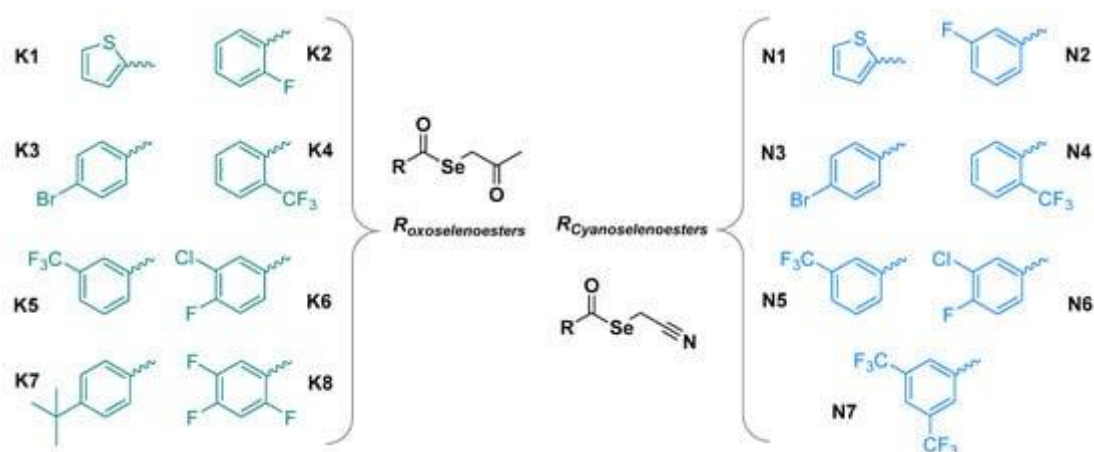
*Se*-(Cyanomethyl) 2-(Trifluoromethyl)benzoselenoate (**N4**)

*Se*-(Cyanomethyl) 3-(Trifluoromethyl)benzoselenoate (**N5**)

*Se*-(Cyanomethyl) 3-Chloro-4-fluorobenzoselenoate (**N6**)

*Se*-(Cyanomethyl) 3,5-Bis(trifluoromethyl)benzoselenoate (**N7**)





**Appendix 2.** Structure of the oxoselenoesters, **K1–K8**, and of the cyanoselenoesters, **N1–N7**

Synthetic procedure has been described in [122].

**Appendix 3.** Complete results of the combination assay in the presence of ketone- or cyanoselenoesters and doxorubicin on Colo 320 cell line.

Compounds	Starting conc. ( $\mu\text{M}$ )	Ratio*	CI at ED <sub>50</sub>	SD (+/-)	Type of interaction
<b>K1</b>	5	0.6:1	2.6	0.73	Antagonism
		1.2:1	1.03	0.11	Additive effect
		2.4:1	0.94	0.09	Additive effect
		4.8:1	0.88	0.13	<b>Slight synergism</b>
		9.6:1	1.18	0.15	Slight antagonism
<b>K2</b>	6	0.7:1	1.77	0.22	Antagonism
		1.4:1	2.95	0.16	Antagonism
		2.8:1	1.2	0.22	Slight antagonism
		5.6:1	1.02	0.22	Additive effect
		11.2:1	1.5	0.27	Antagonism
		22.4:1	2.34	0.59	Antagonism
<b>K3</b>	6	0.7:1	1.32	0.8	Moderate antagonism
		1.4:1	0.37	0.15	<b>Synergism</b>
		2.8:1	0.73	0.1	Moderate synergism
		5.6:1	1.5	0.24	Antagonism
		11.2:1	1.3	0.07	Moderate antagonism
		22.4:1	1.72	0.08	Antagonism
<b>K4</b>	5	0.6:1	0.54	0.07	<b>Synergism</b>
		1.2:1	1.03	0.05	Additive effect
		2.4:1	1.1	0.05	Additive effect
		4.8:1	0.74	0.1	Moderate synergism
		9.6:1	0.85	0.06	<b>Slight synergism</b>
		19.2:1	0.97	0.12	Additive effect
<b>K5</b>	6	0.7:1	0.51	0.06	<b>Synergism</b>

		1.4:1	0.81	0.05	<b>Moderate synergism</b>
		2.8:1	0.55	0.04	<b>Synergism</b>
		5.6:1	0.58	0.02	<b>Synergism</b>
		11.2:1	0.64	0.02	<b>Synergism</b>
		22.4:1	0.68	0.06	<b>Synergism</b>
<b>K6</b>	6	0.7:1	0.51	0.06	<b>Synergism</b>
		1.4:1	0.81	0.05	<b>Moderate synergism</b>
		2.8:1	0.55	0.04	<b>Synergism</b>
		5.6:1	0.58	0.02	<b>Synergism</b>
		11.2:1	0.64	0.02	<b>Synergism</b>
		22.4:1	0.68	0.06	<b>Synergism</b>
<b>K7</b>	6	0.7:1	1.4	0.2	Moderate antagonism
		1.4:1	3.1	0.41	Antagonism
		2.8:1	1.36	0.2	Moderate antagonism
		5.6:1	1.3	0.07	Moderate antagonism
		11.2:1	2.8	0.15	Antagonism
		22.4:1	2.28	0.15	Antagonism
<b>K8</b>	6	0.7:1	0.12	0.09	<b>Strong synergism</b>
		1.4:1	2.4	0.62	Antagonism
		2.8:1	3.3	0.8	Antagonism
		5.6:1	2.01	0.97	Antagonism
		11.2:1	3.3	0.74	Antagonism

<b>Compounds</b>	<b>Starting conc. (µM)</b>	<b>Ratio*</b>	<b>CI at ED<sub>50</sub></b>	<b>SD (+/-)</b>	<b>Type of interaction</b>
<b>N1</b>	15	1.7:1	1.9	0.2	Antagonism
		3.4:1	0.34	0.04	<b>Synergism</b>
		6.8:1	0.51	0.04	<b>Synergism</b>
		13.6:1	0.95	0.15	Additive effect
		27.2:1	0.56	0.09	<b>Synergism</b>
		54.4:1	0.21	0.21	<b>Strong synergism</b>
<b>N2</b>	15	54.4:1	0.21	0.21	Strong synergism
		1.7:1	0.62	0.19	<b>Synergism</b>
		3.4:1	3.1	0.38	Antagonism
		6.8:1	0.58	0.03	<b>Synergism</b>
		13.6:1	1.36	0.05	Moderate antagonism
		27.2:1	2.8	0.12	Antagonism
<b>N3</b>	10	54.4:1	2.3	0.15	Antagonism
		1.2:1	1.7	0.44	Antagonism
		2.4:1	3.7	0.5	Strong antagonism
		4.8:1	0.85	0.1	<b>Moderate synergism</b>
		9.6:1	1.01	0.15	Additive effect
		19.2:1	1.19	0.17	Slight antagonism
<b>N4</b>	10	38.4:1	1.3	0.21	Moderate antagonism
		1.2:1	1.7	0.44	Antagonism
		2.4:1	3.7	0.5	Strong antagonism

		4.8:1	0.85	0.1	<b>Moderate synergism</b>
		9.6:1	1.01	0.15	Additive effect
		19.2:1	1.19	0.17	Slight antagonism
		38.4:1	1.3	0.21	Moderate antagonism
<b>N5</b>	10	1.2:1	5.7	1.6	Strong antagonism
		2.4:1	3.7	0.5	Strong antagonism
		4.8:1	1.2	0.95	Slight antagonism
		9.6:1	1.01	0.15	Additive effect
		19.2:1	1.19	0.17	Slight antagonism
		38.4:1	1.3	0.21	Moderate antagonism
<b>N6</b>	10	1.2:1	2.9	0.31	Antagonism
		2.4:1	4.5	0.5	Additive effect
		4.8:1	1.5	0.1	Antagonism
		9.6:1	1.78	0.21	Antagonism
		19.2:1	1.96	0.11	Antagonism
		38.4:1	1.96	0.105	Antagonism
<b>N7</b>	8	0.9:1	2.7	0.23	Antagonism
		1.8:1	5.3	1.02	Strong antagonism
		3.6:1	0.9	0.23	<b>Slight synergism</b>
		7.2:1	1.84	0.18	Antagonism
		14.4:1	1.89	0.29	Antagonism
		28.8:1	0.92	0.6	Additive effect

**Appendix 4** Inhibition of the MDR efflux pump ABCB1 by selenoesters on Colo 320 colon adenocarcinoma cells. Tariquidar was used as a positive control at 0.2  $\mu$ M, while DMSO served as solvent control at 2%. FSC: forward scatter count; SSC: side scatter count; FL1: fluorescence; FAR: fluorescence activity ratio.

Compounds	Concentration ( $\mu$ M)	FSC	SSC	FL-1	FAR
<b>K1</b>	0.2	2144	989	2.5	1.37
	2	1866	1067	83	<b>45.73</b>
<b>K2</b>	0.2	1916	1061	2.56	1.41
	2	1945	1156	67.8	<b>37.35</b>
<b>K3</b>	0.2	1706	982	7.25	<b>3.99</b>
	2	2040	1031	71.1	<b>39.17</b>
<b>K4</b>	0.2	1808	861	3.19	1.76
	2	1830	1008	9.06	<b>4.99</b>
<b>K5</b>	0.2	1982	1096	3.34	1.84
	2	1949	1053	59.2	<b>32.62</b>
<b>K6</b>	0.2	1996	873	2.7	1.48
	2	1833	1043	53.4	<b>29.42</b>
<b>K7</b>	0.2	1889	938	2.78	1.53
	2	1920	1045	73.3	<b>40.39</b>
<b>K8</b>	0.2	1804	853	6.14	<b>3.38</b>
	2	1990	1131	65.5	<b>36.09</b>
<b>Tariquidar</b>	0.2	1957	1074	50.9	<b>28.04</b>
<b>DMSO</b>	2.00%	1904	1001	1.72	0.95

**Appendix 5.** Apoptosis induction by ketone-selenoesters on MDR Colo 320 adenocarcinoma cells. The positive control, 12*H*-benzo( $\alpha$ )phenothiazine (M627), was used for comparison.

Compounds	Concentration ( $\mu$ M)	Early apoptosis %	Late apoptosis %	Cell death %
<b>M627</b>	<b>20</b>	<b>13.3</b>	<b>36.1</b>	<b>0</b>
<b>K1</b>	<b>2</b>	3.7	28.9	2.15
<b>K2</b>	<b>2</b>	0.3	33.9	0.95
<b>K3</b>	<b>2</b>	<b>18.6</b>	25.6	0
<b>K4</b>	<b>2</b>	3.4	16.1	5.95
<b>K5</b>	<b>2</b>	1.8	30.9	1.35
<b>K6</b>	<b>2</b>	4.5	27.8	0.17
<b>K7</b>	<b>2</b>	6.1	27.5	0.1
<b>K8</b>	<b>2</b>	4.9	26.7	0.85

## **PUBLICATIONS**

### **I.**

Article

# Ketone- and Cyano-Selenoesters to Overcome Efflux Pump, Quorum-Sensing, and Biofilm-Mediated Resistance

Nikoletta Szemerédi <sup>1</sup>, Annamária Kincses <sup>1</sup>, Katerina Rehorova <sup>2</sup>, Lan Hoang <sup>2</sup>,  
Noemi Salardón-Jiménez <sup>3</sup>, Clotilde Sevilla-Hernández <sup>3</sup>, Jitka Viktorová <sup>2</sup>,  
Enrique Domínguez-Álvarez <sup>3,\*</sup> and Gabriella Spengler <sup>1,\*</sup>

<sup>1</sup> Department of Medical Microbiology and Immunobiology, Faculty of Medicine, University of Szeged, Dóm tér 10, 6720 Szeged, Hungary; szemeredi.nikoletta@med.u-szeged.hu (N.S.); kincses.annamaria90@gmail.com (A.K.)

<sup>2</sup> Department of Biochemistry and Microbiology, Faculty of Food and Biochemical Technology, University of Chemistry and Technology Prague, Technická 3, 166 28 Prague, Czech Republic; katerina.rehorova@vscht.cz (K.R.); hoangl@vscht.cz (L.H.); jitka.prokesova@vscht.cz (J.V.)

<sup>3</sup> Instituto de Química Orgánica General (IQOG-CSIC), Consejo Superior de Investigaciones Científicas, Juan de la Cierva 3, 28006 Madrid, Spain; noemi.sj.95@gmail.com (N.S.-J.); clo.sh.1995@gmail.com (C.S.-H.)

\* Correspondence: e.dominguez-alvarez@iqog.csic.es (E.D.-Á.); spengler.gabriella@med.u-szeged.hu (G.S.)

Received: 12 November 2020; Accepted: 10 December 2020; Published: 11 December 2020



**Abstract:** The emergence of drug-resistant pathogens leads to a gradual decline in the efficacy of many antibacterial agents, which poses a serious problem for proper therapy. Multidrug resistance (MDR) mechanisms allow resistant bacteria to have limited uptake of drugs, modification of their target molecules, drug inactivation, or release of the drug into the extracellular space by efflux pumps (EPs). In previous studies, selenoesters have proved to be promising derivatives with a noteworthy antimicrobial activity. On the basis of these results, two series of novel selenoesters were synthesized to achieve more potent antibacterial activity on Gram-positive and Gram-negative bacteria. Fifteen selenoesters (eight ketone-selenoesters and seven cyano-selenoesters) were investigated with regards to their efflux pump-inhibiting, anti-quorum-sensing (QS), and anti-biofilm effects in vitro. According to the results of the antibacterial activity, the ketone-selenoesters proved to be more potent antibacterial compounds than the cyano-selenoesters. With regard to efflux pump inhibition, one cyano-selenoester on methicillin-resistant *S. aureus* and one ketone-selenoester on *Salmonella* Typhimurium were potent inhibitors. The biofilm inhibitory capacity and the ability of the derivatives to disrupt mature biofilms were noteworthy in all the experimental systems applied. Regarding QS inhibition, four ketone-selenoesters and three cyano-selenoesters exerted a noteworthy effect on *Vibrio campbellii* strains.

**Keywords:** selenoesters; *Salmonella* species; *Staphylococcus aureus*; *Pseudomonas aeruginosa*; biofilm; quorum sensing; multidrug resistance; antibacterial activity

## 1. Introduction

The rapid emergence of multidrug-resistant bacteria is jeopardizing the effectiveness of antibiotics that have saved millions of lives previously [1]. Microbes have become resistant to common antibiotics due to the irresponsible use of the antibiotics; therefore, the appearance of resistant bacterial strains makes the treatment of infections more complicated [2]. The improper use of antibiotics has also occurred in veterinary practice and in food-producing animal farms [3]. This has led to the

emergence of superbugs that are resistant to several classes of antibiotics, such as carbapenem resistant *Enterobacteriaceae* [4] and biofilm-producing methicillin-resistant *Staphylococcus aureus* (MRSA) [5].

Numerous bacterial isolates produce biofilms, which are the surface-attached bacterial cells embedded into an extracellular matrix that can protect the bacterial population against antibiotics. These biofilm-producing bacteria are more resistant to antibiotics compared to the planktonic cells, which are more susceptible to biocides [6].

It was believed that bacteria are independent and unicellular organisms [7]. Nevertheless, planktonic growth of bacteria seldom exists in nature. It has been shown that bacteria in nature exist in a large, contiguous, and dynamic surface-associated community, called biofilm, and this population has a unique behavior, namely, the properties of the community depend on population density [8]. The cells in biofilms are in contact with each other. Bacteria in the biofilm secrete small extracellular molecules to communicate with each other [9]. Several bacteria have been shown to regulate different physiological processes and activities *via* a mechanism called quorum sensing (QS), in which bacterial cells produce, detect, and reply to small diffusible signal molecules [10]. It is known that these bacteria need to achieve a critical cell density before they express virulence factors and attack the host organism.

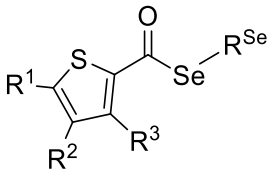
In addition, the over-expression of bacterial efflux pumps can also contribute to bacterial multidrug resistance (MDR). The efflux pumps are transmembrane transport proteins involved in the extrusion of toxic substances into the external milieu. Furthermore, these efflux pumps might be involved in the regulation of the expression of QS-dependent virulence factors. Therefore, the inhibition of efflux pumps may decrease the virulence of resistant bacteria [11].

Different selenocompounds and selenium nanoparticles have shown a significant antibacterial and anti-biofilm activity. Among the selenoparticles (SeNPs), SeNPs synthesized using aqueous berry extract of *Murraya koenigii* showed antibacterial activity against *Enterococcus faecalis*, *Streptococcus mutans*, *Shigella sonnei*, and *Pseudomonas aeruginosa*, as well as anti-biofilm activity against *P. aeruginosa* [12]. Alternatively, SeNPs conjugated with antibiotics were potent antibacterial agents and biofilm disruptors against MRSA [13]. Among selenocompounds, a series of steroidal  $\beta$ -hydroxy-phenylselenides also showed antibacterial activity against *P. aeruginosa*, and prevented its biofilm formation [14]. Similarly, ebselen derivatives were anti-biofilm and potent antibacterial agents against MRSA, with minimum inhibitory concentration (MIC) values below 2  $\mu\text{g}/\text{mL}$  [15].

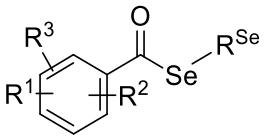
In this context, our group reported previously that selenoesters and selenoanhydrides are bioactive selenium-containing compounds initially designed as potential anticancer and MDR-reversing agents [16] with antioxidant activity [17]. Selenium (Se) and the Se-containing compounds are known antioxidants because this essential trace element allows the antioxidant activity of the glutathione peroxidase, the enzyme that empowers the deactivation of hydrogen peroxides [18–20]. In line with this, patients with bacterial and viral infections generally show high oxidative stress levels, as well as low levels of selenium in blood. Besides the reduction of this oxidative stress, Se can also boost the response of the immune system against infectious diseases [21,22]. The antibacterial activity of the abovementioned selenoesters and selenoanhydrides was evaluated, finding that they showed a potent antibacterial activity against MRSA, *Salmonella enterica* serovar Typhimurium, and *Chlamydia trachomatis* serovar D. Additionally, they exerted a noteworthy anti-biofilm activity, as well as being inhibitors of bacterial efflux pumps [23–25].

On the basis of these antecedents, we tested the antibacterial, anti-biofilm, and anti-quorum sensing activity of 15 selenoesters in this study, comprising 8 ketoneselenoesters ( $\text{R}=\text{COCH}_3$ , compounds K1–K8, Table 1) and 7 cyanoselenoesters ( $\text{R}=\text{CN}$ , compounds N1–N7, Table 1). With our selenocompounds, we aimed to reduce the intercellular communication and thus reduce biofilm formation and reverse resistance.

**Table 1.** Ketone- and cyano-selenoesters evaluated. Cpds. = Compounds.



Ring: Thiophene



Ring: Benzene

Ring: Thiophene						Ring: Benzene					
Cpds.	R <sup>Se</sup>	R <sup>1</sup>	R <sup>2</sup>	R <sup>3</sup>	Ring	Cpds.	R <sup>Se</sup>	R <sup>1</sup>	R <sup>2</sup>	R <sup>3</sup>	Ring
K1	-CH <sub>2</sub> COCH <sub>3</sub>	-H	-H	-H	Thiophene	N1	-CH <sub>2</sub> CN	-H	-H	-H	Thiophene
K2	-CH <sub>2</sub> COCH <sub>3</sub>	2-F	-H	-H	Benzene	N2	-CH <sub>2</sub> CN	3-F	-H	-H	Benzene
K3	-CH <sub>2</sub> COCH <sub>3</sub>	4-Br	-H	-H	Benzene	N3	-CH <sub>2</sub> CN	4-Br	-H	-H	Benzene
K4	-CH <sub>2</sub> COCH <sub>3</sub>	2-CF <sub>3</sub>	-H	-H	Benzene	N4	-CH <sub>2</sub> CN	2-CF <sub>3</sub>	-H	-H	Benzene
K5	-CH <sub>2</sub> COCH <sub>3</sub>	3-CF <sub>3</sub>	-H	-H	Benzene	N5	-CH <sub>2</sub> CN	3-CF <sub>3</sub>	-H	-H	Benzene
K6	-CH <sub>2</sub> COCH <sub>3</sub>	3-Cl	4-F	-H	Benzene	N6	-CH <sub>2</sub> CN	3-Cl	4-F	-H	Benzene
K7	-CH <sub>2</sub> COCH <sub>3</sub>	4-C(CH <sub>3</sub> ) <sub>3</sub>	-H	-H	Benzene	N7	-CH <sub>2</sub> CN	3-CF <sub>3</sub>	5-CF <sub>3</sub>	-H	Benzene
K8	-CH <sub>2</sub> COCH <sub>3</sub>	2-F	4-F	5-F	Benzene						

## 2. Results

### 2.1. Determination of Minimum Inhibitory Concentrations by Microdilution Method

On the basis of the results obtained on Gram-positive and Gram-negative bacteria, we found that the ketone-selenoesters demonstrated a strong antibacterial activity against the Gram-positive strains investigated. The most potent derivatives were **K1**, **K7**, and **K8**—they were effective on all three *S. aureus* strains tested, even reaching the submicromolar range (MIC between 0.39 and 1.56  $\mu$ M, Table 2).

**Table 2.** Antibacterial activity of selenoesters on Gram-positive and Gram-negative bacteria (*S. aureus* = *Staphylococcus aureus*, *S. Typhimurium* = *Salmonella enterica* serovar Typhimurium, *P. aeruginosa* = *Pseudomonas aeruginosa*).

Cpds.	MIC Determination ( $\mu$ M)									
	<i>S. aureus</i> ATCC 25923	<i>S. aureus</i> MRSA ATCC 43300	<i>S. aureus</i> MRSA 272123	<i>S. Typhimurium</i> SE01 Wild-Type	<i>S. Typhimurium</i> SE02 $\Delta$ <i>acrB</i>	<i>S. Typhimurium</i> SE03 $\Delta$ <i>acrA</i>	<i>S. Typhimurium</i> SE39 $\Delta$ <i>tolC</i>	<i>P. aeruginosa</i> CCM 3955	<i>P. aeruginosa</i> NEM 986	
K1	1.56	1.56	0.78	50	100	100	100	100	50	
K2	1.56	3.125	0.78	>100	>100	>100	>100	100	50	
K3	1.56	3.125	0.78	50	50	50	50	>100	>100	
K4	3.125	3.125	1.56	>100	>100	>100	>100	100	50	
K5	1.56	3.125	0.78	100	50	50	>100	100	50	
K6	1.56	3.125	0.39	100	100	100	100	100	50	
K7	1.56	1.56	0.39	50	>100	100	>100	100	100	
K8	1.56	1.56	0.78	50	>100	100	100	100	50	
N1	12.5	100	25	50	50	100	100	>100	>100	
N2	12.5	100	50	50	100	100	100	>100	>100	
N3	12.5	50	25	50	50	50	50	>100	>100	
N4	12.5	100	50	100	100	100	100	>100	>100	
N5	12.5	50	50	100	100	100	100	>100	>100	
N6	12.5	50	25	100	50	100	100	>100	>100	
N7	12.5	50	25	50	50	50	100	>100	>100	

Regarding the cyano-selenoesters, they were also more active on Gram-positive strains. Nevertheless, they were less effective on the MRSA strains (MIC: 25–100  $\mu$ M) compared to the methicillin-susceptible reference American Type Culture Collection (ATCC) 25923 strain (MIC: 12.5  $\mu$ M). Considering this antibacterial potency, three out of the seven cyano-selenoesters evaluated seemed to be more powerful, namely, **N3**, **N6**, and **N7**. On the contrary, the ketone-selenoesters and the cyano-selenoesters were not effective on the tested *P. aeruginosa* strain and had a mild antibacterial activity on the *S. Typhimurium* strains investigated (MIC: 50–100  $\mu$ M) (Table 2).



## 2.2. Real-Time Ethidium Bromide Accumulation Assay

In this study, the ketone- and cyano-selenoesters were tested for their ability to inhibit efflux pumps on Gram-negative and Gram-positive model bacterial strains (Table 3). The efflux pump inhibitor (EPI) activity was investigated on *S. aureus* ATCC MRSA 43300 and *S. Typhimurium* SE01, SE02, SE03, and SE39 strains. Regarding the *Salmonella* strains tested, the ketone-selenoester **K7** was the most potent EPI because it increased the ethidium bromide (EB) accumulation in the efflux pump gene-inactivated mutant *S. Typhimurium* ( $\Delta$ *acrA* and  $\Delta$ *tolC*) strains (relative fluorescence index (RFI): 1.15 and 1.67, respectively), probably because this compound may cause membrane destabilizing effects. It was observed that **K7** inhibited the efflux activity of the wild-type SE01 strain as well (RFI: 1.02). The inhibition by **K7** in  $\Delta$ *tolC* strain was stronger than inhibition in the presence of the reference compound CCCP (carbonyl cyanide m-chlorophenyl hydrazone). In addition, ketone-selenoesters **K4** and **K5** inhibited the EB accumulation in the *tolC*-inactivated mutant strain (Figure 1). Regarding cyano-selenoesters, the most pronounced activity was exerted by **N4** and **N7** on the *tolC*-inactivated mutant strain (Figure 2). The significance level was determined between the negative and positive controls and between the tested substances and the negative control.

**Table 3.** Efflux pump inhibitory effects of selenoesters on *Staphylococcus aureus* and *S. Typhimurium* strains in terms of RFI (relative fluorescence index) values. Higher RFI values indicate more efficient efflux pump inhibition.

Cpds.	Relative Fluorescence Index (RFI)					
	<i>S. aureus</i> MRSA ATCC 43300	<i>S. aureus</i> ATCC 25923	<i>S. Typhimurium</i> SE01 wild-type	<i>S. Typhimurium</i> SE02 $\Delta$ <i>acrB</i>	<i>S. Typhimurium</i> SE03 $\Delta$ <i>acrA</i>	<i>S. Typhimurium</i> SE39 $\Delta$ <i>tolC</i>
<b>K1</b>	−0.02	1.19	0.17	0.20	0.29	0.31
<b>K2</b>	−0.04	1.12	0.18	0.21	0.30	0.42
<b>K3</b>	−0.10	1.17	0.60	0.27	0.24	0.44
<b>K4</b>	−0.09	1.02	0.19	0.35	0.68	0.95
<b>K5</b>	−0.08	1.17	0.41	0.11	0.35	0.91
<b>K6</b>	−0.09	1.19	0.17	0.43	0.52	0.80
<b>K7</b>	−0.02	1.13	1.02	0.30	1.15	1.67
<b>K8</b>	−0.04	1.10	0.08	0.31	0.28	0.70
<b>N1</b>	0.05	1.40	0.04	0.10	0.37	0.84
<b>N2</b>	−0.02	1.31	−0.06	−0.05	0.16	0.19
<b>N3</b>	−0.05	1.49	0.003	0.03	0.38	0.24
<b>N4</b>	0.35	1.78	0.22	0.39	0.36	1.00
<b>N5</b>	−0.03	1.43	0.02	0.02	0.32	0.43
<b>N6</b>	−0.01	1.32	0.03	−0.03	0.45	0.38
<b>N7</b>	−0.06	0.28	0.003	0.14	0.32	1.11
CCCP	-	-	3.37	1.83	3.30	1.61
RES	0.30	5.5	-	-	-	-

CCCP: carbonyl cyanide m-chlorophenyl hydrazone; RES: reserpine.

In case of *S. aureus* ATCC MRSA 43300, only one derivative (the cyano-selenoester **N4**) showed a potent EPI activity (Figure 3); in addition, this effect was more pronounced (RFI: 0.351) than the one obtained in the presence of the reference EPI reserpine (RFI: 0.300).

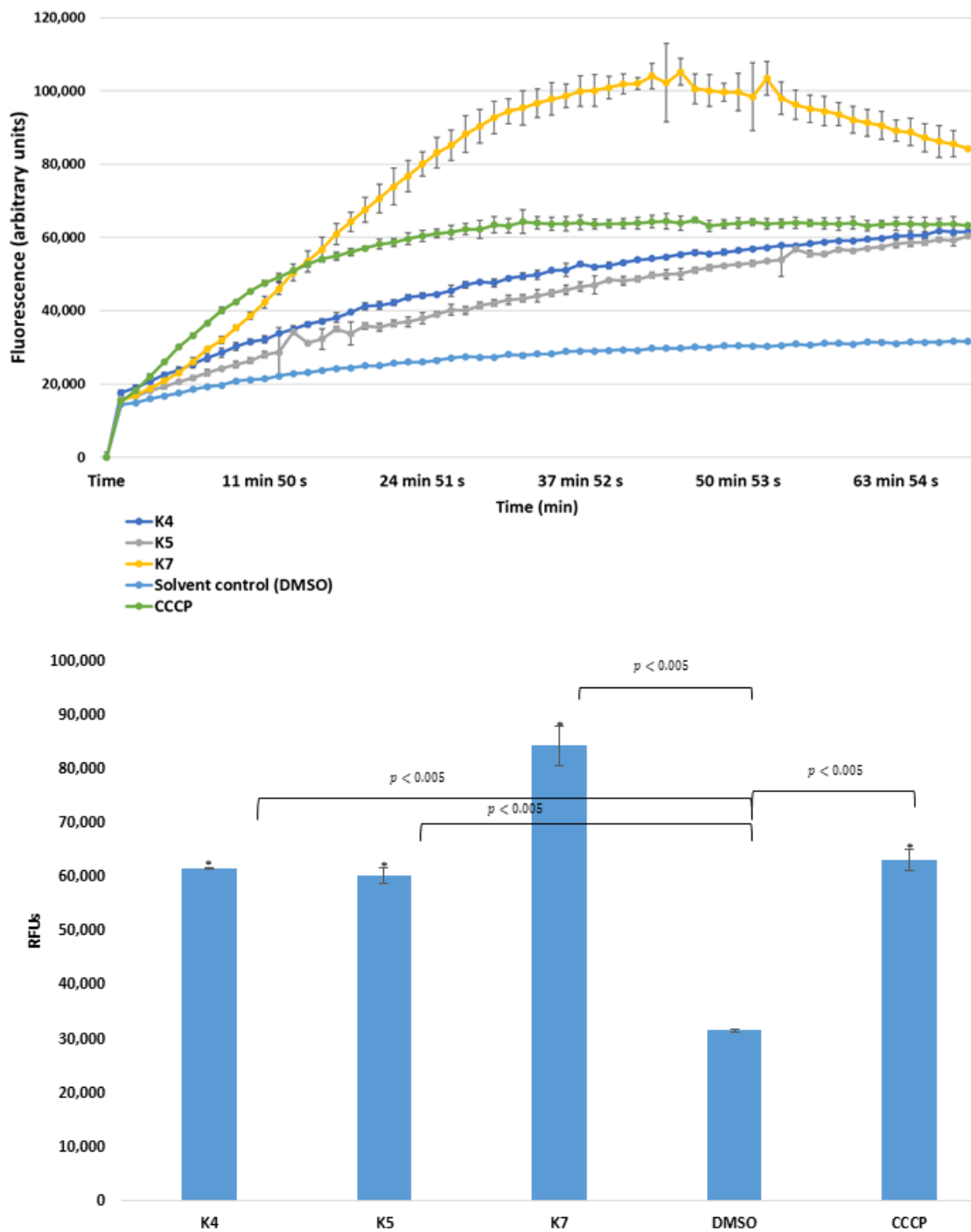


**Figure 1.** Accumulation of ethidium bromide (EB) in the presence of selenoesters **K4**, **K5**, and **K7** on *S. Typhimurium* SE39  $\Delta tolC$  strain. DMSO: dimethyl sulfoxide (solvent); CCCP: carbonyl cyanide 3-chlorophenylhydrazine (positive control). The level of significance was lower than  $p = 0.005$  in all cases;  $\alpha = 0.05$ ;  $p$  values less than 0.005 are marked with an asterisk.

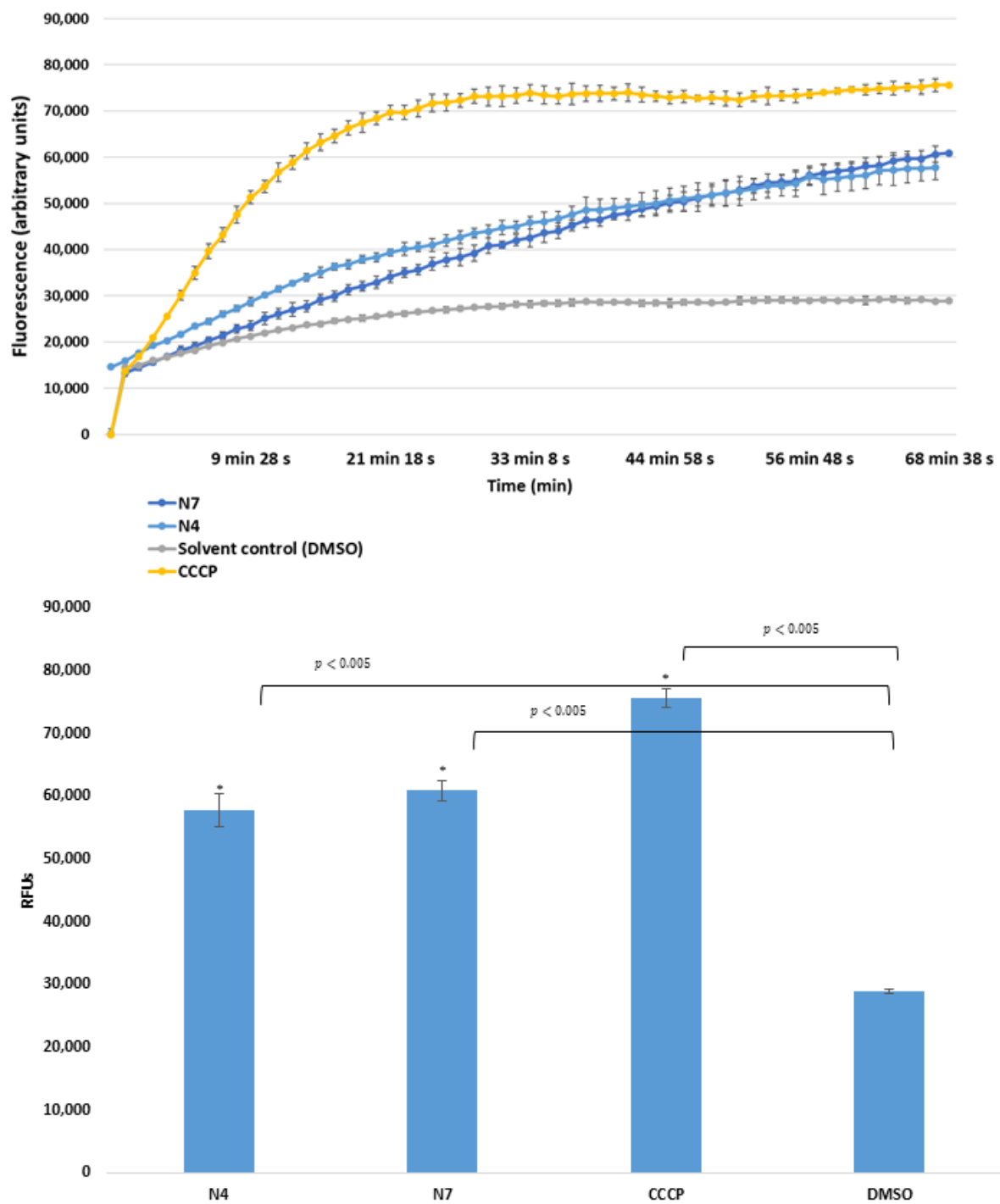


**Figure 2.** Accumulation of EB in the presence of N4 and N7 at one-half minimum inhibitory concentration (MIC) on *S. Typhimurium* SE39  $\Delta tolC$  strain. DMSO: dimethyl sulfoxide (solvent); CCCP: carbonyl cyanide 3-chlorophenylhydrazone (positive control). The level of significance was lower than  $p = 0.005$  in all cases;  $\alpha = 0.05$ ;  $p$  values less than 0.005 are marked with an asterisk.

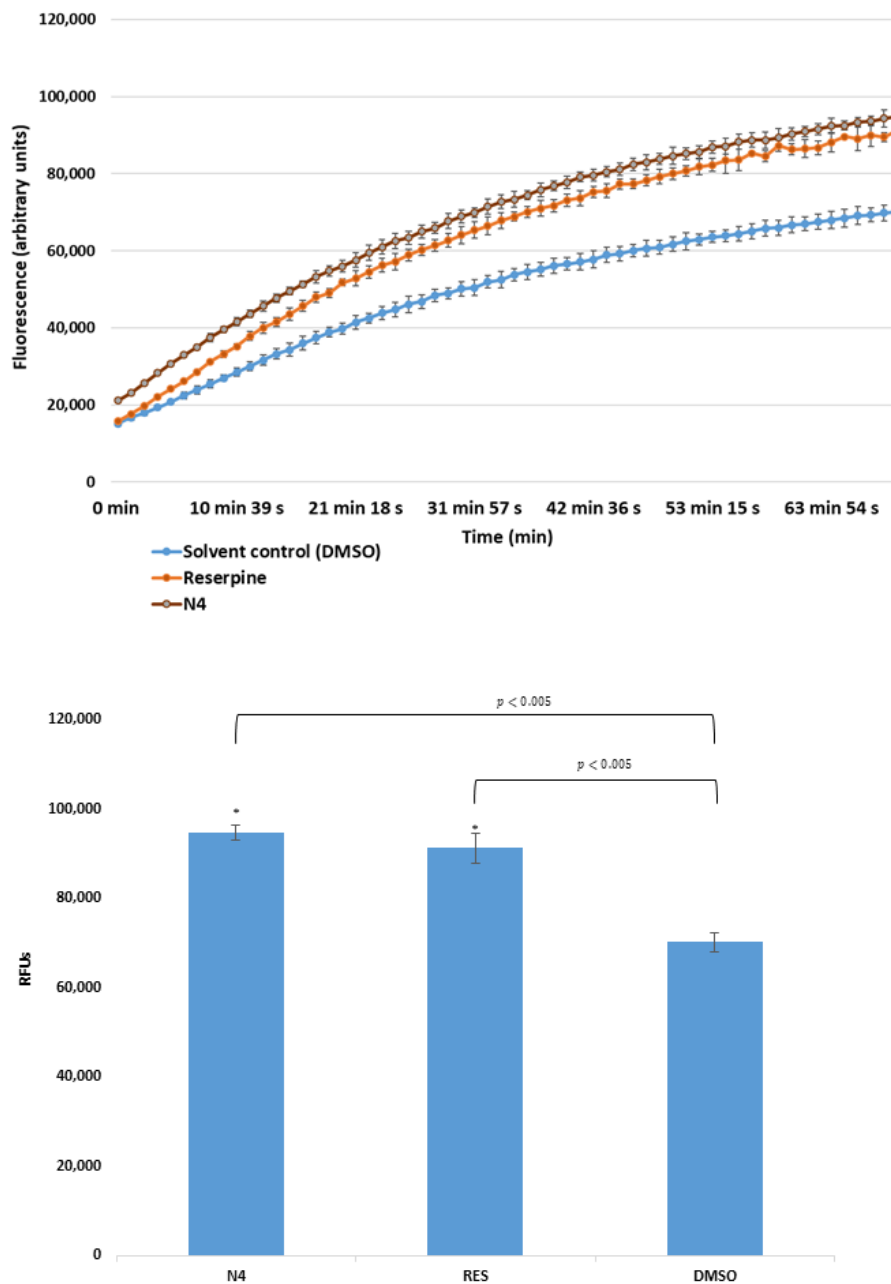


**Figure 3.** Accumulation of EB in the presence of selenoester N4 at one-half MIC on *S. aureus* MRSA (methicillin-resistant *Staphylococcus aureus*) 43300. DMSO: dimethyl sulfoxide (solvent); reserpine: positive control. The level of significance was lower than  $p = 0.005$  in all cases;  $\alpha = 0.05$ ;  $p$  values less than 0.005 are marked with an asterisk.

### 2.3. Assay for Quorum Sensing (QS) Inhibition

In this case, the concentration that halves the viability ( $IC_{50}$ ) was compared to the concentration halving the cell-to-cell communication ( $EC_{50}$ ). This was a necessary step to differentiate between the toxic concentration and the quorum-sensing inhibiting concentration. If the dose for toxicity was higher than the dose needed for quorum sensing (QS) inhibition, the tested compound was considered efficient. Therefore, the comparison of toxicity and QS inhibiting concentrations was evaluated by means of the selectivity index (SI), which was calculated as the ratio of  $IC_{50}$  and  $EC_{50}$ . A higher index is related to a more potent efficacy of the compound in QS inhibition. As can be seen in Table 4, all tested compounds (except for the compound N5) were able to inhibit the bacterial communication.

Table 4. Anti-quorum sensing effects of selenocompounds on *Vibrio* strains.

Cpd.	<i>Vibrio campbellii</i> BAA 1118			<i>Vibrio campbellii</i> BAA 1119		
	IC <sub>50</sub> (μM)	EC <sub>50</sub> (μM)	SI	IC <sub>50</sub> (μM)	EC <sub>50</sub> (μM)	SI
<b>K1</b>	5.76 ± 0.07	0.22 ± 0.01	26.2	2.02 ± 0.15	0.71 ± 0.05	2.8
<b>K2</b>	4.38 ± 0.47	0.25 ± 0.03	17.5	3.23 ± 0.14	0.22 ± 0.02	14.7
<b>K3</b>	1.12 ± 0.02	0.17 ± 0.01	6.6	0.77 ± 0.07	0.23 ± 0.02	3.3
<b>K4</b>	33.18 ± 3.45	4.68 ± 0.32	7.1	6.66 ± 0.13	0.29 ± 0.05	23.0
<b>K5</b>	2.42 ± 0.29	1.35 ± 0.03	1.8	1.32 ± 0.10	0.45 ± 0.01	2.9
<b>K6</b>	3.28 ± 0.19	2.29 ± 0.02	1.4	0.97 ± 0.09	1.20 ± 0.00	0.8
<b>K7</b>	10.54 ± 0.19	1.77 ± 0.19	6.0	4.27 ± 0.23	0.15 ± 0.01	28.5
<b>K8</b>	1.23 ± 0.07	0.11 ± 0.01	11.2	1.39 ± 0.03	0.46 ± 0.03	3.0
<b>N1</b>	2.21 ± 0.19	1.45 ± 0.02	1.5	2.28 ± 0.12	0.26 ± 0.03	8.8
<b>N2</b>	7.36 ± 0.70	0.34 ± 0.04	21.6	2.40 ± 0.12	0.73 ± 0.02	5.1
<b>N3</b>	2.199 ± 0.16	0.34 ± 0.04	6.5	2.35 ± 0.03	<0.06	37.6
<b>N4</b>	2.52 ± 0.03	1.29 ± 0.04	2.0	6.41 ± 0.42	0.73 ± 0.02	8.8
<b>N5</b>	12.51 ± 0.05	>5	-	3.57 ± 0.08	>5	-
<b>N6</b>	1.37 ± 0.02	0.37 ± 0.05	3.7	2.28 ± 0.12	0.22 ± 0.00	10.4
<b>N7</b>	3.84 ± 0.15	1.44 ± 0.06	2.7	7.71 ± 0.10	0.25 ± 0.02	30.8

Usually, for the practical application, indexes should be higher than 10 [26]. On the basis of this criterion, the promising ketone-selenoesters are **K1**, **K2**, and **K8**, whereas the most effective cyano-selenoester is **N2**. The ability of selenocompounds to inhibit quorum sensing was tested using two strains of *Vibrio campbellii*. The wild-type of these bacteria uses both autoinducer-1 (AI-1) and autoinducer-2 (AI-2) types of molecules for its communication. Strain 1118 is deficient in communication on the basis of AI-2, while strain 1119 is deficient in AI-1 type communication. Out of the tested compounds, only **K2** was able to inhibit the communication on the basis of either AI-1 or AI-2 molecules, with a selectivity index higher than 10 (17.5 and 14.7, respectively). The ketone-selenoester **K1** resulted in being the most promising compound in the inhibition of AI-1-based communication showing the SI of 26.2. The second most potent AI-1 inhibitor was **N2** (SI = 21.6), which was also the only cyano-selenoester capable of inhibiting AI-1-based communication. In contrast, the cyano-selenocompounds were more effective inhibitors of AI-2-based communication, with **N3** (SI = 37.6) and **N7** (SI = 30.8) being the most effective compounds among them (Table 4).

#### 2.4. Anti-Biofilm Activity

The anti-biofilm activity was evaluated against typical pathogenic bacteria known for biofilm formation, such as the Gram-positive *S. aureus* and the Gram-negative *P. aeruginosa*. The ability of the compounds to affect the biofilm formation (the inhibition of cell adhesion) was tested, followed by the determination of their ability to disrupt mature biofilms. As can be seen in Table 5, all of the tested compounds were able to affect both stages of the biofilm formation. As is known, biofilm is a layer of cells protected from the adverse external conditions; therefore, the concentrations needed to halve the mature biofilm are several times higher than those needed for halving the adhesion of bacteria. This difference was most pronounced for compound **N3**, which required up to 26- and 11-fold higher concentration for achieving the disruption of the biofilm produced by *S. aureus* and *P. aeruginosa*, respectively, compared to the concentrations at which the inhibition of the adhesion takes place. In contrast, compound **K5** possessed the least noticeable difference in cell adhesion and biofilm disruption, which was only five and four times higher for *S. aureus* and *P. aeruginosa*, respectively. Almost in all cases, the selenocompounds evaluated were slightly more active against *P. aeruginosa* than against *S. aureus*.

**Table 5.** Concentration of selenoesters halving (IC<sub>50</sub>) the adhesion and disrupting the biofilm of *S. aureus* ATCC 25923 and *P. aeruginosa* CCM 3955 strains.

Compounds	<i>Staphylococcus aureus</i> ATCC 25923		<i>Pseudomonas aeruginosa</i> CCM 3955	
	Anti-Adhesion (μM)	Anti-Biofilm (μM)	Anti-Adhesion (μM)	Anti-Biofilm (μM)
<b>K1</b>	1.84 ± 0.26	32.80 ± 3.25	1.15 ± 0.01	10.21 ± 0.48
<b>K2</b>	1.72 ± 0.17	28.08 ± 1.17	1.10 ± 0.11	8.78 ± 0.66
<b>K3</b>	1.39 ± 0.13	11.64 ± 0.99	1.14 ± 0.05	6.00 ± 0.74
<b>K4</b>	3.59 ± 0.48	28.70 ± 4.18	3.04 ± 0.33	21.85 ± 2.04
<b>K5</b>	2.84 ± 0.13	15.44 ± 0.42	1.51 ± 0.22	6.45 ± 0.30
<b>K6</b>	2.96 ± 0.16	12.87 ± 0.37	2.33 ± 0.25	14.29 ± 1.62
<b>K7</b>	3.08 ± 0.24	40.80 ± 3.12	2.16 ± 0.29	11.06 ± 1.92
<b>K8</b>	1.35 ± 0.16	9.22 ± 0.61	0.86 ± 0.09	6.98 ± 0.22
<b>N1</b>	2.46 ± 0.15	24.79 ± 2.65	1.78 ± 0.07	15.51 ± 1.65
<b>N2</b>	3.14 ± 0.12	48.08 ± 3.82	2.86 ± 0.17	18.06 ± 0.72
<b>N3</b>	1.19 ± 0.15	30.46 ± 2.72	0.92 ± 0.01	10.56 ± 0.95
<b>N4</b>	1.49 ± 0.08	28.91 ± 2.00	2.49 ± 0.43	13.48 ± 0.82
<b>N5</b>	3.01 ± 0.35	34.55 ± 3.00	3.40 ± 0.10	24.81 ± 2.12
<b>N6</b>	1.83 ± 0.15	21.75 ± 2.61	1.34 ± 0.08	13.46 ± 1.77
<b>N7</b>	1.99 ± 0.26	16.53 ± 0.76	1.81 ± 0.04	11.09 ± 0.82

### 3. Discussion

#### 3.1. Antibacterial Activity

Previously, it was described by our group that a methylketone selenoester had antibacterial activity against Gram-positive bacteria, and two selenocompounds (a selenoanhydride and a diselenodiester) were active inhibitors of the AcrAB-TolC system [25]. In addition, a series of symmetrical selenoesters were investigated with respect to their anti-biofilm and efflux pump-inhibiting properties. In this study, we observed that the methyloxycarbonyl selenoesters showed a significant biofilm and efflux pump inhibition, and that a strong QS inhibiting activity was exerted by a methyloxycarbonyl selenoester [24].

As a continuation of our former studies, we synthesized new classes of Se-containing compounds and investigated them as potential antibacterial agents in this work. According to the results of the antibacterial activity, the ketone-selenoesters proved to be more potent antibacterial compounds than the cyano-selenoesters against the strains of *Staphylococcus aureus* evaluated. The ketone-selenoesters exerted potent activity on sensitive and methicillin-resistant *S. aureus* strains. Interestingly, the cyano-selenoesters were slightly more active than the ketone-selenoesters against the *Salmonella enterica* serovar Typhimurium strains evaluated—the seven cyano-selenoesters tested showed MIC values of 50 or 100 μM, whereas half of the eight ketone-containing selenoesters had MIC values above 100 μM. None of the 15 derivatives had antibacterial activity on *Pseudomonas aeruginosa*.

A few structure–activity relationships (SAR) can be concluded on the basis of the activity of ketone-selenoesters against *S. aureus*, taking into account that the number of compounds was not enough and thus more experiments should be performed in the future in order to confirm these empirical observations. The most active compound was **K6**, which had a *tert*-butyl group in *para*-position, with MIC values of 1.56 μM on the sensitive strains and 0.39–3.13 μM for the MRSA strains. **K6** was the unique compound with an electron-donating substituent in this work, as previous evaluations of selenoesters pointed out that electron-withdrawing substituents generally showed higher biological activity. Further studies should explore additional compounds with electron-donating substituents to confirm if they have higher antibacterial activity against *S. aureus*. In any case, the differences were small, as **K1** (unsubstituted), **K6** (3-chloro-4-fluoro substituted), and **K8** (2,4,5-trifluoro substituted) showed similar MIC values on two *S. aureus* bacterial strains.

Among the nitrile derivatives **N1–N7**, all exerted similar activity (MIC = 12.5 μM) against the sensitive *S. aureus* ATCC 25923 strain. Taking together the results on the MRSA and *S. Typhimurium* strains, the most active ones were **N1** (unsubstituted), **N3** (4-Br-substituted), **N6** (3-Cl-substituted), and

**N7** (3,5-bis(trifluoromethyl)-substituted). These data suggest that, among monosubstituted compounds, those that include a bromine or a chlorine atom bound to the ring have better activity than those with a fluoro or a trifluoromethyl group, and that the inclusion of a second trifluoromethyl group contributes to an antibacterial activity similar to the one observed for the bromine or chlorine derivatives.

It is noteworthy to mention that the less active compound (**K4**) had a bulky substituent (trifluoromethyl group) at the *ortho* position of the selenoester. This fact may produce a steric hindrance that may hamper the hydrolysis of the selenoester inside the cells, which is the suggested mechanism underlying the biological activity [16]. When this bulky substituent was replaced by the smallest possible substituent (–H in compound **K1**), the MIC value was twofold lower on the three strains of *S. aureus* tested. Additionally, its replacement by a fluorine atom (intermediate between –H and –CF<sub>3</sub>) led to a twofold MIC reduction on *S. aureus* ATCC 25923 and in *S. aureus* MRSA 272123, but maintaining the MIC value on the third strain (*S. aureus* MRSA 43300). In this case, the inclusion of additional –F atoms at positions -4 and -5 (selenoester **K8**) managed to reduce the MIC value on the third strain, achieving an activity comparable to **K1**. Interestingly, the same effect of the steric hindrance was observed in the cyano-selenoesters between the compounds with a 2-CF<sub>3</sub> (**N4**) and a 2-H (**N1**); as in the ketone derivatives, the bulky derivative was less active than the unsubstituted derivative.

### 3.2. Efflux Pump Inhibitory Assay

Multidrug resistance due to drug efflux mechanisms protects bacteria through the extrusion of antibiotics out of the bacterial cells. Thus, this efflux-related phenomenon can make bacterial infections untreatable due to the lack of activity of the antibiotics. Thus, a promising strategy to restore the sensitivity of bacteria to antibiotics could be their administration together with efflux pump inhibitors, also known as EPIs [27].

In order to reverse the multidrug-resistant phenotype and re-sensitize multidrug-resistant bacteria to antibiotic therapy, the application of EPIs is an adequate approach, and natural and synthetic molecules have been described as EPIs against Gram-negative and Gram-positive bacteria [27]. Regarding the present ketone- and cyano-selenoesters, only one cyano-selenoester—**N4**—showed a potent EPI activity on methicillin-resistant *S. aureus*; furthermore, this inhibition was stronger than the effect of the reference EPI reserpine. In addition, ketone-selenoester **K7** was an effective EPI on *Salmonella* Typhimurium strains, supposedly due to its membrane-destabilizing activity. Interestingly, all of the compounds that have at least one trifluoromethyl group (**K4**, **K5**, **N4**, and **N7**), with the exception of **N5**, showed moderate efflux pump inhibitory effects on *S. Typhimurium* SE39  $\Delta tolC$  strain in terms of the real-time ethidium bromide accumulation assay. Consequently, this –CF<sub>3</sub> moiety and the –C(CH<sub>3</sub>)<sub>3</sub> moiety of **K7** seemed to be relevant for this efflux pump inhibition activity in *S. Typhimurium* SE39  $\Delta tolC$  strain.

In this work, we explored the ability of the compounds to inhibit efflux pumps, and at the sight of the promising inhibitory results obtained, we wanted to explore whether the compounds were able to synergistically enhance the activity of commercial antibiotics against multidrug-resistant bacterial strains.

### 3.3. Quorum Sensing (QS) Inhibition and Anti-Biofilm Assay

Inhibition of bacterial cell to cell communication finds its application in the prevention and spreading of bacterial infections. The communication is used by bacteria to sense their count, and in specific breakpoints, they switch their behavior and start to produce biofilm, thus regulating their virulence and metabolism [28]. Nowadays, the quorum-sensing modulators offer new tools in the fight against bacterial resistance and in the diagnosis of the disease, and also act as novel antimicrobial agents. Quorum sensing is based on three types of molecules: homoserine lactones, peptides, and boron structures. AI-1 communication is based on homoserine lactones and is provided by LuxI protein, which is responsible for AI production, and LuxR protein, which becomes activated by AI [29]. AI-2 communication is based on boron structures, which are produced by LuxS, and recognized



by the sensor kinase. Usually, the communication of Gram-negative bacteria is due to the homoserine lactones, whereas Gram-positive bacteria use peptides as AI-1 type of molecules. AI-2 molecules are more universal and serve for communication in both Gram-positive and Gram-negative bacteria. While the homoserine lactones can diffuse freely across the cell membrane, peptide autoinducers usually require special transport mechanisms. These transport mechanisms are generally provided by ABC transporters (ATP-binding cassette), which are similar to those used by mammalian cells as efflux pumps. The inhibitors of the bacterial communication based on peptides could therefore find an application in the inhibition of the related-mammalian ABC transporters, whose overproduction is responsible for, e.g., chemotherapeutic-resistant cancer or drug-resistant epilepsy [30].

On the basis of our results, several compounds appear promising for their use as communication inhibitors. Compound **K2** inhibited both types of communication with a significant selectivity to inhibit communication rather than growth of bacteria. This selectivity is favorable for non-pathogenic (symbiotic) bacteria that constitute the human microflora. The ketone-selenoester **K1** was evaluated as the most promising compound inhibiting AI-1-based communication, followed by **N2**, which was the only cyano-selenocompound that was capable of inhibiting this AI-1-based communication. Both **K1** and **N2** were able to inhibit the communication at concentrations as low as 0.25 and 0.34  $\mu\text{M}$ , respectively. Furthermore, both the ketone-selenoester **K2** and the cyano-selenoester **N2** share a 2-fluorophenyl moiety bound to the selenoester, which seems important for this inhibition of AI-1 communication. Interestingly, the substitution with fluorine atoms in the absence of other substituents was profitable for the activity, as the fourth most active compound was the one with a 2,4,5-trifluoro substitution. Alternatively, the activity of the unsubstituted derivative **K1** (the most active inhibitor) may not be related to the lack of substitution because its nitrile equivalent (**N1**) is devoid of activity. The communication of *P. aeruginosa* is usually based on homoserine lactones (AI-1); therefore, its adhesion should be dominantly inhibited by the same compounds inhibiting AI-1-based communication of *V. campbellii* (strain BAA 1118). Compounds **K1**, **K2**, and **K8** showed QS selectivity indexes higher than 10, and they were also the most active inhibitors of the adhesion of *P. aeruginosa* in the anti-biofilm assay.

Otherwise, the cyano-selenocompounds were more effective in the inhibition of AI-2-based communication—**N3** and **N7** were the most effective compounds among the others, with **N3** being capable of exerting its inhibition at a concentration as low as 60 nM. Intriguingly, they had a quite different substitution at the phenyl ring than the compounds active in AI-1—a bulky bromine atom (**N3**) or a more bulky di-substitution with trifluoromethyl groups (**N7**). Furthermore, the two more potent inhibitors among the ketone-selenoesters also included bulky substituents—trifluoromethyl (**K4**) or *tert*-butyl (**K7**) derivatives that support this observation. Compound **K2**, with a fluorine atom, was also active, but with a selectivity index (SI) of 14.7, significantly lower than the ones of **N3**, **N7**, **K4**, and **K7**: 37.6, 30.8, 23.0, and 28.5, respectively.

Quorum sensing of Gram-positive bacteria is usually based on peptide molecules, which are not typical of *Vibrio* communication; therefore, these results could not be correlated. However, many of tested compounds showed a significant inhibition of *S. aureus* adhesion; thus, the Se-compounds should be investigated more in depth to determine their ability to modulate the activity of ABC transporters. Autoinducers-2 are commonly used by many Gram-positive and Gram-negative bacteria. For example, *S. aureus*, bacteria belonging to the *Enterobacteriaceae* family or to the genus *Bacillus*, use the ABC transporters as a part of their communication [31]. However, in the AI-2 system, these transporters are used for uptake of communication molecules [32]. This universal system of communication spreading in both Gram-positive and Gram-negative bacteria was significantly inhibited by compounds **K2**, **K4**, **K7**, **N3**, **N6**, and **N7**.

Regarding the anti-biofilm assay, all compounds were able to prevent the biofilm adhesion in the two bacterial strains evaluated (*S. aureus* ATCC 25923 and *P. aeruginosa* CCM 3955) at concentrations below 4  $\mu\text{M}$ . Two of them (**K8** and **N3**) exerted this inhibition of the *P. aeruginosa* biofilm at nanomolar range: 0.86  $\mu\text{M}$  and 0.92  $\mu\text{M}$ , respectively. Seven additional compounds exerted this effect at



concentrations from 1 to 2  $\mu\text{M}$  in *P. aeruginosa*, whereas eight showed this range of activity against *S. aureus*. A tendency can be observed—the compounds monosubstituted with halogens (**K1–K3**, **N1–N3**), with the exception of **N1** and **N2**, tended to have anti-adhesion activity at concentrations below 2  $\mu\text{M}$ . In the anti-biofilm evaluation, all compounds were disruptors of existing biofilms at concentrations below 25  $\mu\text{M}$  in *P. aeruginosa*, and below 50  $\mu\text{M}$  in *S. aureus*. Out of them, **K2**, **K3**, **K5**, and **K8** disrupted the biofilm at concentrations below 10  $\mu\text{M}$  in *P. aeruginosa*, and **K8** in *S. aureus*. In this case, no SARs could be extracted, and besides this, the ketone-selenoesters resulted in being more potent disruptors than the cyano-selenoesters; moreover, the compounds were more effective against *P. aeruginosa* biofilms than against those of *S. aureus*.

## 4. Materials and Methods

### 4.1. Compounds

The 15 selenoesters evaluated in this work were previously synthesized and evaluated as described at the patent application EP17382693 [33]. Briefly, a selenation of an acyl chloride was initially performed in aqueous media, being the selenating agent, and sodium hydrogen selenide was prepared in situ by reduction of metallic selenium with sodium borohydride. Later, the intermediate generated, with no purification (one-pot synthesis), reacted with the adequate alkyl halide to render the desired selenoester. When necessary for not being commercially available, the acyl chloride was synthesized by the chlorination of the corresponding carboxylic acid using thionyl chloride.

Before each biological assay, the stock solution of selenoesters (10 mM) was prepared in dimethyl sulfoxide (DMSO).

### 4.2. Reagents and Media

DMSO (Sigma-Aldrich, St Louis, MO, USA), phosphate-buffered saline (PBS; pH 7.4), Mueller–Hinton (MH) broth, autoinducer bioassay (AB-A) medium, resazurin sodium salt (Sigma-Aldrich), tryptic soy broth (TSB), tryptic soy agar (TSA), brain heart infusion (BHI), Luria–Bertani broth (LBB), Luria–Bertani agar (LBA), reserpine, CCCP (carbonyl cyanide 3-chlorophenylhydrazone).

### 4.3. Bacterial Strains

As Gram-positive strains, *Staphylococcus aureus* American Type Culture Collection (ATCC) 25923 strain was used as methicillin-susceptible reference and biofilm-producing strain; the clinical isolate *S. aureus* MRSA 272123 and the methicillin and oxacillin-resistant *S. aureus* MRSA ATCC 43300 strains were investigated in the study.

As Gram-negative strains, the biofilm-producing *Pseudomonas aeruginosa* CCM 3955/ATCC 27853, multidrug-resistant *P. aeruginosa* NEM 986 strain, the wild-type *Salmonella enterica* serovar Typhimurium SL1344 (SE01) expressing the AcrAB-TolC pump system and its *acrB* gene-inactivated mutant *S. Typhimurium* SL1344 strain (SE02), *acrA* gene-inactivated mutant *S. Typhimurium* SL1344 (SE03), and *tolC* gene-inactivated mutant *S. Typhimurium* SL1344 strain (SE39) were used in the study. In terms of QS tests, the Gram-negative *Vibrio campbellii* ATCC BAA-1118 and ATCC BAA-1119 strains were applied. Microorganisms were obtained from the Czech Collection of Microorganisms (CCM, Masaryk University, Czech Republic) and the Collection of Laboratory of Medical Microbiology (NEM, Czech Laboratory, Ltd., Prague, Czech Republic).

### 4.4. Determination of Minimum Inhibitory Concentrations (MIC) by Microdilution Method

The minimum inhibitory concentrations (MICs) of ketone- and cyano-selenoesters were obtained according to the Clinical and Laboratory Standard Institute guidelines (CLSI) [34]. The MIC values of the compounds were established by visual inspection. The solvent DMSO did not exert any antibacterial activity. The MIC determination was performed in 4 parallels for each compound and strain, respectively.

#### 4.5. Real-Time Ethidium Bromide Accumulation Assay

The efflux pump inhibiting activity of Se-compounds was tested on *S. aureus* ATCC 25923 and *S. aureus* MRSA ATCC 43300 strains by real-time fluorimetry monitoring the intracellular accumulation of the efflux pump substrate EB using a CLARIOstar Plus plate reader (BMG Labtech, Ortenberg, Germany). Reserpine (RES) was applied at 25  $\mu$ M as a positive control; the solvent DMSO was applied at 1 v/v %. The bacterial strains were cultured at 37 °C in a shaking incubator until they reached an optical density (OD) of 0.6 at 600 nm. The cells were then washed with phosphate-buffered saline (PBS; pH 7.4) and centrifuged at 13,000 $\times$  g for 2 min; the pellet was re-suspended in PBS. The Se-compounds were applied at one-half MIC concentration to PBS supplemented with a non-toxic concentration of EB (2  $\mu$ g/mL). Then, the solutions were pipetted into a 96-well black microtiter plate (Greiner Bio-One Hungary Kft, Hungary), and 50  $\mu$ L of bacterial suspension (OD<sub>600</sub> 0.6) was pipetted to the wells. Then, the plates were inserted into the CLARIOstar plate reader, and the fluorescence was recorded at excitation and emission wavelengths of 530 nm and 600 nm, respectively, every minute for 1 hour. From the real-time data, the relative fluorescence index (RFI) of the last time point (minute 60) of the EB accumulation assay was calculated according to the subsequent equation:

$$\text{RFI} = (\text{RF}_{\text{treated}} - \text{RF}_{\text{untreated}}) / \text{RF}_{\text{untreated}}$$

where  $\text{RF}_{\text{treated}}$  is the relative fluorescence (RF) at the last time point of EB retention curve in the presence of an inhibitor, and  $\text{RF}_{\text{untreated}}$  is the RF at the last time point of the EB retention curve of the untreated control having the solvent control (DMSO) [24]. The RFI values were analyzed by *t*-test, and statistical significance was defined as  $p < 0.05$ .

#### 4.6. Assay for Quorum Sensing (QS) Inhibition

Anti-QS activity was monitored by two commercial strains of *V. campbellii* (ATCC BAA-1118 and ATCC BAA-1119). The first one responds by bioluminescence to AI-1 inducer, the second one to AI-2 inducer [35]. The effect of compounds on the luminescence generation was evaluated as described previously. Briefly, the overnight culture of strains was diluted to  $5 \times 10^5$  CFU/mL (colony-forming units per milliliter) in Autoinducer Bioassay medium ((NaCl (17.5 g/L), MgSO<sub>4</sub> (12.3 g/L), casamino acids (2 g/L), 10 mM potassium phosphate (pH 7.0), 1 mM L-arginine, and glycerol (10 mL/L of each)) and split into 96-well plates. After adding the compounds and their twofold serial dilutions, we incubated the plate for 8 h at 30 °C with continuous shaking. Then, luminescence was recorded for 16 h using a microplate reader (SpectraMax i3 Multi-Mode Detection Platform, Molecular Devices, San Jose, CA, USA) set up at 30 °C, integration time of 10,000 ms, and shaking for 60 s prior to measurement. The EC<sub>50</sub> of compounds was determined on the basis of the sum of luminescence. After that, the viability of culture was determined by resazurin assay and the IC<sub>50</sub> of compounds was calculated. The compounds were compared on the basis of EC<sub>50</sub> (the concentration that halves the cell communication) and IC<sub>50</sub> (viability). The EC<sub>50</sub> and IC<sub>50</sub> were calculated by using GraphPad Prism software version 5.00 for Windows with nonlinear regression curve fit (GraphPad Software, San Diego, CA, USA; [www.graphpad.com](http://www.graphpad.com)).

#### 4.7. Anti-Biofilm Activity

##### 4.7.1. Inhibition of Biofilm Formation

The effect of the Se-compounds on biofilm formation was investigated on *S. aureus* ATCC 25923 and *P. aeruginosa* CCM 3955 (ATCC 27853). The experiment was carried out in 96-well microplates [36]. The overnight bacterial was diluted in brain heart infusion (BHI) broth to achieve the optical density of 0.5 McFarland, and the suspension was distributed into 96-well plates in 100  $\mu$ L aliquots per well. The Se-compounds were pipetted to the cells in a concentration range of 100  $\mu$ M to 3.125  $\mu$ M. The plate was kept for 24 h at 37 °C. Then, the viability of adherent cells was determined immediately by

resazurin assay. The medium was discarded, the samples were washed 3 times by phosphate-buffered saline (PBS), and 100  $\mu$ L of resazurin in PBS (0.03 mg/L) was added to the wells [37]. The viability was measured by recording the fluorescence (560/590 nm, ex./em.) by the SpectraMax i3x Multi-Mode Detection Platform (Molecular Devices, San Jose, CA, USA). The assays were performed in four parallels. The relative viability was evaluated as a percentage according to the formula:

$$\text{RA [\%]} = 100 \frac{\text{sample fluorescence} - \text{average fluorescence of NC}}{\text{average fluorescence of PC} - \text{average fluorescence of NC}}$$

where RA is relative activity in percentage, PC is positive control (untreated biofilm), and NC is negative control (resazurin incubated without bacterial cells).

The IC<sub>50</sub> values were calculated using the online tool freely provided by AAT Bioquest–IC50 Calculator.

#### 4.7.2. Disruption of Mature Biofilm

The activity of Se-compounds to damage mature biofilms formed by *S. aureus* ATCC 25923 or *P. aeruginosa* CCM 3955 (ATCC 27853) was investigated by resazurin assay [38]. The assay was carried out in 96-well plates. The overnight bacterial cultures were diluted in BHI broth to the optical density of 0.5 McFarland and pipetted in 100  $\mu$ L aliquots into the wells. After 24 h of incubation at 37 °C, the medium was discarded, and fresh BHI broth containing Se-compounds was measured to the wells. After 24 h of incubation, the medium was discarded, the wells were washed 3 times by PBS (pH 7.4), and 100  $\mu$ L of resazurin in PBS (0.03 mg/L) was measured to the samples. The viability was recorded by measuring fluorescence (560/590 nm, ex./em.) using the SpectraMax i3x Multi-Mode Detection Platform (Molecular Devices, San Jose, CA, USA). The assays were performed in 4 parallels. The IC<sub>50</sub> values were calculated using the online tool freely provided by AAT Bioquest–IC50 Calculator.

## 5. Conclusions

This work describes the biological evaluation of 15 novel selenoesters as antibacterials that have a phenyl ring, with different substituents linked to the carbonyl and a functionalized alkyl chain linked to the selenium atom. Eight selenoesters (**K1–K8**) contain a ketone group in this chain, whereas the seven remaining (**N1–N7**) are functionalized by a cyano group. The ketone-selenoesters exerted a potent antibacterial activity against the three strains of *S. aureus* considered herein (one sensitive and two MRSA), higher than that observed for the cyano-selenoesters. Seven of the ketone derivatives showed submicromolar MIC values on *S. aureus* MRSA 272123. The antibacterial activity seemed to be reduced by the inclusion of bulky substituents. Regarding the inhibition of efflux pumps, compound **N4** was a more potent inhibitor than the reference reserpine in *S. aureus* MRSA 43300, and **K7** was a more potent inhibitor than the reference CCCP in *S. Typhimurium* SE39  $\Delta$ tolC. Furthermore, the substitution with *tert*-butyl or trifluoromethyl groups seemed to enhance the inhibition of efflux pumps. Different compounds inhibited selectively the two main types of quorum sensing (QS)—**K1**, **K2**, **K8**, and **N2** inhibited the AI-1 communication, whereas **K2**, **K4**, **K7**, **N3**, and **N7** inhibited the AI-2 communication. Generally, ketone-selenoesters were better inhibitors of AI-1 and cyano-selenoesters were better inhibitors of AI-2. Finally, all compounds were able to prevent biofilm formation at concentrations below 4  $\mu$ M in both *S. aureus* ATCC 25923 and *P. aeruginosa* CCM 3955. At the same time, all compounds disrupted biofilms produced by *S. aureus* at concentrations below 50  $\mu$ M, and *P. aeruginosa* biofilms at concentrations below 25  $\mu$ M. All these observations highlight the promising antibacterial, efflux pump inhibitory, quorum sensing inhibitory, and anti-biofilm activity of these novel ketone- and cyano-selenocompounds.

**Author Contributions:** G.S. and E.D.-Á. conceived and designed the study. E.D.-Á., N.S.-J., and C.S.-H. synthesized the selenocompounds used in the study. N.S., A.K., K.R., and L.H. performed the laboratory work. G.S., E.D.-Á., and J.V. wrote the article. All authors have read and agreed to the published version of the manuscript.

**Funding:** The study was supported by the projects SZTE ÁOK-KKA 2018/270-62-2 of the University of Szeged, Faculty of Medicine and GINOP-2.3.2-15-2016-00038 (Hungary); Consejo Superior de Investigaciones Científicas (CSIC, Spain, project LINKA20285); and Czech Ministry of Education, Youth and Sports INTER-COST LTC19007, COST Action CA17104 STRATAGEM.

**Acknowledgments:** The authors thank Jessica Blair (Institute of Microbiology and Infection, College of Medical and Dental Sciences, University of Birmingham, Birmingham B15 2TT, UK) for providing the *Salmonella* strains.

**Conflicts of Interest:** The authors declare no conflict of interest. The funders had no role in the design of the study; in the collection, analyses, or interpretation of data; in the writing of the manuscript; or in the decision to publish the results.

## References

1. Ventola, C.L. The antibiotic resistance crisis: part 1: Causes and threats. *P T Peer-Rev. J. Formul. Manag.* **2015**, *40*, 277.
2. Bragg, R.R.; Meyburgh, C.M.; Lee, J.-Y.; Coetzee, M. Potential Treatment Options in a Post-antibiotic Era. *Adv. Exp. Med. Biol.* **2018**, *1052*, 51–61. [[CrossRef](#)] [[PubMed](#)]
3. Coyne, L.A.; Latham, S.M.; Dawson, S.; Donald, I.J.; Pearson, R.B.; Smith, R.F.; Williams, N.J.; Pinchbeck, G.L. Exploring Perspectives on Antimicrobial Use in Livestock: A Mixed-Methods Study of UK Pig Farmers. *Front. Vet. Sci.* **2019**, *6*, 257. [[CrossRef](#)]
4. Dong, L.T.; Espinoza, H.V.; Espinoza, J.L. Emerging superbugs: The threat of Carbapenem Resistant Enterobacteriaceae. *AIMS Microbiol.* **2020**, *7*, 176–182. [[CrossRef](#)] [[PubMed](#)]
5. El-Hamid, M.I.A.; El-Naenaeey, E.-S.Y.; Kandeel, T.M.; Hegazy, W.A.H.; Mosbah, R.A.; Nassar, M.S.; Bakhrebah, M.A.; Abdulaal, W.H.; Alhakamy, N.A.; Bendary, M.M. Promising Antibiofilm Agents: Recent Breakthrough against Biofilm Producing Methicillin-Resistant *Staphylococcus aureus*. *Antibiot* **2020**, *9*, 667. [[CrossRef](#)]
6. Singh, S.; Singh, S.K.; Chowdhury, I.; Singh, R. Understanding the Mechanism of Bacterial Biofilms Resistance to Antimicrobial Agents. *Open Microbiol. J.* **2017**, *11*, 53–62. [[CrossRef](#)] [[PubMed](#)]
7. Costerton, J.W.; Stewart, P.S.; Greenberg, E.P. Bacterial Biofilms: A Common Cause of Persistent Infections. *Science* **1999**, *284*, 1318–1322. [[CrossRef](#)]
8. Davey, M.E.; O’Toole, G.A. Microbial Biofilms: from Ecology to Molecular Genetics. *Microbiol. Mol. Biol. Rev.* **2000**, *64*, 847–867. [[CrossRef](#)]
9. Li, Y.-H.; Tian, X. Quorum Sensing and Bacterial Social Interactions in Biofilms. *Sensors* **2012**, *12*, 2519–2538. [[CrossRef](#)]
10. Miller, M.B.; Bassler, B.L. Quorum Sensing in Bacteria. *Annu. Rev. Microbiol.* **2001**, *55*, 165–199. [[CrossRef](#)]
11. Alcalde-Rico, M.; Hernando-Amado, S.; Blanco, P.; Martínez, J. Multidrug Efflux Pumps at the Crossroad between Antibiotic Resistance and Bacterial Virulence. *Front. Microbiol.* **2016**, *7*, 1483. [[CrossRef](#)] [[PubMed](#)]
12. Yazhiniprabha, M.; Vaseeharan, B. In vitro and in vivo toxicity assessment of selenium nanoparticles with significant larvicidal and bacteriostatic properties. *Mater. Sci. Eng. C* **2019**, *103*, 109763. [[CrossRef](#)] [[PubMed](#)]
13. Cihalova, K.; Chudobova, D.; Michalek, P.; Moulick, A.; Guran, R.; Kopel, P.; Adam, V.; Kizek, R. *Staphylococcus aureus* and MRSA Growth and Biofilm Formation after Treatment with Antibiotics and SeNPs. *Int. J. Mol. Sci.* **2015**, *16*, 24656–24672. [[CrossRef](#)] [[PubMed](#)]
14. Jastrzebska, I.; Mellea, S.; Salerno, V.; Grzes, P.A.; Siergiejczyk, L.; Niemirowicz-Laskowska, K.; Bucki, R.; Monti, B.; Santi, C.; Laskowska, N.-. PhSeZnCl in the Synthesis of Steroidal  $\beta$ -Hydroxy-Phenylselenides Having Antibacterial Activity. *Int. J. Mol. Sci.* **2019**, *20*, 2121. [[CrossRef](#)] [[PubMed](#)]
15. Ngo, H.X.; Shrestha, S.K.; Green, K.D.; Garneau-Tsodikova, S. Development of ebsulfur analogues as potent antibacterials against methicillin-resistant *Staphylococcus aureus*. *Bioorganic Med. Chem.* **2016**, *24*, 6298–6306. [[CrossRef](#)]
16. Gajdács, M.; Spengler, G.; Sanmartín, C.; Marć, M.A.; Handzlik, J.; Domínguez-Álvarez, E. Selenoesters and selenoanhydrides as novel multidrug resistance reversing agents: A confirmation study in a colon cancer MDR cell line. *Bioorganic Med. Chem. Lett.* **2017**, *27*, 797–802. [[CrossRef](#)] [[PubMed](#)]

17. Kharma, A.; Misak, A.; Grman, M.; Brezova, V.; Kurakova, L.; Barath, P.; Jacob, C.; Chovanec, M.; Ondrias, K.; Domínguez-Álvarez, E. Release of reactive selenium species from phthalic selenoanhydride in the presence of hydrogen sulfide and glutathione with implications for cancer research. *New J. Chem.* **2019**, *43*, 11771–11783. [[CrossRef](#)]
18. Reich, H.J.; Hondal, R.J. Why Nature Chose Selenium. *ACS Chem. Biol.* **2016**, *11*, 821–841. [[CrossRef](#)]
19. Fernandez-Lazaro, D.; Fernandez-Lazaro, C.I.; Mielgo-Ayuso, J.; Navascués, L.J.; Córdova, A.; Seco-Calvo, J. The Role of Selenium Mineral Trace Element in Exercise: Antioxidant Defense System, Muscle Performance, Hormone Response, and Athletic Performance. A Systematic Review. *Nutrients* **2020**, *12*, 1790. [[CrossRef](#)]
20. Stolwijk, J.M.; Garje, R.; Sieren, J.C.; Buettner, G.R.; Zakharia, Y. Understanding the Redox Biology of Selenium in the Search of Targeted Cancer Therapies. *Antioxidants* **2020**, *9*, 420. [[CrossRef](#)]
21. Sumner, S.E.; Markley, R.L.; Kirimanjeswara, G.S. Role of Selenoproteins in Bacterial Pathogenesis. *Biol. Trace Element Res.* **2019**, *192*, 69–82. [[CrossRef](#)] [[PubMed](#)]
22. Rayman, M.P. The importance of selenium to human health. *Lancet* **2000**, *356*, 233–241. [[CrossRef](#)]
23. Mosolygó, T.; Kincses, A.; Mosolygó, T.; Marć, M.A.; Nové, M.; Gajdács, M.; Sanmartín, C.; McNeil, H.E.; Blair, J.M.A.; Domínguez-Álvarez, E. Antiviral, Antimicrobial and Antibiofilm Activity of Selenoesters and Selenoanhydrides. *Molecules* **2019**, *24*, 4264. [[CrossRef](#)]
24. Nové, M.; Kincses, A.; Szalontai, B.; Rácz, B.; Blair, J.M.A.; González-Prádena, A.; Benito-Lama, M.; Domínguez-Álvarez, E.; Spengler, G. Biofilm Eradication by Symmetrical Selenoesters for Food-Borne Pathogens. *Microorganisms* **2020**, *8*, 566. [[CrossRef](#)]
25. Mosolygó, T.; Kincses, A.; Csonka, A.; Tönki, Á.S.; Witek, K.; Sanmartín, C.; Marć, M.A.; Handzlik, J.; Kieć-Kononowicz, K.; Domínguez-Álvarez, E.; et al. Selenocompounds as Novel Antibacterial Agents and Bacterial Efflux Pump Inhibitors. *Molecules* **2019**, *24*, 1487. [[CrossRef](#)]
26. Peña-Morán, O.A.; Villarreal, M.L.; Alvarez, L.; Meneses-Acosta, A.; Rodríguez-López, V. Cytotoxicity, Post-Treatment Recovery, and Selectivity Analysis of Naturally Occurring Podophyllotoxins from *Bursera fagaroides* var. *fagaroides* on Breast Cancer Cell Lines. *Molecules* **2016**, *21*, 1013. [[CrossRef](#)]
27. Spengler, G.; Kincses, A.; Gajdács, M.; Amaral, L. New Roads Leading to Old Destinations: Efflux Pumps as Targets to Reverse Multidrug Resistance in Bacteria. *Molecules* **2017**, *22*, 468. [[CrossRef](#)]
28. Yong, Y.-C.; Zhong, J.-J. Impacts of Quorum Sensing on Microbial Metabolism and Human Health. In *Future Trends in Biotechnology*; Zhong, J.-J., Ed.; Springer: Berlin/Heidelberg, Germany, 2012; Volume 131, pp. 25–61. [[CrossRef](#)]
29. Chatterjee, R.; Shreenivas, M.M.; Sunil, R.; Chakravorty, D. Enteropathogens: Tuning Their Gene Expression for Hassle-Free Survival. *Front. Microbiol.* **2019**, *9*, 3303. [[CrossRef](#)]
30. Gibbons, S.; Oluwatuyi, M.; Kaatz, G.W. A novel inhibitor of multidrug efflux pumps in *Staphylococcus aureus*. *J. Antimicrob. Chemother.* **2003**, *51*, 13–17. [[CrossRef](#)]
31. Rezzonico, F.; Smits, T.H.M.; Duffy, B. Detection of AI-2 Receptors in Genomes of Enterobacteriaceae Suggests a Role of Type-2 Quorum Sensing in Closed Ecosystems. *Sensors* **2012**, *12*, 6645–6665. [[CrossRef](#)]
32. Taga, M.E.; Semmelhack, J.L.; Bassler, B.L. The LuxS-dependent autoinducer AI-2 controls the expression of an ABC transporter that functions in AI-2 uptake in *Salmonella typhimurium*. *Mol. Microbiol.* **2008**, *42*, 777–793. [[CrossRef](#)] [[PubMed](#)]
33. Domínguez Álvarez, E.; Spengler, G.; Jacob, C.; Sanmartín Grijalba, M.C. Selenoester-Containing Compounds for Use in the Treatment of Microbial Infections or Colorectal Cancer. European Patent EP18382693, 28 September 2018.
34. Christopher, P.J.; Polgar, E.P. (Eds.) *Methods for Dilution Antimicrobial Susceptibility Tests for Bacteria That Grow Aerobically*, 11th ed.; Clinical and Laboratory Standards Institute: Wayne, MI, USA, 2018.
35. Viktorova, J.; Stupák, M.; Rehorova, K.; Dobiasova, S.; Hoang, L.; Hajslova, J.; Van Thanh, T.; Van Tri, L.; Van Tuan, N.; Ruml, T. Lemon Grass Essential Oil does not Modulate Cancer Cells Multidrug Resistance by Citral—Its Dominant and Strongly Antimicrobial Compound. *Foods* **2020**, *9*, 585. [[CrossRef](#)] [[PubMed](#)]
36. Hoang, L.; Beneš, F.; Fenclova, M.; Kronusova, O.; Švarcová, V.; Rehorova, K.; Švecová, E.B.; Vosátka, M.; Hajslova, J.; Kaštánek, P.; et al. Phytochemical Composition and In Vitro Biological Activity of *Iris* spp. (Iridaceae): A New Source of Bioactive Constituents for the Inhibition of Oral Bacterial Biofilms. *Antibiot* **2020**, *9*, 403. [[CrossRef](#)] [[PubMed](#)]



37. Sandberg, M.E.; Schellmann, D.; Brunhofer, G.; Erker, T.; Busygin, I.; Leino, R.; Vuorela, P.; Fallarero, A. Pros and cons of using resazurin staining for quantification of viable *Staphylococcus aureus* biofilms in a screening assay. *J. Microbiol. Methods* **2009**, *78*, 104–106. [[CrossRef](#)] [[PubMed](#)]
38. Haney, E.F.; Trimble, M.J.; Cheng, J.T.; Vallé, Q.; Hancock, R.E.W. Critical Assessment of Methods to Quantify Biofilm Growth and Evaluate Antibiofilm Activity of Host Defence Peptides. *Biomolecules* **2018**, *8*, 29. [[CrossRef](#)]

**Publisher’s Note:** MDPI stays neutral with regard to jurisdictional claims in published maps and institutional affiliations.



© 2020 by the authors. Licensee MDPI, Basel, Switzerland. This article is an open access article distributed under the terms and conditions of the Creative Commons Attribution (CC BY) license (<http://creativecommons.org/licenses/by/4.0/>).

**II.**

## Article

# Cyano- and Ketone-Containing Selenoesters as Multi-Target Compounds against Resistant Cancers

Nikoletta Szemerédi <sup>1</sup>, Simona Dobiasová <sup>2</sup>, Noemi Salardón-Jiménez <sup>3</sup>, Annamária Kincses <sup>1</sup>, Márta Nové <sup>1</sup>, Giyallah Habibullah <sup>2</sup>, Clotilde Sevilla-Hernández <sup>3</sup>, Miguel Benito-Lama <sup>3</sup>, Francisco-Javier Alonso-Martínez <sup>3</sup>, Jitka Viktorová <sup>2,\*</sup>, Gabriella Spengler <sup>1,\*</sup> and Enrique Domínguez-Álvarez <sup>3,\*</sup>

<sup>1</sup> Department of Medical Microbiology, Albert Szent-Györgyi Health Center and Faculty of Medicine, University of Szeged, Semmelweis utca 6, 6725 Szeged, Hungary; szemeredi.nikoletta@med.u-szeged.hu (N.S.); kincses.annamaria90@gmail.com (A.K.); nove.marta@med.u-szeged.hu (M.N.)

<sup>2</sup> Department of Biochemistry and Microbiology, Faculty of Food and Biochemical Technology, University of Chemistry and Technology Prague, Technická 3, 166 28 Prague 6, Czech Republic; dobiasoo@vscht.cz (S.D.); habibuli@vscht.cz (G.H.)

<sup>3</sup> Instituto de Química Orgánica General (IQOG-CSIC), Consejo Superior de Investigaciones Científicas, Juan de la Cierva 3, 28006 Madrid, Spain; noemi.sj.95@gmail.com (N.S.-J.); clo.sh.1995@gmail.com (C.S.-H.); miguelbenitodelama@gmail.com (M.B.-L.); franalonso9112@gmail.com (F.-J.A.-M.)

\* Correspondence: prokesoj@vscht.cz (J.V.); spengler.gabriella@med.u-szeged.hu (G.S.); e.dominguez-alvarez@iqog.csic.es (E.D.-Á.)



**Citation:** Szemerédi, N.; Dobiasová, S.; Salardón-Jiménez, N.; Kincses, A.; Nové, M.; Habibullah, G.; Sevilla-Hernández, C.; Benito-Lama, M.; Alonso-Martínez, F.-J.; Viktorová, J.; et al. Cyano- and Ketone-Containing Selenoesters as Multi-Target Compounds against Resistant Cancers. *Cancers* **2021**, *13*, 4563. <https://doi.org/10.3390/cancers13184563>

Academic Editor: Fortunato Ciardiello

Received: 12 July 2021

Accepted: 8 September 2021

Published: 11 September 2021

**Publisher's Note:** MDPI stays neutral with regard to jurisdictional claims in published maps and institutional affiliations.



**Copyright:** © 2021 by the authors. Licensee MDPI, Basel, Switzerland. This article is an open access article distributed under the terms and conditions of the Creative Commons Attribution (CC BY) license (<https://creativecommons.org/licenses/by/4.0/>).

**Simple Summary:** The search for novel anticancer agents has been the hot topic of interest in cancer research, due to the phenomenon of multidrug resistance (MDR) in cancer that can make cancer cells resistant to the current available chemotherapeutic agents. In this context, we have designed, synthesized, and biologically evaluated 15 novel selenoesters, with the aim to explore their activity against resistant cancer cell lines. Some of these described selenocompounds showed noteworthy cytotoxicity and selectivity, the ability to inhibit the ABCB1 efflux pump, the capacity to modulate the ATPase activity of this pump, the capability to trigger apoptotic events, the ability to interact in a synergistic manner with doxorubicin in resistant cancer cells, and the power to promote wound healing. Consequently, these results validate the design of these selenocompounds and justify further research to evaluate the possibilities of these compounds to be used in the future in the fight against resistant cancers.

**Abstract:** Fifteen selenocompounds, comprising of eight ketone-containing selenoesters (**K1–K8**, also known as oxoselenoesters) and seven cyano-containing selenoesters (**N1–N7**, known also as cyanoselenoesters), have been designed, synthesized, and evaluated as novel anticancer agents. These compounds are derivatives of previously reported active selenoesters and were prepared following a three-step one-pot synthetic route. The following evaluations were performed in their biological assessment: cytotoxicity determination, selectivity towards cancer cells in respect to non-cancer cells, checkerboard combination assay, ABCB1 inhibition and inhibition of ABCB1 ATPase activity, apoptosis induction, and wound healing assay. As key results, all the compounds showed cytotoxicity against cancer cells at low micromolar concentrations, with cyanoselenoesters being strongly selective. All of the oxoselenoesters, except **K4**, were potent ABCB1 inhibitors, and two of them, namely **K5** and **K6**, enhanced the activity of doxorubicin in a synergistic manner. The majority of these ketone derivatives modulated the ATPase activity, showed wound healing activity, and induced apoptosis, with **K3** being the most potent, with a potency close to that of the reference compound. To summarize, these novel derivatives have promising multi-target activity, and are worthy to be studied more in-depth in future works to gain a greater understanding of their potential applications against cancer.



**Keywords:** multidrug resistance; efflux pump; ABCB1; apoptosis; selenium; cancer

## 1. Introduction

The occurrence of multidrug resistance (MDR) to chemotherapeutic drugs has become a significant challenge in cancer therapy. One of the most important factors contributing to MDR is the overexpression of efflux pumps. P-glycoprotein (P-gp)—also known as multidrug resistance protein 1 (MDR1), ATP-binding cassette sub-family B member 1 (ABCB1), or the cluster of differentiation 243 (CD243)—was discovered in 1970 as a member of the ATP-binding cassette (ABC) transporter family [1,2]. These ABC transporters fulfil physiological functions in the gastrointestinal tract, liver, and lungs. They are localized in different barriers that separate blood vessels from specific organs, such as the blood–brain barrier (BBB), the blood–cerebrospinal fluid (B-CSF), the blood–retina barrier (BRB), the blood–testis barrier (BTB), and in the placenta [3]. In humans, this transporter is encoded by the MDR1, also known as *ABCB1* gene [4]. ABCB1 substrates are typically amphiphilic compounds. ABCB1 is comprised of two nucleotide-binding domains and 12 transmembrane domains which constitute a drug-binding pocket. This transporter is a natural cell protective protein whose function is the removal of xenobiotic compound out of the cells, as this compound can be toxic for the cells [5,6]. ABCB1 can remove various chemotherapeutic agents, e.g., daunorubicin, doxorubicin, vinblastine, vincristine, epirubicin, etoposide, imatinib, irinotecan, paclitaxel, or colchicine, thus leading to treatment failure in anticancer therapy [7]. It has been reported that ABCB1, together with the multidrug resistance-associated protein 1 (MRP1)/ATP Binding Cassette Subfamily C Member 1 (ABCC1) (encoded by *ABCC1* gene), is the major determinant of innate drug sensitivity, even at the lowest level of expression [8,9]. The design of inhibitors of efflux pumps, especially in regard to ABCB1, is a promising strategy in cancer therapy [10].

Selenium, and the organic and inorganic compounds that contain this element, are essential in various biological processes. It is known that selenium deficiency can cause disorders or augment risk of developing cancers [11]. Alternatively, epidemiological studies reported that dietary supplementation with selenium can reduce the incidence of certain types of cancers. These starting works in selenium supplementation led to the reporting of a wide variety of organic and inorganic selenocompounds with chemopreventive, antiproliferative, and cytotoxic activity against cancer [12]. Sodium selenite is probably the most deeply studied inorganic selenium salt with anticancer activity. Among organic selenocompounds with chemopreventive and anticancer activity, methylselenol, methylseleninic acid, selenocyanates, and diphenyl diselenide can be cited [13]. Finally, the number of works that study the anticancer and multidrug resistance reversing activities of selenium nanoparticles is significantly increasing nowadays [14].

Considering these lines of evidence, we have designed, synthesized, and determined the biological activity of selenium-containing anticancer agents, mostly of them selenoesters. It has been demonstrated that a selenoanhydride derivative and some selenoester derivatives have potent anticancer activity against ABCB1 expressing in MDR mouse T-lymphoma cells and MDR colon adenocarcinoma cells due to ABCB1 inhibition and apoptosis induction [15]. In addition, these derivatives exerted potent anticancer activity on sensitive and resistant breast cancer cell lines [16]. It has been confirmed that selenium compounds synergistically enhance the activity of anticancer drugs when they are administered in combination [17]. Furthermore, as a drug-repurposing approach, phenothiazines with a known pharmacological and toxicity profile were combined with the previously mentioned selenoanhydride and selenoester, and several Se-compounds exhibited synergistic activity in combination with promethazine, chlorpromazine, and thioridazine [18]. The synergistic effects observed suggest that selenium compounds are able to reverse MDR and potentiate the activity of reference anticancer drugs or compounds with well-defined anticancer activity.

Based on these results, 15 newly synthesized selenoesters, shown in Figure 1, have been investigated in this study with regard to their anticancer and MDR reversing capacity in sensitive and resistant colon adenocarcinoma cell lines. Out of them, eight contain a ketone in the alkyl group directly bound to the selenium atom (oxoselenoesters or ketone-selenoesters, **K1–K8**); and seven contain a cyano group in the same alkyl moiety (cyanoselenoesters, **N1–N7**).

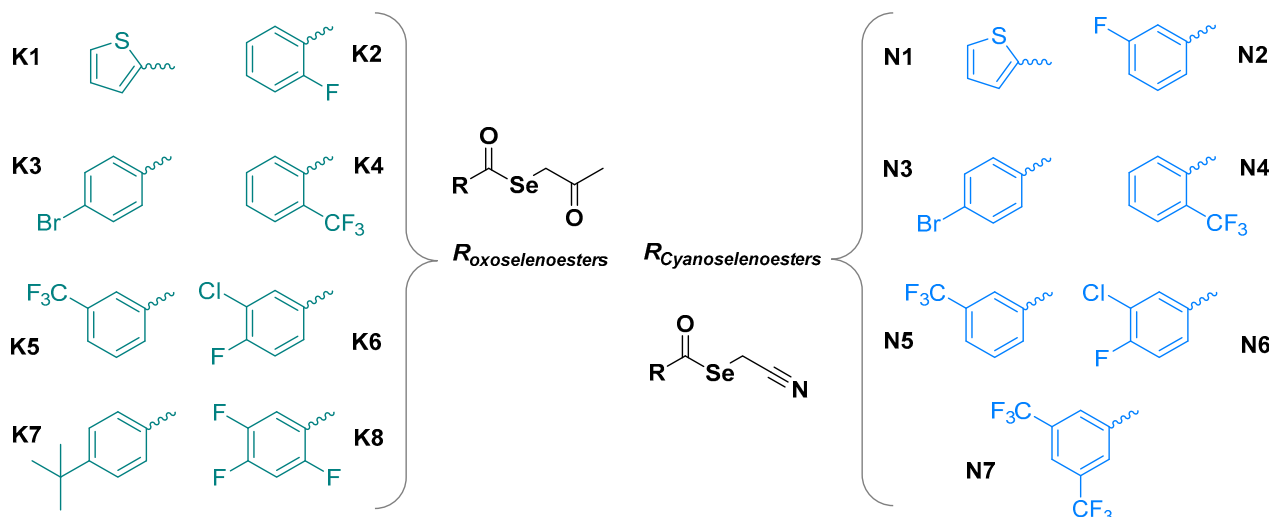


**Figure 1.** Structure of the oxoselenoesters, **K1–K8**, and of the cyanoselenoesters, **N1–N7**, presented in this work.

## 2. Materials and Methods

### 2.1. Chemical Reagents and Chemical Characterization

The chemical reagents, solvents, and materials used to synthesize the cyanoselenoesters and the oxoselenoesters presented herein were acquired at different vendors: Acros Organics and Alfa Aesar (both brands of Thermo Fisher Scientific, Geel, Belgium); Fluorochem (Hadfield, Derbyshire, UK); Honeywell Riedel de Haën (Seelze, Germany); Panreac Química S.L.U (Castellar del Vallés, Barcelona, Spain); Scharlab S.L. Spain (Sentmenat, Barcelona, Spain); and Sigma-Aldrich Merck S.L.U. Spain (Madrid, Spain).

To characterize the compounds, preliminary NMR spectra (Nuclear Magnetic Resonance) were taken using a Varian Inova-300 spectrometer (Agilent Technologies, Santa Clara, CA, USA) to monitor the reactions. The purity of the compounds, with a clean spectrum at the 300 MHz spectrometer, was assessed by means of elemental analysis using a LECO CHNS-932 microanalyser (LECO Europe B.V., Geleen, The Netherlands), at a temperature of 990 °C, using He as a carrier gas, and using silver capsules to introduce the sample in the analyser. Each compound must show a deviation of less than 0.40% in each element analysed (C, H, N, S) to be considered pure. The spectra included in the Supplementary Materials (Figures S1A–S15F) were taken with the following instruments: (i) NMR-<sup>1</sup>H, NMR-<sup>13</sup>C, and bidimensional COSY (Correlation spectroscopy); HSQC (Heteronuclear Single-Quantum Correlation spectroscopy); HMBC (Heteronuclear Multiple-Bond Correlation spectroscopy); and a Bruker Avance III HD-400 (Billerica, MA, USA) spectrometer using TMS as the internal standard. Next, (ii) mass spectra with a direct insertion probe (MS-DIP); and a quadrupole HP 5973 MSD spectrometer (Hewlett Packard, now Agilent Technologies, Santa Clara, CA, USA) with a direct insertion probe and electronic impact (EI) in positive mode as the ionization source, at a 70 eV ionization energy and with an *m/z* precision of ±0.05. Finally, (iii) Infrared spectroscopy (IR), using a Spectrum One B (Perkin-Elmer, Waltham, MA, USA) spectrophotometer. Solid samples were assayed preparing KBr films, whereas liquid samples were assayed between NaCl crystals. Finally, melting points have been determined in a Reichert-Kofler heating system coupled with a microscope; they are provided as obtained by visual inspection, without correction.

## 2.2. Synthetic Procedure

A synthetic procedure with three consecutive reactions in the same pot has been followed to obtain these 2-oxopropyl selenoesters and cyanomethyl selenoesters. In a first step, an equivalent of selenium grey powder is suspended in 20 mL of water, and 2 equivalents of sodium borohydride are added slowly over it and left stirring, usually for 15 min, or until the end of the gas release. Subsequently, an equivalent of the corresponding acyl chloride is added, and the reaction is stirred for 90 min at 50–70 °C. Then, the crude reaction mixture is filtered to eliminate the formed boron salts, and an equivalent of the appropriate alkyl halide are added at that time over the filtrate. The mixture is then kept reacting until reaction completion, which normally requires 1 h at 50 °C and an additional hour, initially at room temperature, and later ice-cooled.

The desired selenoester is isolated and purified by application of the most adequate techniques in each case, namely, as precipitation if the compound is solid, and extraction plus column chromatography if it is liquid. The purification followed for each compound is described in Section 2.3.

Starting acyl chlorides, if not commercially available at a reasonable cost, can be synthesized through the chlorination of the corresponding carboxylic acid with thionyl chloride. In this case, the appropriate derivative of benzoic acid is solved in an excess of thionyl chloride (at least 5:1 in molar ratio) and kept refluxing while stirring for 5 h. Then, thionyl chloride is removed in the rotary evaporator and the crude is washed 3 times with 50 mL of toluene, removing the toluene each time in the rotary evaporator to take away the remaining amounts of thionyl chloride. The structure of the synthesized acyl chloride is verified by <sup>1</sup>H-NMR, as compared with published data (data not shown). Then, the reagent is used in the synthesis of the respective selenocompound without further purification.

## 2.3. Chemical Description of the Compounds

### 2.3.1. *Se*-(2-Oxopropyl) Thiophene-2-carboselenoate (**K1**)

The reagents used: sodium borohydride (0.119 g, 3.15 mmol), grey selenium (0.120 g, 1.52 mmol), thiophene-2-carbonyl chloride (0.219 g, 0.16 mL, 1.5 mmol), and chloroacetone (0.139 g, 0.12 mL, 1.5 mmol). The final compound precipitated as a yellow solid powder that was isolated by filtration and washed with water, rendering 181 mg (49%). **MW**: 247.17. **Mp**: 52–53 °C. **DIP-MS** *m/z* (abundance %): 57.05 (3); 83.05 (7); 111.05 (100); and 245.95/2.47.95 (1/2, Se, M<sup>+</sup>). **IR** (KBr) (cm<sup>-1</sup>): 3082 (m, C-H<sub>Ar</sub>); 2958, 2922 (m, C-H); 1704 (m, C=O ketone); 1661 (s, C=O selenoester); and 1645, 1514 (m, C-C<sub>Ar</sub>). **<sup>1</sup>H-NMR** (400 MHz, CDCl<sub>3</sub>); δ: 7.83 (dd, *J*<sub>3-4</sub> = 3.9 Hz, *J*<sub>3-5</sub> = 1.0 Hz, 1H, H<sub>3</sub>); 7.72 (dd, *J*<sub>4-5</sub> = 5.0 Hz, 1H, H<sub>5</sub>); 7.16 (dd, 1H, H<sub>4</sub>); 3.90 (s, 2H, SeCH<sub>2</sub>); and 2.33 (s, 3H, COCH<sub>3</sub>). **<sup>13</sup>C-NMR** (101 MHz, CDCl<sub>3</sub>, δ): 203.6 (COCH<sub>3</sub>); 183.0 (COSe); 142.7 (C<sub>2</sub>); 134.2 (C<sub>5</sub>); 132.5 (C<sub>3</sub>); 128.3 (C<sub>4</sub>); 34.5 (SeCH<sub>2</sub>); and 28.7 (COCH<sub>3</sub>). **Elemental analysis** for C<sub>8</sub>H<sub>8</sub>O<sub>2</sub>SSe, calculated/found (%): C: 38.88/39.18; H: 3.26/3.41; and S:12.97/12.93.

### 2.3.2. *Se*-(2-Oxopropyl) 2-Fluorobenzoselenoate (**K2**)

The reagents used: sodium borohydride (0.122 g, 3.22 mmol), grey selenium (0.123 g, 1.55 mmol), 2-fluorobenzoyl chloride (0.239 g, 0.18 mL, 1.51 mmol), and chloroacetone (0.139 g, 0.12 mL, 1.50 mmol). The final compound was obtained as a pale-yellow liquid, rendering 59 mg (15%). **MW**: 259.14. **Mp**: Liquid RT. **DIP-MS** *m/z* (abundance %): 75.05 (16); 95.05 (38); 123.15 (100); 161.05 (8); and 255.95/256.95/257.95/259.95/261.95 (0/0/1/2/0, Se, M<sup>+</sup>). **IR** (KBr) (cm<sup>-1</sup>): 3067, 3005 (s, C-H<sub>Ar</sub>); 2925 (m, C-H); 1707 (m, C=O ketone); 1656 (s, C=O selenoester); and 1609, 1577, 1482, 1452 (m, C-C<sub>Ar</sub>). **<sup>1</sup>H-NMR** (400 MHz, CDCl<sub>3</sub>), δ: 7.86 (td, *J*<sub>6-5</sub> = 7.6 Hz, *J*<sub>6-4</sub> = 1.8 Hz, 1H, H<sub>6</sub>); 7.58 (dddd, *J*<sub>4-3</sub> = 8.3 Hz, *J*<sub>4-5</sub> = 7.5 Hz, *J*<sub>4-F</sub> = 5.0 Hz, *J*<sub>4-6</sub> = 1.7 Hz, 1H, H<sub>4</sub>); 7.26 (td, 1H, H<sub>5</sub>), 7.19 (ddd, *J*<sub>3-F</sub> = 11.0 Hz, 1H, H<sub>3</sub>); 3.90 (s, 2H, SeCH<sub>2</sub>); and 2.35 (s, 3H, COCH<sub>3</sub>). **<sup>13</sup>C-NMR** (101 MHz, CDCl<sub>3</sub>, δ): 203.7 (COCH<sub>3</sub>); 188.4 (d, *J*<sub>COSe-F</sub> = 5.2 Hz, COSe); 160.9 (d, *J*<sub>C(F)-F</sub> = 258.7 Hz, C<sub>2(F)</sub>); 135.4 (d, *J*<sub>6-F</sub> = 9.2 Hz, C<sub>6</sub>); 129.5 (d, *J*<sub>5-F</sub> = 1.4 Hz, C<sub>5</sub>); 126.0 (d, *J*<sub>1-F</sub> = 10.4 Hz, C<sub>1</sub>); 124.8 (d, *J*<sub>4-F</sub> = 3.6 Hz, C<sub>4</sub>); 117.2 (d, *J*<sub>3-F</sub> = 22.2 Hz, C<sub>3</sub>); 34.8 (d, *J*<sub>SeCH<sub>2</sub>-F</sub> = 6.5 Hz, SeCH<sub>2</sub>); and 28.9

(COCH<sub>3</sub>). **Elemental analysis** for C<sub>10</sub>H<sub>9</sub>FO<sub>2</sub>Se, calculated/found (%): C: 46.35/46.54; and H: 3.50/3.55.

### 2.3.3. *Se*-(2-Oxopropyl) 4-Bromobenzoselenoate (**K3**)

The reagents used: sodium borohydride (0.200 g, 5.29 mmol), grey selenium (0.200 g, 2.53 mmol), 4-bromobenzoyl chloride (0.551 g, 2.51 mmol), and chloroacetone (0.230 g, 0.20 mL, 2.51 mmol). The final compound precipitated as a white-pale-pink solid that was isolated by filtration, washed with water, and dried, rendering 331 mg (41%). **MW**: 320.04. **Mp**: 55–57 °C. **DIP-MS** *m/z* (abundance %): 50.15 (10); 75.05 (16); 76.05 (18); 154.95/156.95 (31/30, Br); 182.95/184.95 (100/97, Br); and 317.90/319.90/31.85 (0/1/1, Br + Se, M<sup>+</sup> – 2/M<sup>+</sup>/M<sup>+</sup> + 2). **IR** (KBr) (cm<sup>−1</sup>): 2954, 2917 (w, C-H<sub>Alk</sub>); 1706 (m, C=O ketone); 1665 (s, C=O selenoester); and 1582, 1564, 1481 (m, C-C<sub>Ar</sub>). **<sup>1</sup>H-NMR** (400 MHz, CDCl<sub>3</sub>); δ: 7.76 (td, *J*<sub>2-3,6-5</sub> = 8.7 Hz, *J*<sub>2-Br,6-Br</sub> = 2.3 Hz, 2H, H<sub>2</sub>+H<sub>6</sub>); 7.62 (td, *J*<sub>3-Br,5-Br</sub> = 2.3 Hz, 2H, H<sub>3</sub>+H<sub>5</sub>); 3.91 (s, 2H, SeCH<sub>2</sub>); and 2.34 (s, 3H, COCH<sub>3</sub>). **<sup>13</sup>C-NMR** (101 MHz, CDCl<sub>3</sub>, δ: 203.7 (COCH<sub>3</sub>); 192.3 (COSe); 137.2 (C<sub>4Ph(Br)</sub>); 132.8 (C<sub>3Ph</sub>+C<sub>5Ph</sub>); 129.8 (C<sub>1Ph</sub>); 129.2 (C<sub>2Ph</sub>+C<sub>6Ph</sub>); 35.1 (SeCH<sub>2</sub>); and 29.2 (COCH<sub>3</sub>). **Elemental analysis** for C<sub>10</sub>H<sub>9</sub>BrO<sub>2</sub>Se, calculated/found (%): C: 37.53/37.53; and H: 2.83/2.78.

### 2.3.4. *Se*-(2-Oxopropyl) 2-(Trifluoromethyl)benzoselenoate (**K4**)

The reagents used: sodium borohydride (0.197 g, 5.21 mmol), grey selenium (0.195 g, 2.47 mmol), 2-(trifluoromethyl)benzoyl chloride (0.523 g, 0.37 mL, 2.51 mmol), and chloroacetone (0.239 g, 0.20 mL, 2.5 mmol). The final compound was extracted with dichloromethane (4 × 30 mL), dried, and evaporated in vacuum. A column using dichloromethane–toluene (3:1) was performed to purify the compound, rendering 158 mg of a pale-yellow liquid (21%). **MW**: 247.17. **Mp**: Liquid RT. **DIP-MS** *m/z* (abundance %): 75.05 (5); 95.05 (8); 125.05 (6); 126.05 (3); 145.05 (59); 173.15 (100); and 307.95/309.95 (0/0, Se, M<sup>+</sup>). **IR** (KBr) (cm<sup>−1</sup>): 3074, 3006 (m, C-H<sub>Ar</sub>); 2925 (m, C-H<sub>Alk</sub>); 1697 (s, broad, overlapping bands of selenoester and ketone C=O); and 1601, 1582, 1448 (w, C-C<sub>Ar</sub>). **<sup>1</sup>H-NMR** (400 MHz, CDCl<sub>3</sub>); δ: 7.76–7.79 (m, 2H, H<sub>3Ph</sub>+H<sub>6Ph</sub>); 7.63–7.69 (m, 2H, H<sub>4Ph</sub>+H<sub>5Ph</sub>); 3.93 (s, 2H, SeCH<sub>2</sub>); and 2.35 (s, 3H, COCH<sub>3</sub>). **<sup>13</sup>C-NMR** (101 MHz, CDCl<sub>3</sub>, δ: 203.3 (COCH<sub>3</sub>); 193.3 (COSe); 138.6 (q, *J*<sub>1-CF3</sub> = 1.8 Hz, C<sub>1Ph</sub>); 132.1 (d, *J*<sub>4-CF3</sub> = 0.7 Hz, C<sub>4Ph</sub>); 132.0 (C<sub>5Ph</sub>), 128.4 (C<sub>6Ph</sub>); 127.4 (q, *J*<sub>3-CF3</sub> = 5.3 Hz, C<sub>3Ph</sub>); 126.4 (q, *J*<sub>6-CF3</sub> = 33.0 Hz, C<sub>2Ph</sub>); 121.8 (q, *J*<sub>C-F[CF3]</sub> = 274.5 Hz, CF<sub>3</sub>); 36.0 (SeCH<sub>2</sub>); and 28.6 (COCH<sub>3</sub>). **Elemental analysis** for C<sub>9</sub>H<sub>11</sub>F<sub>3</sub>O<sub>2</sub>Se, calculated/found (%): C: 42.74/42.42; and H: 2.93/3.09.

### 2.3.5. *Se*-(2-Oxopropyl) 3-(Trifluoromethyl)benzoselenoate (**K5**)

The reagents used: sodium borohydride (0.119 g, 3.15 mmol), grey selenium (0.120 g, 1.52 mmol), 3-(trifluoromethyl)benzoyl chloride (0.313 g, 0.23 mL, 1.53 mmol), and chloroacetone (0.139 g, 0.12 mL, 1.50 mmol). The final compound was extracted with dichloromethane (4 × 30 mL), dried, and evaporated in vacuum. A column using dichloromethane–toluene (3:1) was performed to purify the compound, rendering 133 mg of a pale-yellow liquid (29%). **MW**: 238.15. **Mp**: Liquid RT. **DIP-MS** *m/z* (abundance %): 75.05 (6); 95.05 (9); 125.05 (7); 126.05 (5); 145.05 (74); 173.15 (100); and 305.95/306.95/307.95/309.95/311.95 (0/0/1/2/0, Se, M<sup>+</sup>). **IR** (KBr) (cm<sup>−1</sup>): 3073, 3007 (m, C-H<sub>Ar</sub>); 2925 (m, C-H<sub>Alk</sub>); 1712 (s, C=O ketone); 1679 (s, C=O selenoester); and 1611, 1590, 1484 (m, C-C<sub>Ar</sub>). **<sup>1</sup>H-NMR** (400 MHz, CDCl<sub>3</sub>); δ: 8.14 (s, 1H, H<sub>2Ph</sub>); 8.08 (d, *J*<sub>6-5</sub> = 7.9 Hz, 1H, H<sub>6Ph</sub>); 7.88 (d, *J*<sub>4-5</sub> = 7.8 Hz, 1H, H<sub>4Ph</sub>); 7.64 (t, 1H, H<sub>5Ph</sub>); 3.96 (s, 2H, SeCH<sub>2</sub>); and 2.36 (s, 3H, COCH<sub>3</sub>). **<sup>13</sup>C-NMR** (101 MHz, CDCl<sub>3</sub>, δ: 203.1 (COCH<sub>3</sub>); 192.1 (COSe); 138.8 (C<sub>1Ph</sub>); 131.9 (q, *J*<sub>3-CF3</sub> = 33.3 Hz, C<sub>3Ph</sub>); 130.7 (d, *J*<sub>6-CF3</sub> = 1.0 Hz, C<sub>6Ph</sub>); 130.6 (q, *J*<sub>4-CF3</sub> = 3.5 Hz, C<sub>4Ph</sub>); 129.9 (C<sub>5Ph</sub>); 124.2 (q, *J*<sub>2-CF3</sub> = 3.9 Hz, C<sub>2Ph</sub>); 123.5 (q, *J*<sub>C-F[CF3]</sub> = 272.5 Hz, CF<sub>3</sub>); 35.0 (SeCH<sub>2</sub>); and 28.9 (COCH<sub>3</sub>). **Elemental analysis** for C<sub>9</sub>H<sub>6</sub>ClNOSe, calculated/found (%): C: 42.74/42.43; and H: 2.93/3.05. The acyl chloride (3-fluorobenzoyl chloride) was synthesized from 3-fluorobenzoic acid (15.859 g, 113.19 mmol) and thionyl chloride (50 mL, excess), obtaining

11.675 g of the acyl chloride (65% yield). Complete yield of the full synthetic route is then 19%.

### 2.3.6. *Se*-(2-Oxopropyl) 3-Chloro-4-fluorobenzoselenoate (**K6**)

The reagents used: sodium borohydride (0.159 g, 4.20 mmol), grey selenium (0.161 g, 2.04 mmol), 3-chloro-4-fluorobenzoyl chloride (0.389 g, 2.02 mmol), and chloroacetone (0.186 g, 0.16 mL, 2.01 mmol). The final compound precipitated as a white solid that was isolated by filtration, washed with water, and purified in the column chromatography using dichloromethane as the eluent; obtaining, after column, 106 mg of a white solid powder (18%). **MW**: 238.15. **Mp**: 42–44 °C. **DIP-MS** *m/z* (abundance %): 74.05 (3); 93.05 (5); 94.05 (7); 109.05/110.95 (5/2, Cl); 129.05/130.95 (9/5, Cl); 157.05/158.95 (100/33, Cl); and 289.95/290.95/291.95/293.95/295.95 (0/0/1/1/0, Se, M<sup>+</sup>). **IR** (KBr) (cm<sup>-1</sup>): 3097, 3050 (m, C-H<sub>Ar</sub>); 2978, 2898 (m, C-H); 1717 (m, C=O ketone); 1672 (s, C=O selenoester); and 1591, 1494 (m, C-C<sub>Ar</sub>). **<sup>1</sup>H-NMR** (400 MHz, CDCl<sub>3</sub>); δ: 7.97 (dd, *J*<sub>2-F</sub> = 6.9 Hz, *J*<sub>2-6</sub> = 2.2 Hz, 1H, H<sub>2Ph</sub>); 7.82 (ddd, *J*<sub>6-5</sub> = 8.6 Hz, *J*<sub>6-F</sub> = 4.4 Hz, 1H, H<sub>6Ph</sub>); 7.25 (t, 1H, H<sub>5Ph</sub>); 3.93 (s, 2H, SeCH<sub>2</sub>); and 2.34 (s, 3H, COCH<sub>3</sub>). **<sup>13</sup>C-NMR** (101 MHz, CDCl<sub>3</sub>, δ: 203.1 (COCH<sub>3</sub>); 190.6 (COSe); 161.7 (d, *J*<sub>C4(F)-F</sub> = 258.7 Hz, C<sub>4Ph(F)</sub>); 135.3 (d, *J*<sub>1-F</sub> = 3.7 Hz, C<sub>1Ph</sub>); 130.1 (d, *J*<sub>2-F</sub> = 1.1 Hz, C<sub>2Ph</sub>); 127.9 (d, *J*<sub>6-F</sub> = 8.6 Hz, C<sub>6Ph</sub>); 122.6 (d, *J*<sub>3-F</sub> = 18.5 Hz, C<sub>3Ph(Cl)</sub>); 117.4 (d, *J*<sub>5-F</sub> = 22.1 Hz, C<sub>5Ph</sub>); 35.1 (SeCH<sub>2</sub>); and 28.9 (COCH<sub>3</sub>). **Elemental analysis** for C<sub>10</sub>H<sub>8</sub>ClFO<sub>2</sub>Se, calculated/found (%): C: 40.91/40.65; and H: 2.75/2.83. The acyl chloride (3-chloro-4-fluorobenzoyl chloride) was synthesized from 3-chloro-4-fluorobenzoic acid (9.426 g, 50 mmol) and thionyl chloride (35 mL, excess), obtaining 9.602 g of the acyl chloride (99.5% yield). Complete yield of the full synthetic route is then 18%.

### 2.3.7. *Se*-(2-Oxopropyl) 4-(*Tert*-butyl)benzoselenoate (**K7**)

The reagents used: sodium borohydride (0.119 g, 3.15 mmol), grey selenium (0.119 g, 1.51 mmol), 4-*tert*-butylbenzoyl chloride (0.292 g, 1.47 mmol), and chloroacetone (0.139 g, 0.12 mL, 1.50 mmol). The final compound was extracted with dichloromethane (4 × 30 mL), dried, and evaporated in vacuum. A column using dichloromethane–hexane (4:1) was performed to purify the compound, rendering 30 mg of a pale-yellow liquid (7%). **MW**: 297.26. **Mp**: Liquid RT. **DIP-MS** *m/z* (abundance %): 65.05 (1); 77.05 (4); 91.05 (9); 105.05 (5); 118.05 (15); 133.15 (2); 146.05 (17); 161.15 (100); and 298.05 (0, Se, M<sup>+</sup>). **IR** (KBr) (cm<sup>-1</sup>): 2964, 2907, 2870 (s, C-H); 1710 (s, C=O ketone); 1678 (s, C=O selenoester); and 1601, 1567, 1465 (m, C-C<sub>Ar</sub>). **<sup>1</sup>H-NMR** (400 MHz, CDCl<sub>3</sub>); δ: 7.85 (d, *J*<sub>2-3,6-5</sub> = 8.6 Hz, 2H, H<sub>2+H<sub>6</sub></sub>); 7.49 (d, 2H, H<sub>3+H<sub>5</sub></sub>); 3.89 (s, 2H, SeCH<sub>2</sub>); 2.33 (s, 3H, COCH<sub>3</sub>); and 1.34 (s, 9H, C<sub>4</sub>H<sub>9</sub>). **<sup>13</sup>C-NMR** (101 MHz, CDCl<sub>3</sub>, δ: 204.1 (COCH<sub>3</sub>); 192.2 (COSe); 158.4 (C<sub>1</sub>); 135.5 (C<sub>4</sub>); 127.5 (C<sub>2+C<sub>6</sub></sub>); 126.1 (C<sub>3+C<sub>5</sub></sub>); 35.5 (C(CH<sub>3</sub>)<sub>3</sub>); 34.2 (SeCH<sub>2</sub>); 31.2 (C(CH<sub>3</sub>)<sub>3</sub>); and 28.6 (s, COCH<sub>3</sub>). **Elemental analysis** for C<sub>14</sub>H<sub>18</sub>O<sub>2</sub>Se, calculated/found (%): C: 56.57/56.52; and H: 6.10/5.97.

### 2.3.8. *Se*-(2-Oxopropyl) 2,4,5-Trifluorobenzoselenoate (**K8**)

The reagents used: sodium borohydride (0.199 g, 5.26 mmol), grey selenium (0.200 g, 2.53 mmol), 2,4,5-trifluorobenzoyl chloride (0.483 g, 2.48 mmol), and chloroacetone (0.244 g, 0.21 mL, 2.63 mmol). The final compound precipitated as a yellow solid powder that was isolated by filtration and washed with water, rendering 306 mg (42%). **MW**: 295.12. **Mp**: 40–43 °C. **DIP-MS** *m/z* (abundance %): 81.05 (10); 92.95(1); 112.05 (1); 131.05 (20); 159.05 (100); and 291.95/292.95/293.95/295.95/297.95 (0/0/1/1/0, Se, M<sup>+</sup>). **IR** (KBr) (cm<sup>-1</sup>): 3058 (s, C-H<sub>Ar</sub>); 2963, 2921 (m, C-H); 1708 (s, C=O ketone); 1650 (s, C=O selenoester); and 1623, 1511 (s, C-C<sub>Ar</sub>). **<sup>1</sup>H-NMR** (400 MHz, CDCl<sub>3</sub>); δ: 7.71 (ddd, *J*<sub>6-F<sub>5</sub></sub> = 10.1 Hz, *J*<sub>6-F<sub>4</sub></sub> = 8.6 Hz, *J*<sub>6-F<sub>2</sub></sub> = 6.4, 1H, H<sub>6</sub>); 7.07 (td, *J*<sub>3-F<sub>4,3-F<sub>2</sub></sub></sub> = 9.8 Hz, *J*<sub>3-F<sub>5</sub></sub> = 6.1 Hz, 1H, H<sub>3</sub>); 3.92 (s, 2H, SeCH<sub>2</sub>); and 2.35 (s, 3H, COCH<sub>3</sub>). **<sup>13</sup>C-NMR** (101 MHz, CDCl<sub>3</sub>, δ: 203.1 (s, COCH<sub>3</sub>); 186.5 (s, COSe); 157.2 (ddd, *J*<sub>2-F<sub>2</sub></sub> = 257.6 Hz, *J*<sub>2-F<sub>4</sub></sub> = 10.1 Hz, *J*<sub>2-F<sub>5</sub></sub> = 2.5 Hz, C<sub>2(F)</sub>); 153.6 (ddd, *J*<sub>4-F<sub>4</sub></sub> = 261.5 Hz, *J*<sub>4-F<sub>5</sub></sub> = 14.7 Hz, *J*<sub>4-F<sub>2</sub></sub> = 12.5 Hz, C<sub>4(F)</sub>); 147.1 (ddd, *J*<sub>5-F<sub>5</sub></sub> = 249.5 Hz, *J*<sub>5-F<sub>4</sub></sub> = 12.9 Hz, *J*<sub>5-F<sub>2</sub></sub> = 3.3 Hz, C<sub>2(F)</sub>); 122.4 (ddd, *J*<sub>1-F<sub>2</sub></sub> = 13.1 Hz, *J*<sub>1-F<sub>5</sub></sub> = 4.3 Hz, *J*<sub>1-F<sub>4</sub></sub> = 3.8 Hz, C<sub>1(F)</sub>); 117.3 (dt, *J*<sub>6-F<sub>5</sub></sub> = 20.5 Hz,

$J_{6-F2,6-F4} = 3.1$  Hz, C<sub>6</sub>); 107.3 (dd,  $J_{3-F4} = 28.6$  Hz,  $J_{3-F6} = 21.3$  Hz, C<sub>3</sub>); 35.1 (SeCH<sub>2</sub>); and 29.1 (COCH<sub>3</sub>). **Elemental analysis** for C<sub>10</sub>H<sub>7</sub>F<sub>3</sub>O<sub>2</sub>Se, calculated/found (%): C: 40.70/40.61; and H: 2.39/2.45. The acyl chloride (2,4,5-trifluorobenzoyl chloride) was synthesized from 2,4,5-trifluorobenzoic acid (8.805 g, 50 mmol) and thionyl chloride (35 mL, excess), obtaining 9.538 g of the acyl chloride (98% yield). Complete yield of the full synthetic route is then 41%.

### 2.3.9. *Se-(Cyanomethyl) Thiophene-2-carboselenoate (N1)*

The reagents used: sodium borohydride (0.197 g, 5.21 mmol), grey selenium (0.194 g, 2.46 mmol), thienyl chloride (0.370 g, 0.27 mL, 2.54 mmol), and chloroacetonitrile (0.191 g, 0.16 mL, 2.53 mmol). The final compound precipitated as a beige solid that was isolated by filtration and washed with water, rendering 85 mg (15% yield). **MW**: 230.14. **Mp**: 50–52 °C. **DIP-MS**  $m/z$  (abundance %): 57.05 (9); 83.05 (21); 111.15 (100); and 230.95 (0, M<sup>+</sup>). IR (KBr, cm<sup>-1</sup>): 3111, 3082, 3068 (w, C-H<sub>Ar</sub>); 2990, 2935 (m, C-H<sub>Alk</sub>); 2246 (m, C≡N); 1662 (s, C=O); and 1512, 1406 (m, C-C<sub>Thiophene</sub>). **<sup>1</sup>H-NMR** (400 MHz, CDCl<sub>3</sub>);  $\delta$ : 7.81 (dd,  $J_{2-3} = 3.9$  Hz,  $J_{2-4} = 1.1$  Hz, 1H, H<sub>2Tp</sub>); 7.81 (dd,  $J_{2-4} = 5.0$  Hz, 1H, H<sub>4Tp</sub>); 7.19 (dd, 1H, H<sub>3Tp</sub>); and 3.71 (s, 2H, SeCH<sub>2</sub>). **<sup>13</sup>C-NMR** (101 MHz, CDCl<sub>3</sub>,  $\delta$ ): 180.4 (CO); 141.5 (C<sub>1Tp</sub>); 135.2 (C<sub>4Tp</sub>); 133.0 (C<sub>2Tp</sub>); 128.5 (C<sub>3Tp</sub>); 117.2 (C≡N); and 5.5 (SeCH<sub>2</sub>). **Elemental analysis** for C<sub>7</sub>H<sub>5</sub>NOSse, calculated/found (%): C: 36.53/36.69; H: 2.19/2.32; N: 6.09/6.22; and S: 13.93/13.89.

### 2.3.10. *Se-(Cyanomethyl) 3-Fluorobenzoselenoate (N2)*

The reagents used: sodium borohydride (0.199 g, 5.26 mmol), grey selenium (0.198 g, 2.51 mmol), 3-fluorobenzoyl chloride (0.391 g, 0.30 mL, 2.47 mmol), and chloroacetonitrile (0.190 g, 0.16 mL, 2.53 mmol). The final compound was extracted with dichloromethane (4 × 30 mL), dried, and evaporated in vacuum. A column using dichloromethane–hexane (4:1) was performed to purify the compound, rendering 138 mg (23%) of a pale-yellow liquid. **MW**: 242.11. **Mp**: Liquid at room temperature. **DIP-MS**  $m/z$  (abundance %): 50.15 (6); 69.05 (6); 75.15 (35); 95.15 (93); 123.15 (100); and 242.95 (0, M<sup>+</sup>). IR (NaCl, cm<sup>-1</sup>): 3075 (w, C-H<sub>Ar</sub>); 2998, 2944 (m, C-H<sub>Alk</sub>); 2246 (m, C≡N); 1690 (s, C=O); and 1589, 1482, 1437 (m, C-C<sub>Ar</sub>). **<sup>1</sup>H-NMR** (400 MHz, CDCl<sub>3</sub>);  $\delta$ : 7.66 (td,  $J_{6-5} = 7.8$  Hz,  $J_{6-2} = 1.0$  Hz, 1H, H<sub>6Ph</sub>); 7.55 (dt,  $J_{2-F} = 9.1$  Hz,  $J_{2-4} = 2.3$  Hz, 1H, H<sub>2Ph</sub>); 7.50 (td,  $J_{5-4,5-6} = 8.2$  Hz,  $J_{5-F} = 5.6$  Hz, 1H, H<sub>5Ph</sub>); 7.37 (tdd, 1H, H<sub>4Ph</sub>); and 3.71 (s, 2H, SeCH<sub>2</sub>). **<sup>13</sup>C-NMR** (101 MHz, CDCl<sub>3</sub>,  $\delta$ ): 189.5 (CO); 163.0 (d,  $J_{3-F} = 250.4$  Hz, C<sub>3Ph</sub>); 139.1 (d,  $J_{2-F} = 6.6$  Hz, C<sub>1Ph</sub>); 131.1 (d,  $J_{5-F} = 7.8$  Hz, C<sub>5Ph</sub>); 123.5 (d,  $J_{6-F} = 3.1$  Hz, C<sub>6Ph</sub>); 121.9 (d,  $J_{4-F} = 21.5$  Hz, C<sub>4Ph</sub>); 117.1 (C≡N), 114.2 (d,  $J_{2-F} = 23.3$  Hz, C<sub>2Ph</sub>); and 5.7 (SeCH<sub>2</sub>). **Elemental analysis** for C<sub>9</sub>H<sub>6</sub>FNOSse, calculated/found (%): C: 44.65/44.42; H: 2.50/2.62; and N: 5.79/6.83. The acyl chloride (3-fluorobenzoyl chloride) was synthesized from 3-fluorobenzoic acid (15.859 g, 113.19 mmol) and thionyl chloride (50 mL, 82 g, excess), obtaining 11.675 g of the acyl chloride (65% yield). Complete yield of the full synthetic route is then 15%.

### 2.3.11. *Se-(Cyanomethyl) 4-Bromobenzoselenoate (N3)*

The reagents used: sodium borohydride (0.200 g, 5.29 mmol), grey selenium (0.199 g, 2.52 mmol), 4-bromobenzoyl chloride (0.551 g, 2.51 mmol), and chloroacetonitrile (0.191 g, 0.16 mL, 2.53 mmol). The final compound precipitated as a white solid that was isolated by filtration and washed with water, rendering 340 mg (45%). **MW**: 303.02. **Mp**: 105–107 °C. **DIP-MS**  $m/z$  (abundance %): 50.10 (14); 75.00 (23); 76.00 (23); 154.90/156.90 (37/37, Br); and 182.90/184.90 (100/98, Br). IR (KBr, cm<sup>-1</sup>): 3082, 3007 (m, C-H<sub>Ar</sub>); 2241 (m, C≡N); 1667 (s, C=O); and 1586, 1565, 1394 (m, C-C<sub>Ar</sub>). **<sup>1</sup>H-NMR** (400 MHz, CDCl<sub>3</sub>);  $\delta$ : 7.73 (td,  $J_{2-3,6-5} = 8.7$  Hz,  $J_{2-Br,6-Br} = 2.0$  Hz, 2H, H<sub>2</sub>+H<sub>6</sub>); 7.66 (td,  $J_{3-Br,5-Br} = 2.1$  Hz, 2H, H<sub>3</sub>+H<sub>5</sub>); and 3.70 (s, 2H, SeCH<sub>2</sub>). **<sup>13</sup>C-NMR** (101 MHz, CDCl<sub>3</sub>,  $\delta$ ): 189.6 (COSe); 136.0 (C<sub>4Ph(Br)</sub>); 131.7 (C<sub>3Ph</sub>+C<sub>5Ph</sub>); 130.2 (C<sub>1Ph</sub>); 128.9 (C<sub>2Ph</sub>+C<sub>6Ph</sub>); 117.1 (C≡N); and 5.6 (SeCH<sub>2</sub>). **Elemental analysis** for C<sub>9</sub>H<sub>6</sub>BrNOSse, calculated/found (%): C: 35.67/35.37; H: 2.00/2.03; and N: 4.62/4.72.

### 2.3.12. *Se*-(Cyanomethyl) 2-(Trifluoromethyl)benzoselenoate (N4)

The reagents used: m sodium borohydride (0.197 g, 5.21 mmol), grey selenium (0.197 g, 2.49 mmol), 2-(trifluoromethyl)benzoyl chloride (0.524 g, 2.51 mmol), and chloroacetonitrile (0.191 g, 0.16 mL, 2.53 mmol). The final compound precipitated as a white powder that was isolated by filtration and washed with water, rendering 294 mg (40%). **MW**: 292.12. **Mp**: 65–67 °C. **DIP-MS**  $m/z$  (abundance %): 50.15 (4); 75.05 (11); 95.05 (15); 125.05 (11); 126.05 (5); 145.05 (88); and 173.15 (100). **IR** (KBr,  $\text{cm}^{-1}$ ): 2992, 2936 (w, C-H<sub>Alk</sub>); 2239 (s, C≡N); 1706 (s, C=O); and 1584, 1390 (m, C-C<sub>Ar</sub>). **<sup>1</sup>H-NMR** (400 MHz, CDCl<sub>3</sub>);  $\delta$ : 7.81 (dd,  $J_{6-5} = 5.4$  Hz,  $J_{6-4} = 3.7$  Hz, 1H, H<sub>6Ph</sub>); 7.76 (dd,  $J_{3-4} = 5.5$  Hz,  $J_{3-5} = 3.8$  Hz, 1H, H<sub>3Ph</sub>); 7.71 (t, 1H, H<sub>4Ph</sub>); 7.69 (t, 1H, H<sub>5Ph</sub>); and 3.72 (s, 2H, SeCH<sub>2</sub>). **<sup>13</sup>C-NMR** (101 MHz, CDCl<sub>3</sub>,  $\delta$ ): 191.2 (COSe); 137.3 (C<sub>1Ph</sub>); 132.6 (C<sub>5Ph</sub>); 132.4 (d,  $J_{4-CF3} = 0.7$  Hz, C<sub>4Ph</sub>); 128.4 (C<sub>6Ph</sub>); 127.6 (q,  $J_{5-CF3} = 5.3$  Hz, C<sub>3Ph</sub>); 126.8 (q,  $J_{6-CF3} = 33.1$  Hz, C<sub>2Ph</sub>); 123.0 (q,  $J_{C-F[CF3]} = 274.1$  Hz, CF<sub>3</sub>); 116.8 (C≡N); and 7.0 (SeCH<sub>2</sub>). **Elemental analysis** for C<sub>10</sub>H<sub>6</sub>F<sub>3</sub>N<sub>1</sub>OSe, calculated/found (%): C: 41.12/41.08; H: 2.07/2.15; and N: 4.79/4.75.

### 2.3.13. *Se*-(Cyanomethyl) 3-(Trifluoromethyl)benzoselenoate (N5)

The reagents used: sodium borohydride (0.198 g, 5.23 mmol), grey selenium (0.198 g, 2.51 mmol), 3-(trifluoromethyl)benzoyl chloride (0.526 g, 2.52 mmol), and chloroacetonitrile (0.191 g, 0.16 mL, 2.53 mmol). The final compound was a liquid non-miscible with water that was separated by decantation. Crude liquid was dissolved in 100 mL of dichloromethane and treated with silica, activated charcoal, and anhydrous sodium sulfate. After filtration and removal of the solvent in a rotary, 157 mg (21%) of a pale-yellow liquid was obtained. **MW**: 292.12. **Mp**: Liquid at room temperature. **DIP-MS**  $m/z$  (abundance %): 50.15 (5); 75.05 (10); 95.05 (13); 125.05 (9); 126.05 (5); 145.05 (85); 173.15 (100); and 292.95 (0, M<sup>+</sup>). **IR** (KBr,  $\text{cm}^{-1}$ ): 3074, 3000 (s, C-H<sub>Ar</sub>); 2946 (m, C-H<sub>Alk</sub>); 2247 (s, C≡N); 1683 (s, C=O); and 1612, 1440 (s, C-C<sub>Ar</sub>). **<sup>1</sup>H-NMR** (400 MHz, CDCl<sub>3</sub>);  $\delta$ : 8.11 (s, 1H, H<sub>2Ph</sub>); 8.05 (d,  $J_{6-5} = 7.9$  Hz, 1H, H<sub>6Ph</sub>); 7.93 (d,  $J_{4-5} = 7.8$  Hz, 1H, H<sub>4Ph</sub>); 7.68 (t, 1H, H<sub>5Ph</sub>); and 3.74 (s, 2H, SeCH<sub>2</sub>). **<sup>13</sup>C-NMR** (101 MHz, CDCl<sub>3</sub>,  $\delta$ ): 189.7 (COSe); 137.9 (C<sub>1Ph</sub>); 132.2 (q,  $J_{3-CF3} = 33.5$  Hz, C<sub>3Ph</sub>); 131.2 (q,  $J_{4-CF3} = 3.5$  Hz, C<sub>4Ph</sub>); 130.8 (d,  $J_{6-CF3} = 1.0$  Hz, C<sub>6Ph</sub>); 130.2 (C<sub>5Ph</sub>); 124.3 (q,  $J_{2-CF3} = 3.8$  Hz, C<sub>2Ph</sub>); 123.4 (q,  $J_{C-F[CF3]} = 272.8$  Hz, CF<sub>3</sub>); 116.9 (CN); and 5.9 (SeCH<sub>2</sub>). **Elemental analysis** for C<sub>10</sub>H<sub>6</sub>F<sub>3</sub>N<sub>1</sub>OSe, calculated/found (%): C: 41.12/41.13; H: 2.07/2.12; and N: 4.79/4.83.

### 2.3.14. *Se*-(Cyanomethyl) 3-Chloro-4-fluorobenzoselenoate (N6)

The reagents used: sodium borohydride (0.200 g, 5.29 mmol), grey selenium (0.197 g, 2.49 mmol), 3-chloro-4-fluorobenzoyl chloride (0.484 g, 2.51 mmol), and chloroacetonitrile (0.191 g, 0.16 mL, 2.53 mmol). The final compound precipitated as a white powder that was isolated by filtration and washed with water, rendering 279 mg (41%). **MW**: 276.55. **Mp**: 73–75 °C. **DIP-MS**  $m/z$  (abundance %): 74.00 (4); 93.00 (8); 94.00 (9); 109.00/110.95 (7/2, Cl); 129.00/130.95 (38/12, Cl); and 156.90/158.90 (100/33, Cl). **IR** (KBr,  $\text{cm}^{-1}$ ): 3101, 3051, 3010 (s, C-H<sub>Ar</sub>); 2953 (m, C-H<sub>Alk</sub>); 2242 (s, C≡N); 1679 (s, C=O); and 1587, 1495, 1398 (s, C-C<sub>Ar</sub>). **<sup>1</sup>H-NMR** (400 MHz, CDCl<sub>3</sub>);  $\delta$ : 7.94 (dd,  $J_{2-F} = 6.8$  Hz,  $J_{2-6} = 2.2$  Hz, 1H, H<sub>2Ph</sub>); 7.79 (ddd,  $J_{6-5} = 8.5$  Hz,  $J_{6-F} = 4.3$  Hz, 1H, H<sub>6Ph</sub>); 7.29 (t, 1H, H<sub>5Ph</sub>); and 3.71 (s, 2H, SeCH<sub>2</sub>). **<sup>13</sup>C-NMR** (101 MHz, CDCl<sub>3</sub>,  $\delta$ ): 188.2 (COSe); 162.1 (d,  $J_{C4(F)-F} = 259.9$  Hz, C<sub>4Ph(F)</sub>); 134.3 (d,  $J_{1-F} = 3.7$  Hz, C<sub>1Ph</sub>); 130.3 (d,  $J_{2-F} = 1.3$  Hz, C<sub>2Ph</sub>); 128.1 (d,  $J_{6-F} = 8.7$  Hz, C<sub>6Ph</sub>); 123.0 (d,  $J_{3-F} = 18.6$  Hz, C<sub>3Ph(Cl)</sub>); 117.7 (d,  $J_{5-F} = 22.2$  Hz, C<sub>5Ph</sub>); 116.9 (CN); and 5.9 (SeCH<sub>2</sub>). **Elemental analysis** for C<sub>9</sub>H<sub>5</sub>ClFNOSe, calculated/found (%): C: 39.09/39.12; H: 1.82/1.89; and N: 5.06/5.03. The acyl chloride (3-chloro-4-fluorobenzoyl chloride) was synthesized from 3-chloro-4-fluorobenzoic acid (9.426 g, 50 mmol) and thionyl chloride (35 mL, excess), obtaining 9.602 g of the acyl chloride (99.5% yield). Complete yield of the full synthetic route is then 40%.



### 2.3.15. *Se*-(Cyanomethyl) 3,5-Bis(trifluoromethyl)benzoselenoate (N7)

The reagents used: sodium borohydride (0.197 g, 5.22 mmol), grey selenium (0.197 g, 2.49 mmol), 3,5-bis(trifluoromethyl)benzoyl chloride (0.6874 g, 2.48 mmol), and chloroacetonitrile (0.191 g, 0.16 mL, 2.53 mmol). The final compound precipitated as a white solid powder that was isolated by filtration and washed with water, rendering 209 mg (23%). **MW**: 360.12. **Mp**: 63–65 °C. **DIP-MS** *m/z* (abundance %): 75.00 (3); 125.00 (2); 144.00 (5); 192.90 (2); 193.95 (4); 213.00 (45); 221.95 (2); and 241.00 (100). **IR** (KBr,  $\text{cm}^{-1}$ ): 3098, 3029, 3004 (m, C-H<sub>Ar</sub>); 2948 (s, C-H<sub>Alk</sub>); 2246 (m, C≡N); 1687 (s, C=O); and 1616, 1462 (m, C-C<sub>Ar</sub>). **<sup>1</sup>H-NMR** (400 MHz, CDCl<sub>3</sub>);  $\delta$ : 8.28 (s, 2H, H<sub>2Ph</sub>+H<sub>6Ph</sub>); 8.17 (s, 1H, H<sub>4Ph</sub>); and 3.79 (s, 2H, SeCH<sub>2</sub>). **<sup>13</sup>C-NMR** (101 MHz, CDCl<sub>3</sub>);  $\delta$ : 188.9 (CO); 139.0 (C<sub>1Ph</sub>); 133.3 (q,  $J_{3-CF3(3),5-CF3(5)} = 34.5$  Hz, C<sub>3Ph</sub>+C<sub>5Ph</sub>); 127.9 (p,  $J_{4-CF3(3),4-CF3(5)} = 3.5$  Hz, C<sub>4Ph</sub>); 127.4 (q,  $J_{2-CF3(3),6-CF3(5)} = 2.9$  Hz, C<sub>2Ph</sub>+C<sub>6Ph</sub>); 122.6 (q,  $J_{C(CF3)-F} = 273.3$  Hz, C<sub>CF3(3)}</sub>+C<sub>CF3(5)}</sub>); 116.4 (CN); and 6.4 (SeCH<sub>2</sub>). **Elemental analysis** for C<sub>11</sub>H<sub>5</sub>F<sub>6</sub>NOSe, calculated/found (%): C: 36.69/36.61; H: 1.40/1.43; and N: 3.89/3.89. The acyl chloride (3,5-bis(trifluoromethyl)benzoyl chloride) was obtained from 3,5-bis(trifluoromethyl)benzoic acid (12.906 g, 50 mmol) and thionyl chloride (35 mL, excess), obtaining 7.422 g of the acyl chloride (54% yield). Complete yield of the full synthetic route is then 13%.

### 2.4. Reagents, Medias, and Chemicals Used in the Biological Evaluation

Analytical grade (to enable its use without further purification) rhodamine 123 (R123); sodium dodecyl sulfate (SDS); 3-(4,5-dimethylthiazol-2-yl)-2,5-diphenyltetrazolium bromide (MTT); Dulbecco's Modified Eagle's medium–high glucose (DMEM) with 10% fetal bovine serum (FBS) and 1% penicillin-streptomycin mixture; resazurin sodium salt; trypsin-EDTA solution; allantoin; and tariquidar and dimethyl sulfoxide (DMSO) were acquired at Sigma-Aldrich (St. Louis, MO, USA). Doxorubicin hydrochloride was acquired from Teva Pharmaceuticals (Petah Tikva, Israel). Eagle's Minimal Essential Medium (EMEM, Sigma-Aldrich) containing 4500 mg/L glucose, supplemented with a non-essential amino acid (NEAA) mixture (Sigma-Aldrich); a selection of vitamins and 10% heat-inactivated FBS; 2 mM L-glutamine (Sigma-Aldrich); 1 mM Na-pyruvate (Sigma-Aldrich); nystatin (Sigma-Aldrich); a penicillin-streptomycin mixture at concentrations of 100 U/L and 10 mg/L; RPMI 1640 medium (Sigma-Aldrich), supplemented with 10% FBS; 2 mM L-glutamine; 1 mM Na-pyruvate; 100 mM HEPES (Sigma-Aldrich); nystatin; and a penicillin-streptomycin mixture at concentrations of 100 U/L and 10 mg/L were used in the biological evaluation. Pgp-Glo™ Assay Systems (Promega), and an Annexin V-FITC Apoptosis Detection Kit were used (Calbiochem, EMD Biosciences, Inc. La Jolla, CA, USA).

### 2.5. Preparations of Compounds for Biological Assays

The fifteen selenoesters (Figure 1) evaluated in this work, whose synthesis and characterization have been described above, were dissolved in dimethyl sulfoxide (DMSO) to obtain stock solutions with a 10 mM concentration to perform their biological evaluation.

### 2.6. Cell Lines and Their Maintenance

Three cell lines have been used in this study: the doxorubicin-sensitive Colo 205 (CCL-222, ATCC, Manassas, VA, USA) human colonic adenocarcinoma cell line; the multidrug resistant Colo 320/MDR-LRP expressing P-gp (MDR1)-LRP (CCL-220.1, ATCC) human colonic adenocarcinoma cell line; and the MRC-5 human embryonal lung fibroblast cell line (CCL-171, ATCC). The colon adenocarcinoma cell lines were purchased from LGC Promochem (Teddington, UK), and the MRC-5 cell line was purchased from Sigma-Aldrich (Merck KGaA, Darmstadt, Germany). Their culture conditions are as follows: Colo 205 (CCL-222, ATCC) and Colo 320/MDR-LRP expressing P-gp (MDR1)-LRP (CCL-220.1, ATCC) human colon adenocarcinoma cell lines were cultured in RPMI 1640 medium, supplemented with 10% FBS, 2 mM L-glutamine, 1 mM Na-pyruvate, and 100 mM HEPES. The cell lines were incubated at 37 °C, 5% CO<sub>2</sub>, and 95% air atmosphere. The semi-adherent human colon cancer cells were detached with a Trypsin-Versene (EDTA) solution for 5 min



at 37 °C. MRC-5 human embryonal lung fibroblast cells were cultured in EMEM containing 4.5 g/L of glucose and supplemented with a non-essential amino acid mixture, a selection of vitamins, and 10% FBS. The cell lines were incubated at 37 °C, 5% CO<sub>2</sub>, and 95% air atmosphere.

The activity of selenoesters was tested on several cancer cell lines, including HepG2 (hepatocellular carcinoma, CCL-23TM, ATCC); HeLa (cervical adenocarcinoma, CCL-2TM, ATCC); B16 (skin melanoma, CCL-6322TM, ATCC); and a non-cancerous cell line, HDF (human dermal fibroblasts, Sigma-Aldrich). HepG2, HeLa, B16, and HDF cell lines were cultivated in EMEM medium supplemented with 10% FBS, 2 mM L-glutamine, and 1% penicillin-streptomycin mixture. The HaCaT cell line was cultivated in DMEM medium supplemented with 10% FBS and 1% penicillin-streptomycin mixture. All of the cells were cultivated in a CO<sub>2</sub> incubator (5% CO<sub>2</sub>, 37 °C). Twice per week, the cell lines were passaged according to a standardized protocol with a trypsin-EDTA solution.

Wound healing activity was realized using human keratinocyte (HaCaT, Thermo Fisher Scientific, Waltham, MA, USA).

### 2.7. Cytotoxicity

The effects of increasing concentrations of the compounds on cell growth were tested in 96-well flat-bottomed microtiter plates. Moreover, 10<sup>4</sup> of human colonic adenocarcinoma cells in 100 µL of the medium (RPMI-1640) were added to each well, except for the medium control wells. The adherent human embryonal lung fibroblast cell line was seeded in the EMEM medium for 4 h before the assay. The two-fold serial dilutions of the compounds were made in a separate plate (0.19–100 µM), and then transferred to the plates containing the adherent corresponding cell line. Culture plates were incubated at 37 °C for 24 h. At the end of the incubation period, 20 µL of MTT (thiazolyl blue tetrazolium bromide) solution (from a 5 mg/mL stock solution) were added to each well. After incubation at 37 °C for 4 h, 100 µL of sodium dodecyl sulfate (SDS) solution (10% SDS in 0.01 M HCl) was added to each well, and the plates were further incubated at 37 °C overnight. Cell growth was determined by measuring the optical density (OD) at 540 nm (ref. 630 nm) with a Multiscan EX ELISA reader (Thermo Labsystems, Cheshire, WA, USA). Inhibition of cell growth was expressed as IC<sub>50</sub> values, defined as the inhibitory dose that reduces the growth of the cells exposed to the tested compounds by 50%. IC<sub>50</sub> values and the SD of triplicate experiments were calculated by using GraphPad Prism software version 5.00 for Windows, with a non-linear regression curve fit (GraphPad Software, San Diego, CA, USA; [www.graphpad.com](http://www.graphpad.com), accessed on 12 July 2021). Doxorubicin (from a 2 mg/mL stock solution, Teva Pharmaceuticals) was used as a positive control. The solvent (DMSO) did not have any effect on the cell growth in the tested concentrations.

The selectivity indexes (SI) were calculated as the ratio of the IC<sub>50</sub> value in the non-tumour cells and the IC<sub>50</sub> in the cancer cell lines. The compound's activity towards cancer cells is considered as strongly selective if the selectivity index (SI) value is higher than 6, moderately selective if 3 < SI < 6, slightly selective if 1 < SI < 3, and non-selective if SI is lower than 1 [16].

### 2.8. Checkerboard Combination Assay

A checkerboard microplate method was applied to study the effect of drug interactions between the selenocompounds and the chemotherapeutic drug doxorubicin on resistant Colo 320 colon adenocarcinoma cells expressing the ABCB1 transporter. Results were expressed in terms of the combination index (CI) values at 50% growth inhibition (ED<sub>50</sub>), which were determined by using CompuSyn software to plot 4 or 5 data points for each ratio. CI values were calculated by means of the median-effect equation, where CI < 1, CI = 1, and CI > 1 represent synergism, an additive effect (or no interaction), and antagonism, respectively (Table 1).

To perform the experiment, the dilutions of doxorubicin were made in a horizontal direction in 100 µL, and the dilutions of the Se-compounds were made vertically in the

microtiter plate in a volume of 50  $\mu\text{L}$ . The cells were re-suspended in the culture medium and distributed into each well in 50  $\mu\text{L}$  portions containing 6000 cells. The plates were incubated for 72 h at 37  $^{\circ}\text{C}$  in a  $\text{CO}_2$  incubator. The cell growth rate was determined after MTT staining. At the end of the incubation period, 20  $\mu\text{L}$  of MTT solution was added to each well. After incubation at 37  $^{\circ}\text{C}$  for 4 h, 100  $\mu\text{L}$  of SDS was added to each well and the plates were further incubated at 37  $^{\circ}\text{C}$  overnight. The optical density (OD) was measured at 540/630 nm with the Multiscan EX ELISA reader.

**Table 1.** Type of interactions based on the combination indexes.

Combination Index (CI)	Type of Interaction	Combination	Type of Interaction
0–0.1	very strong synergism	0.9–1.1	additive effect
0.1–0.3	strong synergism	1.1–1.2	slight antagonism
0.3–0.7	synergism	1.2–1.45 1.45–3.3	moderate antagonism antagonism
0.7–0.85	moderate synergism	3.3–10	strong antagonism
0.85–0.9	slight synergism	>10	very strong antagonism

### 2.9. ABCB1 Inhibition in the Presence of Selenoesters

The inhibition of the ABCB1 multidrug efflux pump ABCB1 by the tested compounds was evaluated using flow cytometry, measuring the retention of rhodamine 123 by ABCB1 (P-glycoprotein) in Colo 320 colonic adenocarcinoma cells. Briefly, the cell number of colonic adenocarcinoma cells were adjusted to  $2 \times 10^6$  cells/mL, re-suspended in serum-free RPMI-1640 medium in the case of colonic adenocarcinoma cells, and distributed in 0.5 mL aliquots into Eppendorf centrifuge tubes. The tested compounds were added at different concentrations (0.2 and 2  $\mu\text{M}$ ; from 1 and 10 mM stock solutions, respectively), and the samples were incubated for 10 min at room temperature. Tariquidar was applied as the positive control (0.2  $\mu\text{M}$  final concentration), and DMSO was used as the solvent control (at 2 v/v%). Next, 10  $\mu\text{L}$  (5.2  $\mu\text{M}$  final concentration) of the fluorochrome rhodamine 123 (Sigma, St. Louis, MO, USA) was added to the samples and the cells were incubated for 20 min at 37  $^{\circ}\text{C}$ . After the incubation period, the cells were washed twice and re-suspended in 0.5 mL PBS for analysis. The fluorescence of the gated cell population was measured with a Partec CyFlow<sup>®</sup> flow cytometer (Partec, Münster, Germany). The percentage of the mean fluorescence intensity was calculated for the treated MDR cells as compared with the untreated cells. The results were obtained from a representative flow cytometry experiment in which at least 20,000 individual cells of the overall population were evaluated for the rhodamine 123 retained inside the cells. The fluorescence activity ratio (FAR) was calculated based on the following equation, which relates the measured fluorescence values:

$$\text{FAR} = \frac{\text{Colo320}_{\text{treated}} / \text{Colo320}_{\text{control}}}{\text{Colo205}_{\text{treated}} / \text{Colo205}_{\text{control}}}$$

### 2.10. P-gp ATPase Activity Assay

P-glycoprotein ATPase activity was determined using the Pgp-Glo<sup>™</sup> Assay System (Promega, WI, USA). The assay was performed according to the manufacturer's instructions. Next, 20  $\mu\text{L}$  of recombinant human P-gp membranes (1.25 mg/mL) were incubated for 5 min in 20  $\mu\text{L}$  of the Pgp-Glo<sup>™</sup> assay buffer at 37  $^{\circ}\text{C}$ . Compounds were tested at 25  $\mu\text{M}$ . Sodium orthovanadate ( $\text{Na}_3\text{VO}_4$ , 0.25 mM) was applied as an inhibitor control, and verapamil was used as a substrate control (0.5 mM). DMSO at 2% was applied as a solvent control. The reaction was initiated by adding 10  $\mu\text{L}$  of 25 mM MgATP, and incubated at 37  $^{\circ}\text{C}$  for 40 min. The reaction was stopped after adding 50  $\mu\text{L}$  of ATP Detection Reagent. Then, the samples and controls were incubated at room temperature for 20 min. The emitted luciferase-generated luminescent signal was measured in a CLARIOstar Plus

plate reader (BMG Labtech, UK) at 580 nm. The relative ATPase activity was calculated based on the ratio between the luminescence measured of the P-gp ATPase activity of each compound and the basal P-gp ATPase activity according to the following equation:

$$\text{Relative ATPase activity} = \frac{\text{Lum}_{\text{treated}} - \text{Lum}_{\text{untreated}}}{\text{Lum}_{\text{Na}_3\text{VO}_4} - \text{Lum}_{\text{untreated}}}$$

The effect of the tested compounds was evaluated according to the instructions of the manufacturer (Table 2).

**Table 2.** Evaluation of Pgp ATPase activity.

$\Delta\text{RLU}_{\text{TC}} > \Delta\text{RLU}_{\text{basal}}$	the tested compound is a stimulator of Pgp ATPase activity
$\Delta\text{RLU}_{\text{TC}} = \Delta\text{RLU}_{\text{basal}}$	the tested compound has no effect on Pgp ATPase activity
$\Delta\text{RLU}_{\text{TC}} < \Delta\text{RLU}_{\text{basal}}$	the tested compound is an inhibitor of Pgp ATPase activity

RLU = Relative Light Unit; TC = tested compound. The difference in luminescent signal between  $\text{Na}_3\text{VO}_4$ -treated samples and untreated samples represents the basal Pgp ATPase activity.

### 2.11. Apoptosis

The assay was carried out using an Annexin V-FITC Apoptosis Detection Kit Cat. No. PF 032 from Calbiochem (EMD Biosciences, Inc. La Jolla, CA), according to the manufacturer's instructions. The concentration of the Colo 320 cell suspension was adjusted to approximately  $1 \times 10^6$  cells/mL. The cell suspension was distributed into 1 mL aliquots ( $1 \times 10^6$  cells) into a 24-well microplate and incubated overnight at 37 °C, with 5%  $\text{CO}_2$ . On the following day, the medium was removed and a fresh medium was added to the cells. The cells were incubated in the presence of Se-compounds for 3 h at 37 °C. The concentration for the apoptosis induction (2  $\mu\text{M}$ ) was selected based on previous cytotoxicity results ( $\text{IC}_{50}$  values). Moreover, 12H-benzo( $\alpha$ )phenothiazine (M627) was used as positive control at 20  $\mu\text{M}$  final concentration. After a 3 h induction period, the culture medium was removed, the cells were washed with PBS, and a fresh medium was added to the cells. The 24-well plates were incubated overnight at 37 °C, with 5%  $\text{CO}_2$ . After the incubation, the supernatant was collected in a microfuge tube and 200  $\mu\text{L}$  of 0.25 trypsin (Trypsin-Versene) was added to the wells until the cells detached from the surfaces of the wells. The cells were centrifuged at  $2000 \times g$  for 2 min at room temperature, the supernatant was removed, and the cells were re-suspended in fresh serum-free medium. After this procedure, apoptosis assay was carried out according to the rapid protocol of the kit using Annexin V-FITC and propidium iodide staining. The fluorescence was analysed immediately using a ParTec CyFlow<sup>®</sup> flow cytometer (Partec, Münster, Germany), and the results were obtained from a representative flow cytometry experiment in which at least 20,000 individual cells of the overall population in a sample were evaluated. The data were analysed by FlowJo<sup>™</sup> software (BD Biosciences, San Jose, NJ, USA).

### 2.12. Wound Healing Assay

Wound healing was measured in vitro by scratch assay, as the migration rate of the cells to close the gap was created, as described by Ling et al. [19], with slight modifications. Briefly, HaCaT cells at the concentration of  $5 \times 10^5$  cells were seeded into 12-well plates and incubated at 37 °C and 5%  $\text{CO}_2$  until the cells formed a uniform layer. After layer formation, the cells were washed with PBS and then scratched with a sterile micropipette tip. The debris was removed by further gentle washing with PBS, then the samples ( $\text{IC}_{10}$ ), along with the positive control (Allantoin, 50  $\mu\text{g}/\text{mL}$ ), were mixed with DMEM and added directly to the cells. The images of the scratch area were captured using an inverted microscope in  $4 \times$  magnification at different time intervals (0 h, 24 h, 48 h) and evaluated using ImageJ software (National Institutes of Health, Bethesda, MD, USA). All of the experiments were performed in four replicates, and a minimum of five measurements were considered from each image captured. Dean–Dixon's test was used to remove the

outliners in the values measured, and further statistical significances between the groups were established by *t*-test (Excel, Microsoft Office, Redmond, WA, USA). The wound closure was calculated as the ratio of the gap size at the beginning minus the gap size at the evaluated time.

### 3. Results

#### 3.1. Synthesis and Characterization of the Compounds

The ketone derivatives have been designed as derivatives of the potent oxoselenoesters previously reported [15–18], attempting to improve their activity and selectivity. The compounds published in these works were the Se-(2-oxopropyl) 4-chlorobenzoselenoate (compound 9), the Se-(3,3-dimethyl-2-oxobutyl) 4-chlorobenzoselenoate (compound 10), and the Se-(3,3-dimethyl-2-oxobutyl) 3,5-dimethoxybenzoselenoate (compound 11). Cyanoselenoesters have been designed as a variation of the ones included in a previous patent of the group [18], with the same improvement aim of the activity showed by the initial cyanoselenoesters included in this patent.

Seeing the noteworthy activity in previous works [15–18] shown by derivatives that contain halogens, we have considered herein different halogenated substituents (bromine, fluorine, trifluoromethyl, chlorine), as well their polysubstitution, to determine which ones enhanced the biological effects. Additionally, compounds with a thiophene ring or with a 4-*tert*-butyl substituent are included to evaluate the activity of compounds that contain heterocycles or electron-donating substituents, respectively.

The new 15 compounds reported in this work were pure and chemically stable at room temperature. All of them were pure in the Elemental Analysis, following the threshold of a maximum variation of  $\pm 0.4\%$  for every element tested (C, H, N, S). The yield is markedly affected by the state of the matter of the product: generally, liquid compounds require purification by column chromatography, and its handling is more troublesome, which is reflected in the yields. Typically, solid compounds showed yields in the range from 40% to 50%, with the exception of compound **K6** (18%); whereas liquid compounds have lower yields, from 7% to 29%. As mentioned above, the synthetic route consisted of three steps: an initial in situ preparation of the selenating agent, and the attack of this agent to the suitable benzoyl or thienyl chloride to form an acyl selenide salt that exerts a nucleophilic attack over a suitable alkyl halide (chloroacetone for derivatives **K1–K8** and chloroacetonitrile for compounds **N1–N7**). A few derivatives needed a preliminary step to prepare the required benzoyl chloride from the respective benzoic acid. These compounds were: **K5** and **N5** from 3-(trifluoromethyl)benzoic acid; **K6** and **N6** from 3-chloro-4-fluorobenzoic acid; **K8** from 2,4,5-trifluorobenzoic acid; and **N7** from 3,5-bis(trifluoromethyl)benzoic acid.

Compounds **K1–K8** have, as a common feature the  $-\text{COSeCH}_2\text{COCH}_3$  moiety bound to the phenyl or thienyl ring. In  $^1\text{H-NMR}$ , the  $\text{CH}_2$  appears as a singlet accompanied by two small satellite peaks (due to the influence of the adjacent selenium atom) in the range 3.89–3.96 ppm, and the  $\text{CH}_3$  in the range 2.33–2.36 ppm. Alternatively, in  $^{13}\text{C-NMR}$ , the  $\text{CH}_2$  again appears as a singlet accompanied by two small satellite peaks (due to the influence of the adjacent selenium atom) in the range 34.5–36.0 ppm, and the  $\text{CH}_3$  in the range 28.6–29.2 ppm. The carbonyls appear in different ranges in  $^{13}\text{C-NMR}$ : there is a higher and narrower range of 203.1–204.1 ppm for the ketone carbonyl, and a less displaced and wider range of 183.0–193.3 ppm for the carbonyl group of the selenoester. The width of the ranges is logical, as the width increases when the substituted phenyl ring is closer. Similarly, in the case of the **N1–N7** derivatives, the common structural moiety is the  $-\text{COSeCH}_2\text{CN}$  bound to the phenyl or thienyl ring. The  $-\text{CH}_2$  bound to the selenium and to the cyano group, which appears in  $^1\text{H-NMR}$  in the range from 3.70 to 3.79 ppm. This carbon is seen in  $^{13}\text{C-NMR}$  at a very low displacement (ranging from 5.5 to 7.0 ppm). The  $-\text{CN}$  group is observed in a very narrow range (116.4–117.2 ppm), and the  $-\text{COSe}$  appears at a slightly lower range than the  $-\text{COSe}$  of the ketone derivatives (180.4–191.2). The remaining signals depend on the ring (thienyl for **K1** and **N1**, and phenyl for the remaining compounds), and on the substituents (and their position) bound to the phenyl

ring. For a few compounds (**K1**, **K3**, **K7**, **K8**, **N1**, and **N5**), bidimensional NMR spectra as  $^1\text{H}$ - $^1\text{H}$  COSY,  $^1\text{H}$ - $^{13}\text{C}$  HSQC, and  $^1\text{H}$ - $^{13}\text{C}$  HMBC have been recorded to help in the correct assignment of the signals. Of these bidimensional spectra, HMBC was of particular interest, as the spectra obtained proof of the  $-\text{COSeCH}_2\text{CN}$  or the  $-\text{COSeCH}_2\text{COCH}_3$  thanks to the long-distance interactions between the different atoms involved (see spectra in Supplementary: Figures S1H, S3H, S7G, S8I, S9H, and S13I).

In mass spectrometry, the most abundant ion is always the product of the breakage of the carbon–selenium bond of the selenoester, releasing as a positive ion the acyl cation (which is the peak with 100% of abundance) and an anion that includes the selenium atom. From this acyl cation, different cations are also observed, including the release of the thiophenium cation (compounds **K1** and **N1**) or the appropriate phenyl cation. The latest overcomes different releases (for example: HF, HCl, and HBr) depending on the substituents present at the ring. The easiness of the breakage of the C–Se bond implies that the molecular ion always has a very low abundance, and it was even not observed in four compounds (**N3**, **N4**, **N6**, and **N7**). Additionally, the molecular ion showed an abundance below 0.5% in 5 compounds of the 11 remaining. Interestingly, abundances of the molecular ion were always higher at ketone-selenoesters (from 0% to 2%) than at cyanoselenoesters (not observed or below 0.5%). Perhaps this fact may point out that, at least in the conditions of the ionization chamber, the first are more stable.

Regarding infrared spectroscopy, all ketone-selenoesters showed two peaks in the range of 1720–1650, where the C=O stretch of carbonyl compounds are usually observed. The carbonyl of the selenoester had a lower (from 1650 to 1679  $\text{cm}^{-1}$ ), and a wider range than the one experimentally determined for the carbonyl of the ketone (from 1697 to 1712  $\text{cm}^{-1}$ ), due to the fact that it was the carbonyl group in the molecule which is closer to the substituents than the ketone carbonyl. The exception was the compound **K4**, which produced a wider overlapping signal that incorporated the two carbonyl compounds. Alternatively, the IR spectra of the nitrile derivatives have, as a common feature, the  $\text{C}\equiv\text{N}$  stretch and the C=O stretch of the selenoester. They appeared in the ranges 2239–2247  $\text{cm}^{-1}$  and 1662–1706  $\text{cm}^{-1}$ , respectively.

### 3.2. Cytotoxicity

Based on the obtained results, ketone-selenoesters showed a potent cytotoxic effect on both sensitive and resistant colon cancer cell lines, where the  $\text{IC}_{50}$  values were between 1 and 4  $\mu\text{M}$  on both cell lines. In addition, similar toxic activity was observed on MRC-5 normal lung fibroblast cells, indicating that ketone-selenoesters have no selectivity towards cancer cells. Cyanoselenoesters showed no effect on the MRC-5 cell line ( $\text{IC}_{50}$  was more than 100  $\mu\text{M}$ ); however, they were very toxic on both colon cancer cell lines. Comparing the sensitive Colo 205 ( $\text{IC}_{50}$ : 1.98–2.96  $\mu\text{M}$ ) to the resistant Colo 320 cells ( $\text{IC}_{50}$ : 3.78–7.64  $\mu\text{M}$ ), cyanoselenoesters were less potent on the resistant cells. Furthermore, both ketone- and cyanoselenoesters were more active on cancer cell lines than the positive control doxorubicin. Selectivity indexes (SI) were calculated as described above. Cyanoselenoesters showed high selectivity ( $>6$ ) in each case, and ketone-selenoesters showed moderate ( $3 < \text{SI} < 6$ ) and slight ( $1 < \text{SI} < 3$ ) selectivity, except **K2** ( $\text{SI} < 1$ ). (Table 3).

Similar results were obtained in cancer cells from other locations, such as liver, cervix, and skin. Ketone-selenoesters showed the following range of  $\text{IC}_{50}$  values in these cancer cells (Table 4): from 2.2 to 4.3  $\mu\text{M}$  towards hepatocellular carcinoma (HepG2) cells, from 1.9 to 2.7  $\mu\text{M}$  towards cervical adenocarcinoma (HeLa) cells, and from 1.1 to 2.0  $\mu\text{M}$  towards skin murine melanoma (B16) cells. Regarding cyanoselenoesters, the observed range of  $\text{IC}_{50}$  values in the abovementioned cell lines were from 5.2 to 11.8  $\mu\text{M}$  towards HepG2 cells, from 1.3 to 5.2  $\mu\text{M}$  towards the HeLa cell line, and from 1.4 to 2.6  $\mu\text{M}$  towards B16 cells. SI values were again higher than 6 for all of the cyanoselenoesters in HepG2 and HeLa cells, indicating that all of the cyanoselenoesters were strongly selective towards the cancer cells in respect to MRC-5 cells. In contrast, none of the ketone-selenoesters showed an SI value higher than three (moderately selective) for these two additional human cancer cells.



**Table 3.** Cytotoxic effect of selenocompounds on sensitive (Colo 205) and resistant (Colo 320) colon adenocarcinoma, and MRC-5 normal embryonal fibroblast cell lines and selectivity indexes (SI). Doxorubicin was used as a positive control.

Cpds.	Colo 205 (IC <sub>50</sub> μM)		Colo 320 (IC <sub>50</sub> μM)		MRC-5 (IC <sub>50</sub> μM)		SI	
	Mean	SD	Mean	SD	Mean	SD	MRC-5/Colo 205	MRC-5/Colo 320
K1	1.53	±0.46	1.47	±0.02	2.24	±0.29	1.46	1.52
K2	3.35	±0.58	2.38	±0.23	2.53	±0.40	0.76	1.06
K3	2.28	±0.05	2.15	±0.03	2.86	±0.36	1.25	1.33
K4	1.05	±0.04	1.48	±0.06	3.63	±0.37	3.46	2.45
K5	2.14	±0.08	2.17	±0.27	3.11	±3.93	1.45	1.43
K6	2.10	±0.02	2.10	±0.05	3.62	±0.41	1.73	1.72
K7	2.69	±0.07	2.57	±0.15	3.72	±0.17	1.38	1.45
K8	2.24	±0.16	2.37	±0.11	2.50	±0.06	1.12	1.05
N1	2.37	±0.27	7.64	±0.15	>100	-	>6 *	>6 *
N2	2.96	±0.09	7.01	±0.69	>100	-	>6 *	>6 *
N3	2.10	±0.06	4.37	±0.10	>100	-	>6 *	>6 *
N4	1.97	±0.14	5.57	±0.23	>100	-	>6 *	>6 *
N5	2.10	±0.10	5.22	±0.08	>100	-	>6 *	>6 *
N6	2.24	±0.07	5.19	±0.37	>100	-	>6 *	>6 *
N7	1.98	±0.16	3.78	±0.23	>100	-	>6 *	>6 *
Dox.	3.46	±0.34	7.61	±0.29	2.73	±0.34	0.79	0.36

Data are presented as the average of three measurements with the respective standard error of the mean. Dox. = doxorubicin. \* The derivatives were not toxic on normal human fibroblast (MRC-5). For this reason, the numeric value of selectivity could not be precisely determined; however, all derivatives proved to be selective.

**Table 4.** Cytotoxic effect of selenocompounds on hepatocellular carcinoma (HepG2), cervical adenocarcinoma (HeLa), and skin melanoma (B16) cell lines and selectivity indexes (SI).

Cpds.	HepG2 (IC <sub>50</sub> μM)		HeLa (IC <sub>50</sub> μM)		B16 (IC <sub>50</sub> μM)		SI		
	Mean	SD	Mean	SD	Mean	SD	MRC-5/HepG2	MRC-5/HeLa	MRC-5/B16
K1	2.3	±0.2	2.5	±0.2	1.4	±0.1	1.6	1.5	2.6
K2	2.2	±0.215	2.5	±0.5	1.2	±0.1	1.1	1.0	2.1
K3	3.1	±0.2	2.1	±0.2	1.7	±0.2	0.7	1.1	1.3
K4	4.3	±0.1	1.9	±0.0	2.0	±0.2	0.7	1.5	1.4
K5	2.4	±0.2	2.5	±0.1	1.1	±0.1	1.3	1.2	2.8
K6	2.9	±0.3	2.3	±0.1	1.3	±0.1	1.3	1.6	2.8
K7	3.7	±0.3	2.7	±0.3	1.4	±0.1	1.0	1.4	2.7
K8	4.0	±0.2	2.0	±0.0	1.4	±0.1	0.6	1.3	1.8
N1	11.3	±0.9	2.0	±0.1	1.9	±0.4	>6 *	>6 *	>6 *
N2	5.6	±0.3	5.2	±0.5	2.6	±0.4	>6 *	>6 *	>6 *
N3	9.6	±0.9	2.4	±0.1	2.8	±0.5	>6 *	>6 *	>6 *
N4	5.2	±0.3	2.5	±0.0	1.4	±0.3	>6 *	>6 *	>6 *
N5	9.8	±0.6	2.5	±0.2	1.4	±0.3	>6 *	>6 *	>6 *
N6	9.6	±0.4	1.3	±0.1	1.7	±0.3	>6 *	>6 *	>6 *
N7	11.8	±1.2	2.1	±0.1	1.6	±0.4	>6 *	>6 *	>6 *

\* The derivatives were not toxic on normal human fibroblast cells (MRC-5) up to 100 μM. For this reason, the numeric value of selectivity could not be precisely determined; however, all derivatives proved to be selective.

### 3.3. Checkerboard Combination Assay

The checkerboard combination assay is a widely used and convenient *in vitro* method for the assessment of drug interactions among various pharmacological agents. This program enables the calculation of the combination indices, and also allows the determination of the most effective ratios of combinational agents. Ketone- and cyanoselenoesters were combined with doxorubicin, and their interactions were determined after MTT staining. The data obtained were analysed using CalcuSyn software.

Six ketone-selenoesters (K1, K3, K4, K5, K6, K8) were found to interact synergistically with doxorubicin. Furthermore, K5 and K6 showed a synergistic interaction with doxorubicin in all ratios (Table 5). Additionally, a synergistic effect can be seen for five

cyanoselenoesters (N1, N2, N3, N4, N7) (Table 6). The type of interaction in the combination studies was evaluated using the Chou–Talalay method for drug combination, which is based on the median-effect equation. The prerequisite for the calculation is the dose-effect curves for each drug alone. The combination of two drugs at a certain ratio behaves like a third drug to the cells. In this way, the parameters can be obtained for the mixture, just in case the of the single drugs, by using the automated median-effect plot with computer software. Applying this method, several ratios can be tested and different types of interactions can be obtained, allowing for a more precise description of the interaction of the compounds [20].

**Table 5.** Interaction of ketone-selenoesters with doxorubicin on MDR Colo 320 cells.

Compounds	Starting Conc. ( $\mu\text{M}$ )	Ratio *	CI at $\text{ED}_{50}$	SD ( $\pm$ )	Type of Interaction
K1	5	0.6:1	2.6	0.73	Antagonism
		1.2:1	1.03	0.11	Additive effect
		2.4:1	0.94	0.09	Additive effect
		4.8:1	0.88	0.13	<b>Slight synergism</b>
		9.6:1	1.18	0.15	Slight antagonism
K2	6	0.7:1	1.77	0.22	Antagonism
		1.4:1	2.95	0.16	Antagonism
		2.8:1	1.2	0.22	Slight antagonism
		5.6:1	1.02	0.22	Additive effect
		11.2:1	1.5	0.27	Antagonism
		22.4:1	2.34	0.59	Antagonism
K3	6	0.7:1	1.32	0.8	Moderate antagonism
		1.4:1	0.37	0.15	<b>Synergism</b>
		2.8:1	0.73	0.1	<b>Moderate synergism</b>
		5.6:1	1.5	0.24	Antagonism
		11.2:1	1.3	0.07	Moderate antagonism
		22.4:1	1.72	0.08	Antagonism
K4	5	0.6:1	0.54	0.07	<b>Synergism</b>
		1.2:1	1.03	0.05	Additive effect
		2.4:1	1.1	0.05	Additive effect
		4.8:1	0.74	0.1	<b>Moderate synergism</b>
		9.6:1	0.85	0.06	<b>Slight synergism</b>
		19.2:1	0.97	0.12	Additive effect
K5	6	0.7:1	0.51	0.06	<b>Synergism</b>
		1.4:1	0.81	0.05	<b>Moderate synergism</b>
		2.8:1	0.55	0.04	<b>Synergism</b>
		5.6:1	0.58	0.02	<b>Synergism</b>
		11.2:1	0.64	0.02	<b>Synergism</b>
		22.4:1	0.68	0.06	<b>Synergism</b>
K6	6	0.7:1	0.51	0.06	<b>Synergism</b>
		1.4:1	0.81	0.05	<b>Moderate synergism</b>
		2.8:1	0.55	0.04	<b>Synergism</b>
		5.6:1	0.58	0.02	<b>Synergism</b>
		11.2:1	0.64	0.02	<b>Synergism</b>
		22.4:1	0.68	0.06	<b>Synergism</b>
K7	6	0.7:1	1.4	0.2	Moderate antagonism
		1.4:1	3.1	0.41	Antagonism
		2.8:1	1.36	0.2	Moderate antagonism
		5.6:1	1.3	0.07	Moderate antagonism
		11.2:1	2.8	0.15	Antagonism
		22.4:1	2.28	0.15	Antagonism
K8	6	0.7:1	0.12	0.09	<b>Strong synergism</b>
		1.4:1	2.4	0.62	Antagonism
		2.8:1	3.3	0.8	Antagonism
		5.6:1	2.01	0.97	Antagonism
		11.2:1	3.3	0.74	Antagonism

\* Ratio: the applied combination and the concentration of selenoester–doxorubicin combination. CI at  $\text{ED}_{50}$ : combination index value (CI) at the 50% growth inhibition dose ( $\text{ED}_{50}$ ). The most effective interactions (types of synergism) for each derivative are highlighted in bold.

**Table 6.** Interaction of cyanoselenoesters with doxorubicin on MDR Colo 320 colon adenocarcinoma cells.

Compounds	Starting Conc. ( $\mu\text{M}$ )	Ratio *	CI at ED <sub>50</sub>	SD ( $\pm$ )	Type of Interaction
N1	15	1.7:1	1.9	0.2	Antagonism
		3.4:1	0.34	0.04	<b>Synergism</b>
		6.8:1	0.51	0.04	<b>Synergism</b>
		13.6:1	0.95	0.15	Additive effect
		27.2:1	0.56	0.09	<b>Synergism</b>
		54.4:1	0.21	0.21	<b>Strong synergism</b>
N2	15	54.4:1	0.21	0.21	Strong synergism
		1.7:1	0.62	0.19	<b>Synergism</b>
		3.4:1	3.1	0.38	Antagonism
		6.8:1	0.58	0.03	<b>Synergism</b>
		13.6:1	1.36	0.05	Moderate antagonism
		27.2:1	2.8	0.12	Antagonism
N3	10	54.4:1	2.3	0.15	Antagonism
		1.2:1	1.7	0.44	Antagonism
		2.4:1	3.7	0.5	Strong antagonism
		4.8:1	0.85	0.1	<b>Moderate synergism</b>
		9.6:1	1.01	0.15	Additive effect
		19.2:1	1.19	0.17	Slight antagonism
N4	10	38.4:1	1.3	0.21	Moderate antagonism
		1.2:1	1.7	0.44	Antagonism
		2.4:1	3.7	0.5	Strong antagonism
		4.8:1	0.85	0.1	<b>Moderate synergism</b>
		9.6:1	1.01	0.15	Additive effect
		19.2:1	1.19	0.17	Slight antagonism
N5	10	38.4:1	1.3	0.21	Moderate antagonism
		1.2:1	5.7	1.6	Strong antagonism
		2.4:1	3.7	0.5	Strong antagonism
		4.8:1	1.2	0.95	Slight antagonism
		9.6:1	1.01	0.15	Additive effect
		19.2:1	1.19	0.17	Slight antagonism
N6	10	38.4:1	1.3	0.21	Moderate antagonism
		1.2:1	2.9	0.31	Antagonism
		2.4:1	4.5	0.5	Additive effect
		4.8:1	1.5	0.1	Antagonism
		9.6:1	1.78	0.21	Antagonism
		19.2:1	1.96	0.11	Antagonism
N7	8	38.4:1	1.96	0.105	Antagonism
		0.9:1	2.7	0.23	Antagonism
		1.8:1	5.3	1.02	Strong antagonism
		3.6:1	0.9	0.23	<b>Slight synergism</b>
		7.2:1	1.84	0.18	Antagonism
		14.4:1	1.89	0.29	Antagonism
N7	8	28.8:1	0.92	0.6	Additive effect

\* Ratio: the applied combination and the concentration of selenocompound–doxorubicin. CI at ED<sub>50</sub>: combination index value (CI) at the 50% growth inhibition dose (ED<sub>50</sub>). The most effective interactions (types of synergism) for each derivative are highlighted in bold.

### 3.4. ABCB1 Inhibition in the Presence of Selenoesters

The inhibition of the ABCB1 transporter was assessed by measuring the intracellular accumulation of its fluorescent substrate rhodamine 123 at 0.2 and 2  $\mu\text{M}$ . Based on the flow cytometric evaluation, ketone-selenoesters inhibited the activity of the ABCB1 transporter, and the most potent derivatives were **K1**, **K2**, **K3**, **K7**, and **K8**, exhibiting a FAR value of 45.73, 37.35, 39.17, 40.38, and 36.09 at 2  $\mu\text{M}$ , respectively. Even the less potent derivatives showed similar activity at 2  $\mu\text{M}$ : in the case of **K5**, the FAR value was 32.61. Furthermore, in the presence of **K6**, a FAR of 29.4 was obtained. The less active derivative was **K4**, with a



FAR value of 4.99 at 2  $\mu\text{M}$ . **K3** and **K8** were effective at 0.2  $\mu\text{M}$  and 2  $\mu\text{M}$  concentration (FAR at 0.2;  $\mu\text{M}$  at 3.99 and 3.38, respectively), while the other compounds were only effective at 2  $\mu\text{M}$  concentration (Figure 2). Cyanoselenoesters did not show ABCB1 modulating activity.

Compounds	Concentration ( $\mu\text{M}$ )	FSC	SSC	FL-1	FAR
<b>K1</b>	0.2	2144	989	2.5	1.37
	2	1866	1067	83	<b>45.73</b>
<b>K2</b>	0.2	1916	1061	2.56	1.41
	2	1945	1156	67.8	<b>37.35</b>
<b>K3</b>	0.2	1706	982	7.25	<b>3.99</b>
	2	2040	1031	71.1	<b>39.17</b>
<b>K4</b>	0.2	1808	861	3.19	1.76
	2	1830	1008	9.06	<b>4.99</b>
<b>K5</b>	0.2	1982	1096	3.34	1.84
	2	1949	1053	59.2	<b>32.62</b>
<b>K6</b>	0.2	1996	873	2.7	1.48
	2	1833	1043	53.4	<b>29.42</b>
<b>K7</b>	0.2	1889	938	2.78	1.53
	2	1920	1045	73.3	<b>40.39</b>
<b>K8</b>	0.2	1804	853	6.14	<b>3.38</b>
	2	1990	1131	65.5	<b>36.09</b>
Tariquidar	0.2	1957	1074	50.9	<b>28.04</b>
DMSO	2.00%	1904	1001	1.72	0.95

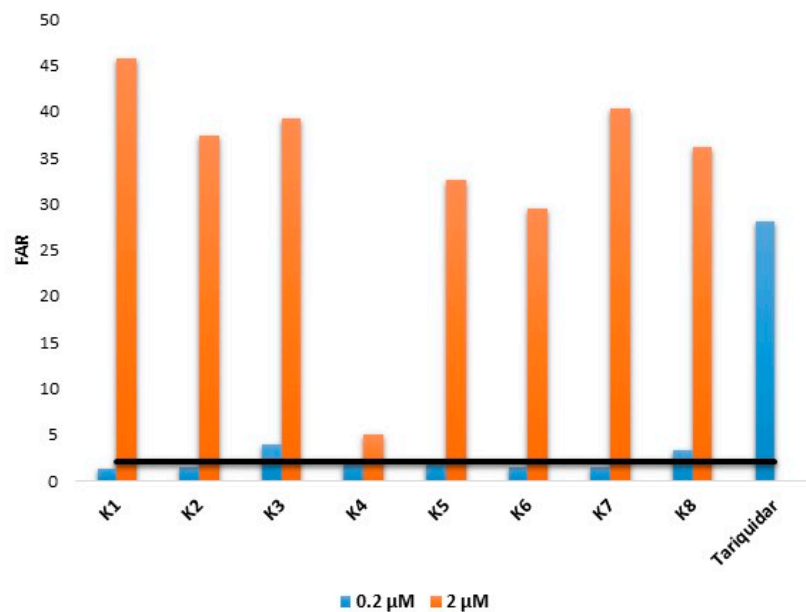


**Figure 2.** ABCB1 (P-gp) inhibition in the presence of selenoesters in MDR Colo 320 cells measuring the intracellular accumulation of the ABCB1 substrate rhodamine 123 by flow cytometry. The FAR (fluorescence activity ratio) values were calculated based on the equation given in Section 2.9. Tariquidar was applied as positive control; DMSO was used as solvent control. Results above FAR 2 (black line, highlighted in bold) are considered effective.

The parameters evaluated from flow cytometry experiments were: Forward Scatter Count (FSC, provides information about cell size); Side Scatter Count (SSC, proportional to cell granularity or internal complexity); FL-1 (Mean fluorescence of the cells), and Fluorescence Activity Ratio (FAR), which was calculated by the equation given above.

### 3.5. P-gp ATPase Activity Assay

Only the compounds with ABCB1 inhibitory activity were tested in this assay. As shown in Figure 3,  $\Delta\text{RLU}$  of **K1**, **K7**, and **K8** were significantly lower than  $\Delta\text{RLU}_{\text{basal}}$ .

demonstrating that these compounds are inhibitors of P-gp ATPase activity. The rest of the compounds are stimulators of P-gp ATPase activity. Verapamil is a P-gp substrate that stimulates ATPase activity and served as a control in this assay. In the cases of **K2** and **K6**, the P-gp ATPase activity could not be determined (Figure 3).

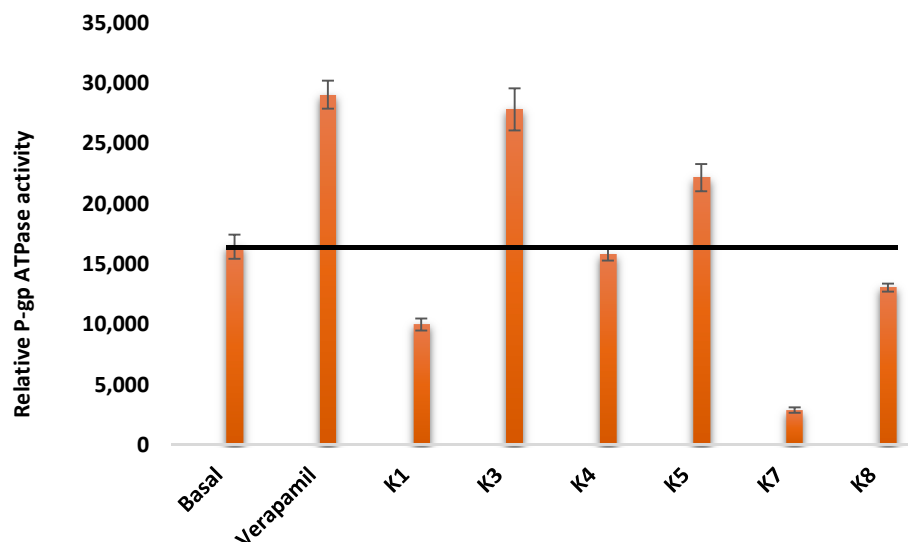


**Figure 3.** Relative ABCB1 (P-gp) ATPase inhibition activity of selected ketone-selenoesters. The effects are presented as the relative ATPase activity. The decrease in luminescence of untreated samples compared to samples treated with sodium-vanadate represents basal P-gp ATPase activity. The decrease in luminescence of verapamil-treated samples represents verapamil-stimulated P-gp ATPase activity. The lower the relative ATPase activity, the better the inhibitor. Results are calculated as the means  $\pm$  SD from experiments performed in triplicate. The level of basal activity is presented as a black line.

### 3.6. Induction of Apoptosis

The potent ABCB1 inhibiting ketone-selenoesters were tested regarding their apoptosis-inducing activity on MDR Colo 320 colon adenocarcinoma cells (Table 7 and Figure 4).

The results were compared to 12*H*-benzo( $\alpha$ )phenothiazine (M627) as a positive control. The most potent compound, **K3**, could induce early apoptosis in 18.6% of the cell population, showing a higher capacity to trigger these early apoptotic events than the reference. Interestingly, all derivatives contributed to late apoptosis, and their activity ranged from 16.1 to 33.9%. **K3** induced late apoptosis in 25.6% of the cell population. Considering together the early and late apoptosis (as total apoptotic events), all of the compounds, with the exception of **K4**, induced apoptotic events in more than 30% of the gated cells. After defining the apoptosis quotient as the quotient of the total apoptotic events of the compound divided by the reference and expressed as a percentage, all of the compounds, except **K4**, showed an apoptosis induction ability equal to 64–90% more than the reference, and a concentration 10-fold lower than the reference. Compound **K3** was the most potent with 89.5%, followed by **K2** with 69.2%. The least effective was **K4**, with 39.5%. During early apoptosis, phosphatidyl serine (PS) appears on the outer membrane, which can be detected by annexin V; however, the membrane has not yet disintegrated. During late apoptosis, the cell membrane is already damaged (in this case, annexin is also able to bind to PS), resulting in the release of DNA, to which propidium iodide is able to bind.

**Table 7.** Apoptosis induction by ketone-selenoesters on MDR Colo 320 adenocarcinoma cells. The 12*H*- benzo( $\alpha$ )phenothiazine (M627) was applied as a positive control.

Conc. ( $\mu$ M)	Early Apoptosis (%) Treated Sample-Untreated Sample	Late Apoptosis (%) Treated Sample-Untreated Sample	Cell Death (%) Treated Sample-Untreated Sample	Total Apoptotic Events (Early + Late, %)	Apoptosis Quotient (%)
M627 20	13.3	36.1	0.00	49.4	100%
K1 2	3.7	28.9	2.15	32.6	66.0%
K2 2	0.3	33.9	0.95	34.2	69.2%
K3 2	<b>18.6</b>	25.6	0.00	44.2	89.5%
K4 2	3.4	16.1	5.95	19.5	39.5%
K5 2	1.8	30.9	1.35	32.7	66.2%
K6 2	4.5	27.8	0.17	32.3	65.4%
K7 2	6.1	27.5	0.10	33.6	68.0%
K8 2	4.9	26.7	0.85	31.6	64.0%

Apoptotic quotient is defined as the quotient of the total apoptotic events determined for the respective compound and the reference M627, expressed in percentage. The most effective early apoptosis induction is highlighted in bold.

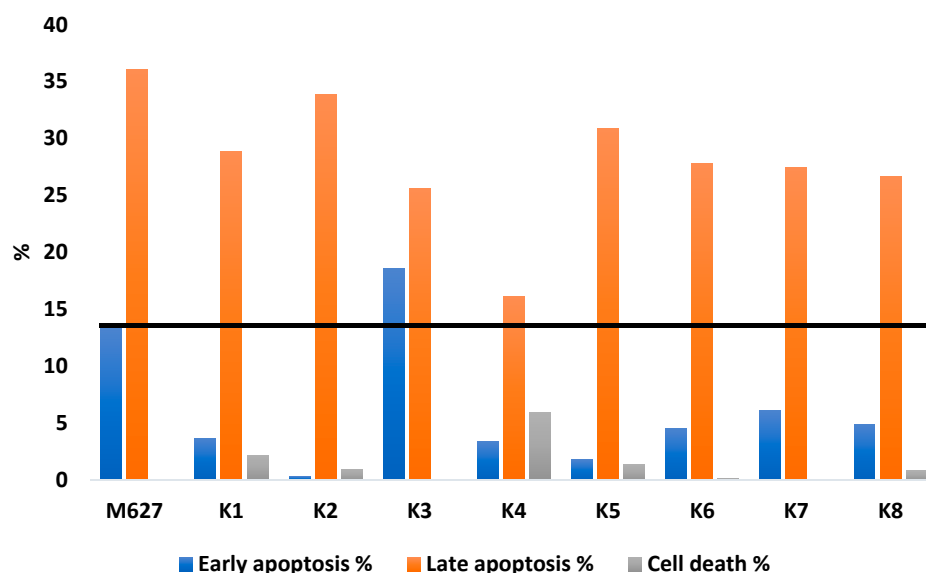


**Figure 4.** Apoptosis induction by ketone-selenoesters on MDR Colo 320 adenocarcinoma cells. The 12*H*- benzo( $\alpha$ )phenothiazine (M627) was applied as a positive control. The cell populations were analysed by flow cytometry after Annexin V-FITC and propidium iodide staining. The figure represents the percentage of early apoptotic cells (annexin positive, propidium iodide negative); late apoptotic cells (annexin positive, propidium iodide positive) (A+, PI+); and dead cells (annexin negative, propidium iodide positive) (A−, PI+). The black line demonstrates the percentage of early apoptosis in the presence of the positive control M627.

### 3.7. Wound Healing Assay

Wound healing activity of selenoesters was evaluated as the ability of the cells to migrate and close the gap created on the monolayer of human keratinocytes (HaCaT cell line). The tested substances were applied in the highest possible non-toxic concentration (IC<sub>10</sub>, concentration inhibiting 10% of the population). In general, ketone-selenoesters were more toxic (except K4 and K1) than cyano-selenoesters (except N4); therefore, they were applied at lower doses (0.17–0.30  $\mu$ M) when compared to cyanoselenoesters (0.36–0.64  $\mu$ M). Compounds K1, K4, and N4 were applied at a concentration of 0.30, 0.46, and 0.20  $\mu$ M, respectively. As could be seen in Table 8, all ketone-selenoesters stimulated wound healing more effectively in comparison to both untreated control ( $p < 0.0000005$ ) and allantoin ( $p < 0.00005$ ). As a result, all of the tested ketone-selenoesters exhibited around 80% of gap closure within 24 h. After 48 h, samples K1, K2, K3, K5, K7, and K8 exhibited complete gap closure, and samples K4 and K6 were able to close the gap with a closure percentage

of 86% and 93%, respectively. In contrast, cyano-selenoesters were less active than ketone-selenoesters, as none of the samples were able to close the gap completely. Samples **N3**, **N5**, and **N6** exhibited slower closure of the wound, and was slower than in the untreated control ( $p < 0.005$ ) within 24 h (closure percentage was only around 45%). Only samples **N1**, **N2**, **N4**, and **N7** closed effectively the damaged wound in 24 h, with the gap closure around 70%. Despite the fact that cyano-selenoesters were less potent in exhibiting the cell mobility for the wound healing, the samples **N1**, **N4**, and **N7** were still even slightly better than the positive control ( $p < 0.005$ ,  $p < 0.05$ , and  $p < 0.05$ , respectively), and other cyano-selenoesters, with a closure percentage of around 80%.

**Table 8.** Wound healing activity determined as keratinocytes' (HaCaT) wound closure (%) after 24 and 48 h. Allantoin (50 µg/mL) served as a positive control. Data represent the average of twenty repetitions (four biological, five technical) with corresponding standard error of the mean. The data were analysed with *t*-test, where the difference between the group and negative control was considered statistically significant when  $p < 0.0000005$  (\*\*\*\*\*), 0.000005 (\*\*\*\*), 0.00005 (\*\*\*), 0.0005 (\*\*), 0.005 (\*\*), and 0.05 (\*).

Compound	Dose		24 h			48 h		
	IC <sub>10</sub> (µM)	Closure (%)	SEM	<i>t</i> -Test	Closure (%)	SEM	<i>t</i> -Test	
<b>K1</b>	0.30	83.64	1.03	*****	100.00		*****	
<b>K2</b>	0.20	85.90	0.97	*****	100.00		*****	
<b>K3</b>	0.24	87.49	1.92	*****	100.00		*****	
<b>K4</b>	0.46	79.17	1.81	*****	86.29	2.47	****	
<b>K5</b>	0.25	88.56	1.44	*****	100.00		*****	
<b>K6</b>	0.22	83.02	1.54	*****	92.65	1.34	*****	
<b>K7</b>	0.24	82.71	1.22	*****	100.00		*****	
<b>K8</b>	0.17	88.55	1.84	*****	100.00		*****	
<b>N1</b>	0.40	75.53	1.52	*****	85.41	1.63	*****	
<b>N2</b>	0.36	72.23	1.20	*****	77.51	1.98	*	
<b>N3</b>	0.64	46.46	2.00	*****	75.70	1.44		
<b>N4</b>	0.20	73.65	1.92	*****	83.84	2.09	*****	
<b>N5</b>	0.60	53.25	1.86	**	64.21	2.78	****	
<b>N6</b>	0.60	46.13	1.25	*****	60.98	3.13	****	
<b>N7</b>	0.61	74.84	1.77	*****	82.41	1.50	*****	
<b>PC</b>		70.37	2.56	*****	84.63	2.21	*****	
<b>NC</b>		56.33	1.75		75.55	1.71		

SEM, standard error of the mean; *t*-test, 2-tailed *t*-test with unequal variances.

## 4. Discussion

### 4.1. Synthesis and Characterization of the Compounds

As mentioned in the Results section, the yield of the synthesis depends mostly on the purification procedure and on the matter state of the compound: generally, liquids are required to perform column chromatography, which reduces the yield. Solids showed a yield between 40% and 50%, and liquids showed a yield between 7% and 29%. Even for solids, the yield tends to be low. This may be related to the solubility of the compounds in water. As compounds are obtained (when they are solid) as a precipitate that is formed in the reaction media, part of the compound can remain in solution. Even knowing from previous works that selenoesters are poorly soluble in water, the usage of a significant volume during washings can be reflected in a significantly lower yield than the one expected.

The spectral data are fully described in the compound descriptions of Section 2.3, which discusses the chemical description of the compounds. Spectra enabled the correct assignments and the proper characterization of the structure of the compounds. As mentioned in the Results section, HMBC spectra were of particular interest to ensure the formation of the selenoester. A second proof was the isotopic pattern observed in the mass spectra of the oxoselenoesters in which the molecular ion has a higher abundance, as indicated by **K2**, **K5**, **K6**, and **K8**. Another indirect proof is the observation in <sup>13</sup>C-NMR

that the range of the peak chemical shift is always narrower for the carbonyl of the ketone or for the cyano group than for the carbonyl of the selenoesters. This is logical as the ketone or the cyano group are at a higher distance from the ring substituents, which are more responsible for the observed variations, than the carbonyl of the selenoester. A similar observation was found with the range of the bond stretches, C=O (COCH<sub>3</sub>) and C≡N, as compared to the C=O (COSe) stretch.

#### 4.2. Anticancer Activity

Oxoselenoesters, in general (a few exceptions are observed), showed a more potent cytotoxicity than cyanoselenoesters in MDR Colo 320, HepG2, and B16 cancer cell lines. This difference of activity is particularly marked in Colo 320 and HepG2 cells. Cyanoselenoesters showed no activity on the MRC-5 cells; however, they were very toxic on both colon cancer cell lines, and were less potent on the resistant cells. Regarding the most active compound in each cell line (the second and third most active in brackets after cell line), these were as follows: **K4** in Colo 205 (**K1**, **N4**); **K1** in Colo 320 (**K4**, **K6**); **K2** in HepG2 (**K1**, **K5**); **N6** in HeLa (**K4**, **K3**); and **K5** in B16 cells (**K2**, **K6**). In line with the overall impression, the majority of them are oxoselenoesters, and among them, all appeared at least once, except **K7** and **K8**. This may point out that the presence of substituents without halogen(s)—as is the case of **K7**—reduces the activity, as the compounds that include a trifluoromethyl group or that have one or two halogens bound to the phenyl ring showed better activity. However, the inclusion of a third fluorine at the phenyl ring (**K8**) is also less profitable for the cytotoxicity. On the other hand, the recurrent appearance of **K1** and **K4** among the most active compounds (three times each) against each cell line points out that the thionyl ring favours the cytotoxicity, as well as the presence of a trifluoromethyl group in ortho position (in the phenyl ring) in respect to the selenoester. Interestingly, **K5** (which has a 3-CF<sub>3</sub> substituent at the ring) also exerts noteworthy activity, and the cyanoselenoester, **N4**, with a 2-CF<sub>3</sub> substituent at the ring, is perhaps the most active derivative among the cyanoselenoesters. This supports the empirical observation of the relevance of this trifluoromethyl group (preferable in ortho position, although the compound with this substituent in meta position has a comparable activity in all cell lines, except in HepG2, in which it is significantly less active) for the cytotoxic activity.

The ketone-containing selenoesters showed toxicity towards normal MRC-5 cells, whereas none of the cyano-containing derivatives exerted toxicity against this cell line at concentrations below 100 µM. This implies that all of the cyanoselenoesters were strongly selective (SI > 6) towards cancer cells. They were especially selective towards B16 skin melanoma cells, as **N4** and **N5** showed an SI higher than 71.4, and **N7** showed an SI higher than 62.5. Compound **N6** was also extremely selective towards HeLa cervical adenocarcinoma cells (SI >76.9). More compounds showed SI values higher than 50 towards cancer cells: **N1** and **N6** in B16 cells, **N1** in HeLa cells, and **N4** and **N7** in Colo 205 cells. Ketone-selenoesters, in contrast, were much less selective. Only **K4** showed a moderate selectivity towards Colo205 cells (3 < SI < 6). The remaining compounds were slightly selective (1 < SI < 3) towards the tested cancers cells in respect to MRC-5 non-cancer cells. Even a few ones were non-selective (SI < 1): **K3**, **K4**, and **K6** towards HepG2 cells, and **K2** towards Colo205 cells. This indicates a risk of side effects, and further research is necessary to find compounds with a similar potency and more selectivity.

Regarding the combination of ketone-selenoesters and cyanoselenoesters with the cytotoxic drug doxorubicin, eleven of the fifteen selenoesters evaluated interacted in a synergistic manner with doxorubicin in at least one of the ratios tested: **K1**, **K3**, **K4**, **K5**, **K6**, **K8**, **N1**, **N2**, **N3**, **N4**, and **N7**. No logical structure-activity relationships (SARs) can be extracted, as **K5** and **K6** interacted in different synergism degrees with doxorubicin in all of the ratios, whereas their nitrile equivalents (**N5** and **N6**) showed antagonistic interactions for five of the six ratios tested. Similarly, the thiophene cyanoselenoester **N1** showed a synergistic interaction with doxorubicin in four of the six ratios assayed, while its ketone

analogue **K1** only showed synergism in one ratio out of five. This **N1** derivative was also capable of interacting with a strong synergism, at a 54.4:1 ratio with doxorubicin.

To reverse efflux-related MDR, the inhibition of the ABCB1 pump was investigated in the presence of selenocompounds. The 2-oxopropyl moiety of the ketone-selenoesters is crucial for the activity, as all ketone-selenoesters, except **K4**, were more potent ABCB1 inhibitors, whereas none of the cyanoselenoesters showed ABCB1 inhibiting activity. This is also in line with previous works [15,16], in which both this moiety and a 3,3-dimethyl-2-oxobutyl moiety showed very potent activity.

The most active compound is **K1**, which contains a thiophene ring instead of a phenyl ring. In this case, the insertion of a bulky trifluoromethyl group at the two-position of the phenyl ring significantly reduced the activity (**K4**): simply moving this group to the three-position and eliminating the steric hindrance produced a sixfold increase of the activity (**K5**). Interestingly, two oxoselenoesters that showed a less marked cytotoxicity (**K7**, with a 4-tert-butylphenyl ring; and **K8**, with a 2,4,5-trifluorophenyl ring) were strong inhibitors of ABCB1, with a similar activity to **K2** and **K3**, with 2-fluorophenyl and 4-bromophenyl moieties, respectively.

Regarding the P-gp ATPase activity, only the oxoselenoesters were tested as they were the only ones with ABCB1 inhibitory activity. Among them, the P-gp ATPase activity of **K2** and **K6** could not be determined, and all of the remaining tested compounds, except **K4** (whose activity was similar to the one observed for the basal control), modulated the ATPase activity. Interestingly, **K1** and **K7**, which were the most potent ABCB1 inhibitors, inhibited the ATPase activity, especially in the case of **K7**. Besides, **K8** exerted a milder inhibition of the ATPase. Since the activity of ABCB1 can protect the cells from apoptosis, the inhibition of the energy supply of this pump can promote apoptosis, as demonstrated by our results [21]. The abovementioned derivatives (**K1**, **K7**, and **K8**) induced late apoptosis in MDR Colo 320 cells, confirming the connection between ABCB1 inhibition and apoptosis induction.

On the other hand, **K3** stimulated the P-gp ATPase with a comparable intensity to the reference verapamil, whereas **K5** produced a milder stimulation. Then—keeping in mind that the data available are scarce—with this data, the thienyl ring and the 4-tert-butylphenyl and 2,4,5-trifluorophenyl moieties inhibited the ATPase activity, whereas the 4-bromophenyl and the 3-(trifluoromethyl)phenyl moiety stimulated it. Finally, moving the trifluoromethyl group from the three- to the two-position eliminated this promotion of the ATPase activity.

The connection between ABCB1 inhibition and apoptosis induction was investigated in the case of ketone-selenoesters. The ketone-selenoesters showed a significant ability to trigger apoptotic events, with the exception of **K4**. Compound **K3** was more effective than the reference phenothiazine in the induction of early apoptosis, and is the one that, considering together the early and late apoptosis, induced apoptosis with a potency closer to the reference (89.5%). As all of the remaining derivatives assayed showed a similar ability to induce apoptosis, no SARs can be extracted with the available data. Besides, it is evident that the inclusion of a bromine atom at the four-position of the phenyl ring increases the apoptosis induction (**K3**), and the inclusion of a bulky substituent at the two-position (as the trifluoromethyl moiety) of the phenyl ring reduces the ability to trigger apoptotic events. In addition, the presence of selenium can induce the formation of free radicals, resulting in apoptosis and cell death in cancer cells [22–24]. The functions of MDR transporter proteins (most notably ABCB1) have been described in apoptosis evasion, mediated by a dampening of the extrinsic apoptotic pathway (through suppression of TRAIL protein and caspases three and eight) and the stabilization of cell membrane phospholipids (through acting as an outwardly directed flippase). The inter-relatedness of overexpressed efflux pumps and programmed cell death may explain the results obtained in the apoptosis detection assay [21].

In general, selenium in the form of selenoproteins and selenocompounds has always been known as an excellent candidate for wound healing, as some of them have exhibited



their ability to act as antioxidants and inhibitors of inflammation. Selenocompounds act as inhibitors of cytokines and eliminators of peroxynitrate, which is a super radical ion in the inflammatory phase [25]. As described in the results, all of the eight ketone-selenoesters stimulated an effective wound healing process, demonstrating a better healing ability than the positive control allantoin. Six of them (**K1**, **K2**, **K3**, **K5**, **K7**, and **K8**) were even capable of repairing the wound completely. Only the compounds with a bulky substituent in the *ortho* position (trifluoromethyl, **K4**) or with two different substituents (**K6**, 3-chloro-4-fluorophenyl) were not capable of completely closing the wound. Regarding the cyano-selenoesters, they were significantly less effective in this assay than the ketone-selenoesters. Only one of the seven cyano-containing derivatives, compound **N1**, displayed better closure than allantoin (especially after 24). Three additional ones, **N2**, **N4**, and **N7**, were more effective than the negative control. In this case, no reliable SARs can be extracted, but the removal of one of the two trifluoromethyl substituents from compound **N7** resulted in significant wound healing activity loss, which serves as the main reason for the inability of compound **N5** to close the gap. Similarly, compound **N6** and **N3** had the same effect as compound **N5**.

If a few compounds would need to be selected among all derivatives to proceed to more in-depth studies, perhaps the most promising are **K1**, **K3**, and **K5**. The oxoselenoester **K1**, which has a thiophene ring bound to the carbonyl of the selenoester, is a potent cytotoxic compound that exerts a strong inhibition of the ABCB1 efflux pump and of the ATPase activity, and also has the ability of apoptosis induction and the capacity to promote a complete closure of a wound. Similarly, the 2-oxopropyl 4-bromobenzoselenoate (**K3**) has a noteworthy cytotoxic activity, and strongly inhibits the ABCB1 efflux pump, but stimulates the ATPase activity. Besides, it is the most potent apoptosis inducer among the tested compounds and also manages to complete the closure of a wound in 48 h. Finally, the 2-oxopropyl 3-(trifluoromethyl)benzoselenoate (**K5**) has a similar effect than **K3**, but with a less potent apoptosis-inducing ability and less capacity to enhance P-gp ATPase activity. In exchange, it could interact in a synergistic manner with doxorubicin when administered in combination, in the six ratios tested. Between these three derivatives, all of the activities tested are covered, as are the two ways of action in the case of the ATPase assay. The compound 2-oxopropyl 3-(trifluoromethyl)benzoselenoate (**K4**) seemed to be a promising derivative in cytotoxicity assay, but later showed a poor effectivity in ABCB1 inhibition, ATPase modulation, apoptosis induction, and wound healing, so it is clearly a less multitarget compound than **K1**, **K3**, and **K5**. Perhaps the presence of a bulky substituent in a position close to the selenoester can affect the interaction of the selenium atom with the different cellular targets. On the other hand, it may affect its hydrolysis, as this is the hypothesized mechanism of action for these compounds, according to previous works [16].

In contrast, the cyanoselenoesters are more selective compounds, but they are generally less cytotoxic, weaker promoters of wound healing, interacted in a less synergistic manner with doxorubicin in combination assay, and did not inhibit the ABCB1 protein.

## 5. Conclusions

Herein, we described the design, synthesis, and characterization of fifteen novel selenoesters, as well as the evaluation of their activity against a wide selection of different targets related to cancer multidrug resistance. Of these selenoesters, the alkyl moiety of eight included a ketone group, whereas the seven remaining contained a cyano group. All of the compounds showed  $IC_{50}$  values between 1 and 12  $\mu$ M in the five cancer cell lines evaluated. The oxoselenoesters were generally more cytotoxic, while the cyanoselenoesters were more selective towards cancer cells in respect to non-cancer cells. Besides, the majority of the obtained oxoselenoesters were potent ABCB1 inhibitors, enhanced the activity of doxorubicin in a synergistic manner (at least in any of the ratio concentrations tested), and modulated the P-gp ATPase activity. All of the oxoselenoesters showed an apoptosis induction capacity and an ability to promote wound healing. Therefore, these

novel selenocompounds have shown noteworthy multi-target anticancer activity that converts them into a promising starting point to develop more effective and selective anticancer agents.

**Supplementary Materials:** The following are available online at <https://www.mdpi.com/article/10.3390/cancers13184563/s1>. Figure S1: Compound **K1**: Se-(2-oxopropyl) thiophene-2-carboselenoate, Figure S2: Compound **K2**: Se-(2-oxopropyl) 2-fluorobenzoselenoate, Figure **S3**: Compound **K3**: Se-(2-oxopropyl) 4-bromobenzoselenoate, Figure S4: Compound **K4**: Se-(2-oxopropyl) 2-(trifluoromethyl) benzoselenoate, Figure S5: Compound **K5**: Se-(2-oxopropyl) 3-(trifluoromethyl)benzoselenoate, Figure S6: Compound **K6**: Se-(2-oxopropyl) 3-chloro-4-fluorobenzoselenoate, Figure S7: Compound **K7**: Se-(2-oxopropyl) 4-(tert-butyl)benzoselenoate, Figure S8: Compound **K8**: Se-(2-oxopropyl) 2,4,5-trifluorobenzoselenoate, Figure S9: Compound **N1**: Se-(cyanomethyl) thiophene-2-carboselenoate, Figure S10: Compound **N2**: Se-(cyanomethyl) 3-fluorobenzoselenoate, Figure S11: Compound **N3**: Se-(cyanomethyl) 4-bromobenzoselenoate, Figure S12: Compound **N4**: Se-(cyanomethyl) 2-(trifluoromethyl)benzoselenoate, Figure S13. Compound **N5**: Se-(cyanomethyl) 3-(trifluoromethyl) benzoselenoate, Figure S14. Compound **N6**: Se-(cyanomethyl) 3-chloro-4-fluorobenzoselenoate, Figure S15. Compound **N7**: Se-(cyanomethyl) 3,5-bis(trifluoromethyl)benzoselenoate.

**Author Contributions:** Conceptualization, G.S., J.V., and E.D.-Á.; methodology, J.V., G.S., and E.D.-Á.; chemical synthesis and analysis, N.S.-J., C.S.-H., M.B.-L., F.-J.A.-M., and E.D.-Á.; biological evaluation and data processing, N.S., S.D., G.H., A.K., and M.N.; writing—original draft preparation, N.S.-J., S.D., G.S., J.V., and E.D.-Á.; writing—review and editing, G.S., J.V., and E.D.-Á.; supervision, G.S., J.V., and E.D.-Á.; project administration, J.V., G.S., and E.D.-Á.; funding acquisition, G.S., J.V., and E.D.-Á. All authors have read and agreed to the published version of the manuscript.

**Funding:** The study was supported by the projects SZTE ÁOK-KKA 2018/270-62-2 of the University of Szeged, Faculty of Medicine and GINOP-2.3.2-15-2016-00038 (Hungary); and Consejo Superior de Investigaciones Científicas (CSIC, Spain, project LINKA20285). This research was funded by VISEGRAD FUND, grant number 22010090; and by the mobility project from the Czech Ministry of Education, Youth and Sports INTER-COST, grant number LTC19007. This article is based upon work from COST Action 17104 <STRATAGEM>, supported by COST (European Cooperation in Science and Technology), (<http://www.cost.eu>, accessed on 17 September 2021). The study was supported also by two cultural associations: “Trevinca” and “Iniciativas Ropelanas”.

**Institutional Review Board Statement:** Not applicable.

**Informed Consent Statement:** Not applicable.

**Data Availability Statement:** The data presented in this study are available in this article (and supplementary material). Additional data are available on request from the corresponding author.

**Conflicts of Interest:** The authors declare no conflict of interest. The funders had no role in the design of the study; in the collection, analyses, or interpretation of data; in the writing of the manuscript; or in the decision to publish the results.

## References

1. Bellamy, W.T. P-Glycoproteins and multidrug resistance. *Annu. Rev. Pharmacol. Toxicol.* **1996**, *36*, 161–183. [[CrossRef](#)] [[PubMed](#)]
2. Smyth, M.J.; Krasovskis, E.; Sutton, V.R.; Johnstone, R.W. The drug efflux protein, P-Glycoprotein, additionally protects drug-resistant tumor cells from multiple forms of caspase-dependent apoptosis. *Proc. Natl. Acad. Sci. USA* **1998**, *95*, 7024–7029. [[CrossRef](#)]
3. Sharom, F.J.; Liu, R.; Romsicki, Y.; Lu, P. Insights into the structure and substrate interactions of the P-Glycoprotein multidrug transporter from spectroscopic studies. *Biochim. Biophys. Acta (BBA)—Biomembr.* **1999**, *1461*, 327–345. [[CrossRef](#)]
4. Brinkmann, U. Functional Polymorphisms of the Human Multidrug Resistance (MDR1) Gene: Correlation with P Glycoprotein Expression and Activity in vivo. In *Novartis Foundation Symposia*; Bock, G., Goode, J.A., Eds.; John Wiley & Sons, Ltd.: Chichester, UK, 2008; pp. 207–212. ISBN 978-0-470-84146-4.
5. Pokharel, D.; Roseblade, A.; Oenarto, V.; Lu, J.F.; Bebawy, M. Proteins regulating the intercellular transfer and function of P-Glycoprotein in multidrug-resistant cancer. *Ecancer* **2017**, *11*, 768. [[CrossRef](#)] [[PubMed](#)]
6. Hiller, D.; Sanglard, D.; Morschhäuser, J. Overexpression of the MDR1 Gene is sufficient to Confer increased resistance to toxic compounds in *Candida Albicans*. *Antimicrob. Agents Chemother.* **2006**, *50*, 1365–1371. [[CrossRef](#)] [[PubMed](#)]
7. Barrand, M.A.; Bagrij, T.; Neo, S.-Y. Multidrug resistance-associated protein: A protein distinct from P-Glycoprotein involved in cytotoxic drug expulsion. *Gen. Pharmacol. Vasc. Syst.* **1997**, *28*, 639–645. [[CrossRef](#)]



8. Allen, J.D.; Brinkhuis, R.F.; van Deemter, L.; Wijnholds, J.; Schinkel, A.H. Extensive contribution of the multidrug transporters P-Glycoprotein and Mrp1 to basal drug resistance. *Cancer Res.* **2000**, *60*, 5761–5766.
9. Allen, J.D.; Van Dort, S.C.; Buitelaar, M.; van Tellingen, O.; Schinkel, A.H. Mouse breast cancer resistance protein (Bcrp1/Abcg2) mediates etoposide resistance and transport, but etoposide oral availability is limited primarily by P-Glycoprotein. *Cancer Res.* **2003**, *63*, 1339–1344.
10. Palmeira, A.; Sousa, E.; Vasconcelos, M.H.; Pinto, M.; Fernandes, M.X. Structure and ligand-based design of P-Glycoprotein inhibitors: A historical perspective. *Curr. Pharm. Des.* **2012**, *18*, 4197–4214. [[CrossRef](#)] [[PubMed](#)]
11. Prabhu, K.S.; Lei, X.G. Selenium. *Adv. Nutr.* **2016**, *7*, 415–417. [[CrossRef](#)]
12. Vinceti, M.; Filippini, T.; Cilloni, S.; Crespi, C.M. The Epidemiology of Selenium and Human Cancer. In *Advances in Cancer Research*; Elsevier: Cambridge, MA, USA, 2017; Volume 136, pp. 1–48. ISBN 978-0-12-812016-3.
13. Álvarez-Pérez, M.; Ali, W.; Marć, M.A.; Handzlik, J.; Domínguez-Álvarez, E. Selenides and diselenides: A review of their anticancer and chemopreventive activity. *Molecules* **2018**, *23*, 628. [[CrossRef](#)]
14. Maiyo, F.; Singh, M. Selenium nanoparticles: Potential in cancer gene and drug delivery. *Nanomedicine* **2017**, *12*, 1075–1089. [[CrossRef](#)] [[PubMed](#)]
15. Domínguez-Álvarez, E.; Gajdács, M.; Spengler, G.; Palop, J.A.; Marć, M.A.; Kieć-Kononowicz, K.; Amaral, L.; Molnár, J.; Jacob, C.; Handzlik, J.; et al. Identification of selenocompounds with promising properties to reverse cancer multidrug resistance. *Bioorganic Med. Chem. Lett.* **2016**, *26*, 2821–2824. [[CrossRef](#)] [[PubMed](#)]
16. Gajdács, M.; Spengler, G.; Sanmartín, C.; Marć, M.A.; Handzlik, J.; Domínguez-Álvarez, E. Selenoesters and selenoanhydrides as novel multidrug resistance reversing agents: A confirmation study in a colon cancer MDR cell line. *Bioorganic Med. Chem. Lett.* **2017**, *27*, 797–802. [[CrossRef](#)] [[PubMed](#)]
17. Spengler, G.; Gajdács, M.; Marć, M.; Domínguez-Álvarez, E.; Sanmartín, C. Organoselenium compounds as novel adjuvants of chemotherapy drugs—A promising approach to fight cancer drug resistance. *Molecules* **2019**, *24*, 336. [[CrossRef](#)]
18. Gajdács, M.; Nové, M.; Csonka, Á.; Varga, B.; Sanmartín, C.; Domínguez-Álvarez, E.; Spengler, G. Phenothiazines and selenocompounds: A potential novel combination therapy of multidrug resistant cancer. *Anticancer Res.* **2020**, *40*, 4921–4928. [[CrossRef](#)]
19. Liang, C.-C.; Park, A.Y.; Guan, J.-L. In vitro scratch assay: A convenient and inexpensive method for analysis of cell migration in vitro. *Nat. Protoc.* **2007**, *2*, 329–333. [[CrossRef](#)]
20. Chou, T.-C. Drug combination studies and their synergy quantification using the Chou-Talalay method. *Cancer Res.* **2010**, *70*, 440–446. [[CrossRef](#)]
21. Stavrovskaya, A.A.; Moiseeva, N.I. Non-canonical functions of the cellular transporter P-Glycoprotein. *Biochem. Mosc. Suppl. Ser. A* **2016**, *10*, 241–250. [[CrossRef](#)]
22. Zhu, Z.; Kimura, M.; Itokawa, Y.; Aoki, T.; Takahashi, J.A.; Nakatsu, S.; Oda, Y.; Kikuchi, H. Apoptosis induced by selenium in human glioma cell lines. *Biol. Trace Element Res.* **1996**, *54*, 123–134. [[CrossRef](#)]
23. Ghosh, J. Rapid induction of apoptosis in prostate cancer cells by selenium: Reversal by metabolites of arachidonate 5-lipoxygenase. *Biochem. Biophys. Res. Commun.* **2004**, *315*, 624–635. [[CrossRef](#)] [[PubMed](#)]
24. Zu, Y.; Yang, Z.; Tang, S.; Han, Y.; Ma, J. Effects of P-Glycoprotein and its inhibitors on apoptosis in K562 cells. *Molecules* **2014**, *19*, 13061–13075. [[CrossRef](#)] [[PubMed](#)]
25. Hariharan, S.; Dharmaraj, S. Selenium and selenoproteins: It's role in regulation of inflammation. *Inflammopharmacology* **2020**, *28*, 667–695. [[CrossRef](#)] [[PubMed](#)]